2013-09-11

Formation, Functionalization, Characterization, and Applications of a Mixed-Mode, Carbon/Diamond-Based, Core-Shell Phase for High Performance Liquid Chromatography

Landon A. Wiest
Brigham Young University - Provo

Formation, Functionalization, Characterization, and Applications of a Mixed-Mode, Carbon/Diamond-Based, Core-Shell Phase for High Performance Liquid Chromatography

Landon Andrew Wiest

A dissertation submitted to the faculty of
Brigham Young University
in partial fulfillment of the requirements for the degree of

Doctor of Philosophy

Matthew R. Linford, Chair
Daniel E. Austin
Steven L. Castle
Robert C. Davis
Milton L. Lee

Department of Chemistry and Biochemistry

Brigham Young University

September 2013

ABSTRACT

Formation, Functionalization, Characterization, and Applications of a Mixed-Mode, Carbon/Diamond-Based, Core-Shell Phase for High Performance Liquid Chromatography

Landon Andrew Wiest
Department of Chemistry and Biochemistry, BYU
Doctor of Philosophy

My work has focused on a variety of different types of diamond-based, core-shell particles. These particles are formed with inert cores and poly(allylamine)/nanodiamond shells. Their intended purpose is to form an LC stationary phase that is stable from pH 1 – 14 and at elevated temperatures. At the beginning of my studies, the particles that had been made in the Linford laboratory were pH stable, but irregular and had poor mechanical stability. Since that time, I have worked to improve the particles by using more spherical zirconia and carbon cores, and I have improved their mechanical stability via chemical crosslinking with epoxides. I have performed van Deemter and van't Hoff analyses to understand the properties of these columns. Efficiencies greater than 100,000 N/m are routinely achieved with these carbon/nanodiamond-based phases. In addition I contributed to two patents that show innovations in diamond functionalization. My contributions involved reduction of an oxidized diamond surface with $LiAlH_4$ prior to functionalization with isocyanates. I also wrote some application notes for the Flare mixed-mode column, which was recently introduced to the market and contains particles comprised of a carbon core and a polymer/nanodiamond shell. These application notes show the gradient separations of four essential oils (lavender, melaleuca, peppermint and eucalyptus), and the isocratic separations of various triazine herbicides and a mixture of β_2-agonists and amphetamines.

This dissertation contains the following sections. Chapter 1 is a review of liquid chromatographic history and theory. It also includes a history of the use of diamonds in liquid chromatography. Chapter 2 is a study on a glassy carbon core - polymer/nanodiamond shell particle made in our laboratory. Stability studies at pH 11.3 and 13 were performed and different analytes were retained and/or separated on the column. Chapter 3 is a study performed on the Flare mixed-mode column. Separations of tricyclic antidepressants, β_2-andrenergic receptor agonists, and linear chain alkylbenzenes were demonstrated with this phase. Van Deemter and van't Hoff studies were also performed to probe the efficiency and selectivity of this column with different classes of analytes. Chapter 4 chronicles, via SEM and van Deemter analysis, the improvements that have taken place in our column after many iterations of improved synthetic methods and new materials. These include better particle uniformity, particle stability, and column efficiency. Three different carbon cores were analyzed, each better than the previous one. Appendices 1 – 6 are application notes published by Diamond Analytics of β_2-andrenergic receptor agonists and amphetamines, triazine herbicides, and lavender, melaleuca, eucalyptus and peppermint essential oils. Appendices 7 and 8 are patents that contain ideas and research contributed by the author.

Keywords: diamond, reversed-phase chromatography, mixed-mode, scanning electron microscopy, liquid chromatography, elevated temperature chromatography, van't Hoff plots, van Deemter curves

ACKNOWLEDGEMENTS

I am grateful for the mentorship, insightful discussions, fascinating research opportunites and encouragement provided by Dr. Matthew R. Linford. I am thankful that I had the opportunity to work in his group. He provided many opportunities to present my research at conferences and to travel abroad where research and valuable networking could occur.

I appreciate the suggestions and support given from my committee members, Dr. Robert C. Davis, Dr. Steven L. Castle, Dr. Daniel E. Austin and Dr. Milton L. Lee who encouraged me to excel, but also focus on the basics.

I am grateful for all the members, undergraduates, and friends from the Linford group: Dr. Li Yang, Dr. Guarav Saini, Dr. Feng Zhang, Dr. Lei Pei, Dr. David S. Jensen, Nitesh Madaan, Chuan-Hsi Hung, Supriya S. Kanyal, Bhupinder Singh, Jon Strum, Katherine N. Biggs, Sarah Copland, Adam Larsen, Rachel Djurich, Loryn Killpack and James Christensen.

I thank Diamond Analytics, a US Synthetic company, for financial support throughout my graduate study tenure. I thank Andrew E. Dadson, Dr. Michael A. Vail, Andrew J. Miles, Trent Butcher, Daniel Law, Bob Smith and Brad Lee for their camaraderie and insight.

I thank the Department of Chemistry and Biochemistry at Brigham Young University for a stimulating work environment, excellent teaching opportunities and the facilities where I was able to perform the major part of my research.

Finally, I am grateful for the love and support of my family, personal friends, the Triad and especially my wife, Vanessa.

Table of Contents

LIST OF TABLES

LIST OF FIGURES

Chapter 1: Brief History of Chromatography, Chromatographic Theory and Diamond-Based Chromatography

1.1 Foundational Applications and Theory

Chromatography, which translates to "color writing," was named by Tswett, who used it to separate plant pigments like chlorophyll (green) and carotenoids (orange and yellow).[1-3] He used calcium carbonate as his stationary phase and petroleum ether as the mobile phase. His monumental studies were the first documented chromatographic separations. The initial theories of partition chromatography were later proposed in 1941 by Martin and Synge,[4] which earned them the Nobel Prize in Chemistry in 1952.

The work by Martin and Synge marked the first time silica gel had been used as a stationary phase/support that held water on its surface while an organic solvent flowed through the column. Analytes, such as amino acids and other organic compounds in wool, would partition between the stationary and mobile phases and elute individually. This work also established the use of the height equivalent of a theoretical plate (HETP) in chromatography. When this original theory was proposed, distillation columns, from which the theoretical plate concept had originated, had HETP efficiencies on the order of 1 cm. The initial columns created by Martin and Synge had HETPs of 20 μm.

When Martin and Synge published their theory of chromatography, they assumed, as did others, that chromatography was analogous to distillation in the way it purified or separated compounds. Their work was the first valid theory of chromatography. To simplify the equations supporting their theory, they had to assume that the diffusion of a solute from one 'plate' to another was negligible, and that at equilibrium the distribution ratio of a solute between the

mobile phase and the stationary phase was independent of concentration and the presence of other solutes.

From their observations, they recognized that HETP was dependent upon "factors controlling diffusion" and the flow rate of the mobile phase. According to their findings, the HETP was proportional to the flow rate of the mobile phase and the square of the particle diameter. They noted that efficiency increases (HETP decreases) as particle size decreases. Their theory also took into account the ability of the analyte to diffuse. If the analyte had a difficult time diffusing, e.g., a large protein, it would have a poorer efficiency than a smaller analyte.

When considering the limitations of their own theory, they recognized that (1) the partition coefficient is not usually constant, (2) peak asymmetry resulting from high solute concentration can be mitigated by lowering solute concentration, (3) interactions between analytes do occur and, according to their theory, can actually assist in the separation efficiency between two analytes and (4) a considerable loss in efficiency comes from a lack of uniform fluid flow through the column bed.

Giddings was also a significant figure in defining the theory and fundamentals of chromatography.[5-11] Much of his work focused on the fundamentals of gas chromatography,[12,13] and he pioneered field flow fractionation, which is a single phase separation technique.[14] Using his understanding of gas chromatography, he theorized that a thin film of stationary phase surrounding small particles packed in a small diameter column should improve the resolving power in liquid chromatography (LC).

1.2 Van Deemter Theory

In an effort to describe the effects of longitudinal diffusion and resistance to mass transfer on band broadening/plate height, van Deemter et al.,[15] and others,[16] derived equations that are known as van Deemter equations. The original form of the equation is as follows:

$$H = 2\lambda d_p + 2\gamma \frac{D_I}{u} + \frac{8}{\pi^2} \frac{KF_I u d_f^2}{(1+KF_I/F_{II})^2 D_{II} F_{II}} \quad (1.1)$$

where λ is the eddy diffusion factor, d_p is the particle diameter, γ is the labyrinth factor, D_I is the molecular diffusivity of the analyte in the mobile phase, D_{II} is its molecular diffusivity in the stationary phase, u is the linear velocity of the mobile phase, K is the distribution factor, F_I is the fractional volume of the mobile phase, F_{II} is the fractional volume of the stationary phase, and d_f is the effective liquid film thickness. The van Deemter equation is often written in the following form for packed columns:

$$H = 2\lambda d_p + \frac{2\gamma D_M}{u} + \left(\frac{\omega d_p^2}{D_M} + \frac{R d_f^2 \mu}{D_S}\right) u \quad (1.2)$$

where D_M is the diffusion coefficient of the analyte in the mobile phase, D_s is the diffusion coefficient of the analyte in the stationary phase, and ω and R are constants. The van Deemter equation has been further simplified to the following very familiar form:

$$H = A + B/u + Cu \quad (1.3)$$

where the A-term is the eddy diffusion term attributed to band broadening caused by multiple pathways, the B-term accounts for longitudinal diffusion, and the C-term is from broadening caused by resistance to mass transfer.

Another simplified form of the van Deemter equation separates the C-term into two components, rather than a single component as seen in Equation 1.3. This form takes into account the resistance to mass transfer in the stationary phase and the mobile phase as seen here:

$$H = A + \frac{B}{u} + (C_S + C_M)u \quad (1.4)$$

In this form, C_S is the resistance to mass transfer in the stationary phase and C_M is the resistance to mass transfer in the mobile phase. Each of these expressions can be explained as follows:

$$C_S \propto \frac{d_f^2}{D_s} \quad (1.5)$$

$$C_M \propto \frac{d_p^2}{D_M} \quad (1.6)$$

As it is, of course, desirable to have smaller plate heights, the smaller each term is in the van Deemter equation, the smaller *H* becomes, which results in an improved optimal efficiency. Simply put, poor packing and larger particle diameters increase the *A*-term. Extra time in the mobile phase as a result of lower linear velocity increases the *B*-term. Smaller analytes diffuse more readily than larger ones, also leading to an increased *B*-term. Higher flow rates along with greater stationary phase film thicknesses result in an increased *C*-term or more resistance to mass transfer. The *C*-term is also affected by the diffusion of solutes into and out of fully porous particles, i.e., it depends on d_p^2, hence the development of fused-core[17] or core-shell[18] particles that provide shorter flow paths and, consequently, smaller *C*-terms. One can find the best possible efficiency under a given set of conditions by performing a van Deemter analysis. This is done by measuring *H* for a range of linear velocities and thereafter working at the linear velocity at the van Deemter minimum (H_{min}) where efficiency is highest.

1.3 Peak Resolution

While efficiency is an important parameter that contributes to the usefulness of a column, other factors must be taken into account in a separation. That is, efficiency alone is insufficient to guarantee an acceptable separation, and sufficient resolution, *R*, must be present to allow critical

pairs of peaks (closely eluting analytes) to be separated. Knox, Said and Purnell have proposed different equations for calculating resolution.

The Knox Resolution Equation is:[19]

$$R_s = \sqrt{\frac{N}{16}} \cdot \frac{k_1}{1+k_2} \cdot \alpha - 1 \qquad (1.7)$$

The Exact Resolution Equation by Said is:[20]

$$R_s = \sqrt{\frac{N}{4}} \cdot \frac{k}{k+1} \cdot \frac{\alpha-1}{\alpha+1} \qquad (1.8)$$

And the Purnell Resolution Equation is:[21]

$$R_s = \sqrt{\frac{N}{16}} \cdot \frac{k_2}{k_2+1} \cdot \frac{\alpha-1}{\alpha} \qquad (1.9)$$

Where N is the number of theoretical plates for each analyte:

$$N = 5.545\left(\frac{t_r}{W_{1/2}}\right)^2 \qquad (1.10)$$

$$N = 16\left(\frac{t_r}{W}\right)^2 \qquad (1.11)$$

with W representing the full peak width at baseline, $W_{1/2}$ expressing the peak width at half height, and t_r equaling the solute retention time.

The capacity or retention factor, k, is given by:

$$k = \frac{t_r - t_m}{t_m} \qquad (1.12)$$

where t_m is the dead time or elution time for an unretained species. The selectivity factor, α, is defined as follows:

$$\alpha = \frac{k_2}{k_1} \qquad (1.13)$$

The Knox, Said and Purnell resolution equations give similar results – they share the same variables: number of plates, retention factor, and selectivity, with similar relationships between them. Of the three, the Knox equation gives the highest prediction of resolution while the Purnell equation provides the most conservative prediction and will be used here for the discussion of resolution in chromatography. When considering the same analytes, Said's "exact resolution equation" actually yields R_s values that are the averages of the Knox and Purnell results. For any of the three equations, peak widths are assumed to be identical and R_s must be greater than 1.5 for a critical pair to be considered completely resolved.

To separate a critical pair, it may be possible to manipulate N, k, and α in the resolution equations to produce the desired resolution.[22] Perhaps the easiest variable to change is k as one must only weaken the mobile phase to increase it. However, either very large or very small values of k are less than optimal. When k is small and the retention time approaches t_m, the middle term of the resolution equation approaches 0, which reduces the resolution to zero. On the other hand, as retention increases, k approaches its maximum possible value of 1. Accordingly, it is typically recommended that the retention factor range from 2 – 10, or at most from 2 – 20, because beyond these values, little improvement in resolution will be obtained as an analyte simply spends more time on the column, ineffectively increasing the separation time and increasing the analyte peak width.[23] Selectivity and efficiency will be discussed in greater detail in the following sections.

1.3.1 Leveraging Efficiency

In general, the best options available for increasing resolution by increasing the number of plates (efficiency) in a separation are (1) performing a van Deemter analysis to find the optimal flow rate, which as noted corresponds to optimal resolution for a given set of conditions, (2) changing the length of the column (efficiency is directly proportional to column length), or (3) decreasing the particle diameter. Options (2) and (3) result in greater system back pressures and/or a need for a different column. Clearly, however, there is a diminishing return in the effects of N in the resolution equation because resolution goes as $N^{1/2}$. Accordingly, efforts are sometimes more focused on changing selectivity to achieve a desired resolution. The effects of α will be discussed below and changing the selectivity can be an important way to improve resolution in a separation. In practice, other factors, such as solute concentration and peak tailing also affect the resolution of peaks.[22]

1.3.2 Responses and Consequences to the Need for Greater Efficiency

As the need for greater efficiency and faster analysis time has increased, particle sizes have decreased. These changes have followed the predictions of chromatographic theory.[24,25] For example, as noted above, if particle size decreases, the A-term also decreases, allowing for lower plate heights and increased efficiency. Particles now exist that are less than 2 µm in diameter, allowing for very fast, high resolution separations. Consequently, as the C-term also depends on particle diameter, d_p, these smaller diameter particles would also give better mass transfer over larger diameter particles.

However these advantages come at a price.[26] Smaller particles decrease the permeability of the particle bed, thereby increasing the column back pressure, which goes as $1/d_p^2$. This results

in increased stress on the pump and other instrument components. Accordingly, new instruments have been developed that can withstand pressures greater than 15 000 psi.[27-29] These elevated pressures can lead to frictional heating within beds of particles, which may lead to thermal gradients in the column that decrease separation efficiencies.[27,30,31]

decrease the *A*- and *C*-term*s*, resulting in lower plate heights, other types of particles with solid cores and porous shells, i.e., superficially porous particles,[32,33] have also been developed that can give similar efficiencies without causing as large an increase in column back pressure.

1.3.2.1 Pellicular, Fused-Core and Core-Shell Particles

Pellicular phases were first introduced by Horvath et al.[34] in 1967 as ion exchangers, and Kirkland introduced controlled surface porosity supports for HPLC two years later.[35] While these fused core, core-shell, or pellicular particles[34,36-40] have been used for many years, they never found the same mainstream adoption or usage as fully porous supports. In 1999, Knox[41] proposed that these "long neglected packings" could be used at higher flow rates because their thin porous shells could improve mass transfer. Superficially porous packings have now found mainstream acceptance since their revival in 2007.[17] Today, these particles have been accepted as high efficiency alternatives to the sub-2 μm fully porous particles.[42-44]

The impetus behind the superficially porous supports is the decrease in the *A*- and *C*-term*s* they offer. Typically, core-shell particles have greater particle uniformity than fully-porous supports resulting in less eddy diffusion. The *C*-term is reduced because the accessible diffusion paths are less in core-shell particles than for comparable fully porous particles, reducing the resistance to mass transfer. This allows for faster separations without as drastic a decrease in efficiency as is observed with fully porous particles at higher flow rates. Indeed, in many cases,

relatively flat van Deemter curves are obtained for core-shell particles, i.e., efficiencies do not decrease substantially with mobile phase velocity. When reduced plate heights of core-shell/fused core particles are compared to fully porous supports, core-shell particles typically have smaller reduced plate heights. [42,44-49]

1.3.3 Leveraging Selectivity with the Mobile Phase

While the relatively new core-shell particles have leveraged efficiency to attain better resolution, another important "lever" that can still be pulled to achieve baseline separations is selectivity. To affect a change in the selectivity factor, α, the retention times of the solutes must change relative to each other. This can often be accomplished by altering the mobile phase or changing the stationary phase, i.e., installing a column with a different selectivity. Changing the mobile phase is likely the easiest of these two options as tables exist that help one predict equivalent hydrophobicities between organic modifiers, allowing nearly the same retentions to be maintained between separations.[50] If acids or bases are being analyzed, changing the mobile phase pH,[51-53] buffers,[54] or buffer concentration,[55] or even altering the ionic strength of the mobile phase can also have profound effects on the selectivity of a separation.[52,53,56-58]

1.3.4 Changing the Selectivity by Changing the Stationary Phase

When changes to a mobile phase do not sufficiently improve a separation, a new column with a different selectivity may be used. Hundreds of different phases with different selectivities have been developed. Most of these have been created by functionalizing silica gel, which in its underivatized form is commonly used in flash chromatography for the purification of organic compounds and which alone has been used for gel permeation chromatography[59] and normal

phase HPLC.[60] With the need for different column selectivities, numerous alkyl phases, especially C_{18} (octadecyl silane, ODS), have been created on silica as reversed-phases.[61,62] Indeed, when reversed-phase chromatography was first developed in the 1950s[63,64] and began to be widely used in the 1970s,[62,65-71] debates arose as to whether the retention mechanism was based on partitioning or adsorption.[72] And while to some degree this debate continues, there is no question as to the usefulness of this phase. Interestingly, the many reversed-phase C_{18} columns now available from the different manufacturers often show quite different selectivities. Even silica itself comes in two different types: there is the Type-A silica,[73] which has more metal impurities, and the newer Type-B silica.[74-76] As expected, both these materials show different selectivities.

Other non-silica based supports[77] or packing materials such as zirconia,[78-91] porous graphitic carbon (PGC),[92-112] other metal oxides,[113,114] and carbon-based,[115-117] polymer-based,[118,119] and diamond-based[120-125] particles also exist and give unique selectivities and stabilities for a variety of LC separations. While each of these packing materials has its own unique characteristics, ODS is still used by the vast majority of chromatographers, as its selectivity is quite well known and it is remarkably effective in separating many diverse mixtures. Nevertheless, there have always been and continue to be mixtures that require selectivities beyond what C_{18} phases can offer.

1.4 Limitations of Reversed-Phases on SiO_2

Many types of compounds are separated using reversed-phase chromatography, yet certain classes, such as bases, still remain difficult to separate because of limitations[126] associated with silica as a phase support, i.e., there is still a need for improvements to C_{18}

stationary phase technology.[127] Bases, in particular, are better retained when they are neutral – at a pH about one pK_a unit above the pK_a values of their conjugate acids, which is around pH 10 or 11. However, elevated pH values challenge most silica-based phases – it is well known that silica has limited pH stability.[126] At lower pH values (ca. pH 2 or below) silane ligands hydrolyze from the silica support. At higher pH values (ca. pH 8 and above), the silica itself is etched. Another drawback of many columns is limited capacity or overloading, which leads to poor peak shape.[118,128,129]

1.4.1 Importance of Basic Analytes and Examples of Phase Stability Under Extreme pH Conditions

Because ca. 70% of all pharmaceuticals are bases,[130] and because liquid chromarography is an extremely important analytical technique for the pharmaceutical industries, this is an important class of compounds in separation science. If analyzed at lower pH values where they are protonated, these compounds may be separated by cation exchange chromatography.[37,131] Nevertheless, many still desire to use a reversed-phase mechanism. To meet this challenge,[130] different reversed phases have been considered, including organic/inorganic hybrid phases.[132-136] Hydrophilic interaction chromatography has also been considered as a method to separate these compounds.[137]

Hybrid organic/inorganic phases have drastically increased the pH stability of silica-based particles. These hybrid phases are made by replacing some of the tetraethoxysilane ($Si(OCH_2CH_3)_4$) used to make the particles with a silane containing either a methyl ($Si(OCH_2CH_3)_3CH_3$) or an ethylene group ($((CH_3CH_2O)_3SiCH_2CH_2Si(OCH_2CH_3)_3$). In many regards, they represent a great improvement in stability over traditional silica-based reversed

phases. Success in separating bases has been obtained with these columns, yet column manufacturers advise that temperatures above 80 °C not be exceeded when working at low pH, and temperatures above 60 °C not be used when operating under high pH conditions with bonded ethylene hybrid (BEH) columns. However, a high temperature stability study performed by Teutenberg et al. showed that a BEH column from Waters was virtually unaffected by 90:10 water/methanol at 150 °C for over 25 h.[138] Other studies also suggest that this column is stable up to 200 °C over extended periods of time.[139,140] Phases stable at low pH have also been developed on silica by hyper crosslinking chlorinated polymers onto a phenyl bonded silica surface via a Friedel-Crafts alkylation.[141-143] Further functionalization has given these materials reversed-phase selectivity and they have shown excellent stability under low pH, but not elevated pH, conditions.

1.5 Van't Hoff Equation

As temperature changes, thermodynamics influences a separation.[139,144-147] To quantitatively understand these effects, two classical definitions of the Gibbs free energy, ΔG°, are combined: the relationship between ΔG° and the equilibrium constant, *K*:

$$\Delta G^\circ = -RT\ lnK \qquad (1.14)$$

and the Gibbs-Holmholtz equation:

$$\Delta G^\circ = \Delta H^\circ - T\Delta S^\circ \qquad (1.15)$$

where ΔH° and ΔS° are the enthalpy and entropy of transfer of the analyte from the mobile phase to the stationary phase, respectively, and T is the absolute temperature. By setting the two equations equal to each other, the following equation is obtained:

$$-RT \ln K = \Delta H^\circ - T\Delta S^\circ \qquad (1.16)$$

Simplification of this expression results in:

$$\ln K = -\frac{\Delta H^\circ}{RT} + \frac{\Delta S^\circ}{R} \quad (1.17)$$

which is the classic van't Hoff equation. For this equation to be useful in chromatography, we use the following expression, which relates the equilibrium consant, *K*, to the retention factor, *k*:

$$K = \frac{k}{\Phi} \quad (1.18)$$

where Φ is the phase ratio. This substitution yields:

$$\ln \frac{k}{\Phi} = -\frac{\Delta H^\circ}{RT} + \frac{\Delta S^\circ}{R} \quad (1.19)$$

leading to the version of the van't Hoff equation that is in a form useful to chromatographers:

$$\ln k = -\frac{\Delta H^\circ}{RT} + \frac{\Delta S^\circ}{R} + ln\Phi \quad (1.20)$$

When ln *k* is plotted vs. 1/T, a linear relationship is often observed. Linear regression of the resulting line gives a slope (-Δ*H*°/*R*) from which ΔH° can be easily calculated. From the intercept (Δ*S*°/*R*+*lnΦ*), ΔS° can be found if the phase ratio is known (often it is not). To better understand the selectivity of a column for a given class of analytes, a homologous series of the analytes can be injected at different temperatures and Δ*H*° and Δ*S*° calculated.[144,145]

1.6 Elevated/High Temperature Chromatography

Depending on the types of analytes, temperature[69,71,144,148-152] can have an effect on the selectivity[153-156] and efficiency[157] of a separation. Increased temperature is often used to increase the speed of a separation[158] as it increases the effect of the entropy term in Equation 1.15.[147,159] Furthermore, it changes the static permitivity of the mobile phase – water effectively becomes less polar with increasing temperature.[160] That is, increased temperatures causes mobile phases to behave similarly to unheated mobile phases with more organic modifier. The effect of

temperature, however, on basic analytes is rather unexpected.[161,162] A study performed by McCalley[161] found that increasing temperatures actually *increase* the retention of basic analytes at pH 3 and 7, rather than decrease them.

Similar to mobile phase gradients, temperature gradients can also be used in liquid chromatography.[163,164] Indeed, as suggested above, the effect of temperature on water is so drastic that water alone can be used as a stationary phase at elevated temperature[157,165,166] because its static permittivity is similar to that of methanol at elevated temperatures. Separations of anticancer drugs have been performed by Teutenberg et al.[165] and Yang et al.[157] using FID detection from a water-only mobile phase at elevated temperature. Obviously, water-only separations are very environmentally friendly. However, high temperature water can be quite corrosive, so proper columns, fittings, and other hardware should be employed. Well-designed column ovens and narrow columns can help to limit thermal gradient and thermal equilibration issues, especially when thermal programming is employed.

As elevated temperatures can damage particles, stability tests have been performed on numerous phases to validate them.[138,139,167,168] Column instability at high temperatures is generally associated with one of two issues: (1) the mobile phase can react more readily with the particles, perhaps hydrolyzing silane ligands or dissolving the support, and (2) thermal expansion and contraction of the column housing and packed particle bed occurs as temperatures increase and decrease, often resulting in an increasingly poorly packed column. This results in an increased *A*-term and decreased column efficiency.

1.7 Diamond-Based Chromatography

As has been demonstrated, numerous chromatographic phases and columns exist. And while reversed phases and supports have been developed that exhibit either outstanding pH or thermal stability, only the BEH phase (XBridge, Waters, Bedford, MA) shows stability under extremes of both pH and temperature. Research in the Linford group at BYU has focused on the development of a diamond/carbon-based column that can withstand both kinds of stresses, and that show unique selectivity compared to silica-based C_{18} columns. We believe that diamond and carbon-based materials might be the key to a column with excellent durability.

The first mention of the use of diamonds in chromatography was by Telepchak.[169] He claimed that natural diamonds should be an excellent reversed-phase chromatographic material as they are inert – according to his understanding, they are terminated in hydrogen and, therefore, very hydrophobic. Columns packed with diamond particles in his study showed a plate height of 660 μm. While a column packed with natural diamonds could be cost prohibitive, synthetic diamonds are much more affordable. These diamonds show heterogeneous surfaces[170] with many different oxygen-containing moieties, e.g., hydroxyl, carbonyl, carboxyl, and epoxide groups. These diamonds, when left unreacted, are not well suited for reversed-phase separations, but might be used in different types of chromatography.

Fedyanina et al.[120] and Nesterenko et al.[121,171,172] separated different classes of compounds using microdispersed sintered detonation nanodiamonds (MSDNs). Fedyanina separated benzoic acids on MSDNs in water/methanol mobile phases and noticed that the retention mechanism depended on the dissociation constant of the tested solutes. Nesterenko performed ion exchange and normal phase chromatography using MSDNs with varying degrees

of success. He achieved efficiencies of 45,300 N/m (plates/m), which at the time was a significant leap forward in the efficiency of diamond-based chromatographic materials.

1.8 Contributions of the Linford Group to Diamond-Based Chromatography

The Linford group saw diamonds as an excellent candidate for a chromatographic support because they exhibit excellent chemical inertness and thermal conductivity. The first steps taken by the Linford group were to discover how to functionalize the diamond surface. Its natural inertness made these studies challenging. Accordingly, the first attempts to functionalize the diamond surface were performed by Saini, Linford, and coworkers.[173] The diamond surface was cleaned with piranha solution to expose its oxidized surface and then coated with a primary amine-containing polymer: poly(allylamine) (PAAm). This surface was cured at 115 °C under vacuum or chemically crosslinked with 1,2,5,6-diepoxycyclooctane. The PAAm-coated diamond was then used as a solid-phase extraction (SPE) medium. Lipid extractions were demonstrated and the particles showed excellent stability from pH 1 to 14 for many hours as evidenced by little or no loss of the N1s peak in x-ray photoelectron spectroscopy (XPS). SPE cartridges packed with this material showed excellent recovery of the extracted analytes. However, as the material had no porosity, analyte capacity was low.

The next study performed by Saini, Wiest, Linford et al.[174] showed the first development of a reversed-phase on diamond via the reaction of PAAm-coated diamonds with hydrophobic, long alkyl chain isocyanate ligands. This isocyanate chemistry bonded alkyl chains to the surfaces through robust urea linkages. Octyl isocyanate, octadecyl isocyanate, and heptadecafluoro isocyanate were reacted with the PAAm surface to create hydrophobic phases for SPE. These reactions were monitored by diffuse reflectance infrared Fourier transform

(DRIFT) spectroscopy and XPS. SPE cartridges made with these diamond particles still had limited capacity (14.5 μg, diazinon), but exhibited high recoveries of the analytes tested.

Yang, Linford, and coworkers[175] attempted to functionalize the diamond surface by treating hydrogen- or deuterium-terminated nanodiamond with di-*tert*-amyl peroxide, styrene, and divinylbenzene (DVB) to create a polystyrene coated/encapsulated diamond material. The surface was then sulfonated by exposure to sulfuric acid. Both DVB-coated diamond and sulfonated DVB-coated diamond particles were used as SPE sorbents. These were also tested under basic conditions and showed excellent stability.

In an effort to form a diamond-based stationary phase with sufficient capacity and efficiency to be used as an HPLC phase, Saini, Wiest, Linford, and coworkers[176] developed diamond core-shell particles by coating irregular (non-spherical) PAAm-coated, micron-sized diamond particles with nanodiamond. These particles were then coated again with PAAm and recoated with nanodiamond so as to increase the porous shell thickness of the support. After 28 bilayers of this layer-by-layer process, the particles were crosslinked with a cyclic diepoxide to add structural stability to the support. These particles were used as both SPE and HPLC sorbents. As more bilayers of PAAm and nanodiamond were added to the core particles, the analyte capacity of the particles increased in SPE. When used as an HPLC sorbent, Saini could successfully separate mixtures of benzophenone and nitrobenzene with this relatively hydrophilic phase. Another more hydrophobic phase treated with 1,2-epoxyoctadecane allowed the separation of a mixture of benzene, toluene, xylene, and mesitylene (36,300 N/m, k = 2.62) and also cyanazine and diazinon (54,800 N/m, k = 1.76). All of these separations occurred with triethylamine (TEA) as an additive to deprotonate the amine-containing surface. The crosslinked

material showed excellent stability, but the core-shell particles treated with only 1,2-epoxyoctadecane were not mechanically stable as they were not crosslinked.

As our original core-shell particles for HPLC were formed with irregular diamond cores, our next step was to build particles from spherical cores to improve the *A*-term. To this end, zirconia was used as the core material as it is known to be chemically inert and could be obtained commercially in spherical form. The 2 μm spherical zirconia particles so obtained from ZirChrom were first etched in hot, aqueous sodium hydroxide overnight. This treatment exposed the oxide to which PAAm was applied. These PAAm-terminated zirconia particles were then treated in an alternating fashion with nanodiamond and PAAm to build up ca. 0.5 μm shells (28 nanodiamond/PAAm bilayers). The growth of these particles was monitored by SEM. When the electron accelerating voltage was set at 30 keV, contrast became apparent between the carbon-based shell and the zirconia core because of the higher atomic number of the zirconium. To further confirm the shell thickness, the particles were ion milled using a focused Ga^+ ion beam, after which their cross sections were analyzed. After the layer-by-layer deposition, the particles were functionalized with a C_{18} ligand using 1,2-epoxyoctadecane and then packed into a 4.6 mm × 30 mm column. Separations were performed using an alkylbenzene test mixture. The analytes showed good peak symmetry in the resulting chromatograms and the mesitylene peak showed an efficiency of 41,700 N/m (k = 8.16). Similar to our previous C_{18} phases, this phase had a short lifetime and degraded rapidly with use, as evidenced by decreasing retention times. SEM also showed that the nanodiamond/polymer shells had been damaged after use, suggesting mechanical instability. (For further information see Chapter 4.)

Zirconia proved to be cost prohibitive as a core material, so a different spherical material was sought. Fortunately, Supelco donated some glassy carbon spherical carbon particles to us.

The same PAAm/nanodiamond bilayer deposition was then performed on these particles. However, their final functionalization was altered slightly. To give greater mechanical stability to the particles, a diepoxide crosslinker was added to the 1,2-epoxyoctadecane in a 1:20 ratio. The resulting particles were then packed in 4.6 mm × 30 mm columns, which were found to be much more stable than the previous columns of uncrosslinked, reversed-phase particles. These particles also withstood high pH mobile phases and showed little to no degradation at pH 11.3 or even pH 13 over 2,600 column volumes. Van Deemter curves of this material showed high *C*-terms. These van Deemter studies, along with SEM and light scattering/particle size distribution (PSD) measurements showed that particle agglomerates were present.

To improve the PSD, some particles were sieved and others were sonicated after each bilayer deposition. These particles were then sieved after the desired shell thickness had been achieved (ca. 30 bilayers). PSDs were determined by taking PAAm-coated particles and measuring them in a light scatting PSD instrument. The more uniform the particle PSD became, the lower the *C*-terms in the corresponding columns, which suggested that the distance the solutes needed to diffuse had been lowered, i.e., lower resistance to mass transfer. The material without sonication showed an optimal efficiency of 56,000 (k = 1.70) – 71,000 N/m (k = 13.4), however on a UHPLC system, where a specialized "sandwich" injection was performed, efficiencies of 120,000 N/m (k = 2.04) were achieved. These were the best efficiencies we have obtained with a diamond-based column, however an exotic injection method was used to decrease band broadening. Other analytes could also be retained on the column, including amitriptyline, diazepam, cholesterol, diazinon and various phenols. (For further information see Chapter 2.)

Further analysis of the carbon core particles from Supelco revealed that they were not the nonporous cores we had originally believed them to be. As their PSD was not ideal either, we decided to develop our own uniform, dense carbon cores. Hung et al.[177] from our group were able to achieve this by first synthesizing polydivinylbenzene spheres poly(DVB). These were then oxidized, carbonized, and acid treated to allow adhesion of PAAm to their surfaces. Bilayer deposition of PAAm and nanodiamond with sonication was done as previously reported by Wiest et al.[178] These particles showed a much tighter PSD than the Supelco cores, along with a good d_{90}/d_{10} indicating that they were fairly uniform. Particles created with these cores showed better efficiencies than the previous material. To further improve on this approach, commercial polydivinylbenzene particles were obtained and treated identically to the ones made in our lab. This yielded material with an even narrower PSD and d_{90}/d_{10} than we had previously created. Scanning electron microscopy also showed evidence for uniform particles.

BET isotherm measurements of the carbonized core particles showed that these particles had formed small pores ($\leq$ 25 Å), giving them a high surface area. After PAAm/nanodiamond bilayer deposition, the surface area decreased to ca. 15 m^2/g, indicating that the polymer had filled the pores or at least made the inner pores inaccessible. Efficiencies for these particles were typically 90,000 – 100,000 N/m for *normal* injections, where the highest efficiency observed was 112,000 N/m under these conditions (hexylbenzene, *k* ca. 4.5). Column to column reproducibility within a batch was shown (see Chapter 4) along with high temperature stability studies (see Chapter 3). Longer columns (2.1 mm × 50 mm) were packed with the same optimized core material, and separations of lavender, peppermint, eucalyptus and melaleuca essential oils, were obtained via gradient elution (see Appendices 3 – 6).

To better understand the optimized column, tricyclic antidepressants (TCAs) and alkylbenzenes were separated at pH 7 and 12. The selectivity of the column appeared to be independent of pH when alkylbenzenes were used as the analytes; however, selectivity changed drastically for the TCAs. At pH 7 the peaks tailed and retention factors were low. At pH 12, peak tailing was reduced and these analytes were well retained (see Chapter 3).

Van Deemter and van't Hoff analyses were performed with optimized columns, which showed that basic analytes had lower optimal linear velocities than the alkylbenzenes, along with larger *C*-terms. The van't Hoff analysis also showed that there was a greater change in slope at what appears to be a phase transition in the column (60 °C) for the basic analytes compared to the alkylbenzenes. This is attributed to hydrogen bonding that may occur with the TCAs at lower temperatures, whereas at higher temperatures, the hydrogen bonding between the analyte and the mobile/stationary phases is disrupted, resulting in more interaction with the stationary phase as evidenced by the increase in $\Delta H°$ but a less favorable change entropy $\Delta S°$. This was the first comparative pH study on our column with different analyte classes. The column showed good stability at elevated pH over two weeks of nearly continuous use. However, after repeated van't Hoff studies, it appears that the expansion and contraction of the column housing and particle bed affected the packing efficiency. Accordingly, the *A*-term increased and efficiency decreased, but selectivity and retention were not drastically changed. (For more information see Chapter 3.)

Many application notes have been developed for this diamond-based phase suggesting that it has mixed-mode character. While we had attempted to form a pure C_{18} phase, it appears that the amine-containing backbone of the PAAm gave the phase weak anion exchange selectivity at low pH and reversed-phase (C_{18}) selectivity at high pH. We had believed at first that the amines would be largely inaccessible; however, we have now performed anion exchange

separations of acidic herbicides at low pH that suggest that this column exhibits mixed-mode character.

I wrote application notes on the separation of melaleuca, peppermint, eucalyptus and lavender essential oils, along with separations of amino acid methyl esters, triazine herbicides, β_2 andrenergic receptor agonists and amphetamines (see Appendices 1 – 6). My experience has also allowed me to contribute ideas to licensed patents as an inventor (see Appendices 7 and 8).

1.9 Conclusions

Modern chromatography began over a century ago and, since that time, great advances have occurred. Silica-based phases (normal and reversed-phase) along with many other stationary phases have been developed over the history of chromatography. As chromatographic science has advanced and required more efficient separations with greater peak resolution, many different functionalities with a variety of selectivities have been incorporated into stationary phases in an attempt to achieve desired separations.

A common challenge has been the separation of basic analytes, requiring phase stability at high pH. Temperature also appears to an important factor in chromatographic separations. Our desire was to develop a column that would have a reversed-phase selectivity and be able to operate with little to no degradation under extreme pH and high temperature conditions. We chose diamond as our stationary phase support with an inert spherical carbon core. We have made great advances over the past years as evidenced in the following chapters.

1.10 References

(1) Tswett, M. S. *Otdelenie Biologii* **1905**, *14*, 20.

(2) Tswett, M. S. *Ber. Deut. Bot. Ges.* **1906**, *24*, 384.

(3) Tswett, M. S. *Ber. Deut. Bot. Ges.* **1906**, *24*, 316.

(4) Martin, A. J.; Synge, R. L. *Biochem. J.* **1941**, *35*, 1358.

(5) Giddings, J. C. *J. Chem. Phys.* **1959**, *31*, 1462.

(6) Giddings, J. C. *Nature* **1959**, *184*, 357.

(7) Giddings, J. C. *Anal. Chem.* **1963**, *35*, 1999.

(8) Giddings, J. C. *Anal. Chem.* **1963**, *35*, 2215.

(9) Giddings, J. C.; Eyring, H. *J. Phys. Chem.* **1955**, *59*, 416.

(10) Giddings, J. C. *Anal. Chem.* **1964**, *36*, 1890.

(11) Giddings, J. C. *Anal. Chem.* **1965**, *37*, 60.

(12) Giddings, J. C.; Myers, M. N.; King, J. W. *J. Chromatogr. Sci.* **1969**, *7*, 276.

(13) Giddings, J. C.; Seager, S. L.; Stucki, L. R.; Stewart, G. H. *Anal. Chem.* **1960**, *32*, 867.

(14) Giddings, J. C. *Science* **1993**, *260*, 1456.

(15) van Deemter, J. J.; Zuiderweg, F. J.; Klinkenberg, A. *Chem. Eng. Sci.* **1956**, *5*, 271.

(16) Lee, M. *Fundamentals of Analytical Separations*; Brigham Young University: Provo, UT, 2010.

(17) Kirkland, J. J.; Langlois, T. J.; DeStefano, J. J. *Am. Lab.* **2007**, *39*, 18.

(18) Gritti, F.; Leonardis, I.; Abia, J.; Guiochon, G. *J. Chromatogr. A* **2010**, *1217*, 3819.

(19) Knox, J. H.; Saleem, M. *J. Chromatogr. Sci.* **1969**, *7*, 614.

(20) Said, A. S. *J. High Res. Chromatog.* **1979**, *2*, 193.

(21) Purnell, J. H. *J. Am. Chem. Soc.* **1960**, *0*, 1268.

(22) Dolan, J. W. *LC GC N. Am.* **2002**, *20*, 430.

(23) Snyder, L. R.; Kirklan, J. J.; Dolan, J. W. *Introduction to Modern Liquid Chromatography*; , Inc.John Wiley & Sons: Hoboken, New Jersey, 2010.

(24) Kirkland, J. J. *J. Chromatogr. Sci.* **2000**, *38*, 535.

(25) Yoshida, T.; Majors, R. E. *J. Sep. Sci.* **2006**, *29*, 2421.

(26) McCalley, D. V. *J. Chromatogr. A* **2011**, *1218*, 2887.

(27) Nguyen, D. T. T.; Guillarme, D.; Rudaz, S.; Veuthey, J. L. *J. Sep. Sci.* **2006**, *29*, 1836.

(28) Swartz, M. E. *J. Liq. Chromatogr. Relat. Technol.* **2005**, 28, 1253.

(29) Wren, S. A. C. *J. Pharm. Biomed. Anal.* **2005**, *38*, 337.

(30) Gritti, F.; Guiochon, G. *Chem. Eng. Sci.* **2010**, *65*, 6310.

(31) Fallas, M. M.; Hadley, M. R.; McCalley, D. V. *J. Chromatogr. A* **2009**, *1216*, 3961.

(32) Kirkland, J. J. *Anal. Chem.* **1992**, *64*, 1239.

(33) McCalley, D. V. *J. Chromatogr. A* **2008**, *1193*, 85.

(34) Horvath, C. G.; Preiss, B. A.; Lipsky, S. R. *Anal. Chem.* **1967**, *39*, 1422.

(35) Kirkland, J. J. *Analytical Chemistry* **1969**, *41*, 218.

(36) Horvath, C.; Lipsky, S. R. *Anal. Chem.* **1969**, *41*, 1227.

(37) Horvath, C. G.; Lipsky, S. R. *Anal. Chem.* **1969**, *41*, 1227.

(38) Kaczmarski, K.; Guiochon, G. *Anal. Chem.* **2007**, *79*, 4648.

(39) Kalghatgi, K. *J. Chromatogr.* **1990**, *499*, 267.

(40) Varady, L.; Kalghatgi, K.; Horvath, C. *J. Chromatogr.* **1988**, *458*, 207.

(41) Knox, J. H. *J. Chromatogr. A* **1999**, *831*, 3.

(42) Abrahim, A.; Al-Sayah, M.; Skrdla, P.; Bereznitski, Y.; Chen, Y. D.; Wu, N. J. *J. Pharm. Biomed. Anal.* **2010**, *51*, 131.

(43) Cunliffe, J. M.; Maloney, T. D. *J. Sep. Sci.* **2007**, *30*, 3104.

(44) Salisbury, J. J. *J. Chromatogr. Sci.* **2008**, *46*, 883.

(45) Gritti, F.; Cavazzini, A.; Marchetti, N.; Guiochon, G. *J. Chromatogr. A* **2007**, *1157*, 289.

(46) Guiochon, G.; Gritti, F. *J. Chromatogr. A* **2011**, *1218*, 1915.

(47) DeStefano, J. J.; Langlois, T. J.; Kirkland, J. J. *J. Chromatogr. Sci.* **2008**, *46*, 254.

(48) MacNair, J. E.; Lewis, K. C.; Jorgenson, J. W. *Anal. Chem.* **1997**, *69*, 983.

(49) MacNair, J. E.; Patel, K. D.; Jorgenson, J. W. *Anal. Chem.* **1999**, *71*, 700.

(50) Rafferty, J. L.; Siepmann, J. I.; Schure, M. R. *J. Chromatogr. A* **2011**, *1218*, 2203.

(51) Gritti, F.; Guiochon, G. *J. Chromatogr. A* **2004**, *1041*, 63.

(52) Ho, J. W. *LC GC N. Am.* **1989**, 7, 348.

(53) Young, P. M.; Astephen, N. E.; Wheat, T. E. *LC GC N. Am.* **1992**, *10*, 26.

(54) McCalley, D. V. *J. Chromatogr. A* **2004**, *1038*, 77.

(55) Claessens, H. A.; van Straten, M. A.; Kirkland, J. J. *J. Chromatogr. A* **1996**, *728*, 259.

(56) Davies, N. H.; Euerby, M. R.; McCalley, D. V. *J. Chromatogr. A* **2006**, *1119*, 11.

(57) Stella, C.; Rudaz, S.; Mottaz, M.; Carrupt, P.-A.; Veuthey, J.-L. *J. Sep. Sci.* **2004**, *27*, 284.

(58) Huang, H. S.; Wu, J. R.; Chen, M. L. *J. Chromatogr.-Biomed. Appl.* **1991**, *564*, 195.

(59) De Vries, A. J.; LePage, M.; Beau, R.; Guillemin, C. L. *Anal. Chem.* **1967**, *39*, 935.

(60) Kirkland, J. J.; Dilks Jr, C. H.; DeStefano, J. J. *J. Chromatogr. A* **1993**, *635*, 19.

(61) Sander, L. C.; Wise, S. A.; Lochmüller, C. H. *C R C Critical Reviews in Analytical Chemistry* **1987**, *18*, 299.

(62) Horvath, C. *Trend Anal. Chem.* **1981**, 1, 6.

(63) Partridge, S. M.; Swain, T. *Nature* **1950**, *166*, 272.

(64) Partridge, M. W.; Chilton, J. *Nature* **1951**, *167*, 79.

(65) Molnar, I.; Horvath, C. *Clin. Chem.* **1976**, *22*, 1497.

(66) Horvath, C.; Melander, W. *Am. Lab.* **1978**, *10*, 17.

(67) Roumeliotis, P.; Unger, K. K. *J. Chromatogr., A* **1978**, *149*, 211.

(68) Horvath, C.; Melander, W.; Nahum, A. *J. Chromatogr.* **1979**, *186*, 371.

(69) Melander, W. R.; Chen, B. K.; Horvath, C. *J. Chromatogr.* **1979**, *185*, 99.

(70) Melander, W. R.; Stoveken, J.; Horvath, C. *J. Chromatogr.* **1979**, *185*, 111.

(71) Melander, W. R.; Nahum, A.; Horvath, C. *J. Chromatogr.* **1979**, *185*, 129.

(72) Vailaya, A.; Horvath, C. *J. Chromatogr. A* **1998**, *829*, 1.

(73) Gilroy, J. J.; Dolan, J. W.; Carr, P. W.; Snyder, L. R. *J. Chromatogr. A* **2004**, *1026*, 77.

(74) Hill, D. W.; Kind, A. J. *J. Liq. Chromatogr.* **1993**, *16*, 3941.

(75) Gilroy, J. J.; Dolan, J. W.; Snyder, L. R. *J. Chromatogr. A* **2003**, *1000*, 757.

(76) Köhler, J.; Kirkland, J. J. *J. Chromatogr. A* **1987**, *385*, 125.

(77) Forgacs, E.; Cserhati, T. *Advances in Chromatography, Vol 40* **2000**, *40*, 359.

(78) Dai, J.; Yang, X. Q.; Carr, P. W. *J. Chromatogr. A* **2003**, *1005*, 63.

(79) Dunlap, C. J.; McNeff, C. V.; Stoll, D.; Carr, P. W. *Anal. Chem.* **2001**, *73*, 598A.

(80) Hu, Y.; Yang, X. Q.; Carr, P. W. *J. Chromatogr. A* **2002**, *968*, 17.

(81) Jackson, P. T.; Carr, P. W. *J. Chromatogr. A* **2002**, *958*, 121.

(82) Li, J. W.; Carr, P. W. *Anal. Chim. Acta* **1996**, *334*, 239.

(83) Li, J. W.; Carr, P. W. *Anal. Chem.* **1996**, *68*, 2857.

(84) Li, J. W.; Carr, P. W. *Anal. Chem.* **1997**, *69*, 2193.

(85) Reeder, D. H.; Li, J. W.; Carr, P. W.; Flickinger, M. C.; McCormick, A. V. *J. Chromatogr. A* **1997**, *760*, 71.

(86) Rigney, M. P.; Weber, T. P.; Carr, P. W. *J. Chromatogr.* **1989**, *484*, 273.

(87) Sarkar, S.; Carr, P. W.; McNeff, C. V.; Subramanian, A. *J. Chromatogr. B* **2003**, *790*, 143.

(88) Xiang, Y. Q.; Yan, B. W.; McNeff, C. V.; Carr, P. W.; Lee, M. L. *J. Chromatogr. A* **2003**, *1002*, 71.

(89) Yan, B. W.; McNeff, C. V.; Carr, P. W.; McCormick, A. V. *J. Am. Ceram. Soc.* **2005**, *88*, 707.

(90) Sun, L. F.; Carr, P. W. *Anal. Chem.* **1995**, *67*, 3717.

(91) Sun, L. F.; McCormick, A. V.; Carr, P. W. *J. Chromatogr. A* **1994**, *658*, 465.

(92) Barrett, D. A.; Pawula, M.; Knaggs, R. D.; Shaw, P. N. *Chromatographia* **1998**, *47*, 667.

(93) Elfakir, C.; Lafosse, M. *J. Chromatogr. A* **1997**, *782*, 191.

(94) Hennion, M. C.; Coquart, V.; Guenu, S.; Sella, C. *J. Chromatogr. A* **1995**, *712*, 287.

(95) Jensen, D. S.; Gupta, V.; Olsen, R. E.; Miller, A. T.; Davis, R. C.; Ess, D. H.; Zhu, Z. H.; Vail, M. A.; Dadson, A. E.; Linford, M. R. *J. Chromatogr. A* **2011**, *1218*, 8362.

(96) Jensen, D. S.; Wiest, L. A.; Vail, M. A.; Dadson, A.; Linford, M. R. *Abstr. Pap. Am. Chem. Soc.* **2009**, *237*, 338.

(97) Kaur, B. *LC GC-Mag. Sep. Sci.* **1990**, *8*, 468.

(98) Knox, J. H.; Kaur, B.; Millward, G. R. *J. Chromatogr.* **1986**, *352*, 3.

(99) Koimur, M.; Lu, B.; Westerlund, D. *Chromatographia* **1996**, *43*, 254.

(100) Lepont, C.; Gunatillaka, A. D.; Poole, C. F. *Analyst* **2001**, *126*, 1318.

(101) Mama, J. E.; Fell, A. F.; Clark, B. J. *Anal. Proc.* **1989**, *26*, 71.

(102) Pereira, L. *LC GC N. Am.* **2006**, 75.

(103) Pereira, L. J. Liq. Chromatogr. Relat. Technol. **2008**, 31, 1687.

(104) Ross, P. *LC GC N. Am.* **2000**, *18*, 14.

(105) Viron, C.; Andre, P.; Dreux, M.; Lafosse, M. *Chromatographia* **1999**, *49*, 137.

(106) Wan, Q. H.; Davies, M. C.; Shaw, P. N.; Barrett, D. A. *Anal. Chem.* **1996**, *68*, 437.

(107) Wan, Q. H.; Shaw, P. N.; Davies, M. C.; Barrett, D. A. *J. Chromatogr. A* **1995**, *697*, 219.

(108) West, C.; Elfakir, C.; Lafosse, M. *J. Chromatogr. A* **2010**, *1217*, 3201.

(109) Zhang, Y. N.; McGuffin, V. L. *J. Liq. Chromatogr. Relat. Technol.* **2007**, *30*, 1551.

(110) Monser, L.; Darghouth, F. *J. Pharm. Biomed. Anal.* **2003**, *32*, 1087.

(111) Monser, L. I.; Greenway, G. M. *Anal. Chim. Acta* **1996**, *322*, 63.

(112) Nazir, T.; Gould, L. A.; Marriott, C.; Martin, G. P.; Brown, M. B. *J. Pharm. Pharmacol.* **1997**, *49*, 90.

(113) Nawrocki, J.; Dunlap, C.; Li, J.; Zhao, J.; McNeff, C. V.; McCormick, A.; Carr, P. W. *J. Chromatogr. A* **2004**, *1028*, 31.

(114) Nawrocki, J.; Dunlap, C.; McCormick, A.; Carr, P. W. *J. Chromatogr. A* **2004**, *1028*, 1.

(115) Knox, J. H.; Ross, P. *Advances in Chromatography,* Brown, P. R., Grushka, E., Eds.; Marcel Dekker: New York, 1997; Vol. 37, p 73.

(116) Ross, P.; Knox, J. H. *Advances in Chromatography,* Brown, P. R., Grushka, E., Eds.; Marcel Dekker: New York, 1997; Vol. 37, p 121.

(117) Leboda, R.; Lodyga, A.; Charmas, B. *Mater. Chem. Phys.* **1998**, *55*, 1.

(118) Buckenmaier, S. M. C.; McCalley, D. V.; Euerby, M. R. *Anal. Chem.* **2002**, *74*, 4672.

(119) McCalley, D. V. *J. Chromatogr. A* **2005**, *1073*, 137.

(120) Fedyanina, O. N.; Nesterenko, P. N. *Russ. J. Phys. Ch.* **2011**, *85*, 1773.

(121) Nesterenko, P.; Haddad, P. *Anal. Bioanal. Chem.* **2010**, *396*, 205.

(122) Nesterenko, P. N.; Fedyanina, O. N. *J. Chromatogr. A* **2010**, *1217*, 498.

(123) Nesterenko, P. N.; Fedyanina, O. N.; Volgin, Y. V.; Jones, P. *J. Chromatogr. A* **2007**, *1155*, 2.

(124) Saini, G.; Jensen, D. S.; Wiest, L. A.; Vail, M. A.; Dadson, A.; Lee, M. L.; Shutthanandan, V.; Linford, M. R. *Anal. Chem.* **2010**, *82*, 4448.

(125) Wiest, L. A.; Jensen, D. S.; Hung, C.-H.; Olsen, R. E.; Davis, R. C.; Vail, M. A.; Dadson, A. E.; Nesterenko, P. N.; Linford, M. R. *Anal. Chem.* **2011**, *83*, 5488.

(126) Wehrli, A.; Hildenbrand, J. C.; Keller, H. P.; Stampfli, R.; Frei, R. W. *J. Chromatogr., A* **1978**, *149*, 199.

(127) Jackson, P. T.; Carr, P. W. *Chemtech* **1998**, *28*, 29.

(128) Davies, N. H.; Euerby, M. R.; McCalley, D. V. *J. Chromatogr. A* **2006**, *1119*, 11.

(129) Gritti, F.; Perdu, C.; Guiochon, G. *J. Chromatogr. A* **2008**, *1180*, 73.

(130) McCalley, D. V. *J. Chromatogr., A* **2010**, *1217*, 858.

(131) Davies, N. H.; Euerby, M. R.; McCalley, D. V. *J. Chromatogr. A* **2007**, *1138*, 65.

(132) Davies, N. H.; Euerby, M. R.; McCalley, D. V. *J. Chromatogr. A* **2008**, *1178*, 71.

(133) Wyndham, K.; Walter, T.; Iraneta, P.; Alden, B.; Bouvier, E.; Hudalla, C.; Lawrence, N.; Walsh, D. *LC GC Europe* **2012**, 15.

(134) Wyndham, K.; Lawrence, N.; Glose, K.; Cook, J.; Walsh, D.; Brousmiche, D.; Iraneta, P.; Alden, B.; Boissel, C.; Walter, T. *Polym. Prepr. Am. Chem. Soc., Div. Polym. Chem.* **2007**, *48*, 278.

(135) O'Gara, J. E.; Wyndham, K. D. *J. Liq. Chromatogr. R. T.* **2006**, 29, 1025.

(136) Wyndham, K. D.; O'Gara, J. E.; Walter, T. H.; Glose, K. H.; Lawrence, N. L.; Alden, B. A.; Izzo, G. S.; Hudalla, C. J.; Iraneta, P. C. *Anal. Chem.* **2003**, *75*, 6781.

(137) McCalley, D. V. *J. Chromatogr. A* **2010**, *1217*, 3408.

(138) Teutenberg, T.; Hollebekkers, K.; Wiese, S.; Boergers, A. *J. Sep. Sci.* **2009**, *32*, 1262.

(139) Liu, Y.; Grinberg, N.; Thompson, K. C.; Wenslow, R. M.; Neue, U. D.; Morrison, D.; Walter, T. H.; O'Gara, J. E.; Wyndham, K. D. *Anal. Chim. Acta* **2005**, *554*, 144.

(140) Shen, S.; Lee, H.; McCaffrey, J.; Yee, N.; Senanayake, C.; Grinberg, N.; Clark, J. *J. Liq. Chromatogr. R. T.* **2006**, *29*, 2823.

(141) Zhang, Y.; Luo, H.; Carr, P. W. *J. Chromatogr. A* **2012**, *1228*, 110.

(142) Luo, H.; Ma, L. J.; Zhang, Y.; Carr, P. W. *J. Chromatogr. A* **2008**, *1182*, 41.

(143) Ma, L. J.; Luo, H.; Dai, J.; Carr, P. W. *J. Chromatogr. A* **2006**, *1114*, 21.

(144) Andersen, S.; Birdi, K. *Surfactants and Macromolecules: Self-Assembly at Interfaces and in Bulk*; Lindman, B., Rosenholm, J., Stenius, P., Eds.; Springer Berlin / Heidelberg: 1990; Vol. 82, p 52.

(145) Chester, T. L.; Coym, J. W. *J. Chromatogr., A* **2003**, *1003*, 101.

(146) Gritti, F.; Guiochon, G. *Anal. Chem.* **2006**, *78*, 4642.

(147) Jensen, D. S.; Teutenbere, T.; Clark, J.; Linford, M. R. *LC GC N. Am.* **2012**, *30*, 992.

(148) Dolan, J. W. *LC GC North Am.* **2002**, *20*, 524.

(149) Guillarme, D.; Heinisch, S.; Rocca, J. L. *J. Chromatogr., A* **2004**, *1052*, 39.

(150) Teutenberg, T. *Chromatography Today* **2010**, *3*, 3.

(151) Teutenberg, T. High-Temperature Liquid Chromatography: A User's Guide for Method Development; RSC: London, 2010.

(152) Wenclawiak, B. W.; Giegold, S.; Teutenberg, T. *Anal. Lett.* **2008**, *41*, 1097.

(153) Buckenmaier, S. M. C.; McCalley, D. V.; Euerby, M. R. *J. Chromatogr. A* **2004**, *1060*, 117.

(154) Dolan, J. W.; Snyder, L. R.; Blanc, T.; Van Heukelem, L. *J. Chromatogr. A* **2000**, *897*, 37.

(155) Dolan, J. W. *J. Chromatogr. A* **2002**, *965*, 195.

(156) Li, J. W.; Carr, P. W. *Anal. Chem.* **1997**, *69*, 2202.

(157) Teutenberg, T. *Anal. Chim. Acta* **2009**, *643*, 1.

(158) Antia, F. D.; Horváth, C. *J. Chromatogr. A* **1988**, *435*, 1.

(159) Jensen, D. S.; Teutenberg, T.; Clark, J.; Linford, M. R. *LC GC N. Am.* **2012**, *30*, 1052.

(160) Teutenberg, T.; Wiese, S.; Wagner, P.; Gmehling, J. *J. Chromatogr. A* **2009**, *1216*, 8480.

(161) McCalley, D. V. *J. Chromatogr. A* **2000**, *902*, 311.

(162) Vervoort, R. J. M.; Ruyter, E.; Debets, A. J. J.; Claessens, H. A.; Cramers, C. A.; de Jong, G. J. *J. Chromatogr. A* **2002**, *964*, 67.

(163) Greibrokk, T.; Andersen, T. *J. Sep. Sci.* **2001**, *24*, 899.

(164) Godin, J.-P.; Hopfgartner, G. r.; Fay, L. *Anal. Chem.* **2008**, *80*, 7144.

(165) Teutenberg, T.; Lerch, O.; Gotze, H. J.; Zinn, P. *Anal. Chem.* **2001**, *73*, 3896.

(166) Yang, Y.; Kondo, T.; Kennedy, T. J. *J. Chromatogr. Sci.* **2005**, *43*, 518.

(167) Teutenberg, T.; Tuerk, J.; Hozhauser, M.; Giegold, S. *J. Sep. Sci.* **2007**, *30*, 1101.

(168) Haun, J.; Oeste, K.; Teutenberg, T.; Schmidt, T. C. *J. Chromatogr. A* **2012**, *1263*, 99.

(169) Telepchak, M. J. *Chromatographia* **1973**, *6*, 234.

(170) Jee, A.-Y.; Lee, M. *Curr. Appl. Phys.* **2009**, *9*, e144.

(171) Nesterenko, P. N.; Fedyanina, O. N. *J. Chromatogr. A* **2010**, *1217*, 498.

(172) Nesterenko, P. N.; Fedyanina, O. N.; Volgin, Y. V.; Jones, P. *J. Chromatogr. A* **2007**, *1155*, 2.

(173) Saini, G.; Yang, L.; Lee, M. L.; Dadson, A.; Vail, M. A.; Linford, M. R. *Anal. Chem.* **2008**, *80*, 6253.

(174) Saini, G.; Wiest, L. A.; Herbert, D.; Biggs, K. N.; Dadson, A.; Vail, M. A.; Linford, M. R. *J. Chromatogr. A* **2009**, *1216*, 3587.

(175) Yang, L.; Vail, M. A.; Dadson, A.; Lee, M. L.; Asplund, M. C.; Linford, M. R. *Chem. Mater.* **2009**, *21*, 4359.

(176) Saini, G.; Jensen, D. S.; Wiest, L. A.; Vail, M. A.; Dadson, A.; Lee, M. L.; Shutthanandan, V.; Linford, M. R. *Anal. Chem.* **2010**, *82*, 4448.

(177) Hung, C.-H.; Wiest, L. A.; Singh, B.; Diwan, A.; Valentim, M. J. C.; Christensen, J. M.; Davis, R. C.; Miles, A. J.; Jensen, D. S.; Vail, M. A.; Dadson, A. E.; Linford, M. R. *Submitted to J. Sep. Sci.* 2013.

(178) Wiest, L. A.; Jensen, D. S.; Hung, C.-H.; Olsen, R. E.; Davis, R. C.; Vail, M. A.; Dadson, A. E.; Nesterenko, P. N.; Linford, M. R. *Anal. Chem.* **2011**, *83*, 5488.

Chapter 2: Pellicular Particles with Spherical Carbon Cores and Porous Nanodiamond/Polymer Shells for Reversed-Phase HPLC*

2.1. Abstract

A new stationary phase for reversed-phase high performance liquid chromatography (RP HPLC) was created by coating spherical 3 μm carbon core particles in a layer-by-layer (LbL) fashion with poly(allylamine) (PAAm) and nanodiamond. Unfunctionalized core carbon particles were characterized by scanning electron microscopy (SEM), x-ray photoelectron spectroscopy (XPS), time-of-flight secondary ion mass spectrometry (ToF-SIMS), and Raman spectroscopy. After LbL of PAAm and nanodiamond, which yields ca. 4 μm core-shell particles, the particles were simultaneously functionalized and cross-linked using a mixture of 1,2-epoxyoctadecane and 1,2,7,8-diepoxyoctane to obtain a mechanically stable C_{18}/C_8 bonded outer layer. Core-shell particles were characterized by SEM, and their surface area, pore diameter, and volume were determined using the Brunauer-Emmett-Teller (BET) method. Short stainless steel columns (30 mm × 4.6 mm ID) were packed and the corresponding van Deemter plots obtained. The retention characteristics of a suite of analytes were investigated using a conventional HPLC system at various organic solvent compositions, pH values of mobile phases, and column temperatures. At 60 °C, a chromatogram of 2,6-diisopropylphenol showed 71,500 plates/m (N/m) (k = 13.4). The possibility of using this composite stationary phase at extreme pH of mobile phase was studied. Chromatograms obtained under acidic conditions (pH 2.7) of a mixture of acetaminophen, diazepam, and 2,6-diisopropylphenol, and a mixture of phenol, 4-methylphenol, 2-chlorophenol, 4-chlorophenol, 4-bromophenol and 1-tert-butyl-4-methylphenol are presented. Retention times

of amitriptyline, cholesterol, and diazinon at temperatures ranging from 35 °C to 80 °C and at pH 11.3 are reported. A series of five basic drugs was also separated at this pH. The stationary phase exhibits considerable hydrolytic stability at high pH (11.3) and even pH 13 over extended periods of time. An analysis made using a UHPLC system with a "sandwich" injection appeared to reduce extra column band broadening and gave best efficiencies of 110,000 – 120,000 N/m (k = 2.04).

2.2. Introduction

Silica is the workhorse of modern liquid chromatography.[1-2] Accordingly, its surface has been extensively studied and modified, which has led to a broad array of available functionalities for the chromatographer.[3] However, despite its flexibility, common silica-based stationary phases lack stability at both high and low pH, where the useful window of pH stability for a typical bonded phase lies between ca. 2 and 8.[4-5] A number of researchers have investigated ways to improve the stability of silica, especially for reversed-phase (RP) HPLC. For example, it has been known for decades that increasing the length of the *n*-alkyl chain in alkylsilica bonded phases or endcapping residual silanols with trimethylchlorosilane or hexamethyldisilazane can improve the hydrolytic stability of bonded phases.[6] A further improvement in the hydrolytic stability of alkylsilicas can be achieved using trichloroalkylsilanes instead of monochlorodimethylalkylsilanes.[4,7] Immobilization of trichloroalkylsilanes on silica in the presence of water causes polycondensation and formation of polymeric layers of good stability, although additional silanols are created during polymerization.[8] Kirkland et al. used sterically protected monofunctional silanes to increase the hydrolytic stability of alkyl bonded phases in highly acidic mobile phases.[3-4] Sagliano and coworkers studied the effect of silane structure on resistance to acid hydrolysis and reported higher stabilities for silanes with bulky or long chain alkyl groups.[9]

Kirkland, Glajch and Farlee disclosed the concept of bidentate silanes of the form $XR_2Si–B–SiR_2X$, where –X is a reactive group such as –Cl or –OMe and –B– is a bridging group of variable nature and length, e.g., it may be an ethylene ($–CH_2CH_2–$) moiety or an oxygen atom, and R is a methyl, *n*-butyl, *n*-octyl or *n*-octadecyl group.[4,10] Their C_{18}/C_{18} bidentate silane with a

propylene bridge as a bonded phase had a very low rate of hydrolysis in mobile phases at both low (0.9) and high (≥11) pH.[10-11]

Another possible improvement in the hydrolytic stability of silica particles is polymer shielding or cross-linking of bonded groups. Kobayashi and coworkers treated octyltrichlorosilane modified silica with a cyclic siloxane monomer, effectively endcapping the bonded phase with a siloxane polymer to improve its stability.[12] Carr and coworkers chemisorbed (chloromethyl)phenylethyltrichlorosilane ($ClCH_2C_6H_4CH_2CH_2SiCl_3$) onto silica and then crosslinked it via Friedel-Crafts alkylation to itself and to a styrene heptamer or triphenylmethane.[13] When it was found that this phase was overly silanophilic compared to a steric-protected C_{18} phase, i.e., it had too many residual silanols that were leading to peak tailing of basic analytes, a monolayer of a monofunctional silane, $ClCH_2C_6H_4CH_2CH_2Si(CH_3)_2Cl$, was deposited, which was then similarly crosslinked with the styrene heptamer. While this assembly was not more stable than the layer prepared with the trifunctional silane ($ClCH_2C_6H_4CH_2CH_2SiCl_3$), it could be further crosslinked and then modified with C_8 groups, also via Friedel-Crafts alkylation, to produce an extremely stable phase. This material showed substantially lower silanophilicity than before; the peak shapes in the resulting separations of basic drugs were at least as good as those obtained using a steric-protected C_{18} phase.[14]

The work cited above focuses on improvements in the low pH stability of bonded phases on silica. An approach for the improvement of the hydrolytic stability of hydrophobic column packings at higher pH values is based on the synthesis of various inorganic-organic hybrid materials. For example, a group at Waters Corporation (Milford, MA) first formed particles by condensing methyltriethoxysilane, $Si(OCH_2CH_3)_3CH_3$, and tetraethoxysilane, $Si(OCH_2CH_3)_4$ (TEOS), which placed methyl groups within and at the surfaces of the particles.[15] These first

generation hybrid particles comprise the companies' XTerra product line. They can be functionalized with C_8 and C_{18} silanes, and show reduced tailing of basic analytes, consistent with a reduction of silanol quantity and activity. A further advance from this group came by the use of silanes with bridging alkyl groups, e.g., $(CH_3O)_3SiCH_2CH_2Si(OCH_3)_3$, which is the basis of their bridged ethyl hybrid technology in their XBridge and ACQUITY product lines.[16-17] Columns packed with the resulting particles were stable for 140 hours at 50 °C in a pH 10 triethylamine-containing mobile phase.[17]

A similar series of inorganic-organic hybrid stationary phases was produced by Phenomenex (Torrance, CA) under the trade name Gemini. Gemini particles consist of a traditional silica core surrounded by an inorganic-organic layer, similar to that of the Waters XTerra particles. Their TWIN-NX technology uses ethylene bridged silanes, like those in Waters' XBridge and ACQUITY products. The temperature and pH-stabilities of the Gemini C_{18}, Gemini C_{18} NX, and XBridge C_{18} columns were recently compared. The Gemini C_{18} column was substantially less stable than the Gemini C_{18} NX, which in turn was less stable than the XBridge C_{18}.[18] In general, the prolonged stability of inorganic-organic hybrid stationary phases in mobile phases at pH 10.0–10.5 has been demonstrated.

Clearly notable advances have been made with regards to creating stable, effective, silica-based materials. However, Teutenberg and coworkers recently compared the stabilities of a series of commercially available columns that are advertized as highly stable and concluded that: "Although some progress has been made to increase the stability of packing materials at very high and low pH, further improvements of silica-based stationary phases regarding dissolution at high temperatures still is a challenge."[18] It appears that a considerable need remains for future innovation.

A significant motivation for creating HPLC stationary phases/supports that are stable at high pH also exists in the pharmaceutical industry. McCalley and coworkers[19-20] expressed the difficulty of separating basic compounds under reversed-phase conditions because these analytes usually exist in their protonated states under the pH conditions appropriate for most silica-based columns. (Protonated species are typically less retained under reversed-phase conditions than the corresponding unprotonated ones.[21]) Thus, high pH values (at least high enough to deprotonate amines) would be advantageous in such separations. McCalley further observes that of all pharmaceutical compounds, 70% are bases.[19] Because the pK_a values of most amines are ca. 9.5 to 11, and at least in aqueous solutions, the pH must be at least one pH unit above the pK_a value of an acidic moiety for ca. 90% or more of these groups to be deprotonated, there is a strong need for a chromatographic material that can withstand a pH where the basic groups on analytes would be largely or even entirely deprotonated. (Note that in this work when we mention the "pK_a of an amine", we are, technically speaking, referring to the pK_a of the conjugate acid of that amine.)

Because of the considerable need to create highly stable stationary phases, other, non-siliceous materials have also been studied. Some of these supports, which include organic polymers, zirconia, titania, alumina, and porous graphitic carbon (PGC), are usually stable over a wide pH range, but sometimes lack efficiency.[22-26] Carr and coworkers developed polymer coated or encapsulated zirconia as both hydrophilic (normal-phase HPLC) and hydrophobic (reversed-phase HPLC) stationary phases,[27-30] where these materials also have stability over a wide pH range.[24,31-32] However, due to Lewis acid sites on the zirconia surface, undesirable secondary interactions occur with certain analytes.[33-35] These specific interactions with analytes bearing carboxylic and phosphonic acid functional groups, in conjunction with the difficulty

associated with functionalizing the zirconia surface,[30] help explain why zirconia-based supports/phases have not become more mainstream products.

PGC is an important material that has been marketed commercially since 1988 by more than one firm, *e.g.*, Hypercarb™ by Thermo Scientific.[36-37] PGC is stable at extreme pH values and also elevated temperatures, although its selectivity is very different from standard reversed phases and noticeable tailing is observed with many analytes. While these differences/limitations have prevented it from being more widely adopted, there is currently a great deal of interest in this material because of its stability and unique selectivity to hydrophilic compounds.

Diamond has also been studied as a support/stationary phase in liquid chromatography.[38] For example, Nesterenko and coworkers employed sintered, microdispersed detonation nanodiamond for normal phase separations[39] and ion exchange chromatography.[40] They performed baseline separations of various compounds using their normal phase material and achieved 15,400 plates/m (N/m) (*o*-xylene, k = 4.31). Their peaks showed considerable asymmetry, especially at longer retention times. In more recent work they have achieved 45,300 N/m (*m*-diisopropylbenzene, k = 2.29).[41]

Work in the Linford group at Brigham Young University has focused on the chemical modification of diamond and its subsequent use in solid phase extraction (SPE) and HPLC. Their first separations were performed on poly(allylamine) (PAAm)-coated 50–70 μm diamond particles,[42-43] where SPE of lipids was demonstrated. It was later shown that various alkyl and a perfluoroalkyl isocyanate would react with the PAAm-coated diamond, forming urea linkages between the isocyanate and PAAm.[44] SPE of pesticides from water was performed on the resulting C_{18} phase. Deuterium-terminated diamond (DTD),[45] was also shown to react with di-*tert*-amyl peroxide, and it could be further functionalized with polymers by radical

polymerization.[46] The resulting diamond materials could be used for SPE. In general, these materials were stable under extreme pH conditions.[43-44]

In spite of these advances, the nonporous particles employed in these earlier studies would probably not be suitable for HPLC. Hence, pellicular particles[47] were formed by coating irregularly shaped ca. 1.7 μm diamond particles with bilayers of PAAm and nanodiamond in a layer-by-layer (LbL) fashion.[48] These PAAm-coated core-shell particles were then reacted with 1,2-epoxyoctadecane, creating a hydrophobic phase, where the C–N bond produced during the reaction between an amine and an epoxide is very resistant to hydrolysis at both low and high pH. This stationary phase was able to separate pesticides (cyanazine and diazinon) and various alkyl benzenes. An efficiency of 54,800 N/m (k = 1.76) was obtained with diazinon, which was a solid improvement over previous diamond-based materials. Unfortunately, after an extended period of time, the material began to degrade. Another PAAm/nanodiamond pellicular phase, this time cross-linked/functionalized with 1,2,5,6-diepoxycyclooctane, was then prepared, and this material showed considerably improved stability, albeit lower efficiencies. However, even with this improved stability, back pressures were high for all of the particles made with irregular diamond particles.

While this earlier work was a step forward, a variety of issues needed to be addressed. First, it would be important to find a spherical, inert support to serve as the core for these particles, where this material would need to be amenable to functionalization via LbL chemistry. A spherical core would also be important because irregular diamond particles would be expected to have a significant negative impact on the eddy diffusion and flow distribution component in peak broadening (A term in the van Deemter equation) and give a higher back pressure. In addition, it was imperative to find a way to stabilize this hydrophobic phase with some sort of

cross-linker so that these phases would be mechanically stable over a longer period of time, but without a loss of efficiency.

In this work, we address these and other issues, showing the development of a new type of stationary phase created by coating spherical, 3 μm carbon particles with layers of PAAm and nanodiamond. The two types of stationary phases described herein were both hydrophobic (C_{18}), but one phase was also cross-linked. As expected, the non-cross-linked phase showed low mechanical stability, but the cross-linked material showed good stability over an extended period of time and at high pH. Particular improvements over our last study[48] include:

1. The use of spherical carbon particles as cores instead of irregular diamond particles.

2. Efficiencies for these new core-shell particles that are higher than those for the previous particles, in spite of the fact that the new particles are larger.

3. The use of two epoxides (a monofunctional epoxide and a bifunctional epoxide) in the functionalization/cross-linking of the PAAm/nanodiamond layers, where the monofunctional epoxide provides C_{18} chains and the bifunctional epoxide provides cross-linking.

4. A demonstration that these new particles are hydrolytically stable for prolonged periods of time in both alkaline mobile phases – at pH 11.3 and even pH 13, and in acidic mobile phases – at pH 2.7.

5. Reduced column back pressures, i.e., higher possible flow rates, which allows, for the first time in our work on diamond-containing pellicular particles, acquisition of complete van Deemter curves in a suitable range of flow rates. An analysis of these curves is presented.

6. Reproducible/repeatable pressure-flow curves.

7. A demonstration that by appropriate particle preparation, relatively tight particle size distributions can be obtained, which translates into the improved mass transfer and expected flattening of the van Deemter curves at increasing flow rates.

8. Separation of many different analytes on a conventional HPLC, including the alkyl benzenes, a series of basic drugs, and various phenols, at either pH 2.7 or pH 11.3. Indeed, more than 70,000 N/m (k = 13.4) were obtained for 2,6-diisopropylphenol at 60 °C under acidic conditions. A "sandwich" injection on a UHPLC system yielded 110,000 – 120,000 N/m (k = 0.66 – 2.0) for three low molecular weight analytes.

2.3. Experimental

2.3.1. Reagents and Materials

Table 2.1 gives the chemicals and materials used to create and test the phases in this work.

Table 2.1 Chemicals and materials used in Chapter 2.

Chemical Name	CAS No	Manufacturer	Location	Purity
Acetaminophen	103-90-2	Sigma-Aldrich	St. Louis, MO	BioXtra, ≥ 99.0 %
Acetonitrile	75-05-8	EMD	Gibbstown, NJ	HPLC grade
Amitriptyline hydrochloride	549-10-8	Restek	St. Louis, MO	≥ 98%
Benzenoid Hydrocarbon Kit		Supelco	St. Louis, MO	Varied by analyte
4-Bromophenol	106-41-2	Sigma-Aldrich	St. Louis, MO	99%
2-*tert*-Butyl-4-methylphenol	2409-55-4	Sigma-Aldrich	St. Louis, MO	99%
2-Chlorophenol	95-57-8	Sigma-Aldrich	St. Louis, MO	98%
4-Chlorophenol	106-48-9	Sigma-Aldrich	St. Louis, MO	≥99%
Cholesterol	57-88-5	Sigma-Aldrich	St. Louis, MO	Approx. 95%
Clomipramine	303-49-1	Sigma-Aldrich	St. Louis, MO	≥ 98%
Cyclohexanol	109-93-0	Fisher Scientific	Fair Lawn, NJ	Reagent grade
Diazepam	439-14-5	Sigma-Aldrich	St. Louis, MO	98%
Diazinon	333-41-5	Fluka	Steinheim, Germany	Pestanal, analytical standard
1,2,7,8-Diepoxyoctane	2426-07-5	Sigma-Aldrich	St. Louis, MO	97%
2,6-Diisopropylphenol	2078-54-8	SAFC Supply Solutions	St. Louis, MO	97+%
Doxepin hydrochloride	1229-29-4	Sigma-Aldrich	St. Louis, MO	
1,2-Epoxyoctadecane	7390-81-0	Alfa Aesar	Ward Hill, MA	Technical Grade, 90%
Imipramine	50-49-7	Sigma-Aldrich	St. Louis, MO	BioXtra, ≥ 99.0 %
Isopropyl alcohol	67-63-0	Mallinkrodt Baker Inc.	Phillipsburg, NJ	ChromAR
Methanol	67-56-1	Fisher Scientific	Fair Lawn, NJ	HPLC grade
4-Methylphenol	106-44-5	Supelco	St. Louis, MO	Analytical standard
Nanodiamond		Advanced Abrasives Corp.	Pannsauken, NJ	8.32 wt. %, 0-100 nm
Phenol	108-95-2	Sigma-Aldrich	St. Louis, MO	~ 99%
Poly(allylamine), avg. 17,000 M_w	30551-89-4	Sigma-Aldrich	St. Louis, MO	20 wt. % in water
Poly(allylamine), avg. 65,000 M_w	30551-89-4	Sigma-Aldrich	St. Louis, MO	20 wt. % in water
Spherical glassy carbon, 3 μm mean size		Supelco	St. Louis, MO	Prototype material, not commercially available.
Tetramethylammonium hydroxide	75-59-2	Sigma-Aldrich	St. Louis, MO	24 wt. % solution in water
Triethylamine	121-44-8	Mallinkrodt Baker Inc.	Phillipsburg, NJ	99.50%
Triton X-100	9002-93-1	Fisher Scientific	Fair Lawn, NJ	Electrophoresis grade
Water	7732-18-5	From a Millipore system	Billerica, MA	18 MΩ Res. (Milli-Q System)
Xylenes	1330-20-7	Mallinkrodt Baker Inc.	Phillipsburg, NJ	ACS grade

Empty stainless steel HPLC columns (30 mm × 4.6 mm ID with 0.5 μm frits) were obtained from Restek, Bellefonte, PA, and 50 mL centrifuge tubes were from Sarstedt, Newton, NC. All analyte solutions were prepared by mixing ca. 20 μL of an analyte in 15 mL of acetonitrile.

2.3.2. Instrumentation

Our HPLC system consisted of a dual wavelength detector (Model No. 2487), a binary HPLC pump (Model No. 1525), and a column oven (Model Number 5CH) all from Waters Corporation, Milford MA. The LC system was run using the Breeze software, Version 3.3. To calculate efficiencies, the software measured the full width at half maximum (FWHM) of a peak and employed the equation, $N = 5.54(R_t/W_{1/2})^2$. Separations performed at the University of Tasmania were done using a Waters Alliance HPLC. A dual wavelength detector (Model No. 2487) was used for detection and the pump, autosampler, and column oven were all part of a 2695 Separations Module. The system was run using Empower, Version 2 software and efficiencies were calculated using the FWHM method. Columns were packed using a Pack-in-a-Box 10,000-psi pump (Chrom Tech, Inc., Apple Valley, MN). All separations were performed under isocratic conditions. For the high and low pH separations, the pH of the water was set to 11.3 by addition of 0.1% (v/v) triethylamine, 13.0 by addition of tetramethylammonium hydroxide, or 2.7 by addition of formic acid. Analytes were injected using a 20 μL sample loop. Samples for SEM (Philips XL30 ESEM FEG, FEI Corporation, Hillboro, OR) were prepared by placing a slurry of particles directly on a stub and then drying the samples in an oven. Imaging was done under high-vacuum conditions with a spot size of 3. (This is an arbitrary number commonly used in SEM that has no units. This number represents the size of the aperture that allows electrons through for imaging.) Specific surface areas of the samples were determined

from N_2 adsorption at 77 K using a TriStar II, (Micromeritics Instrument Corporation, Norcross, GA). The samples were degassed at 200 °C for 12 hours prior to data collection. Particle size distribution measurements were obtained with an LS 13 320 Multi-Wavelength Particle Size Analyzer (Beckman Coulter, Inc., Brea, CA) by placing drops of a suspension of particles in an analysis bath. X-ray photoelectron spectroscopy (XPS) was performed with an SSX-100 instrument from Surface Sciences (maintained by Service Physics in Bend, OR) using an Al Kα source and a hemispherical analyzer. An electron flood gun was employed for charge compensation, and this charge compensation was further enhanced with a fine Ni mesh approximately 0.5 – 1.0 mm above the surface of the sample. Survey scans, as well as narrow scans, were recorded with an 800 μm × 800 μm spot. Carbon powders were mounted onto double-sided tape adhered to silicon wafers for XPS analysis. Static time-of-flight secondary ion mass spectrometry (ToF-SIMS) was performed on an ION TOF IV instrument (Münster, Germany) with a 25 keV Ga^+ source and a 200 μm × 200 μm sample area. For ToF-SIMS analysis, the carbon powders were mounted onto double-sided tape adhered to silicon wafers. Raman spectroscopy was performed on a Chromex Raman 2000 instrument (Billerica, MA) with a 532 nm laser, the CCD was cooled to -40˚C, and the slit width was set at 100 μm. Raman spectra were obtained using conventional methods; loose powder was placed in a sample vessel and analyzed.

2.3.3 Particle Preparation

Particles were prepared using a layer-by-layer (LbL) procedure that was similar to that performed by Saini *et al.* on diamond core particles.[48] About 0.5 g of spherical, carbon particles, 3 μm in diameter, were suspended in 40 mL of a 1:1 water/methanol (H_2O/MeOH) mixture

containing 3.3 mL of a 65,000 M_w poly(allylamine) (PAAm) solution, as obtained from the vendor. The particles were stirred for 24 h in this solution. The particles were then placed in a 50 mL screw cap plastic centrifuge tube, centrifuged at 5,000 rpm and rinsed three times with the 1:1 H_2O/MeOH solution. Nanodiamond (1.5 mL of a 8.32 wt. % slurry) was then added to the PAAm coated particles that were suspended in ca. 40 mL of the rinse solution. The solution with the partially coated particles and nanodiamond was shaken by hand for 5 min and allowed to settle for 1 min. It was then centrifuged and rinsed twice with the 1:1 H_2O/MeOH mixture to remove excess nanodiamond from the particles. To these particles, now coated with a layer of PAAm and nanodiamond, were added 1.5 mL of a 7.5 wt % aqueous solution of PAAm (17,000 M_w). The particles were again agitated by hand for five min and allowed to settle for 1 min. Excess PAAm was removed by centrifuging the particles and rinsing three times with the same H_2O/MeOH mixture. Deposition of nanodiamond (8.32 wt. % slurry) and PAAm (17,000 M_w) was subsequently performed in alternating steps until the desired thickness of the porous shell was reached, terminating in a PAAm coating. To clarify, 60 discrete depositions were performed to form the polymer-nanodiamond shell; to create a particle with a 0.5 μm shell, 30 bilayers were deposited. Deposition occurred in a similar manner to that observed by Saini in his work.[48] There appeared to be an induction period in which the surface was only partially covered, after which deposition appeared to proceed with greater regularity. The thickness was measured periodically during particle growth by scanning electron microscopy.

2.3.4 Particle Optimization

In an effort to improve the particle size distribution, two other batches of particles were prepared. One batch of core particles was sonicated after the initial PAAm deposition, but prior

to nanodiamond deposition, using a Sonifier Cell Disruptor (Heat Systems Co., Model: W1850, Melville, N.Y.). The particles were sonicated in 1 min intervals until they had been sonicated for a total of 5 min. Sonication was performed with the particles in the centrifuge tube that would later be used for deposition. In between sonications, the centrifuge tube was immersed in ice water for a minute to prevent overheating of the sample. Other than this initial sonication, the particles were functionalized, cross-linked, and tested in the same manner as the previous batch of cross-linked particles. This resulted in particles with an improved particle size distribution (PSD) over the previous, non-sonicated batch.

Another batch of particles was prepared where sonication was performed after every PAAm deposition until the desired shell thickness was reached. Otherwise, these particles were prepared in the same manner as the previous batches. This approach yielded the tightest PSD of the three preparation methods. Compared to the uncoated particles, in all of the particle syntheses a significant increase in the mass and volume of the particles was observed after the LbL depositions.

2.3.5 Particle Functionalization

Core-shell particles made through deposition of 30 PAAm/nanodiamond bilayers, and terminated with a PAAm coating, were rinsed three times in isopropanol and three times in 1:1 cyclohexanol/xylenes. The particles were then placed in ca. 15 g of the cyclohexanol/xylenes solution to which functionalizing agents were added. To prepare a non-crosslinked phase, 10 wt. % of 1,2-epoxyoctadecane was added. This was reacted with the particles in a round bottom flask, which was fitted with a water-cooled condenser and heated to 130 °C for 54 h. For the crosslinked phase, both 10 wt. % of 1,2-epoxyoctadecane and 0.5 wt. % of 1,2,7,8-

diepoxyoctane were added, i.e., a 20:1 ratio by weight of functionalizing ligand to crosslinker. The diepoxide served as the crosslinker. The reaction conditions were the same in the preparation of the crosslinked and the non-crosslinked particles.

The reaction mixtures were allowed to cool to room temperature. Excess functionalizing reagent was removed by rinsing and centrifuging three times with the cyclohexanol/xylenes solution, three times with isopropanol, and three times with a 1% (v/v) aqueous solution of Triton X-100.

2.3.6 Particle Sieving

After particle functionalization, the particle size distribution was measured. In the non-sonicated material, there were ca. 100 μm agglomerates, so the particles, in an aqueous solution of Triton X-100 (1% v/v), which worked as a dispersant, were passed through a 40 μm sieve, which removed most of the larger agglomerates. Although improved, the particle size distribution was still far from uniform (see Figure 2.1 A). After sieving, the particles were concentrated by centrifugation.

2.3.7 Column Packing

Packing was performed by suspending the particles in 12 mL of an aqueous solution of Triton X-100 (1% v/v). The Triton solution was also used as the pushing solution during packing. The slurry was poured into the packing chamber which had a 30 mm × 4.6 mm ID column attached at its end. The maximum packing pressure was set at 7,000 psi (8,500 psi for the improved, sonicated particles). Packing occurred over a 25 min period and the pressure was released gradually over a 30 min period.

Another column (50 mm × 4.6 mm ID) was packed at the University of Tasmania using a a pump from Haskel (Burbank, CA). The particles were suspended in isopropanol and packed at 8,000 psi until 25 mL of packing solvent had passed through the column. An insufficient volume of particles was used on the first attempt, so the column was repacked with a mixture of new and previously packed 4 μm particles. This second attempt was successful.

2.3.8 Stability Tests

Two stability tests were performed using the crosslinked material. The first was run under the following conditions: flow rate: 0.5 mL/min, mobile phase composition: 40:60 H_2O/ACN with 0.1% (v/v) triethylamine in the aqueous portion of the mobile phase to set the pH at 11.3, temperature: 35.0 °C. The test occurred over 1,600 column volumes. A stability test at pH 13.0 was then performed on this column. The mobile phase was 40:60 H_2O/ACN, with 1% (v/v) of the tetramethylammonium hydroxide solution (see Table 2.1) in the aqueous component to raise the pH to 13. The column temperature was 35.0 °C. The test occurred over 1,000 column volumes. The analytes used for these tests were from a benzenoid hydrocarbon kit and included benzene, ethylbenzene, *n*-butylbenzene and *n*-hexylbenzene. After the stability tests, the HPLC system was flushed sufficiently with ACN or MeOH and water to remove the corrosive material that might damage the pump and/or detector flow cell. After use, the columns were also flushed with the same mobile phase and stored under MeOH between uses.

2.3.9. UHPLC and Sandwich Injection

A UHPLC system, Agilent Infinity 1290, with a diode array detector (Model No. G4212A, detection at 254 nm), an LC pump (Model No. G4220A), a column oven (Model No.

G1316C), and an autosampler (Model No. G4226A) were used. This system was run with Chem Station Software, version B.04.03, and measurement of the FWHM by the software was used to calculate efficiencies. A "sandwich" injection on this system was performed using a mixture of alkyl benzenes. To wit, a 5 µL sample of an alkylbenzene analyte mixture was injected between 7 µL volumes of water onto our 4 µm particle-packed column at 80 °C using a pH 11.3 mobile phase, with a flow rate of 1.0 mL/min.

2.4. Results and Discussion

2.4.1. Characterization of Core Particles and the LbL Process

The glassy carbon core particles, which are not commercially available and are a prototype material, were characterized by scanning electron microscopy (SEM), x-ray photoelectron spectroscopy (XPS), time-of-flight secondary ion mass spectrometry (ToF-SIMS) and Raman spectroscopy. SEM showed that the glassy carbon cores were largely spherical, but had a fairly broad particle size distribution (Figure 2.1, L0). XPS analyzes the upper ca. 10 nm of a material, and gives insight into the elemental composition of surfaces of materials. An XP survey scan (Figure 2.2) of the core carbon material showed two main peaks from carbon (C1s) and oxygen (O1s), indicating that carbon comprised 83 % of the surface and oxygen the remaining 17 %. These atomic percentages were acquired through XPS narrow scans. The presence of oxygen should be important for adherence of PAAm to the core particles.

ToF-SIMS, a form of surface mass spectrometry, provides chemical information about the upper ca. 3 nm of a surface and is sensitive to all elements. Consistent with the XPS, negative ion ToF-SIMS of the core particles showed fairly intense O^- and OH^- peaks. It also showed the expected C^-, CH^-, C_2^-, and C_2H^- signals.

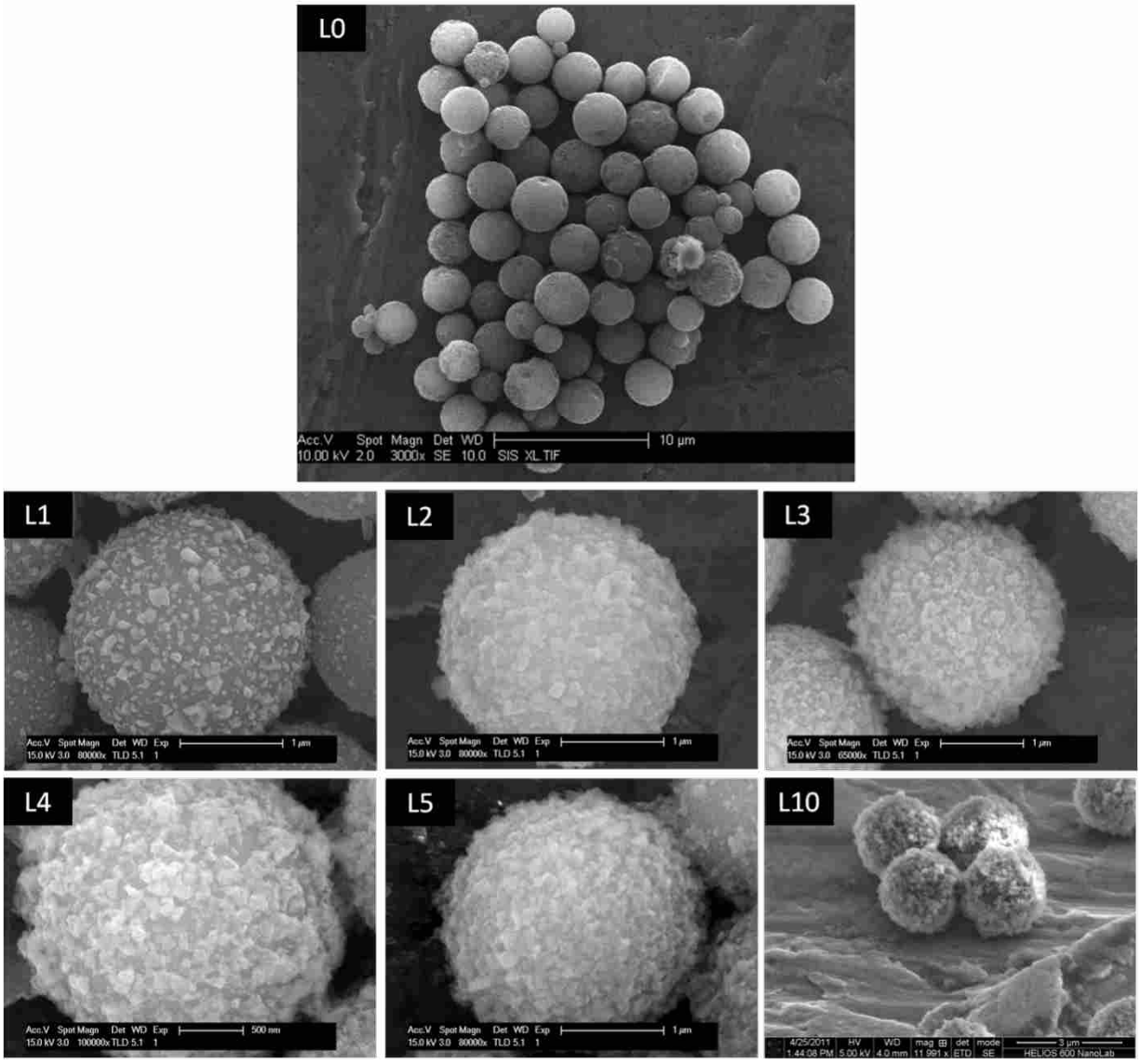

Figure 2.1 (L0) SEM image of the carbon core particles used in all of the chromatographic studies in this chapter. (L1 – L5, L10) SEM of LbL-coated model carbon particles, which were synthesized according to a procedure derived from the literature.[49-53] These particles were coated with nanodiamond that had a broad particle size distribution (ca. 10 – 400 nm, Advanced Abrasives). The particles were oxidized prior to the first PAAm deposition. Particles prepared with the nanodiamond with this broad PSD were not employed in any of the chromatographic studies described in this chapter. It was advantageous to use these particles because they could be easily imaged by SEM. L1 refers to one bilayer of PAAm and nanodiamond, L2 refers to two bilayers of PAAm and nanodiamond, etc.

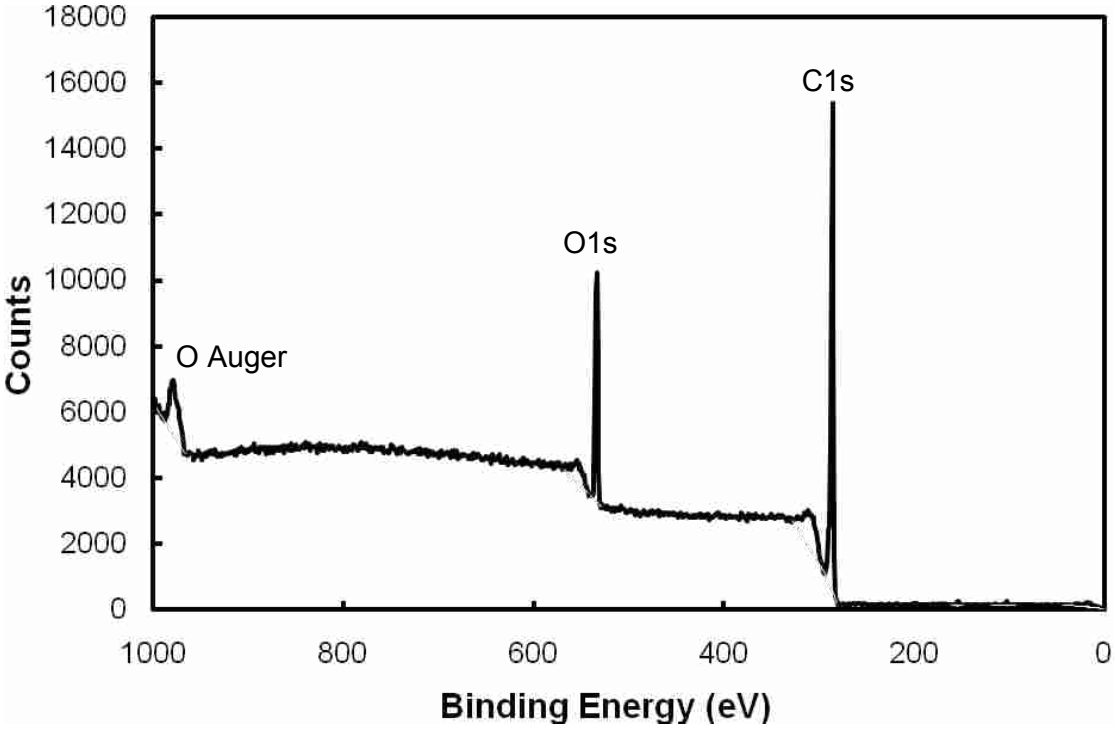

Figure 2.2 XPS of spherical carbon cores. The carbon (C1s) peak (286 eV) comprises ca. 83% of the surface while the oxygen (O1s) peak (534 eV) comprises the other ca. 17% of the surface.

Raman spectroscopy gives the analyst information about the degree of sp^3- or sp^2-bonding in a bulk carbonaceous material.[54-55] The Raman spectrum in Figure 2.3 contains four distinct peaks labeled 1 – 4. Peak 1 represents the T band. It is centered around 1050 cm^{-1} and can be assigned to sp^3-bonded carbon.[56] Peak 2 is designated as the disorder-induced band (or *D* band). It is centered at approximately 1350 cm^{-1} and is also due to sp^3-bonded carbon (diamond-like carbon).[55,57-58] Peak 3 is designated as the *G* band and is centered around 1580 cm^{-1}. It is attributed to sp^2-bonded carbon (graphitic type bonding).[55,58] Peak 4, which is centered around 2700 cm^{-1}, is the *G′* band, which is an overtone of the *D* band.[57] It is clear from this spectrum that both sp^2 and sp^3 hybridized carbon are present in the particles.

` To track the coating process on a spherical carbon material, we prepared core-shell particles with nanodiamond that was larger than the nanodiamond used for our packed pellicular phases, but still considerably smaller than the core particles. This made it easier to follow the LbL process by SEM (see Figure 2.1). It is clear from Figure 2.1 that the core material is nearly completely coated after 5 deposition cycles and that nanodiamond deposition progresses steadily from deposition to deposition. It should also be noted that, despite calling our deposition process 'layer-by-layer,' a complete layer is not obtained after each deposition, which is consistent with previous results.[48] Finally, note that the spherical carbon material used to obtain the SEM images in Figure 2.1, L1 – L5, L10 is different from that employed for the packings used in the chromatographic studies in this paper. Nevertheless, this should be a representative study, as the LbL of PAAm and nanodiamond has now been shown to proceed on micron-sized diamond particles,[48] planar silicon surfaces,[48] and the other carbon cores used in this study.

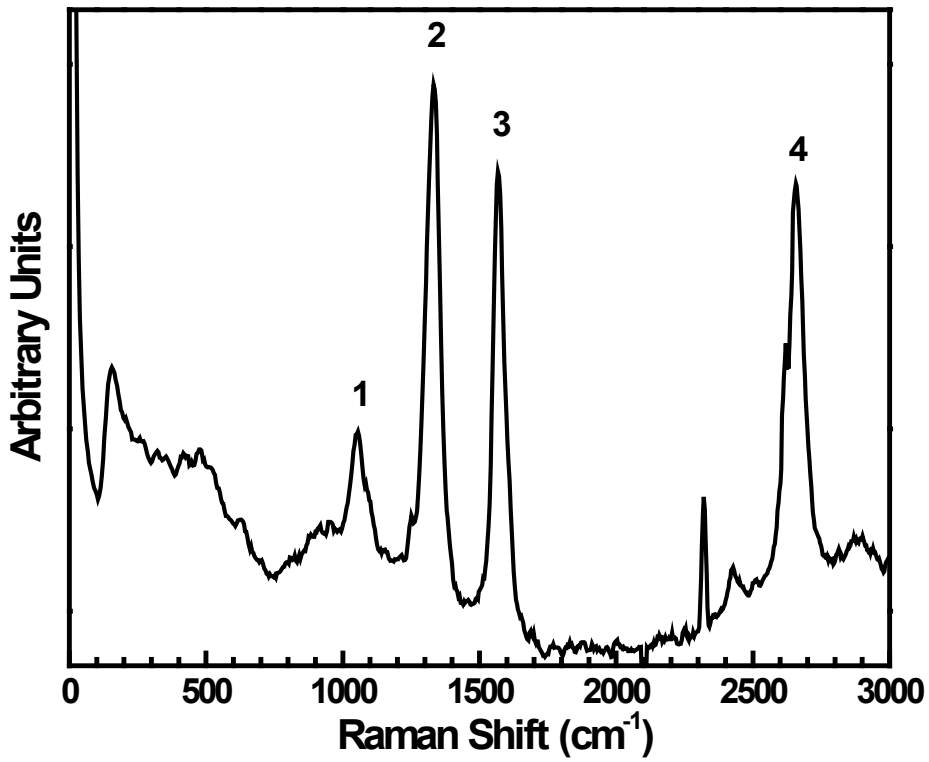

Figure 2.3 Raman spectrum acquired with 532 nm light. Band 1 is the T band (1050 cm^{-1}), corresponding to sp^3-bonded carbon. Band 2 is the D band, also corresponding to sp^3-bonded carbon (diamond-like). Band 3 is the G band, corresponding to graphitic, sp^2-bonded carbon. Band 4 is the G' band, and is an overtone of the D band.

2.4.2 Non-Crosslinked, Hydrophobic Phase

The first batch of core-shell particles made from carbon cores and PAAm/nanodiamond shells was not crosslinked. In the formation of these (and subsequent) particles, the PAAm was expected to deposit as an ultrathin film in a self-limiting fashion.[42,48] The primary amines from the PAAm in the shell layer were only reacted with monofunctional 1,2-epoxyoctadecane resulting in a C_{18} phase. Chromatography was performed on this column using alkyl benzene analytes (see separation conditions in the caption to Figure 2.4). Under all conditions explored, peaks showed a large amount of fronting regardless of analyte concentration. This may be due to non-uniform column packing. Moreover, the non-crosslinked column showed a rapid increase in back pressure over a short period of time which indicated mechanical instability of this material.

During our experimentation with this column, the flow rate was doubled from 0.5 mL/min to 1.0 mL/min. Upon returning to the original flow rate, the back pressure had increased significantly from 2,040 to 3,620 psi. After this experiment, the back pressure steadily increased over a 6 h period to 4,570 psi. At this point, the experiment was terminated. We had previously observed mechanical instability with non-crosslinked phases in our lab,[48] so we opted for a different approach that included crosslinking, with the hope that a more mechanically stable phase could be created.

2.4.3 Crosslinked, Hydrophobic Phases

2.4.3.1 Surface area, Pore Size and Volume

The surface area of the crosslinked particles was 44.2 m^2/g by BET isotherm measurements. The particles had a mean pore size of 28 nm and a pore volume of 0.356 mL/g.

2.4.3.2 Pressure-Flow Relationship and Hydrophobic Character

To determine the effect of crosslinking, the column was reacted with 1,2-epoxyoctadecane under the same conditions as described above, but with the addition of a small amount of crosslinker: 1,2,7,8-diepoxyoctane. The resulting crosslinked stationary phase was then packed under the same conditions as the previous column. From the chromatography, it was immediately clear that this phase was less hydrophobic than the non-crosslinked phase, which would be consistent with the incorporation of the diepoxide into the stationary phase. That is, the diepoxide, which contains eight carbon atoms and will yield two hydroxyl groups upon reaction with PAAm, is less hydrophobic than 1,2-epoxyoctadecane, which contains eighteen carbon atoms and will only yield one –OH group when it reacts with PAAm. For example, under the same conditions used with the non-crosslinked column (mobile phase and pressure), the last eluting peak, n-hexylbenzene, eluted about 1.5 min earlier. Figure 2.4 shows the chromatogram of this and other alkyl benzenes on this crosslinked column. There were also immediate indications that this crosslinked material would be stable over a longer period of time, as evidenced by our ability to increase and decrease repeatedly and reproducibly the mobile phase

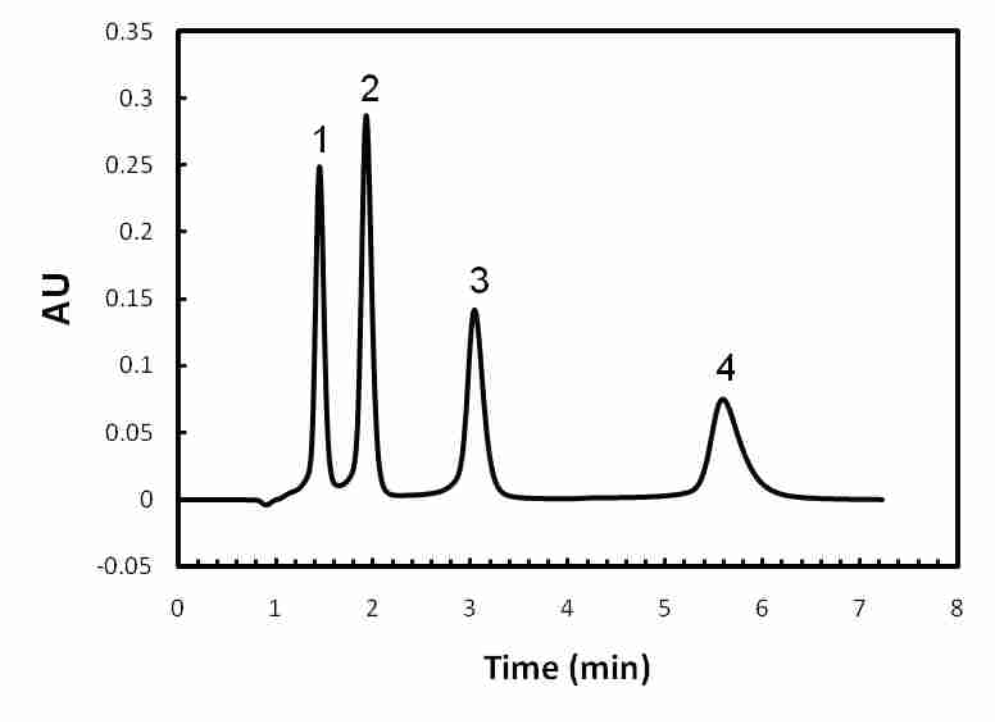

Figure 2.4 Reversed-phase separation of (1) benzene, (2) ethylbenzene, (3) *n*-butylbenzene, (4) *n*-hexylbenzene. Mobile phase: 40:60 H_2O/ACN with 0.1 (v/v) % triethylamine, pH 11.3. Flow rate was 0.5 mL/min. Column temperature was 35 °C. Detection was at 254 nm.

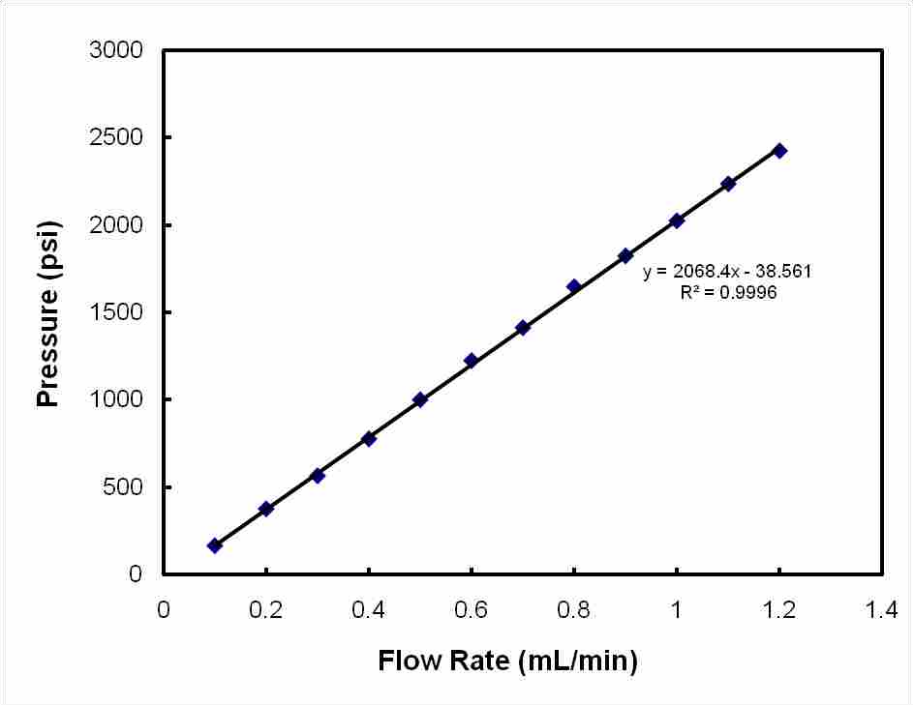

Figure 2.5 Pressure vs. flow curve for the crosslinked column. Pressures obtained at different flow rates were reproducibly observed as the flow was varied.

velocity. A plot of the resulting linear relationship between pressure and flow is shown in Figure 2.5. To compare the hydrophobicity of our materials to the hydrophobicity of other columns, we calculated log *k* for a series of alkyl benzenes: benzene, toluene, ethylbenzene, *n*-butylbenzene, and *n*-hexylbenzene.[59] The data were then fit to the equation:

$$\log k = \alpha(CH_2)C_n + \beta(Ph) \qquad (2.1)$$

where $\alpha(CH_2)$ and $\beta(Ph)$ are the retention increments for the methylene and phenyl groups respectively.[59] That is, the interaction of the stationary phase with the phenyl group will give the y-intercept and that with the methylene units will provide the slope. The value of $\alpha(CH_2)$ thus gives an indication of the hydrophobicity of a column.

One of our columns (4 μm mean particle size, 30 mm × 4.6 mm ID column) that was used for many months prior to this test was evaluated and gave an $\alpha(CH_2)$ of 0.15 under 40:60 (0.1% TEA)/ACN at 30 °C. Another column (4 μm mean particle size, 50 mm × 4.6 mm ID column) was tested at the beginning of its lifetime and gave an $\alpha(CH_2)$ of 0.19 under 55:45 water/ACN at 60 °C. This difference in $\alpha(CH_2)$ values is attributed to different mobile phase conditions, column ages, and operating temperatures. These data were compared to a previous study by Smith et al.[60] reported for a Spherisorb ODS-2 octadecyl modified silica gel. From the retention factors of alkylbenzenes that were separated in a 20 mM sodium phosphate buffer (pH 7.0)/ACN mobile phase (40:60 v/v) at 30 °C we calculate an $\alpha(CH_2)$ value of 0.17. This comparison points to a substantial hydrophobic (RP) character for our materials.

As a further note of comparison, the initial back pressure for the column containing the crosslinked phase was 940 psi, while the starting pressure for the column containing the non-

crosslinked phase was 2,040 psi. (Both columns were packed under identical conditions.) These results for the non-crosslinked particles suggest mechanical instability during packing, which would lead to clogging of the frit or the interstitial spaces between the particles by fines, possibly sloughed off the particles during column packing. However, even the back pressure from the column containing crosslinked material was higher than might be expected for a column containing 4 μm particles. To probe this issue, the back frit (closer to the detector) from one such column, which had been used extensively, was removed and analyzed by SEM. The resulting micrograph showed noticeable plugging of the frit. In the future, it will be determined whether the plugging came as a result of fines that were not removed prior to packing, or as a result of damage to the particles during packing. At present, the data point to the former explanation.

2.4.3.3 Stability at pH 11.3

The first stability test performed on the crosslinked column took place over 1,600 column volumes of mobile phase at pH 11.3. The flow rate was 0.5 mL/min and the column temperature was 35 °C. An analyte mixture containing benzene, ethylbenzene, *n*-butylbenzene and *n*-hexylbenzene was used to probe the column during this test. The trial ran over a 26.6 h period and resulted in a decrease in k of 4.2 – 6.1% (see Figure 2.6). The efficiency (N/m) of the column decreased initially, however it recovered and over the length of the test there was no overall decrease in its efficiency (see also Figure 2.6).

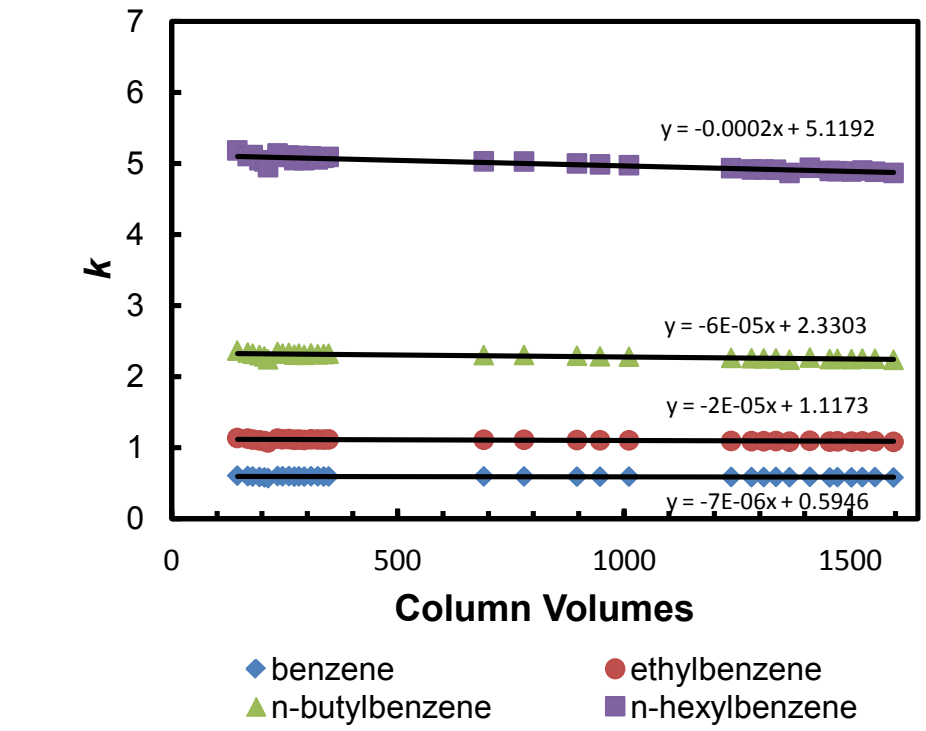

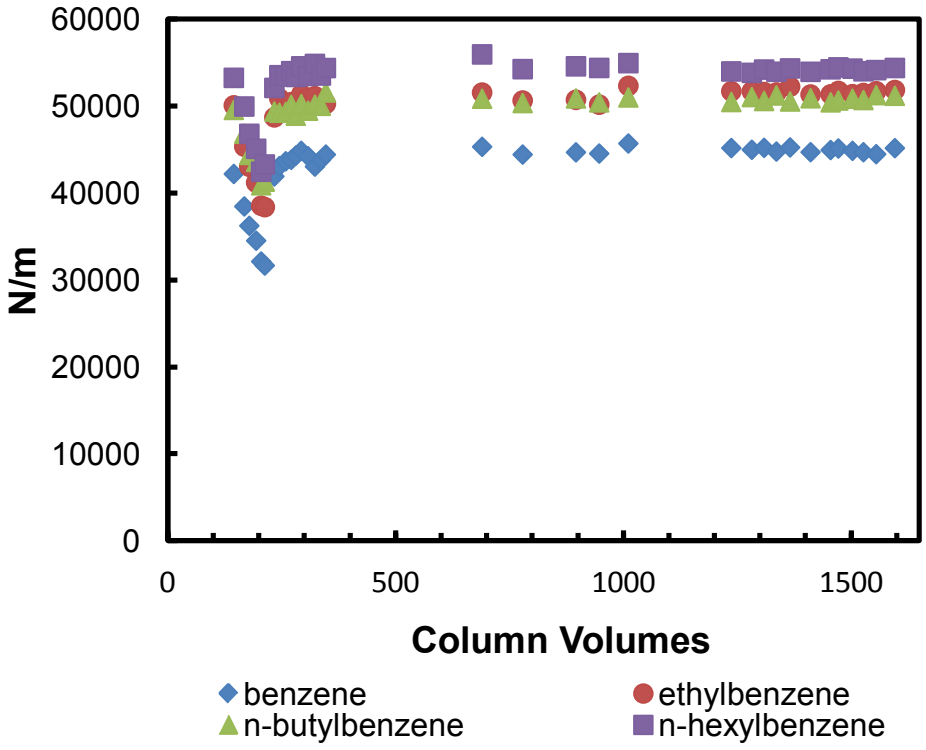

Figure 2.6 Column stability test at pH 11.3. See text for experimental details.

2.4.3.4 Stability at pH 13.0

A second stability test was then performed on this same column at pH 13.0 using the same analyte mixture. The mobile phase was 40:60 H_2O/ACN with the aqueous portion set at pH 13.0 by addition of 1% (v/v) tetramethylammonium hydroxide. The flow rate for this stability test was 0.5 mL/min, and the column temperature was 35 °C. Over the course of this stability test, only a slight decrease (ca. 1%) in *k* was seen. Given the scatter in the data, it was not possible to conclude whether the efficiencies of the columns increased or decreased – they remained nearly constant. (After a careful scrutiny of the data, one might argue that a small decrease in efficiency of ca. 2 – 3% occurred for most of the analytes, although the efficiency for *n*-butylbenzene appeared to *increase* by ca. 3%.) Overall, we can state that little or no change took place in column properties and that this phase shows the greatest stability of any HPLC phase we have created to date.

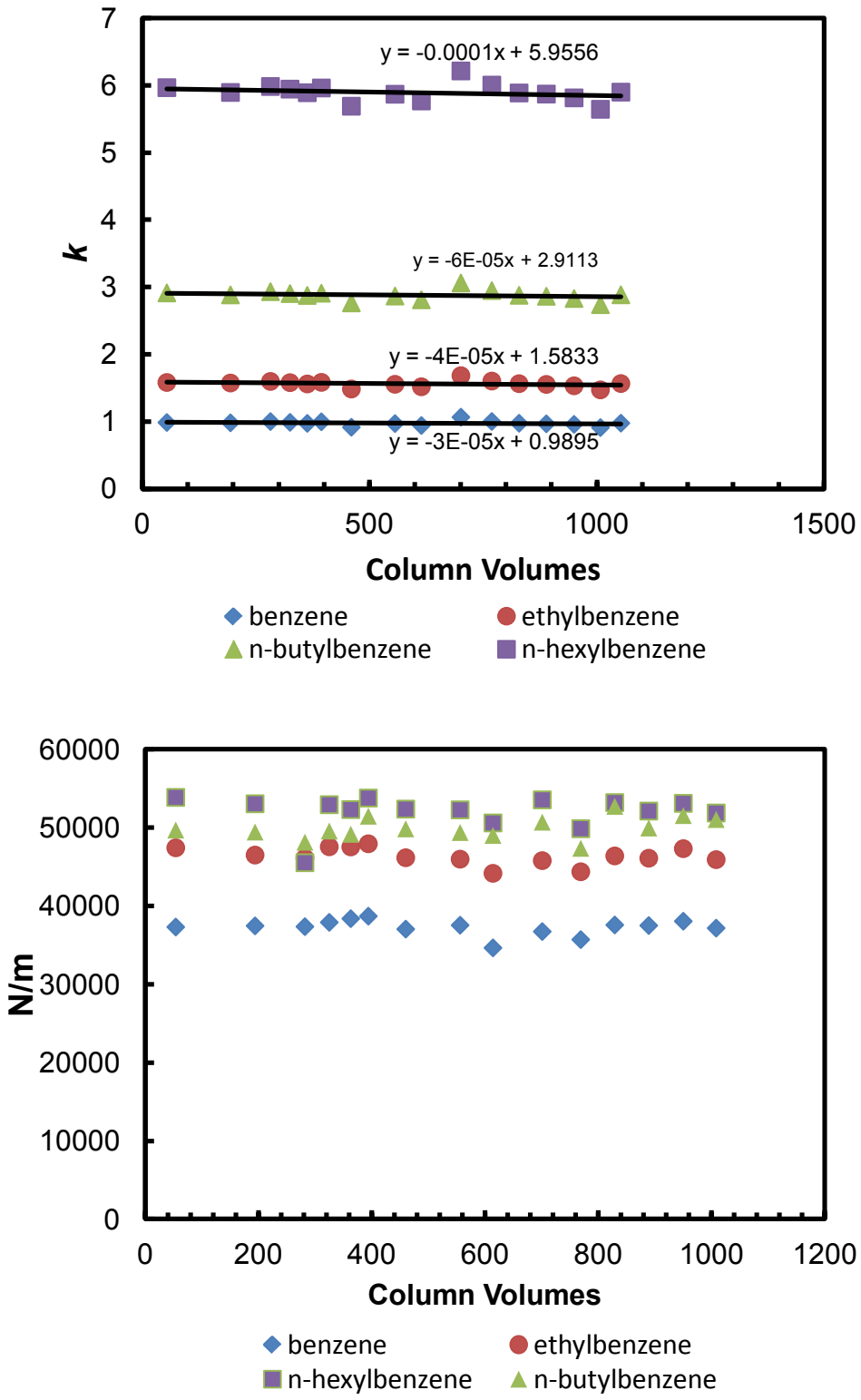

Figure 2.7 Stability test at pH 13.0 with the same column used for Figure 2.6. See text for experimental details.

2.4.3.5 Van Deemter Study and Instrument Response

The reasonable back pressures of this column opened the possibility of varying flow rates enough to obtain van Deemter curves. For this study, the mobile phase was the same as that used for the first stability test (pH 11.3). An analyte mixture consisting of benzene, ethylbenzene, *n*-propylbenzene and *n*-butylbenzene was used, and measurements were taken every 0.1 mL/min from 0.1 to 1.2 mL/min. Table 2.2 gives the results of this van Deemter study, and Figure 2.8 shows a representative van Deemter curve for *n*-butylbenzene, the best performing analyte in this study. The optimal plate height and flow rate for *n*-butylbenzene from the fitted van Deemter data were 18.6 μm (which equates to ca. 53,800 N/m) and 0.44 mL/min. The best efficiency for a single injection of n-butylbenzene was 56,000 N/m (k = 1.70) at 0.5 mL/min. A trend in this van Deemter study (see Table 2.2) was that the A and C terms decreased as the analytes increased in molecular weight. Also shown in Table 2.2 is that with increasing analyte molecular weight, the optimal mobile phase flow rate increased. Furthermore, the improvements we observed in efficiency with retention, which in our case also corresponds to analyte molecular weight, are consistent with extra column contributions to band broadening. The HPLC system used in this work had a dead volume of ca. 100 – 105 μL, which was within the specifications for this instrument. However, for earlier eluting analytes on our short columns, the LC appeared to contribute to decreased efficiencies.

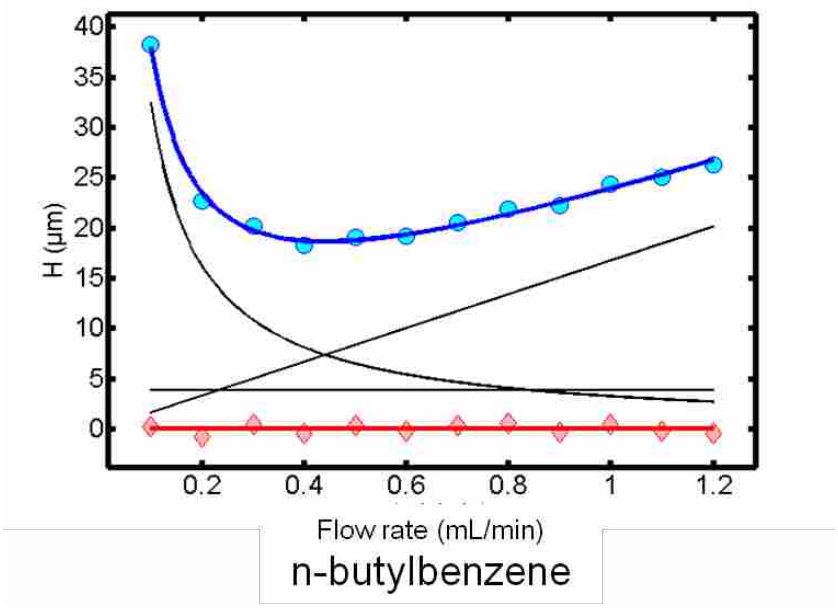

Figure 2.8 Van Deemter curve for *n*-butylbenzene. The raw data and residuals to the data are represented by the symbols: ○ and ◊. The black lines represent the fitted *A*, *B,* and *C* terms.

Table 2.2 Van Deemter terms and optima for each analyte.

	A (μm)	B (μm·mL/min)	C (μm·min/mL)	R^2	Flow $Rate_{opt}$ (mL/min)	H_{opt} (μm)
benzene	8.45	2.31	22.8	0.99955	0.32	23.0
ethylbenzene	6.36	2.62	18.8	0.99924	0.37	20.4
n-propylbenzene	5.71	2.74	17.4	0.99967	0.40	19.5
n-butylbenzene	3.89	3.25	16.8	0.99958	0.44	18.6

It is significant that the plate counts observed using this column are higher than those for phases previously created in our lab,[48] despite previous phases having smaller particle sizes. The peaks also appear to have good symmetries, although some of them show some fronting. Symmetry factors, which appeared to be low, could not be calculated for this separation because the peaks were not fully baseline separated.

A "sandwich" injection of an alkyl benzene analyte mixture was done using a UHPLC system with the pH 11.3 mobile phase used for the stability test in Figure 2.6. The column used was the one corresponding to Figure 2.10 C. This UHPLC system was expected to have substantially lower extra column band broadening contributions than the HPLC system used for our other separations. This separation, which was performed once, pointed to the potential efficiencies of our diamond-based phases when used under more optimized conditions. In the resulting chromatogram (see Figure 2.9), benzene, ethylbenzene, *n*-butylbenzene, *n*-hexylbenzene, *n*-octylbenzene, and *n*-decylbenzene showed efficiencies of 117 000, 120 100, 111 400, 80 900, 52 100, and 21 400 N/m, respectively. Not only did this separation give us much better efficiencies than those obtained previously, but later eluting analytes had lower efficiencies, which is a reversal of the results obtained with our HPLC. Obviously, the instrument can have a large impact on separations.

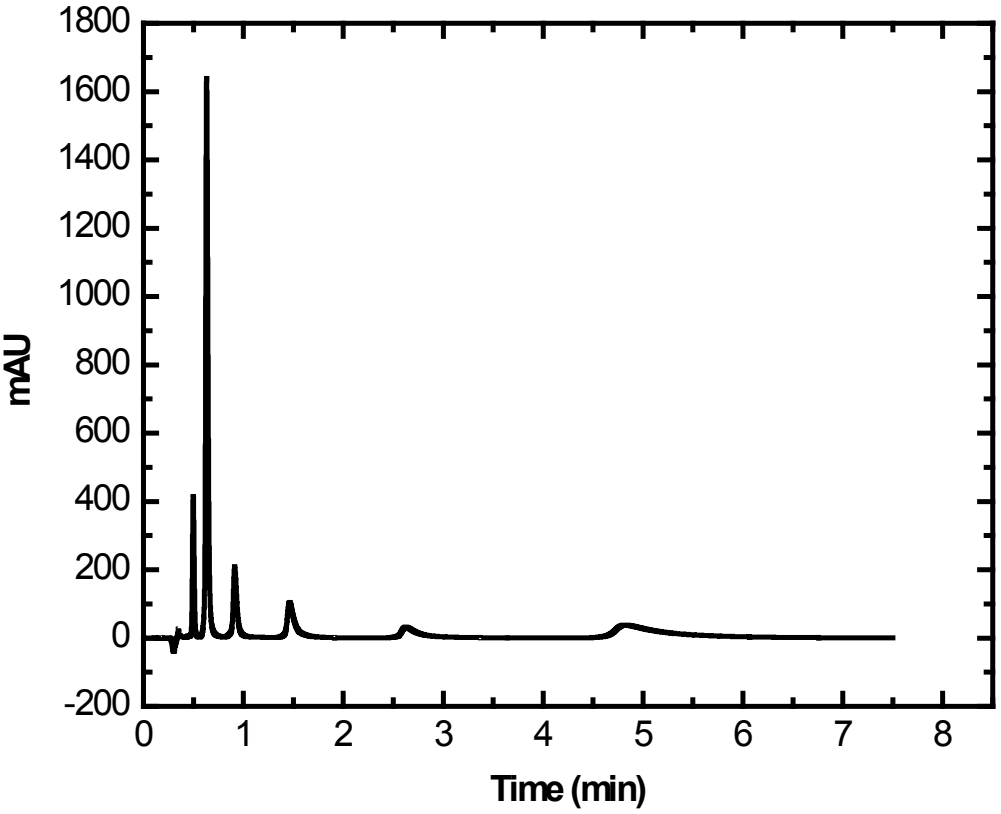

Elution Order	Name	*k*	N/m
1	benzene	0.66	117000
2	ethylbenzene	1.11	120100
3	*n*-butylbenzene	2.04	111400
4	*n*-hexylbenzene	3.88	80900
5	*n*-octylbenzene	7.75	52100
6	*n*-decylbenzene	15.07	21400

Figure 2.9 Separation obtained on an Agilent Infinity 1290 using a “sandwich” injection.

2.4.3.6 PSDs and SEMs of Particles and Particle Optimization

The reduced plate height, $h = H/d_p$, where d_p is the average particle diameter, of a well-packed column of good particles is typically 2. Accordingly, we were concerned with our higher than desired values of h (ca. 5 based on a projected particle size of 4 μm), and were also surprised that our C term had contributed so significantly to our overall plate height since we had created a phase based on a core-shell particle.

To obtain greater insight into these problems, we measured our particles' size distribution (PSD). Despite starting with a material with a 3 μm average particle size and a shell thickness of 0.5 μm (4 μm total), our measurements showed a mean particle size of 14.0 μm and a $D_{90/10}$ (skewness) of 3.9 after functionalization. This less-than-ideal PSD is shown in Figure 2.10 A, which indicates a clear need for particle optimization. Scanning electron microscopy also suggested the presence of agglomerates in this material.

2.4.3.7 Particle Optimization.

Our next goal was to create a new batch of particles with the same crosslinked/C_{18} functionality, but with fewer agglomerates. In this effort, the particles were sonicated after the first PAAm coating (before LbL deposition). After particle formation, a substantially improved PSD was obtained (see Figure 2.10 B), and the mean d_p of this batch was 5 μm.

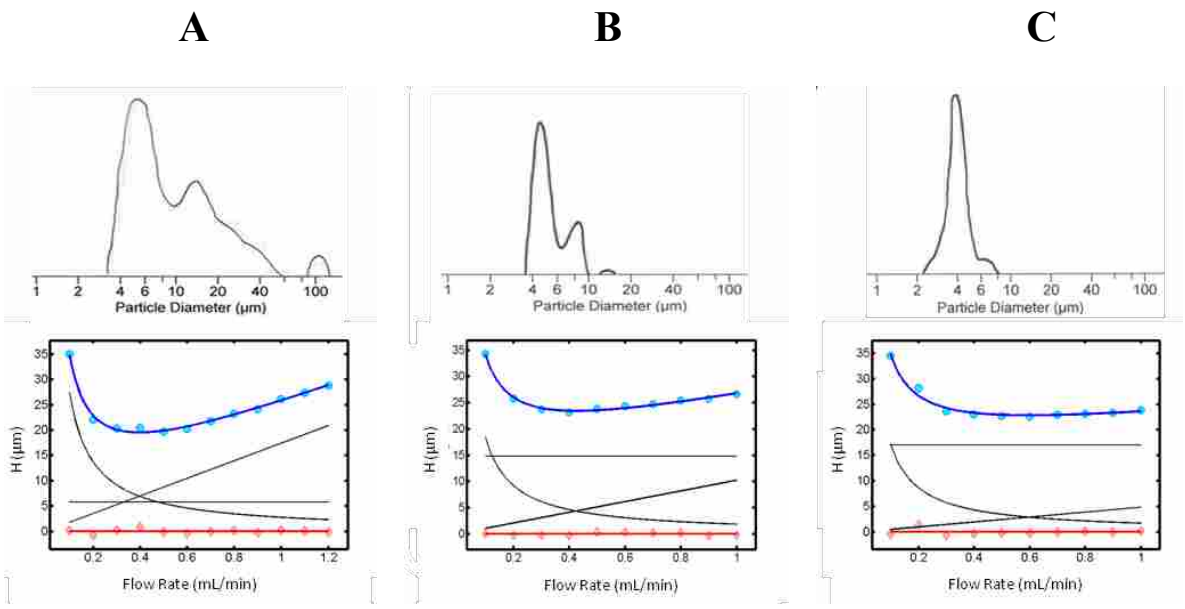

Figure 2.10 PSDs of core-shell particles synthesized in three different ways, and corresponding van Deemter curves from columns packed with these particles, with n-butylbenzene as analyte. For separation conditions see Figure 2.4. (A) Particles that were not sonicated prior to nanodiamond deposition. (B) Particles that were sonicated prior to the first nanodiamond deposition. (C) Particles that were sonicated prior to every nanodiamond deposition. The units on the *A*, *B*, and *C* terms are µm, µm·mL/min, and µm·min/mL, respectively.

The column was characterized as before, and the resulting van Deemter curve showed the expected flattening of its *C* term. Whereas the *C* term for the previous particles was 16.8, the *C* term for the sonicated particles was 7.86. Unfortunately, the *A* term for this new column/material increased, which suggests that our packing procedure was not optimized. A third batch of particles was then created, where sonication was employed after every PAAm deposition. This batch showed an even better PSD, with a mean d_p of 4 μm (see Figure 2.10 C). The *C* term for these particles was even lower than before (4.84), but the *A* term remained high (17.0).

2.4.4 Retention and Separation of Various Analytes

2.4.4.1 Retention of Amitriptyline, Cholesterol, and Diazinon at pH 11.3

Diazinon (a pesticide), amitriptyline (a basic drug), and cholesterol (a lipid) were retained on our second column (d_p = 5 μm in Figure 2.10 B). Better efficiencies and decreased asymmetries were seen at 60 °C, compared to 35 °C (see Figure 2.11).

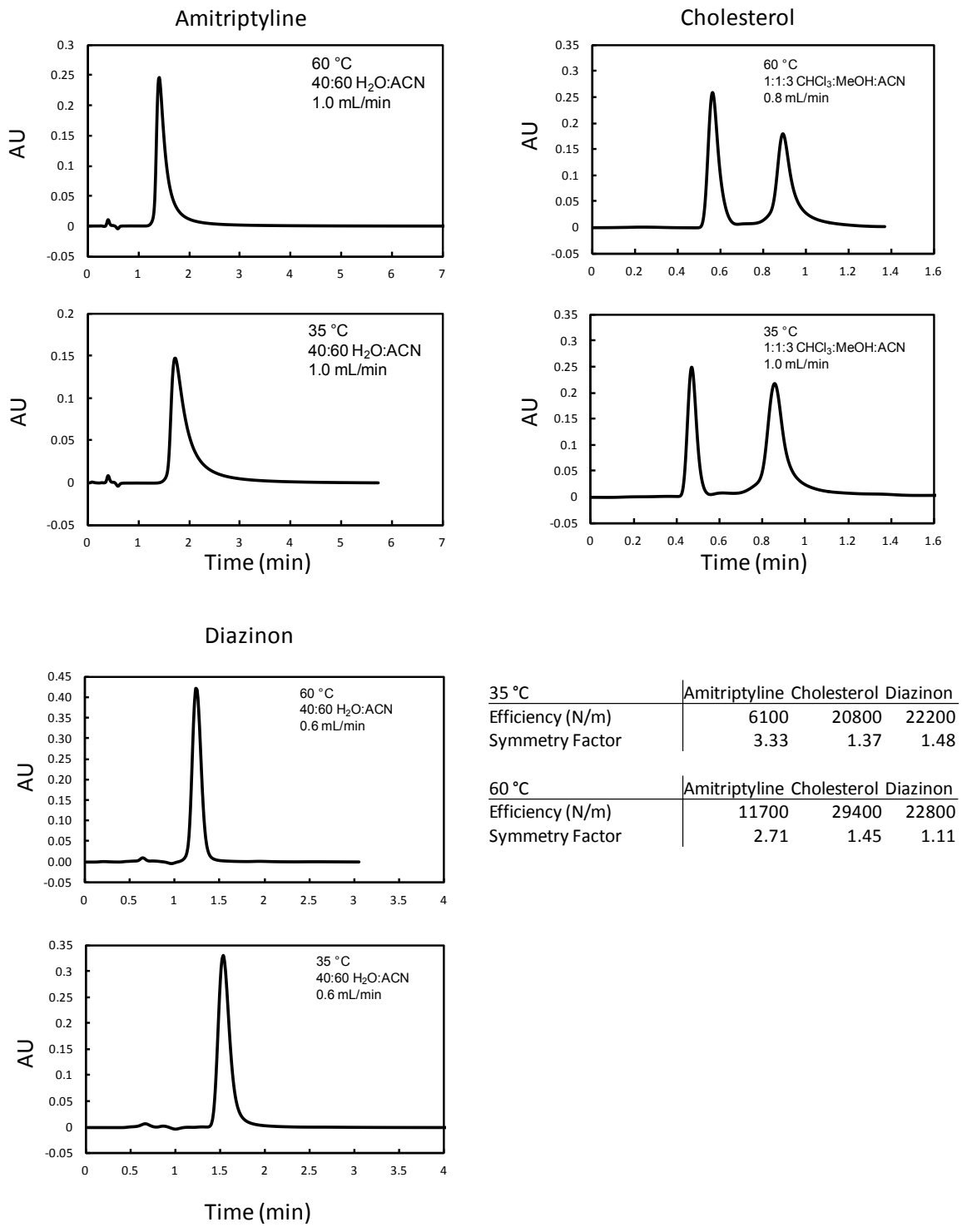

35 °C	Amitriptyline	Cholesterol	Diazinon
Efficiency (N/m)	6100	20800	22200
Symmetry Factor	3.33	1.37	1.48

60 °C	Amitriptyline	Cholesterol	Diazinon
Efficiency (N/m)	11700	29400	22800
Symmetry Factor	2.71	1.45	1.11

Figure 2.11 Effect of column temperature on the retention characteristics of amitriptyline, cholesterol and diazinon using a high pH mobile phase (11.3).

2.4.4.2 Retention of Amitriptyline and Three Organic Acids Under Acidic Conditions

Under acidic conditions (40:60 0.1% formic acid/ACN) different retention mechanisms were seen for amitriptyline and various organic, aromatic acids. Amitriptyline was unretained at 35 °C and 60 °C. In this case, it would be reasonable to assume that ion repulsion was occurring between amitriptyline and the stationary phase and this interaction overrode the hydrophobic character of the stationary phase.

Retention of toluic, benzoic, and *p*-chlorobenzoic acids was seen using a 100% methanol mobile phase containing 0.5 mM formic acid. Analytes exhibited substantial tailing (see Table 2.3). Retention increases with decreasing pK_a (increased acidity) of analyte, consistent with an ion exchange interaction between the stationary phase and analytes.

2.4.4.3 Separation of a Five Component Pharmaceutical Mixture

A mixture of drugs, which included acetaminophen (Tylenol), diazepam (Valium), doxepin (Adapin), imipramine (Tofranil), and clomipramine (Anafranil), was separated at pH 11.3 using our third column (d_p = 4 μm) at 60 °C with a flow rate of 0.8 mL/min using a basic mobile phase of 40:60 water (0.1% TEA, pH 11.3)/ACN (see Figure 2.12). Some tailing was observed. We speculate that hydrogen bond acceptance and/or polar bonds of these basic analytes lead to interactions with the polar groups on the stationary phase, i.e., amine or hydroxyl groups. It is also possible that some of the nanodiamond surfaces may not be completely coated and any oxygenated moieties on those heterogeneous surfaces could also contribute to tailing of more polar analytes.

Table 2.3 Retention of various benzoic acids.

Acid	t_r (min)	Sym.	pK_a
Toluic acid	3.74	3.02	4.37
Benzoic acid	4.90	2.73	4.20
p-chlorobenzoic acid	12.56	2.74	3.99

2.4.4.4 Separation of a Three Component Pharmaceutical Mixture at pH 2.7

Separations at low pH were also attempted on the third column (Figure 2.10 C, d_p = 4 μm), where the first group of analytes was acetaminophen, diazepam and 2,6-diisopropylphenol (propofol) (see Figure 2.13A).

The mobile phase was 40:60 water (0.1% formic acid, pH 2.7)/ACN. While acetaminophen and diazepam were retained longer than in the basic separation, their efficiencies were lower. We were pleased with the separation of propofol from the analyte mixture. Propofol gave higher efficiency (48,300 N/m, k = 6.04) than we had seen with the other non-alkyl benzene analytes, and the peak symmetry was very good. This led us to attempt a separation of various phenols at acidic pH.

2.4.4.5 Separation of Phenolic Compounds and Derivatives at pH 2.7

Six phenolic compounds were separated using a mobile phase of 55:45 water (0.1% formic acid pH 2.7)/ACN (see Figure 2.13 C). All of these analytes separated with an efficiency of ca. 13,500 N/m or better. The less than optimal efficiencies could be attributed to the core-shell particles being packed into the column twice (see Experimental). We were pleased to see fairly good resolution between the 2-chlorophenol and 4-chlorophenol isomers. A trend that seemed apparent from this separation was that electron withdrawing groups appear to cause greater tailing. This may be a result of an exposed diamond surface that retains the more deshielded aromatic ring. Peak asymmetries could not be determined for this separation because most of the compounds were not baseline separated.

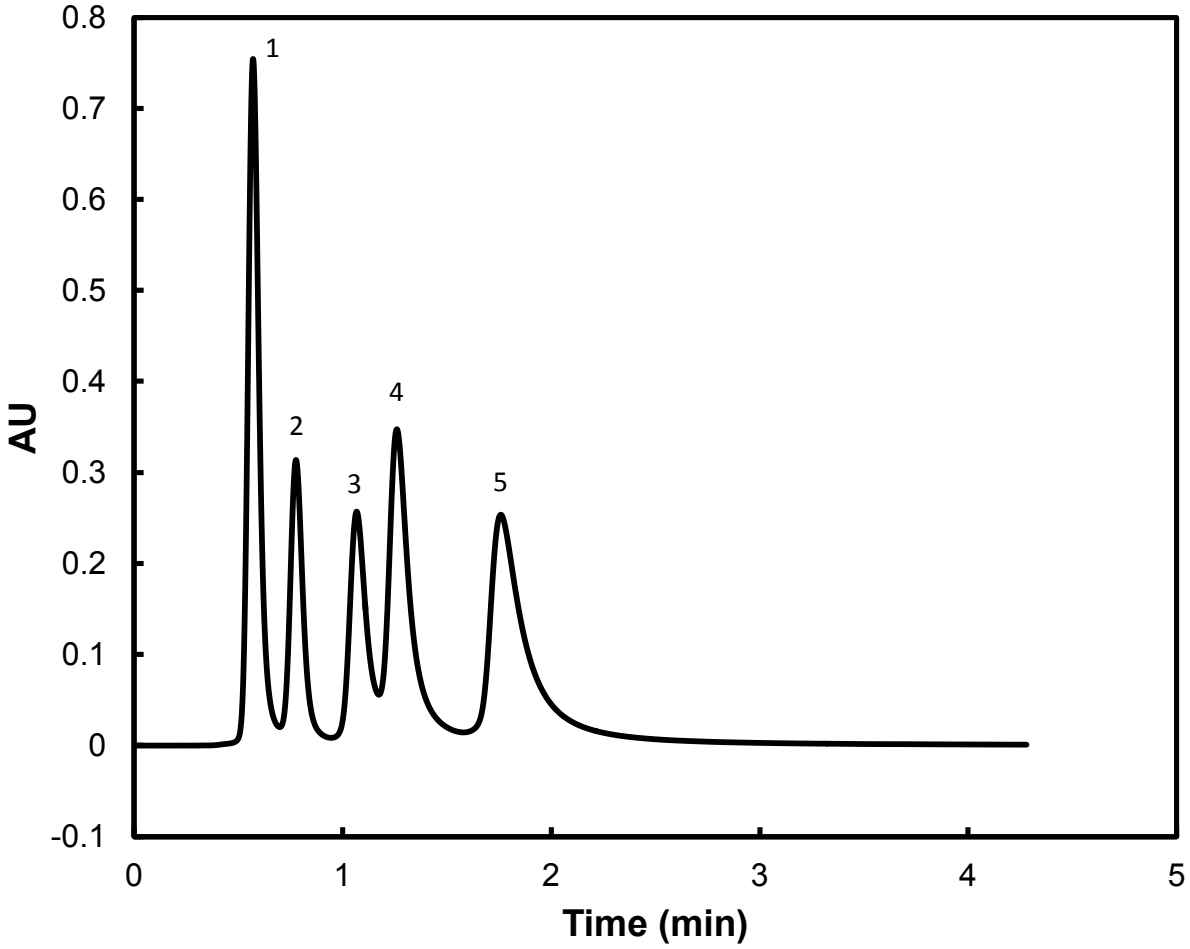

Elution Order	Name	t_r	R	N/m	k
1	Acetaminophen	0.57		19000	0.16
2	Diazepam	0.78	2.01	26600	0.58
3	Doxepin	1.07	2.27	28200	1.17
4	Imipramine	1.26	1.22	29800	1.56
5	Clomipramine	1.76	2.27	22500	2.58

Figure 2.12 Separation of five pharmaceuticals. See text for separation conditions.

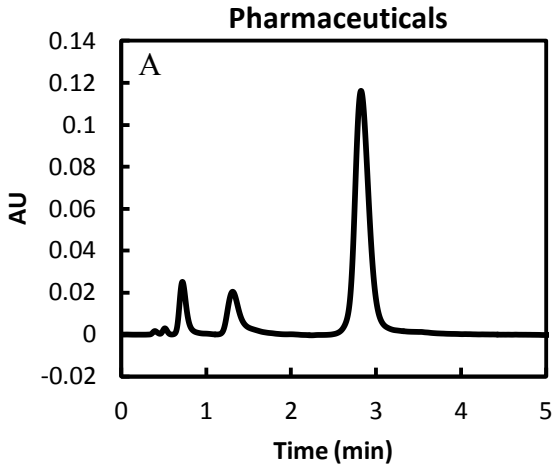

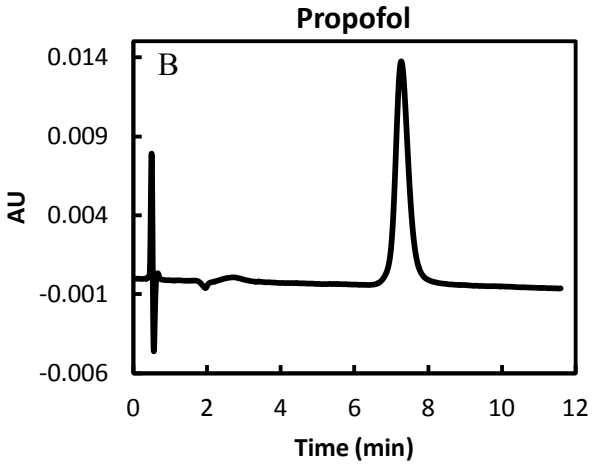

Name	t_r	N/m	*k*	$Sym_{10\%}$
Acetaminophen	0.73	13000	0.81	1.48
Diazepam	1.32	14900	2.28	1.97
2,6-diisopropylphenol	2.83	48300	6.04	1.14

Name	t_r	N/m	*k*	$Sym_{10\%}$
2,6-diisopropylphenol	7.28	71500	13.4	1.12

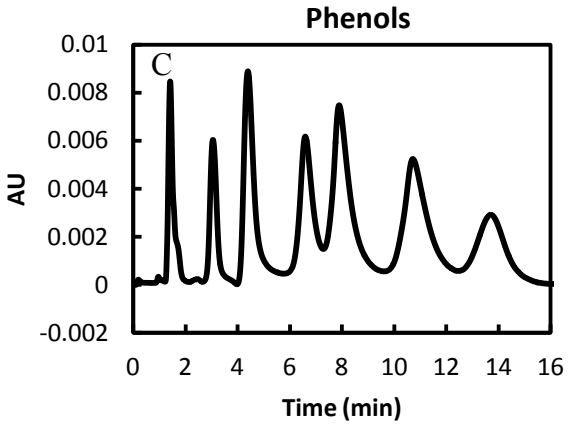

Name	t_r	N/m	*k*
Phenol	3.05	13500	3.08
4-methylphenol	4.39	13600	4.87
2-chlorophenol	6.59	16000	7.81
4-chlorophenol	7.89	15200	9.55
4-bromophenol	10.7	13600	13.3
1-*tert*-butyl-4-methylphenol	13.7	14200	17.3

Figure 2.13 Separations of various analytes. All separations performed at 60 °C and acidic pH (2.7). (A) Separation of three pharmaceuticals using 40:60 water (0.1 v/v % formic acid)/ACN at 0.8 mL/min on the d_p = 4 μm column (Figure 2.10 C). (B) Retention of propofol using 70:30 water (0.1 v/v % formic acid)/ACN at 0.8 mL/min on the same column. (C) A mixture of phenols using 55:45 water (0.1 v/v % formic acid)/ACN at 0.4 mL/min separated using a 50 mm × 4.6 mm ID column.

2.4.4.6 Retention of Propofol

We again chromatographed propofol, and used a 70:30 water (0.1% formic acid, pH 2.7)/ACN mobile phase. The greater retention for this compound can be explained by the increased water in the mobile phase, resulting in a plate count of 71,500 N/m (k = 13.4) and a peak asymmetry of 1.12.

Note that we saw no signs of degradation of the column at low pH, which might have been evidenced by an increase or significant decrease in its back pressure, or by a noticeable loss of performance. It would appear that crosslinking of the PAAm prevents any substantial swelling of the material.

2.5 Conclusions

We have reported the formation of pellicular particles prepared from carbon cores and porous PAAm/nanodiamond shells for HPLC. The carbon cores, which are not commercially available, were characterized by XPS, ToF-SIMS, SEM, and Raman spectroscopy. We first developed a non-crosslinked C_{18} material. The resulting column appeared to be unstable, showed low efficiencies, and resulted in a significant increase in back-pressure over a short period of time, as had our previous non-crosslinked columns.[48]

Our next attempt to create a stable phase included the addition of a crosslinker (1,2,7,8-diepoxyoctane) during functionalization. The back pressures of this column were the lowest observed for any of our diamond-based core-shell particles to date. The pressure-flow behavior was completely reversible and allowed us to obtain a van Deemter curve for this phase. The optimal flow rate and theoretical plate height for our best performing alkylbenzene analyte, *n*-butyl benzene, were 0.44 mL/min and 18.6 µm, respectively. Our best results for a single

injection of n-butylbenzene gave us 56,000 N/m (k = 1.70). Unfortunately, our A and C terms were rather high.

Not only did the crosslinked phase show the best efficiencies yet seen for a diamond-based phase, ca. 71,000 N/m on a conventional HPLC, but it also exhibited good stability under extreme pH conditions, i.e., pH 11.3 and even pH 13. A "sandwich" injection using a UHPLC system showed best efficiencies of 110,000 – 120,000 N/m (k = 0.66 – 2.04) for three low molecular weight analytes.

Improvement in our particle size distributions was accomplished through sonication, which resulted in improved C terms for the columns packed with these particles. On the other hand, the A terms were higher. This was attributed to an unoptimized column packing procedure. Future work will focus on improving the column packing.

The columns packed with the sonicated phases separated a more diverse set of analytes. Separations of pharmaceuticals at high (11.3) and low (2.7) pH were performed and phenols and phenolic derivatives were separated under acidic conditions. While no stability studies, per se, were performed under acidic conditions, there appeared to be no degradation of the phases under these conditions.

ACKNOWLEDGMENTS

I thank Paul Ross from Supelco for providing the spherical glassy carbon particles that served as our core material, Michael Standing at BYU for operating the SEM, Grant Brown (BYU undergraduate) for help with sample and mobile phase preparation, John Kimmel from Agilent for assistance with the UHPLC, US Synthetic for funding and support, and the ARC Discovery Grant of UTAS for supporting the travel of M. Linford to Tasmania.

2.6. References

(1) Miller, J. M. *Chromatography: Concepts and Contrasts*; 2nd ed.; John Wiley & Sons, Inc: Hoboken, NJ, 2005.

(2) Snyder, L. R.; Kirkland, J. J.; Glajch, J. L. *Practical HPLC Method Development*; 2nd ed.; John Wiley: New York, 1997.

(3) Kirkland, J. J. *J. Chromatogr. A* **2004**, *1060*, 9-21.

(4) Kirkland, J. J.; Glajch, J. L.; Farlee, R. D. *Anal. Chem.* **1989**, *61*, 2-11.

(5) Nawrocki, J. *J. Chromatogr. A* **1997**, *779*, 29-71.

(6) Wehrli, A.; Hildenbrand, J. C.; Keller, H. P.; Stampfli, R.; Frei, R. W. *J. Chromatogr. A* **1978**, *149*, 199-210.

(7) Roumeliotis, P.; Unger, K. K. *J. Chromatogr. A* **1978**, *149*, 211-224.

(8) Engelhardt, H.; Nikolov, M.; Arangio, M.; Scherer, M. *Chromatographia* **1998**, *48*, 183-189.

(9) Sagliano Jr, N.; Floyd, T. R.; Hartwick, R. A.; Dibussolo, J. M.; Miller, N. T. *J. Chromatogr. A* **1988**, *443*, 155-172.

(10) Kirkland, J. J.; Adams, J. B.; van Straten, M. A.; Claessens, H. A. *Anal. Chem.* **1998**, *70*, 4344-4352.

(11) Kirkland, J. J.; van Straten, M. A.; Claessens, H. A. *J. Chromatogr. A* **1998**, *797*, 111-120.

(12) Kobayashi, A.; Takezawa, K.; Takasaki, H.; Kanda, T.; Kutsuna, H. *J. Chromatogr. A* **2005**, *1073*, 163-167.

(13) Trammell, B. C.; Ma, L.; Luo, H.; Jin, D.; Hillmyer, M. A.; Carr, P. W. *Anal. Chem.* **2002**, *74*, 4634-4639.

(14) Trammell, B. C.; Ma, L.; Luo, H.; Hillmyer, M. A.; Carr, P. W. *J. Chromatogr. A* **2004**, *1060*, 61-76.

(15) Cheng, Y. F.; Walter, T. H.; Lu, Z.; Iraneta, P.; Alden, B. A.; Gendreau, C.; Neue, U. D.; Grassi, J. M.; Carmody, J. L.; O'Gara, J. E.; Fisk, R. *LC-GC N. Am.* **2000**, *11*, 1162.

(16) Wyndham, K.; Lawrence, N.; Glose, K.; Cook, J.; Walsh, D.; Brousmiche, D.; Iraneta, P.; Alden, B.; Boissel, C.; Walter, T. *Polym. Prepr. (Am. Chem. Soc., Div. Polym. Chem.)* **2007**, *48*, 278-279.

(17) Wyndham, K. D.; O'Gara, J. E.; Walter, T. H.; Glose, K. H.; Lawrence, N. L.; Alden, B. A.; Izzo, G. S.; Hudalla, C. J.; Iraneta, P. C. *Anal. Chem.* **2003**, *75*, 6781-6788.

(18) Teutenberg, T.; Hollebekkers, K.; Wiese, S.; Boergers, A. *J. Sep. Sci.* **2009**, *32*, 1262-1274.

(19) McCalley, D. V. *J. Chromatogr. A* **2010**, *1217*, 858-880.

(20) McCalley, D. V. *Advances in Chromatography*; CRC Press: Boca Raton, FL, 2008; Vol. 46.

(21) Gagliardi, L. G.; Castells, C. B.; Ràfols, C.; Rosés, M.; Bosch, E. *Anal. Chem.* **2006**, *78*, 5858-5867.

(22) Haky, J. E.; Vemulapalli, S.; Wieserman, L. F. *J. Chromatogr. A* **1990**, *505*, 307-318.

(23) Knox, J. H.; Kaur, R. P. *Advances in Chromatography*; CRC Press: Boca Raton, FL, 1997; Vol. 37.

(24) Nawrocki, J.; Rigney, M.; McCormick, A.; Carr, P. W. *J. Chromatogr. A* **1993**, *657*, 229-282.

(25) Tanaka, N.; Araki, M. *Advances in Chromatography*; CRC Press: Boca Raton, FL, 1989; Vol. 30.

(26) Trüdinger, U.; Müller, G.; Unger, K. K. *J. Chromatogr. A* **1990**, *535*, 111-125.

(27) Nawrocki, J.; Dunlap, C.; McCormick, A.; Carr, P. W. *J. Chromatogr. A* **2004**, *1028*, 1-30.

(28) Sun, L.; Carr, P. W. *Anal. Chem.* **1995**, *67*, 3717-3721.

(29) Sun, L.; McCormick, A. V.; Carr, P. W. *J. Chromatogr. A* **1994**, *658*, 465-473.

(30) Nawrocki, J.; Dunlap, C.; Li, J.; Zhao, J.; McNeff, C. V.; McCormick, A.; Carr, P. W. *J. Chromatogr. A* **2004**, *1028*, 31-62.

(31) Cazes, J. *Encyclopedia of Chromatography*; 1st ed.; Marcel Dekker: New York, 2004.

(32) Rigney, M. P.; Weber, T. P.; Carr, P. W. *J. Chromatogr. A* **1989**, *484*, 273-291.

(33) Blackwell, J. *Chromatographia* **1993**, *35*, 133-138.

(34) Blackwell, J. A.; Carr, P. W. *J. Chromatogr. A* **1991**, *549*, 59-75.

(35) Blackwell, J. A.; Carr, P. W. *J. Liq. Chromatogr. Relat. Technol.* **1991**, *14*, 2875-2889.

(36) Pereira, L. *J. Liq. Chromatogr. Relat. Technol.* **2008**, 31, 1687-1731.

(37) West, C.; Elfakir, C.; Lafosse, M. *J. Chromatogr. A* **2010**, *1217*, 3201-3216.

(38) Nesterenko, P.; Haddad, P. *Anal. Bioanal. Chem.* **2010**, *396*, 205-211.

(39) Nesterenko, P. N.; Fedyanina, O. N.; Volgin, Y. V. *Analyst* **2007**, 403-405.

(40) Nesterenko, P. N.; Fedyanina, O. N.; Volgin, Y. V.; Jones, P. *J. Chromatogr. A* **2007**, *1155*, 2-7.

(41) Nesterenko, P. N.; Fedyanina, O. N. *J. Chromatogr. A* **2010**, *1217*, 498-505.

(42) Saini, G.; Gates, R.; Asplund, M. C.; Blair, S.; Attavar, S.; Linford, M. R. *Lab Chip* **2009**, *9*, 1789-1796.

(43) Saini, G.; Yang, L.; Lee, M. L.; Dadson, A.; Vail, M. A.; Linford, M. R. *Anal. Chem.* **2008**, *80*, 6253-6259.

(44) Saini, G.; Wiest, L. A.; Herbert, D.; Biggs, K. N.; Dadson, A.; Vail, M. A.; Linford, M. R. *J. Chromatogr. A* **2009**, *1216*, 3587-3593.

(45) Yang, L.; Lua, Y. Y.; Tan, M.; Scherman, O. A.; Grubbs, R. H.; Harb, J. N.; Davis, R. C.; Linford, M. R. *Chem. Mater.* **2007**, *19*, 1671-1678.

(46) Yang, L.; Vail, M. A.; Dadson, A.; Lee, M. L.; Asplund, M. C.; Linford, M. R. *Chem. Mater.* **2009**, *21*, 4359-4365.

(47) Kirkland, J. J.; Langlois, T. J.; DeStefano, J. J. *Am. Lab.* **2007**, *8*, 18-21.

(48) Saini, G.; Jensen, D. S.; Wiest, L. A.; Vail, M. A.; Dadson, A.; Lee, M. L.; Shutthanandan, V.; Linford, M. R. *Anal. Chem.* **2010**, *82*, 4448-4456.

(49) Ramanathan, T.; Fisher, F. T.; Ruoff, R. S.; Brinson, L. C. *Chem. Mater.* **2005**, *17*, 1290-1295.

(50) Jee, A.-Y.; Lee, M. *Curr. Appl. Phys.* **2009**, *9*, e144-e147.

(51) Li, K.; Stöver, H. D. H. *J. Polym. Sci., Part A: Polym. Chem.* **1993**, *31*, 3257-3263.

(52) Downey, J. S., McMaster University, 2000.

(53) Li, L.; Song, H.; Chen, X. *Mater. Lett.* **2008**, *62*, 179-182.

(54) Jawhari, T.; Roid, A.; Casado, J. *Carbon* **1995**, *33*, 1561-1565.

(55) Ferrari, A. C.; Robertson, J. *Phys. Rev. B: Condens. Matter Mater. Phys.* **2000**, *61*, 14095.

(56) *Properties of Amorphous Carbon*; Silva, S. R. P., Ed.; IEE: London, U.K, 2003; Vol. 29.

(57) Matthews, M. J.; Pimenta, M. A.; Dresselhaus, G.; Dresselhaus, M. S.; Endo, M. *Phys. Rev. B: Condens. Matter Mater. Phys.* **1999**, *59*, R6585.

(58) Nistor, L. C.; Van Landuyt, J.; Ralchenko, V. G.; Obraztsova, E. D.; Smolin, A. A. *Diamond Relat. Mater.* **1997**, *6*, 159-168.

(59) Penner, N.; Nesterenko, P.; Ilyin, M.; Tsyurupa, M.; Davankov, V. *Chromatographia* **1999**, *50*, 611-620.

(60) Smith, R. M.; Burr, C. M. *J. Chromatogr. A* **1989**, *475*, 57-74.

Chapter 3: Core-Shell Particles with Carbon Cores and Nanodiamond/Polymer Shells for Mixed-Mode HPLC at Elevated Temperatures and pH 7 and 12

3.1 Abstract

We report an elevated temperature and pH study of a mixed-mode (C_{18}/anion exchange), core-shell material created by the layer-by-layer deposition of ca. 0.25 μm of poly(allylamine) (PAAm) and nanodiamond onto spherical 3.5 μm carbon particles. Longer/narrower columns were used in this study than previously reported (50 mm × 2.1 mm). Van't Hoff plots were obtained from 30 – 100 °C in regular intervals at pH 7 and pH 12 using three different classes of analytes: alkylbenzenes, tricyclic antidepressants (TCAs) and β_2-andrenergic receptor agonists. Van Deemter data were also obtained and the resulting *A*-, *B*-, and *C*-terms for the alkylbenzenes and TCA analytes are presented. All analyses were performed with water (10 mM phosphate buffer, pH 7 or 12)/acetonitrile (ACN) mobile phases. The particles showed good stability at high pH and at elevated temperatures over an extended period of time.

3.2 Introduction

Interest in elevated temperature high-performance liquid chromatography (HPLC) has increased over the past few years.[1,2] Indeed, numerous studies now show that as column temperature increases in reversed-phase HPLC, retention of analytes almost always decreases and improvement in efficiencies are not uncommon.[3,4] Temperature thus becomes an important parameter for optimizing the speed and resolution,[3,5] and sometimes even selectivity[2] of a separation. The possibility of faster separations at elevated temperatures comes as a result of enhanced transport and diffusion of analytes, and the decreased viscosity of the mobile phase reduces column back pressure. As temperatures increase, optimal flow velocities occur at higher flow rates because of an increase in the *B*-term and a concomitant decrease in the *C*-term of the van Deemter equation:

$$H = A + \frac{B}{u} + (C_S + C_M)u \qquad (3.1)$$

Accordingly, the resultant 'flattening' of the higher flow region of van Deemter curves allows an increase in the speed of a separation without sacrificing much by way of efficiency.[1,2]

Nevertheless, there seems to be a lack of consensus regarding the effects of elevated temperature on efficiency. Li and Carr[6] stated that there is an assumption that the *A*-term often does not depend on temperature, but that this is uncertain because at elevated eluent temperatures, there should be an improvement in laminar flow and lateral mixing of the analytes among different flow channels in a column. They further noted that improvements in efficiency with temperature may not be significant. Xiang and coworkers[7] observed that the effect of temperature on the *A*-term is uncertain, the *B*-term increases, and the *C*-term decreases.

Improvements to the *C*-term with temperature come from improved mass transport between phases and diffusion inside the stationary phase.[1,8] These conclusions are reasonable vis-à-vis the terms in the classical/extended expressions for the van Deemter equation as described by Giddings:[9]

$$B \propto D_M \qquad (3.2)$$

$$C_M \propto \frac{1}{D_M} \qquad (3.3)$$

$$C_S \propto \frac{1}{D_S} \qquad (3.4)$$

where D_M and D_S are the diffusion coefficients of the analyte in the mobile and stationary phases, respectively. Obviously, diffusion coefficients increase greatly with increasing temperature, which leads to a decrease of the C_M and C_S terms. Xiang further noted that elevated temperatures are beneficial for accelerating analysis times without much efficiency loss.[7] While not contradictory, the papers by Li and Xiang suggest that there is currently no complete theory on the effects of temperature on efficiency. Also the authors of both papers used complex adsorbents composed of porous and nonporous zirconia with poly(butadiene) layers. It is possible that conformational changes in the structure of bonded polymer layers may increase with temperature, affecting interactions between analytes and the bonded phase with these zirconia-based materials.

Various studies[10-13] indicate that better efficiencies are obtained at elevated temperatures, but that there is a need for temperature optimization[11,13,14] to obtain the most efficient separation. For example, de Villiers and coworkers[15] showed that efficiencies improved when elevated temperatures were used. This was attributed to reduced contributions of secondary equilibria to plate height. Teutenberg[4] noted that it has been reported that separation efficiency will increase at higher temperatures, but this hypothesis cannot be supported by the van Deemter equation. He

also noted that there is no absolute increase in efficiency when temperature is increased because it is not possible to lower the minimum of the van Deemter curve with temperature.[2] In real chromatographic systems the effect of temperature depends on many experimental details, including column size and geometry, effectiveness of eluent pre-heating and post-cooling, chemical structure of the stationary phase, and even on differences in thermal expansion coefficients between column housings and adsorbents.[16-18] Interest in exploiting the favorable characteristics of elevated temperature LC has been directed towards the separation and analysis of biological macromolecules.[19]

Mobile phase characteristics are altered at elevated temperatures. This effect is especially significant for water, where as temperature increases water becomes less polar due to a change in its static permittivity.[20] Hence, water-only applications have become a possibility for elevated temperature HPLC, where these conditions are not only environmentally friendly, but allow the use of other detection methods,[21-23] including flame ionization detection (FID).[24]

An analysis often used to yield information regarding both the thermodynamics and the consistency of the retention mechanism in elevated temperature separations is based on the van't Hoff equation:[25]

$$\ln k = \frac{-\Delta H^\circ}{RT} + \frac{\Delta S^\circ}{R} + \ln \Phi \qquad (3.5)$$

where k is the retention factor, T is the temperature in Kelvin, R is the ideal gas constant, Φ is the phase ratio, and ΔH° and ΔS° are the enthalpy and entropy of transfer of the analyte from the mobile phase to the stationary phase, respectively. Accordingly, a van't Hoff plot is a plot of ln k vs. 1/T, where the slope yields ΔH° and the intercept gives ΔS° if Φ is known.

The linearity of a van't Hoff plot may be an indication of an unchanging retention mechanism at different temperatures, although there is some question regarding the validity of

this statement.[26] A nonlinear van't Hoff plot points to a change in retention mechanism over the given temperature range.[25] The magnitude and sign of $\Delta H°$ should be a reflection of the interaction between the analyte and the stationary phase; the greater and more negative $\Delta H°$, the more the analyte interacts with the stationary phase. A common set of analytes used for this type of study is the alkylbenzenes.[27,28]

The development and study of stationary phases/supports that are stable at high pH and elevated temperature is a current topic in HPLC. Significant interest exists in this area because of the need to separate basic analytes, many of which are important to the pharmaceutical industry.[29,30] Such compounds often show lower retention[14,31] and greater tailing if the separation is performed at a more neutral pH.[32,33] Hence, it would be advantageous for a column to exhibit stability at high pH values. McCalley stated that the improvements in efficiency due to elevated temperature under low to moderate pH in the separation of basic compounds "are so considerable that more thought should be given to carrying out analysis of basic compounds at elevated temperature and the development of columns which are stable at these temperatures".[34] Evidently, separations using eluents at extreme pH values and at elevated temperature are a current challenge for reversed-phase HPLC.

This chapter is a study of a new core-shell phase that shows good stability at both elevated temperature and high pH (pH 12). These particles are created by coating spherical carbon core particles with poly(allylamine) (PAAm) and nanodiamond in an alternating layer-by-layer deposition, as first outlined by Saini and coworkers,[35] by Wiest and coworkers[36] and by Hung and coworkers.[37] The particles were given the desired functionality by reacting the final PAAm-terminated surface with a mixture of 1,2-epoxyoctadecane (to contribute C_{18} moieties) and 1,2,7,8-diepoxyoctane (for crosslinking). We have previously reported the deposition and

reactivity of PAAm onto diamond particles for solid phase extraction[38,39] and onto patterned silicon substrates for lab-on-a-chip type devices.[40] In this study we perform separations of alkylbenzenes and tricyclic antidepressants (TCAs). Van't Hoff studies are performed from 30 to 100 °C, and van Deemter curves are obtained at pH 7 and 12. A van Deemter study at 22, 40, 60, and 80 °C was also performed with TCA analytes. This work indicates that our mixed-mode (C_{18}/anion-exchange) phase, which is formed by deposition of ca. 0.25 μm of poly(allylamine) (PAAm) and nanodiamond onto spherical 3.5 μm carbon particles, can perform efficient separation of basic analytes at elevated temperature and pH. Longer/narrower columns (50 mm × 2.1 mm) were used in this study than previously reported (30 mm × 4.6 mm) and each separation was performed with aqueous 10 mM phosphate buffer (pH 7 or 12)/acetonitrile (ACN) mobile phases.

Work on diamond-based stationary phases for liquid chromatography has also been performed by Nesterenko and coworkers, who employed sintered, microdispersed detonation nanodiamond for normal phase HPLC separations[41] and ion exchange chromatography.[42] They showed baseline separations of various compounds using their normal phase material and achieved efficiencies of 15,400 plates/m. Their peaks showed considerable asymmetry, especially at longer retention times. In more recent work they have achieved 45,300 plates/m.[43]

3.3 Materials and Methods

3.3.1 Reagents and Materials

Water (18 MΩ resistance, filtered using a Milli-Q Water System, Millipore, Billerica, MA); methanol, (HPLC grade, Fisher Scientific, Fair Lawn, NJ); isopropyl alcohol (ChromAR, Mallinkrodt Baker); acetonitrile (ACN) (HPLC grade, EMD, Gibbstown, NJ); monosodium phosphate monohydrate, disodium phosphate heptahydrate, trisodium phosphate dodecahydrate, benzenoid hydrocarbon kit, doxepin HCl, imipramine HCl, amitriptyline HCl, clomipramine HCl, cimaterol, tulobuterol HCl, mabuterol, HCl and mapenterol HCl (Sigma Aldrich, St Louis, MI).

3.3.2 Particle Preparation and Characterization

Particles were prepared via a layer-by-layer (LbL) procedure, as described previously,[36] to yield particles with carbon cores and poly(allylamine)/nanodiamond shells (see Figure 3.1). The carbon cores were created by oxidizing, carbonizing and acid washing 5 µm polydivinylbenzene spheres as described by Hung et al.[37] The core diameter was 3.5 µm and the final particle size was 4.0 µm. The columns used were from the same batch of synthesized particles. Particle sizes were measured using a scanning electron microscope: Helios Nanolab SEM FEG (FEI Corporation, Hillboro, OR) and BET isotherm measurements were taken using a Tristar II (Micromeritics, Norcross, GA). Columns packed with particles made in a procedure similar to those previously reported[36,37] are marketed as the Flare mixed-mode, C18/anion exchange column (Diamond Analytics, Orem, UT.)

3.3.3 HPLC

We used an Infinity 1290 chromatograph (Agilent, Santa Clara, CA) equipped with a binary pump, autosampler, column heater capable of heating up to 100 °C, and a UV/Vis diode array detector paired with a 10 mm Max-Light flow cell, all operating on OpenLab CDS, ChemStation Edition (Rev. C.01.03.37) software. Alkylbenzenes were analyzed using 45:55 10 mM aqueous phosphate/ACN buffer (pH 7 and 12) mobile phases. The TCAs were analyzed with 60:40 10 mM aqueous phosphate/ACN buffer (pH 7 and 12) mobile phases. The β_2-agonist mixture was analyzed with a 70:30 10 mM aqueous phosphate/ACN buffer (pH 12) mobile phase. The alkylbenzene mixture contained butylbenzene, hexylbenzene, and phenyloctane (octylbenzene) – all had linear alkyl chains, each with a ca. 1 mg/mL concentration. They were dissolved in ACN. Some TCAs, i.e., doxepin, imipramine, amitriptyline and clomipramine, each with concentrations of ca. 0.3 mg/mL were dissolved in 70:30 water 10 mM phosphate/ACN buffer (pH 12). A mixture of β_2-andrenergic receptor agonists (β_2-agonists) (cimaterol, tulobuterol, mabuterol, and mapenterol) each at ca. 0.2 mg/mL were dissolved in 50:50 10 mM aqueous phosphate/ACN buffer (pH 12).

Van Deemter curves were obtained with the TCA mixture at 22, 40, 60, and 80 °C. Injections (0.5 μL) were made with the autosampler. Data for the van't Hoff plots were obtained from 30 – 100 °C in 10 °C increments for the alkylbenzenes, TCAs, and the β_2-agonists. The mobile phase was preheated with a capillary in-line heater prior to entering the column. Data were plotted as van Deemter and van't Hoff plots, where van Deemter data were fitted using a least squares fit in Microsoft Excel 2010.

3.4 Results and Discussion

3.4.1 Particle Characteristics

Spherical carbon cores prepared in our lab were functionalized with porous PAAm/nanodiamond bilayer shells yielding core-shell particles with an average particle diameter of 4 μm, as described previously.[36,37] Figure 3.1A shows an SEM micrograph of the bare carbonized particles. The dimples seen on these particles are likely caused from particle fusion and subsequent separation during the carbonization process. Figure 3.1B shows the particles after deposition of seven PAAm/nanodiamond bilayers and Figure 3.1C shows the particles after deposition of 15 bilayers. These micrographs show uniform shell growth. BET surface area analysis showed that the surface area of these particles was 14.6 m^2/g. While this is a low surface area for a chromatographic support, it appeared adequate for good chromatography when relatively low analyte concentrations and injection volumes were used.

3.4.2 Effect of Mobile Phase pH on the Separations of Alkylbenzenes

Using columns packed with the particles prepared in the previous section, separations of ethylbenzene, butylbenzene, hexylbenzene and octylbenzene were performed (see Figure 3.2). These stationary phases contain many amine groups from the PAAm precursor. At pH 7 the amines are mostly protonated as the pK_a of a molecular analog of PAAm (allylamine) is 9.49. At pH 12, the reverse will occur, namely the amines from the poly(allylamine) will be mostly deprotonated.

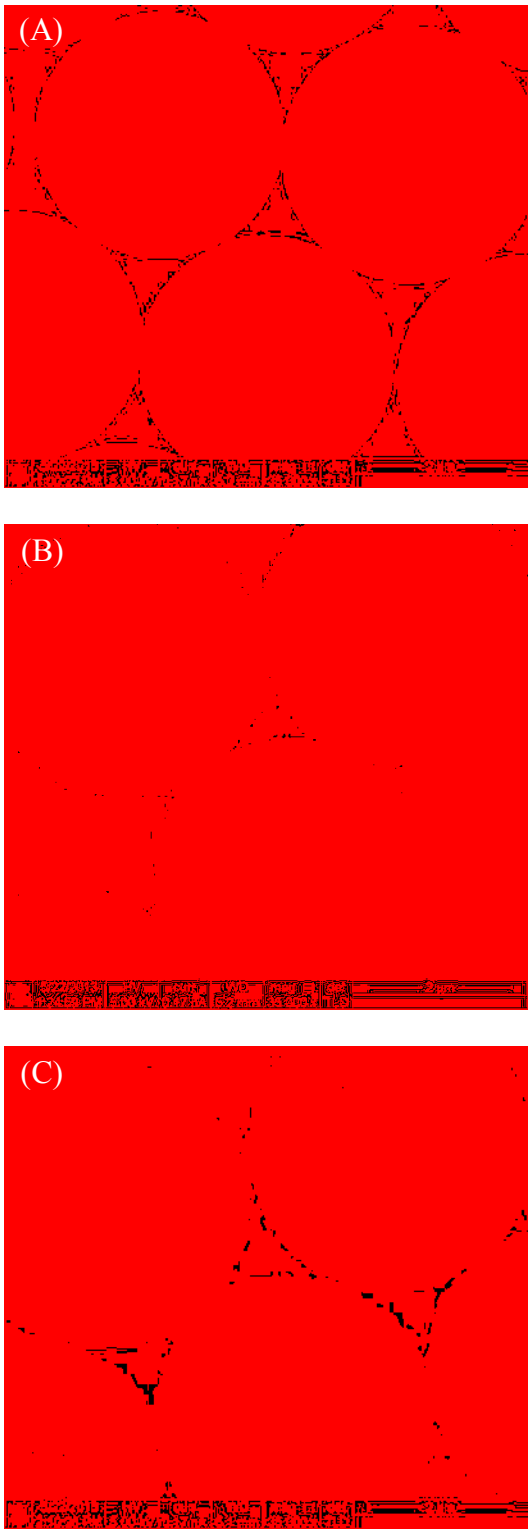

Figure 3.1 SEM of cores and core-shell particles after deposition of (A) 0, (B) 7, and (C) 15 bilayers.

We tested the effects of mobile phase pH, i.e., protonation state of the column, on retention using the alkylbenzenes as probes. Separations performed at pH 7 and 12 were very similar (see Figure 3.2). Indeed, Table 3.1 shows that the selectivities, α, of the separations are nearly identical. The retention of the analytes in the pH 12 separation is ca. 3 % greater than in the pH 7 separation. Somewhat greater retention is expected at elevated pH because the column is deprotonated (more hydrophobic). The most significant difference between the separations was efficiency, which decreased by ca. 6 – 8 % at pH 7 compared to pH 12. Perhaps the protonated (pH 7) stationary phase has greater heterogeneity.

To further understand these separations, van Deemter studies were performed at pH 7 and pH 12 (see Figure 3.3). The results are as expected. For example, the van Deemter curves for octylbenzene as analyte are very similar. The greatest difference between the curves is in their *C*-terms, which may be due to the more swollen (thicker) stationary phase likely present at lower pH. The *A*-term for the pH 7 separation is slightly larger, which may also be a result of a more swollen stationary phase. The *B*-terms are essentially identical. Thus, it appears that the separation of neutral analytes is slightly more efficient at elevated pH. Table 3.2 shows the *A*-, *B*-, and *C*-terms for butyl-, hexyl-, and octylbenzene at pH 12. The *A*- and *C*-terms decrease with increased retention of the analytes, and the *B*-terms and optimal flow rates increase with increased retention. With these nonpolar analytes, increased retention correlates with improved efficiency.

Table 3.1 Separation of alkylbenzenes at pH 7 and 12.

pH 7	k	α*	$T_{5\%}$	$A_{10\%}$	N/m
Ethylbenzene	0.68	-	1.38	1.47	31558
Butylbenzene	1.41	2.07	1.30	1.43	41937
Hexylbenzene	3.07	2.17	1.31	1.41	60785
Octylbenzene	6.99	2.28	1.25	1.23	78280
pH 12	k	α*	$T_{5\%}$	$A_{10\%}$	N/m
Ethylbenzene	0.70	-	1.43	1.46	33289
Butylbenzene	1.46	2.08	1.25	1.42	45435
Hexylbenzene	3.17	2.17	1.30	1.39	65225
Octylbenzene	7.17	2.26	1.25	1.21	82559

*Selectivities calculated as the ratio of *k* for the analyte divided by *k* for the previously eluting analyte.

Table 3.2 Van Deemter terms for the alkylbenzenes and TCAs at pH 12.

	Butylbenzene	Hexylbenzene	Octylbenzene	Doxepin	Imipramine	Amitriptyline	Clomipramine
A	14.05	10.11	9.22	11.2	9.0	9.5	9.8
B	0.078	0.100	0.105	0.027	0.035	0.041	0.043
C	103.26	54.29	23.60	98.5	63.2	67.1	45.1
H_{min}	19.7	14.8	12.4	14.4	12.0	12.8	12.6
u_{min}	0.03	0.043	0.067	0.017	0.023	0.025	0.031

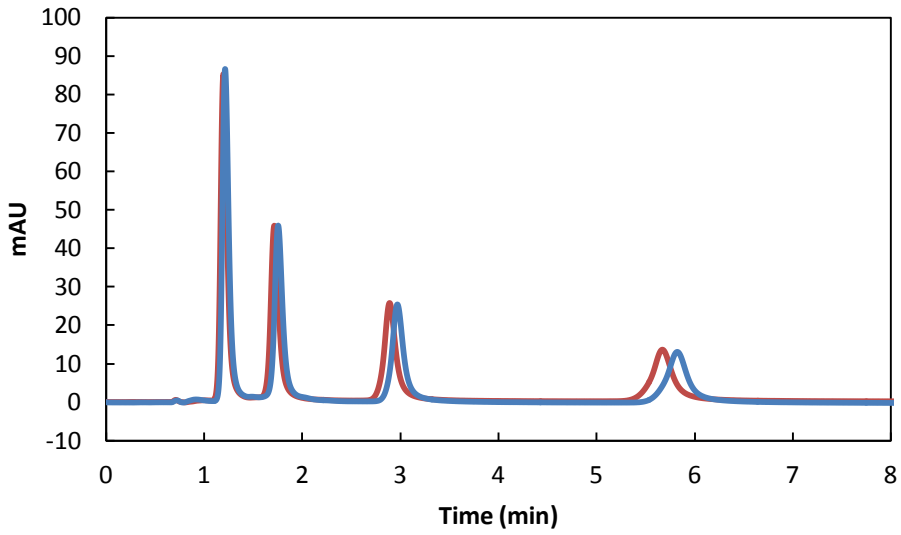

Figure 3.2 Chromatograms of alkylbenzenes separated at pH 7 and 12 using 45:55 10 mM aqueous phosphate/ACN buffer mobile phases at pH 7 (red) and 12 (blue)/ACN mobile phases at 22 °C, 0.13 mL/min.

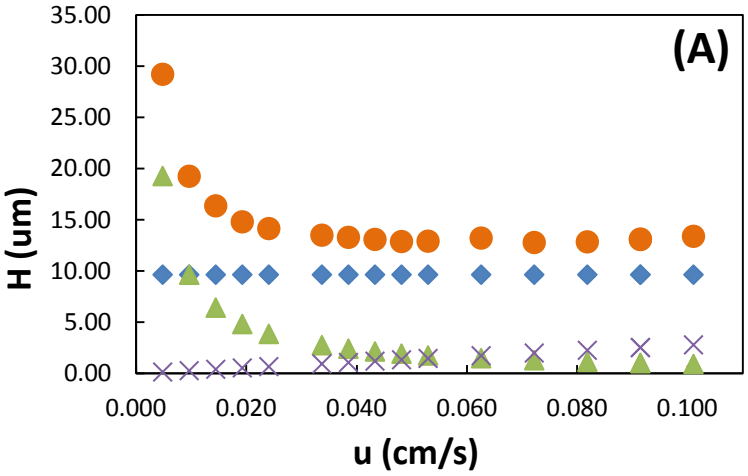

A	9.63	µm
B	0.09	µm·cm/s
C	27.56	µm·s/cm
H_{min}	12.83	µm
h_{min}	3.2	
u_{min}	0.058	cm/s
Flow $Rate_{min}$	0.12	mL/min

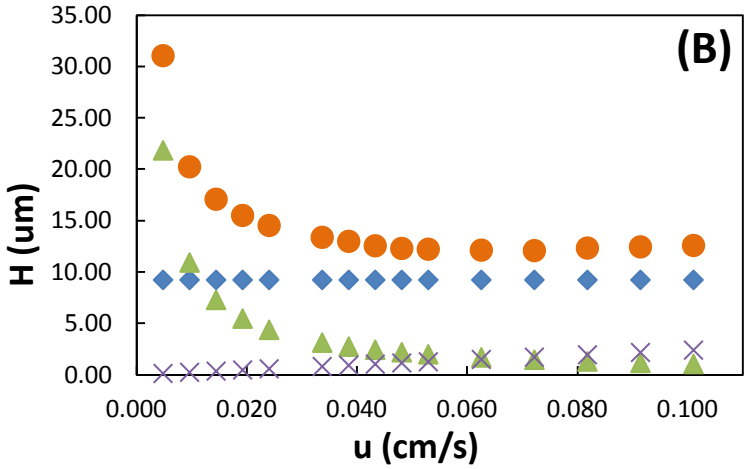

A	9.22	µm
B	0.1	µm·cm/s
C	23.6	µm·s/cm
H_{min}	12.36	µm
h_{min}	3.09	
u_{min}	0.067	cm/s
Flow $Rate_{min}$	0.14	mL/min

Figure 3.3 Van Deemter curves performed at (A) pH 7 and (B) pH 12 for octylbenzene.

3.4.3 Effect of Mobile Phase pH on the Separation of TCAs and van Deemter Analysis

While the separations performed at pH 7 and pH 12 were very similar for the alkylbenzene analytes, the effects of pH on the separation of the tricyclic antidepressants (TCAs) was drastic. Separations performed at pH 7 (see Figure 3.4) showed significant tailing ($A_{10\%}$ ca. 2.7), reduced retention, where the first two analytes coeluted, and relatively poor efficiencies (ca 14,000 N/m). As McCalley has noted,[30,44-46] the separation of basic analytes at moderate pH results in shorter elution times and greater tailing. In contrast, the pH 12 separation showed decreased tailing ($A_{10\%}$ ca. 1.8 – 2.0), increased retention, and substantially improved efficiencies (ca. 60,000 – 80,000 N/m).

Van Deemter curves were obtained at pH 12 for doxepin, imipramine, amitriptyline and clomipramine. Representative van Deemter plots for imipramine and clomipramine are shown in Figure 3.5. Table 3.2 gives the van Deemter data for the four TCAs. The optimal plate heights for the best performing TCAs, imipramine, amitriptyline, and clomipramine, are about the same as H_{min} for octylbenzene, the best performing alkylbenzene, albeit under different mobile phase conditions.

The trends in the *B*- and the *C*-terms for the two sets of analytes give results that are not expected from van Deemter theory. In the van Deemter equation, $B=2\gamma D_M$. Accordingly, one would expect an increase in *B* with increasing diffusion coefficient (decreasing size of an analyte). For the alkylbenzenes, the *B*-term *increases* with increasing analyte size. Also, from van Deemter theory, we would expect similar *B*-terms from the TCAs because of their similar sizes. This was not the case. The *B*-terms vary rather substantially. For both sets of analytes, the *B*-term appears to increase with retention time, however, the *B*-term has no time dependence. The *C*-terms for these analytes also appear not to follow van Deemter theory. Both C_S and C_M

are inversely proportional to analyte diffusion coefficients. Accordingly, *C* should increase with larger analyte size, yet we observe the opposite effect. At this time we do not fully understand these effects.

Table 3.1 shows that the tailing factors and asymmetries for the alkylbenzenes are all below 1.5 and as low as ca. 1.2. In contrast, the TCAs show considerably more tailing – tailing factors and asymmetries at pH 12 from ca. 1.7 – 2.0. These results suggest an increased number of secondary interactions between the TCAs and the stationary phase, which would be expected given the increased complexity of these analytes. It is also interesting to note that the optimal linear velocity for the TCA analytes is less than half of the optimal linear velocity for octylbenzene. This is attributed to the larger *C*-terms of the TCAs. McCalley noted this effect, observing that optimal flow rates decreased for basic analytes, and tailing increased as compared to neutral analytes.[34]

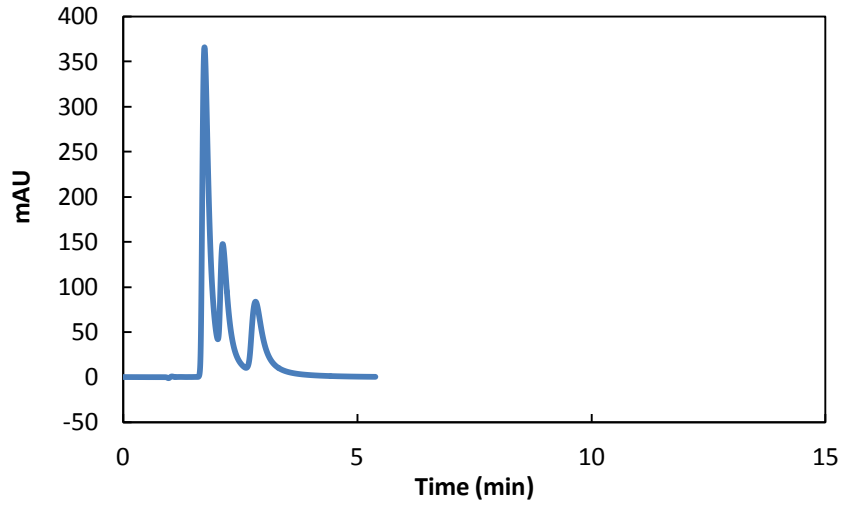

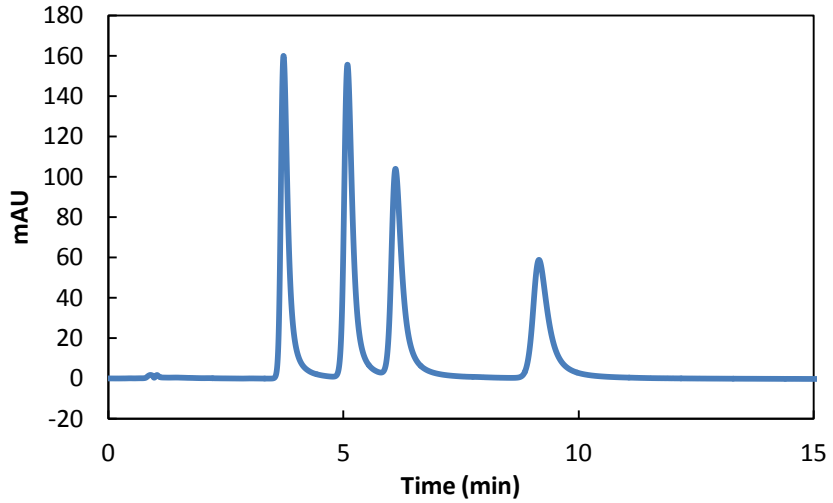

pH 7	k	α	$T_{5\%}$	$A_{10\%}$	N/m
Doxepin Imipramine	0.79	-	-	-	14523
Amitriptyline	1.20	1.50	2.92	2.67	14340
Clomipramine	1.92	1.61	2.50	2.67	12863
pH 12	k	α	$T_{5\%}$	$A_{10\%}$	N/m
Doxepin	3.16	-	1.92	2.02	60449
Imipramine	4.68	1.48	1.69	1.76	77899
Amitriptyline	5.82	1.24	1.71	1.93	73699
Clomipramine	9.23	1.59	1.78	1.95	78253

Figure 3.4 Chromatograms of TCAs at pH 7 and 12 using 60:40 10 mM aqueous phosphate/ACN mobile phases at 22 °C, 0.1 mL/min.

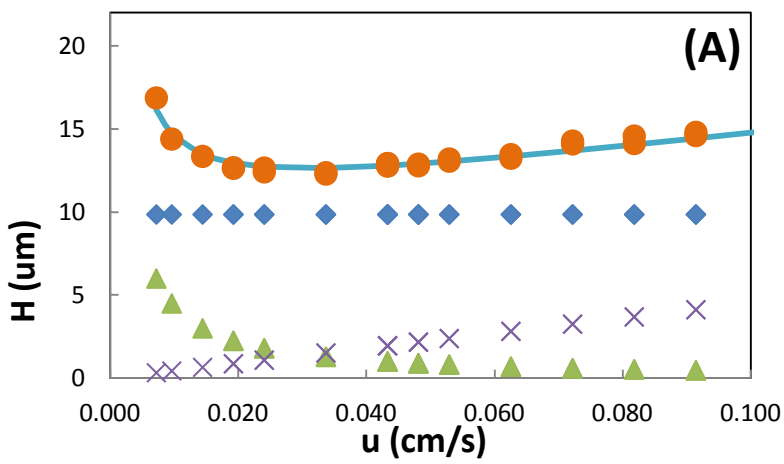

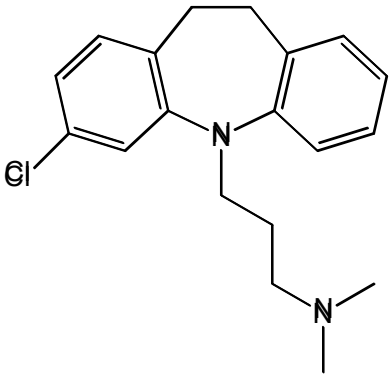

A	9.85	µm
B	0.04	µm·cm/s
C	45.05	µm·s/cm
H_{min}	12.64	µm
h_{min}	3.16	
u_{min}	0.031	cm/s
Flow $Rate_{min}$	0.06	mL/min

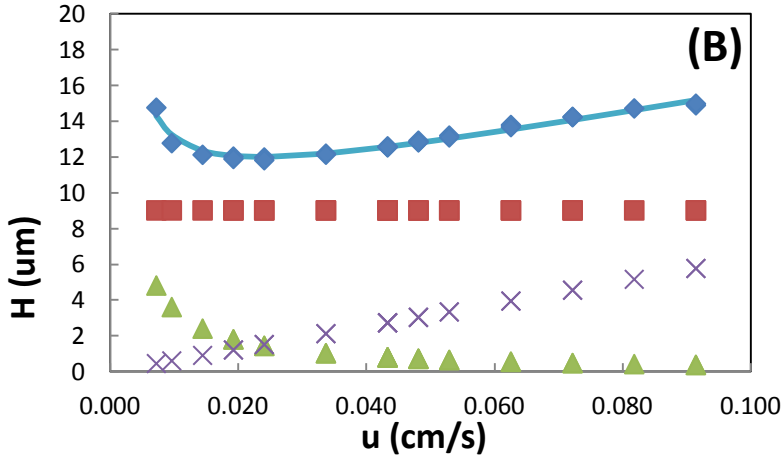

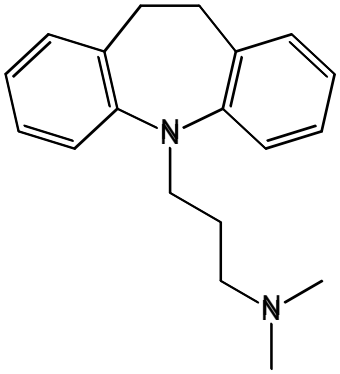

A	9.02	µm
B	0.03	µm·cm/s
C	63.16	µm·s/cm
H_{min}	11.99	µm
h_{min}	3.00	
u_{min}	0.067	cm/s
Flow $Rate_{min}$	0.05	mL/min

Figure 3.5 Van Deemter curves of (A) clomipramine and (B) imipramine performed at pH 12. Structures of the analytes are given on the right.

3.4.4 Effect of Temperature on TCAs and their van Deemter Minima

Van Deemter plots were obtained at 22, 40, 60, and 80 °C for the TCA mixture. The resulting *A*-, *B*- and *C*-terms, and optimal linear velocities and plate heights are given in Table 3.3. The *B*-term increased with increasing temperature, which is expected because of the linear dependence of *B* on D_M, and the exponential dependence of D_M on temperature.[1,2,16] The *A*-terms were roughly constant with temperature. From 22 – 40 °C, we observed a decrease in the *C*-term, which would be expected because of its inverse dependence on analyte diffusion coefficients; however, each *C*-term increased at 80 °C. It is not entirely clear why this latter change occurs. The optimal linear velocity always increased with increasing temperature, which is also expected.[1,2,12,16] Optimal plate heights increased with temperature (efficiencies decreased), which is consistent with Teutenberg's statement that an increase in efficiency is not possible with temperature according to van Deemter theory.[1,2]

3.4.5 Van't Hoff Analysis of Alkylbenzenes from 30 – 100 °C

We performed a van't Hoff analysis from 30 – 100 °C using alkylbenzene analytes (butyl-, hexyl-, and octylbenzene). Measurements were taken in triplicate every 10 °C with a 45:55 10 mM phosphate/ACN (pH 7 and 12) mobile phase. The resulting van't Hoff plots of ln *k* vs. 1/T at both pH 7 and 12 appeared to consist of two linear regions (see Figure 3.6). The transistion point between these two regions was at ca. 60 °C. Similar transitions are often observed with C_{18} type phases and are attributed to phase transitions or changes in retention mechanisms.[18]

Table 3.3 Van Deemter analysis of TCAs performed at 22, 40, 60, and 80 °C. The mobile phase was the same in these experiments (60:40 10 mM aqueous phosphate/ACN, pH 12).

Doxepin	22	40	60	80
A	7.56	8.55	8.41	8.55
B	0.05	0.06	0.08	0.11
C	112.9	80.5	81.0	95.6
u_{min}	0.021	0.028	0.031	0.034
H_{min}	12.3	13.0	13.4	15.0
Imipramine	22	40	60	80
A	5.37	6.70	6.75	5.39
B	0.06	0.07	0.08	0.14
C	91.6	60.1	59.0	79.8
u_{min}	0.025	0.034	0.038	0.041
H_{min}	10.0	10.8	11.2	12.0
Amitriptyline	22	40	60	80
A	5.84	6.86	6.66	5.39
B	0.06	0.08	0.10	0.14
C	91.8	62.3	61.5	79.8
u_{min}	0.026	0.036	0.040	0.041
H_{min}	10.7	11.3	11.5	12.0
Clomipramine	22	40	60	80
A	6.64	6.53	5.96	2.86
B	0.07	0.09	0.12	0.19
C	56.6	51.5	51.3	83.7
u_{min}	0.034	0.042	0.048	0.048
H_{min}	10.5	10.9	10.8	10.9

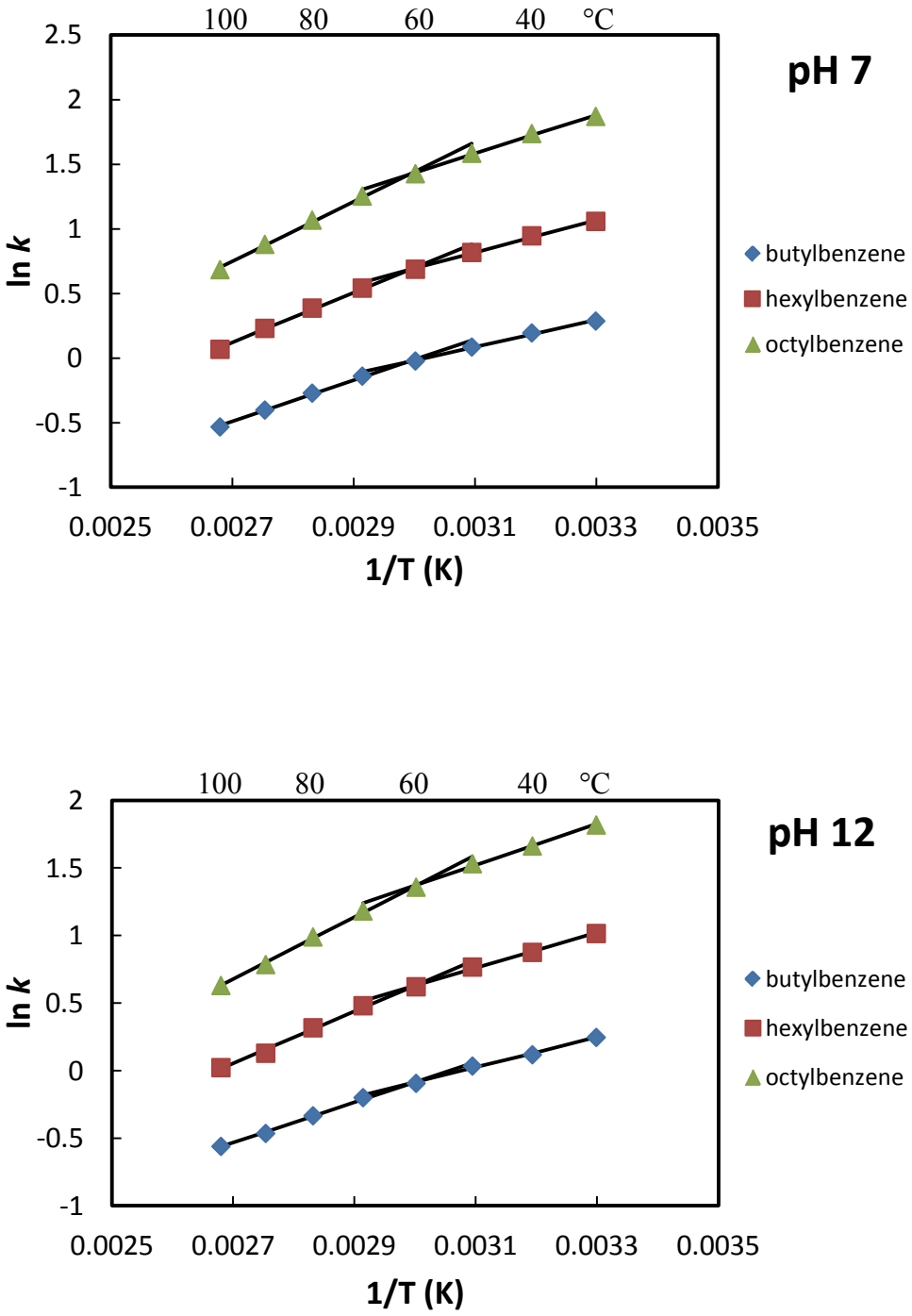

Figure 3.6 Van't Hoff plots from 30 – 100 °C for alkylbenzene analytes.

The enthalpy of transfer of an analyte from the mobile phase to the stationary phase, $\Delta H°$, is easily calculated from the slope of a van't Hoff plot. Table 3.4 gives the enthalpies of transfer for the lower (30 – 60 °C) and higher (60 – 100 °C) temperature regions of the plots. As expected, in both temperature ranges, $\Delta H°$ becomes steadily more negative with increasing alkyl chain-length. Interestingly, the lower temperature region shows smaller enthalpies compared to the elevated temperature region. An increase in enthalpy implies greater interactions between both the analyte and the stationary phase, and perhaps a greater degree of absorption of the analyte in the stationary phase, which, by expulsion of the analyte, would allow more hydrogen bonding to take place in the mobile phase. Thus, these results are consistent with a stationary phase that is less accessible to the analyte at lower temperatures and more accessible at higher temperatures. Also of note: there appeared to be no significant differences between the $\Delta H°$ data obtained at pH 7 and pH 12 for the alkylbenzenes, which is consistent with the similar retention times for the analytes (see Figure 3.2).

3.4.6 Van't Hoff Analysis of TCAs and β_2-Andrenergic Receptor Agonists from 30 – 100 °C

Van't Hoff analysis was also performed on four TCAs and four β_2-agonists. All of these compounds are basic analytes and were separated at pH 12. The TCA mixture, containing doxepine, imipramine, amitripyline, and clomipramine, was analyzed with the same mobile phase used in the previous experiments (60:40 10 mM phosphate/ACN, pH 12). The β_2-agonist mixture, containing cimaterol, tulobuterol, mabuterol, and mapenterol, were separated using a 70:30 10 mM phosphate/ACN (pH 12) mobile phase. As before, measurements were taken in triplicate every 10 °C from 30 – 100 °C (see Figures 3.7 and 3.8).

Table 3.4 Enthalpies of transfer for three alkylbenzenes at two pH values, four TCAs, and four β_2-agonists in the two linear temperature regions of their respective van't Hoff plots. Analytes are arranged based the magnitudes of their $\Delta H°_{60\text{-}100\ °C}$ values. Note that the data from the different classes of analytes were obtained under different mobile phase conditions, and so are not directly comparable.

	$\Delta H°_{30\text{-}60\ °C}$ (kJ/mol)	$\Delta H°_{60\text{-}100\ °C}$ (kJ/mol)
Octylbenzene (pH7)	-12.43	-19.18
Hexylbenzene (pH 7)	-10.39	-16.01
Butylbenzene (pH 7)	-8.69	-13.24
Octylbenzene (pH 12)	-12.67	-19.13
Hexylbenzene (pH 12)	-10.82	-16.00
Butylbenzene (pH 12)	-9.25	-12.37
Clomipramine	-8.54	-16.93
Amitriptyline	-7.41	-15.41
Imipramine	-6.21	-14.75
Doxepin	-6.59	-13.98
Mapenterol	-9.89	-16.30
Mabuterol	-8.52	-14.34
Tulobuterol	-6.64	-11.96
Cimaterol	-8.03	-10.98

As was the case for the alkylbenzenes, the TCAs and β_2-agonists generally show two linear regions with an inflection point at ca. 60 °C in their van't Hoff plots, where the transition is more pronounced for the TCAs. Once again, the higher temperature linear region shows a steeper slope than the lower temperature region, which gives a $\Delta H°$ value that is greater in magnitude (see Table 3.4) and indicates that the analytes interact more strongly with the stationary phase at elevated temperatures. This result would again be consistent with a more open/accessible stationary phase at elevated temperature.

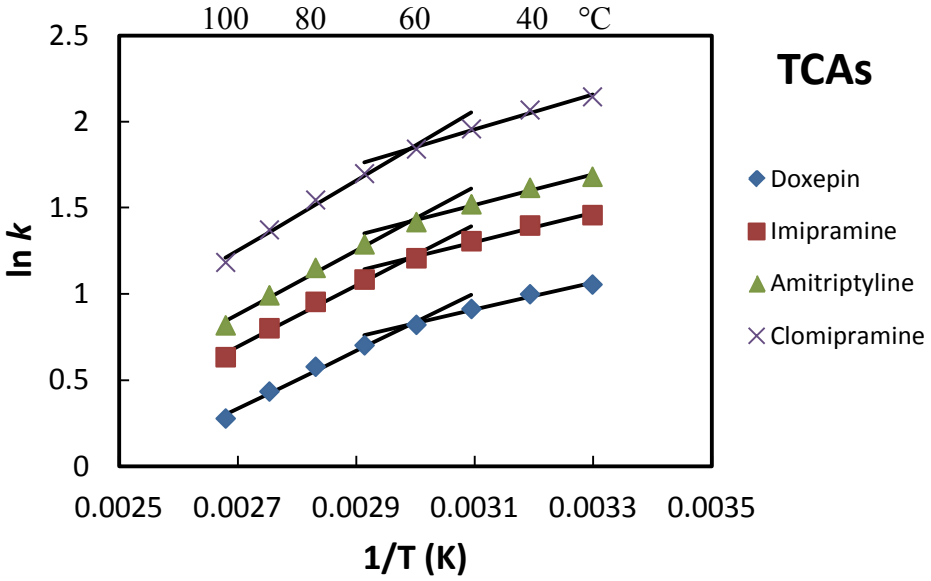

Figure 3.7 Van't Hoff plots of some TCAs from 30 – 100 °C. Note that there appears to be an inflection point around 60 °C.

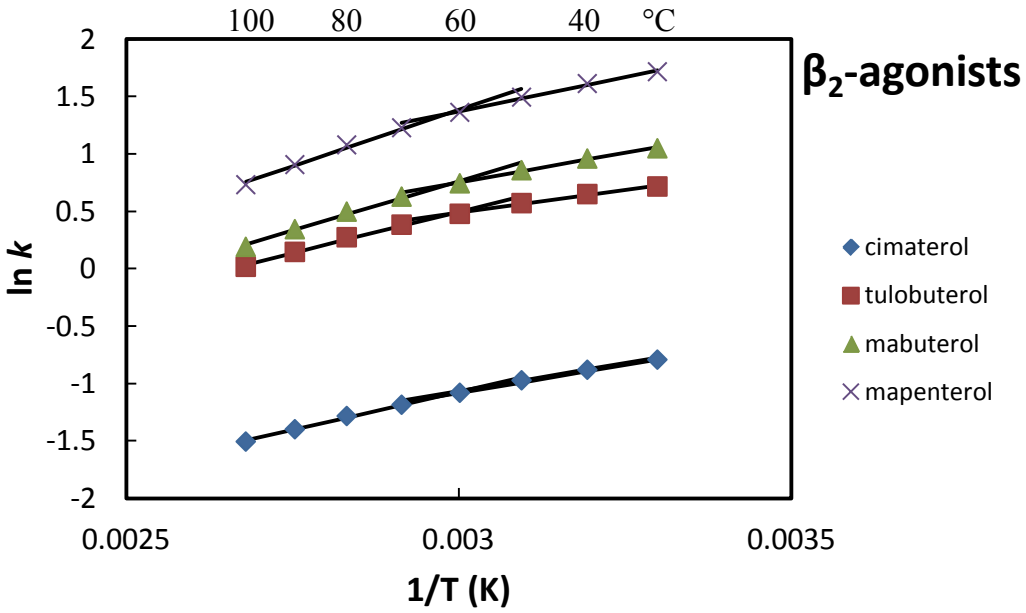

Figure 3.8 Van't Hoff plots of some β_2-Agonists from 30 – 100 °C. Note that there appears to be an inflection point around 60 °C.

3.4.7 Effect of Temperature and Flow Rate on Asymmetry and Tailing Factors for the TCAs

Both flow rate and temperature had an effect on peak tailing. Using the traditional definitions of the tailing factor

$$T_{5\%} = \frac{a+b}{2a} \quad (3.6)$$

and peak asymmetry

$$A_{10\%} = \frac{b}{a} \quad (3.7)$$

where a is the left side of the peak and b is the right side of the peak as defined by a line dropped from the apex of the peak. The instrument software determined $T_{5\%}$ and $A_{10\%}$ for our TCA separations, which showed that as temperature and flow rate increased, these factors changed (see Figure 3.9 and 3.10). When the software did not produce a value, manual attempts were not made to calculate the values in order to avoid adding error into the plots. As flow rate increased, $T_{5\%}$ and $A_{10\%}$ decreased. As temperature increased to ca. 60 °C, $T_{5\%}$ and $A_{10\%}$ also decreased and then remained fairly constant up to 100 °C – this latter statement applies more to the $A_{10\%}$ than $T_{5\%}$ results.

3.4.8 Effects of Elevated Temperature and High pH on the Column

A single Flare mixed-mode column was used to do the van't Hoff and van Deemter analyses of the alkylbenzenes (pH 7 and 12) and the TCAs (pH 12) reported herein. Over 300 injections were made on the column, and it was in use for ca. 200 h, with much of that time spent at elevated temperatures and/or at pH 12. The column did show wear over this time period. About 10% of absolute retention was lost, although selectivity remained nearly constant.

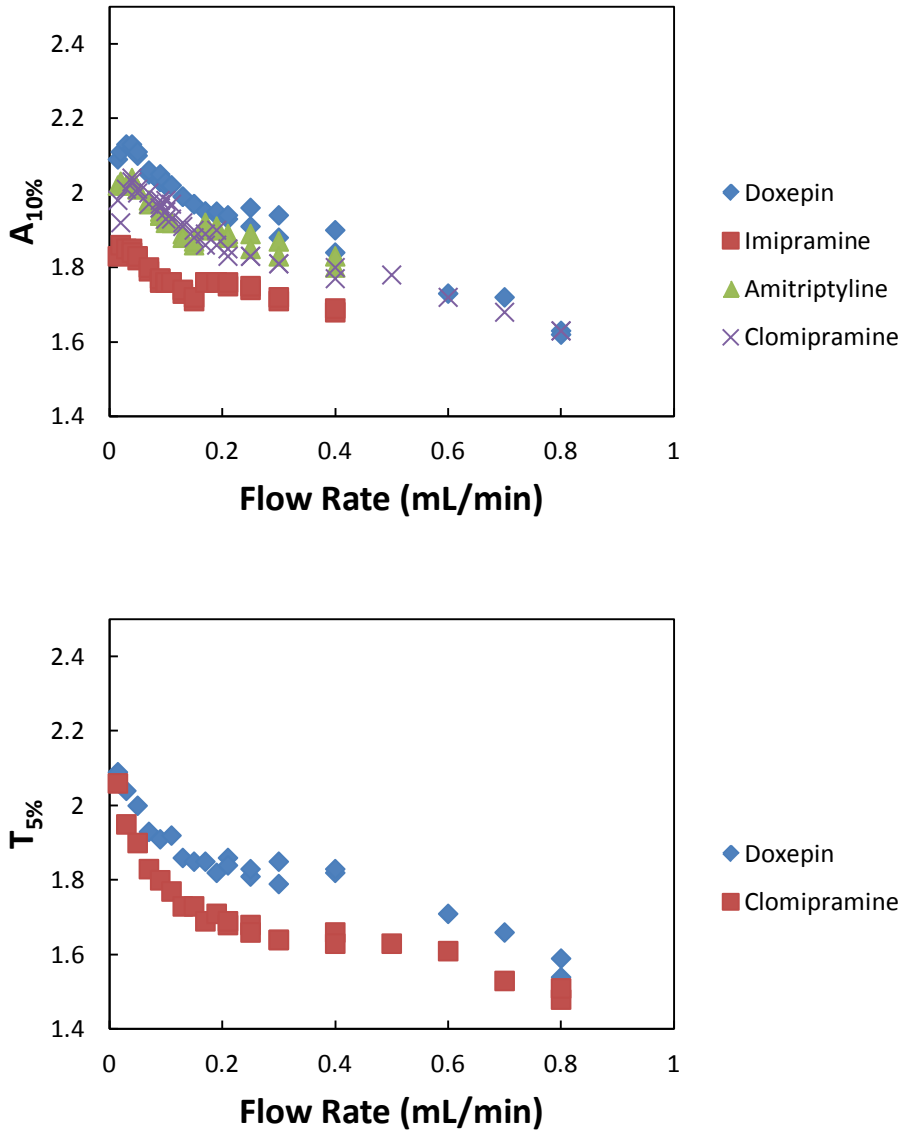

Figure 3.9 Effect of flow rate on $A_{10\%}$ and $T_{5\%}$ for four TCA analytes.

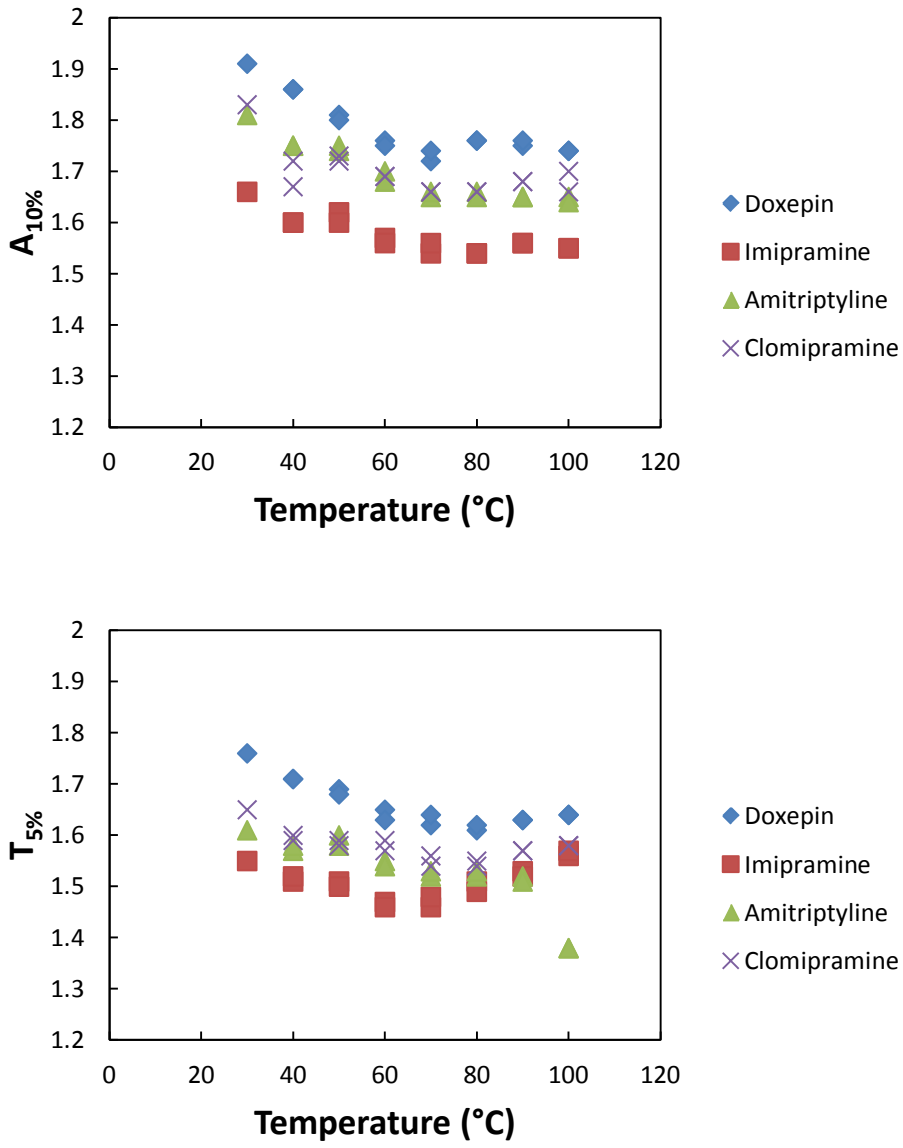

Figure 3.10 Effect of temperature on $A_{10\%}$ and $T_{5\%}$ for four TCA analytes.

A ca. 40% loss in efficiency was observed with the alkylbenzene probes. The data for the van Deemter studies reported herein were collected at the beginning of the column life while efficiencies were quite constant. The van't Hoff studies, which depend solely on retention factor, and not efficiency, were then performed. The efficiency loss corresponded to greater peak fronting, which may be due to some bed degradation and may have been caused by the repeated heating and cooling of the column. A more systematic study of column stability seems warranted.

Another column from the same batch was used to perform the van Deemter study of the TCAs at various temperatures and the van't Hoff analysis of the β_2-agonists. This column and the column referred to in the previous paragraph showed very similar retention factors and selectivities making direct comparisons possible.

3.5 Conclusions

We report the effects of temperature and flow rate on the Flare mixed-mode C_{18}/anion exchange column from Diamond Analytics using tricyclic antidepressants, β_2-andrenergic receptor agonists, and alkylbenzene analytes. The properties of these materials were explored *vis-à-vis* van Deemter and van't Hoff plots. The best efficiencies for the best performing alkylbenzenes and TCAs were comparable and greater than 80,000 N/m. As temperature increased u_{min} also increased. Some of the trends in the *B*- and *C*-terms could not be explained by van Deemter theory. The van't Hoff analysis shows a phase change in the stationary phase at ca. 60 °C for the three different analyte classes. Overall, elution times decreased and peak asymmetries improved as the analysis temperature increased, and good separations of all

analytes were obtained. Some column degradation was observed after repeated exposure to elevated temperature and pH.

ACKNOWLEDGEMENTS

I thank US Synthetic Corporation for funding this research.

3.6 References

(1) Teutenberg, T. *Chromatography Today* **2010**, *3*, 3.

(2) Teutenberg, T. High-Temperature Liquid Chromatography: A User's Guide for Method Development; RSC: London, 2010.

(3) McNeff, C. V.; Yan, B.; Stoll, D. R.; Henry, R. A. *J. Sep. Sci.* **2007**, *30*, 1672.

(4) Teutenberg, T. *Anal. Chim. Acta* **2009**, *643*, 1.

(5) Giegold, S.; Teutenberg, T.; Tuerk, J.; Kiffmeyer, T.; Wenclawiak, B. *J. Sep. Sci.* **2008**, *31*, 3497.

(6) Li, J.; Carr, P. W. *Anal. Chem.* **1997**, *69*, 837.

(7) Xiang, Y.; Yan, B.; Yue, B.; McNeff, C. V.; Carr, P. W.; Lee, M. L. *J. Chromatogr. A* **2003**, *983*, 83.

(8) Greibrokk, T.; Andersen, T. *J. Sep. Sci.* **2001**, *24*, 899.

(9) Giddings, J. C. Dynamics of Chromatography: Principles and theory; M. Dekker, 1965.

(10) Antia, F. D.; Horváth, C. *J. Chromatogr. A* **1988**, *435*, 1.

(11) Dolan, J. W.; Snyder, L. R.; Wolcott, R. G.; Haber, P.; Baczek, T.; Kaliszan, R.; Sander, L. C. *J. Chromatogr. A* **1999**, *857*, 41.

(12) Guillarme, D.; Heinisch, S.; Rocca, J. L. *J. Chromatogr. A* **2004**, *1052*, 39.

(13) Molander, P.; Gundersen, T. E.; Haas, C.; Greibrokk, T.; Blomhoff, R.; Lundanes, E. *J. Chromatogr. A* **1999**, *847*, 59.

(14) Gagliardi, L. G.; Castells, C. B.; Ràfols, C.; Rosés, M.; Bosch, E. *Anal. Chem.* **2006**, *78*, 5858.

(15) de Villiers, A.; Cabooter, D.; Lynen, F.; Desmet, G.; Sandra, P. *J. Chromatogr. A* **2009**, *1216*, 3270.

(16) Jensen, D. S.; Teutenberg, T.; Clark, J.; Linford, M. R. *LC GC N. Am.* **2012**, *30*, 850.

(17) Jensen, D. S.; Teutenbere, T.; Clark, J.; Linford, M. R. *LC GC N. Am.* **2012**, *30*, 992.

(18) Jensen, D. S.; Teutenberg, T.; Clark, J.; Linford, M. R. *LC GC N. Am.* **2012**, *30*, 1052.

(19) Chen, H.; Horváth, C. *Anal. Methods Instrum.* **1993**, *1*, 213.

(20) Teutenberg, T.; Wiese, S.; Wagner, P.; Gmehling, J. *J. Chromatogr. A* **2009**, *1216*, 8480.

(21) Godin, J.-P.; Hopfgartner, G. r.; Fay, L. *Anal. Chem.* **2008**, *80*, 7144.

(22) de Boer, A. R.; Alcaide-Hidalgo, J. M.; Krabbe, J. G.; Kolkman, J.; van Emde Boas, C. N.; Niessen, W. M. A.; Lingeman, H.; Irth, H. *Anal. Chem.* **2005**, *77*, 7894.

(23) Louden, D.; Handley, A.; Taylor, S.; Sinclair, I.; Lenz, E.; Wilson, I. D. *Analyst* **2001**, *126*, 1625.

(24) Yang, Y.; Kondo, T.; Kennedy, T. J. *J. Chromatogr. Sci.* **2005**, *43*, 518.

(25) Vervoort, R. J. M.; Ruyter, E.; Debets, A. J. J.; Claessens, H. A.; Cramers, C. A.; de Jong, G. J. *J. Chromatogr. A* **2002**, *964*, 67.

(26) Gritti, F.; Guiochon, G. *Anal. Chem.* **2006**, *78*, 4642.

(27) Liu, Y.; Grinberg, N.; Thompson, K. C.; Wenslow, R. M.; Neue, U. D.; Morrison, D.; Walter, T. H.; O'Gara, J. E.; Wyndham, K. D. *Anal. Chim. Acta* **2005**, *554*, 144.

(28) Andersen, S.; Birdi, K. In *Surfactants and Macromolecules: Self-Assembly at Interfaces and in Bulk*; Lindman, B., Rosenholm, J., Stenius, P., Eds.; Springer Berlin / Heidelberg: 1990; Vol. 82, p 52.

(29) McCalley, D. V. *Advances in Chromatography*; CRC Press: Boca Raton, 2008; Vol. 46.

(30) McCalley, D. V. *J. Chromatogr. A* **2010**, *1217*, 858.

(31) Neue, U. D.; Phoebe, C. H.; Tran, K.; Cheng, Y.-F.; Lu, Z. *J. Chromatogr. A* **2001**, *925*, 49.

(32) McCalley, D. V. *J. Chromatogr. A* **1997**, *769*, 169.

(33) McCalley, D. V. *J. Chromatogr. A* **1999**, *844*, 23.

(34) McCalley, D. V. *J. Chromatogr. A* **2000**, *902*, 311.

(35) Saini, G.; Jensen, D. S.; Wiest, L. A.; Vail, M. A.; Dadson, A.; Lee, M. L.; Shutthanandan, V.; Linford, M. R. *Anal. Chem.* **2010**, *82*, 4448.

(36) Wiest, L. A.; Jensen, D. S.; Hung, C.-H.; Olsen, R. E.; Davis, R. C.; Vail, M. A.; Dadson, A. E.; Nesterenko, P. N.; Linford, M. R. *Anal. Chem.* **2011**, *83*, 5488.

(37) Hung, C.-H.; Wiest, L. A.; Singh, B.; Diwan, A.; Valentim, M. J. C.; Christensen, J. M.; Davis, R. C.; Miles, A. J.; Jensen, D. S.; Vail, M. A.; Dadson, A. E.; Linford, M. R. *Submitted to J. Sep. Sci.* **2013**.

(38) Saini, G.; Wiest, L. A.; Herbert, D.; Biggs, K. N.; Dadson, A.; Vail, M. A.; Linford, M. R. *J. Chromatogr. A* **2009**, *1216*, 3587.

(39) Saini, G.; Yang, L.; Lee, M. L.; Dadson, A.; Vail, M. A.; Linford, M. R. *Anal. Chem.* **2008**, *80*, 6253.

(40) Saini, G.; Gates, R.; Asplund, M. C.; Blair, S.; Attavar, S.; Linford, M. R. *Lab Chip* **2009**, *9*, 1789.

(41) Nesterenko, P. N.; Fedyanina, O. N.; Volgin, Y. V. *Analyst* **2007**, 403.

(42) Nesterenko, P. N.; Fedyanina, O. N.; Volgin, Y. V.; Jones, P. *J. Chromatogr. A* **2007**, *1155*, 2.

(43) Nesterenko, P. N.; Fedyanina, O. N. *J. Chromatogr. A* **2010**, *1217*, 498.

(44) McCalley, D. V. *J. Chromatogr. A* **1995**, *708*, 185.

(45) McCalley, D. V. *J. Chromatogr. A* **1996**, *738*, 169.

(46) McCalley, D. V. *J. Chromatogr. A* **2004**, *1038*, 77.

Chapter 4: Improvements in Core-Shell Particles with Polymer/Nanodiamond Shells as Revealed by Scanning Electron Microscopy, Fast Ion Bombardment, and van Deemter Analysis

4.1 Abstract

We report advanced microscopy (scanning electron microscopy with focused ion bombardment and energy-dispersive x-ray spectroscopy (EDAX)) and chromatographic (van Deemter analysis) characterization of different generations of core-shell particles coated with polymer/nanodiamond shells. The combination of these techniques has resulted in an in-depth analysis of each new prototype material. Once the properties of a new material are understood, it can be improved upon and a subsequent generation of particles can be developed.

4.2 Introduction

Silica has been used for most chromatographic separations for over half a century.[1,2] Its coated/silanized and uncoated forms give it a plethora of selectivities. However it has some limitations.[3-10] At low pH (below 2), the silane stationary phase hydrolyzes from the silica support and at high pH (above 10), the silica itself dissolves. However, there are many analytes that are best separated outside of this pH range. Thus, there is an interest, especially in the pharmaceutical industry, to have particles that are stable at high and low pH.[11-15] Phases that show greater pH stability have been developed, including organic/inorganic hybrids,[4,16,17] which are an alternative to silica-based phases, having comparable efficiencies, and selectivities. Other materials such as zirconia,[3,18-22] porous graphitic carbon,[23-28] and polymers[29,30] are also stable at high and low pH, but sometimes have relatively low efficiency, tailing, and/or poor batch-to-batch reproducibility. They also have selectivities that are different from the more traditional silica-based reversed-phase materials.

Over the past six years, we have attempted to develop, from the ground up, a particle and phase that are stable under extreme pH conditions and that show high efficiency and selectivity with the batch-to-batch reproducibility expected from a commercial reversed-phase. Progress in these areas has largely relied on the continual analysis of our particles, often by scanning electron microscopy (SEM) in both routine and advanced modes. The resulting SEM micrographs have been complemented by van Deemter analysis of our particles. Accordingly, in this chapter we focus on the characterization of many of the particles we have developed.

The development of a new phase for chromatography is a non-trivial endeavor – many material properties must be considered, including particle uniformity, porosity, and stationary phase thickness, and these physical attributes must ultimately lead to high efficiency separations.

Efficiency, as measured in plates/m (N/m), finds its origins in distillation theory and is an important figure of merit for the quality of a separation.[31] Theoretical plates are "imaginary units" on which chemicals in a gas or liquid phase establish equilibrium. Each successive equilibrium/plate results in greater purification for the chemical, i.e., the efficiency of a separation increases with increasing numbers of theoretical plates. If one divides the length, *L*, of a chromatographic column by its number of plates, *N*, one obtains the plate height, *H*, of a single plate: $H = L/N$. Clearly, column efficiency increases with decreasing plate height.

4.2.1 Van Deemter Theory

The van Deemter equation[32] takes into account the different parameters that affect efficiency. The general form of the van Deemter equation is:

$$H = A + \frac{B}{u} + Cu \qquad (4.1)$$

where *H*, *A, B, C,* and *u* represent the plate height, eddy diffusion, linear diffusion of the analyte along the direction of flow, resistance to mass transfer, and linear velocity of the mobile phase, respectively. These terms will now be described.

The *A*-term takes into account the multiple pathways that an analyte can take through the column – the more paths the greater the term. It is defined as

$$A = 2\lambda d_p \qquad (4.2)$$

where d_p is the particle diameter and λ is a column packing constant. Thus, the smaller the particle diameter and the lower (better) the packing constant, the lower the *A*-term. The packing constant is affected by the uniformity of the packed particle bed and the particle sphericity/roughness. Therefore, column efficiency will decrease if agglomerates are present,

which disturb bed uniformity and increase the average particle diameter, or if the bed is poorly packed.

The *B*-term accounts for longitudinal diffusion and is defined as

$$B = 2\gamma D_M \qquad (4.3)$$

where γ is the labyrinth factor and D_M is the diffusion coefficient of the solute in the mobile phase. Because diffusion in condensed phases is relatively slow, the *B*-term is often of only moderate importance in liquid chromatography. Note also that diffusion coefficients decrease with increasing molecular size, and that temperature affects *B* by decreasing mobile phase viscosity and thereby increasing analyte diffusion.

Resistance to mass transfer, in both the mobile and stationary phases, determines the *C*-term and is defined as follows:

$$C_S \propto \frac{d_f^2}{D_s} \qquad (4.4)$$

$$C_M \propto \frac{d_p^2}{D_M} \qquad (4.5)$$

The *C*-term decreases as particle diameter and stationary phase film thickness decrease, resulting in improved efficiency (smaller plate heights). It is also inversely proportional to the diffusion coefficients of the analytes in the stationary and mobile phases. Thus, the larger a particle is, the more an analyte can diffuse into it, resulting in greater band broadening and poorer efficiences. Over the history of chromatography, particles have been developed with increasingly smaller diameters because a decrease in d_p improves both *A* and *C*. While these particles, which are now smaller than 2 μm, have high efficiencies, they also give high system back pressures, greater frictional heating in the column,[33] thermal gradients[34] and require more expensive instrumentation.

4.2.2 Superficially Porous Particles

In recent years, various manufacturers have introduced particles with nonporous cores and porous shells as an alternative to smaller particles. These are referred to as pellicular, fused-core, superficially porous, or core-shell particles. Compared to fully porous particles, these particles reduce the diffusion path length of analytes in them and, as a result, these particles have reduced *C*-terms.[35-37] In addition, superficially porous particles often have more uniform particle diameters and higher densities, which can lead to improved packing and better *A*-terms. Recently, we have focused on making core-shell particles with inert cores and polymer/nanodiamond shells.[38-40]

4.2.3 Core Materials

Here we consider diamond, zirconia, glassy carbon, and carbonized/oxidized polydivinylbenzene (PolyDVB) microspheres as core particles for the layer-by-layer deposition of poly(allylamine) (PAAm) and nanodiamond shells to form core-shell particles. These core materials were selected because they are inert under extreme pH conditions and complement the inertness of the porous PAAm/nanodiamond shell that is deposited on them. Other beneficial properties of nanodiamond include excellent thermal conductivity, thermal stability, and a low coefficient of thermal expansion. In addition, diamond does not swell when exposed to organic solvents.[41] Because of these outstanding properties and its interesting surface chemistry,[42] diamond has previously been explored as a stationary phase for reversed-phase,[43] normal-phase,[44] and anion exchange[45,46] chromatography.

The first diamond-containing phases created in our group were used for solid phase extraction (SPE).[38,47,48] To prepare these materials, diamond was cleaned and coated with PAAm. The PAAm was then chemically crosslinked or cured to give an amino phase. Subsequent studies used this same PAAm-coated support that was reacted with hydrophobic isocyanates to yield reversed-phase particles. All of the resulting PAAm-coated diamond particles were non-porous and had fairly low capacities. To increase the surface area of the materials, PAAm/nanodiamond bilayers were deposited on micron-sized diamond particles in a layer-by-layer fashion to create porous polymer/nanodiamond shells.[38] The resulting particles were packed and used for HPLC. Separations of pesticides on a crosslinked amino phase and alkylbenzenes on a non-crosslinked reversed-phase were demonstrated.

This work outlines our use of scanning electron microscopy and associated techniques to characterize a variety of different nanodiamond-containing particles and phases. Whenever possible, particles were packed into columns for HPLC and van Deemter analyses were performed to further understand these materials.

4.3 Materials and Methods

4.3.1 Particle Synthesis, Functionalization and Column Packing

Core-shell particles were prepared by applying poly(allylamine) (PAAm) and nanodiamond to core particles in a layer-by-layer (LbL) fashion. Details of this preparation have been reported by Hung et al.,[40] Wiest et al.,[39] and Saini et al.[38] The application of this LbL coating scheme varied slightly when applied to the coating of zirconia core particles, which is first reported herein. Zirconia particles were etched in hot 1 M sodium hydroxide overnight. They were filter rinsed with Millipore water (18 MΩ purity) and subsequently coated with

PAAm. LbL deposition, as previously reported, was then performed until the desired shell thickness was reached. The shell thickness was monitored by SEM. The final PAAm/nanodiamond-coated core-shell particles were functionalized with 1,2-epoxyoctadecane. After the reaction, the zirconia-based core-shell particles were packed into 4.6 mm × 30 mm stainless steel columns.

4.3.2 Instrumentation

The columns were tested on a conventional HPLC: dual wavelength detector (Model No. 2487), binary pump (Model No. 1525), column oven (Model Number 5CH), Waters Corporation, Milford MA and on a UHPLC instrument: Infinity 1290, (Agilent, Santa Clara, CA) equipped with a binary pump, autosampler, and UV/Vis DAD detector. The chromatographic conditions for each set of van Deemter analyses are summarized in Table 4.1. First generation (glassy carbon), second generation (in-house prepared carbonized polyDVB), and third generation (commercially obtained carbonized polyDVB) materials were analyzed with the Waters HPLC. Some generation 3 materials were analyzed using the Agilent UHPLC. The designation of "generation" signifies that van Deemter plots were obtained for the corresponding material.

SEM was performed with a Philips XL30 ESEM FEG or an FEI Helios Nanolab 600. To prepare the microscope samples, rinsed, core-shell particles were dried and placed on weighing paper and an aluminum SEM stub was lightly rubbed on the powders to get them to adhere to the stub's surface. Alternatively, isopropyl alcohol was pipeted onto the stub surface and a small volume of particle-containing slurry was then mixed into the alcohol with a pipet and the stubs were allowed to dry.

For SEM imaging, a spot size of 3 was used with the SFEG instrument. The NanoLab instrument was run at 0.17 nA. The accelerating voltages and imaging types are specified on the individual micrographs shown herein. Ion milling with the FEI Nanolab was performed by first depositing platinum over the surface. The ion current was set at about 6 – 10 pA for both platinum deposition and ion milling.

Energy-dispersive x-ray spectroscopy (EDAX) was performed both in single point mode and mapping mode. The beam energy was set at 30.0 kV and the stage was tilted at 29.9° with a take-off angle of 57.2°. Resolution was 130 and Amp. T was 50.0. Carbon, zirconium, and aluminum were used for 2D x-ray mapping.

4.3.3 Image Processing

Particle diameters were obtained using ImageJ Software (Ver. 1.44p, National Institutes of Health, USA). Each individual image was threshold adjusted, which allowed the image to be made binary. Binary image conversion converts pixels above the established threshold black (features) and pixels below the threshold white (background). This adjustment needed to be performed manually as brightness and contrast were different for each image. After the binary conversion was completed, holes were filled with the software and a watershed function was performed, splitting fused particle projections at their narrowest point. Watershed segmentation is a way to "cut apart" or separate particles that touch each other by calculating the Euclidian distance map and finding the ultimate eroded point, or the narrowest point between the fused particles. Particles were analyzed using the "Analyze Particles" function. The parameters measured were "particle perimeter," and "fit ellipse" (major diameter, minor diameter and angle.)

The fit ellipse function operates as follows: "Major and Minor are the primary and secondary axes of the best fitting ellipse. Angle is the angle between the primary axis and a line parallel to the X-axis of the image."[49] Parameter thresholds for particle analysis were set as follows: circularity: 0.6 – 1.0 and area: 7 – 16 μm^2. Average diameters, standard deviations, and 95 % confidence intervals were calculated in MS Excel.

For all measurements of diameters, the major diameter was calculated so particles fused by the software could be included in the particle analysis. Roughly 40 – 60 particles were measured per image. To obtain a measurement of particle roughness, which would later be correlated with the van Deemter *A*-term, the perimeter (experimental circumference) of the particles was compared to the theoretical circumference for each imaged particle. The theoretical circumference was calculated by measuring the average particle diameter as measured by the fit ellipse function and multiplying it by π. The ratio of the experimental circumference and the theoretical circumference was taken as measure of the roughness of the particle. This roughness calculation was then compared to the *A*-term.

4.4 Results and Discussion

Herein we show the SEM analysis of core-shell particles with diamond, zirconia, glassy carbon and carbonized polyDVB cores. Van Deemter analysis is given where possible.

4.4.1 Diamond Core Materials

Images of diamond materials (see Figure 4.1) showed that the particles were highly irregular. When these particles were packed into a column and used to separate analytes, they had a very high back pressure. The best efficiencies obtained for these particles was 54,800 N/m

for diazinon.[38] This result set the benchmark for future diamond-containing particles as it was the best efficiency obtained with a diamond-based material to date in the world. However, it was clear that improvements in efficiency would be expected from particles with narrower particle size distributions and greater sphericity – the irregular shapes of the particles would be expected to lead to multiple flow paths and a poorly packed bed, resulting in a large packing factor (λ). It was essential to find a material that would be more spherical and also provide chemical and mechanical stability under harsh chromatographic conditions.

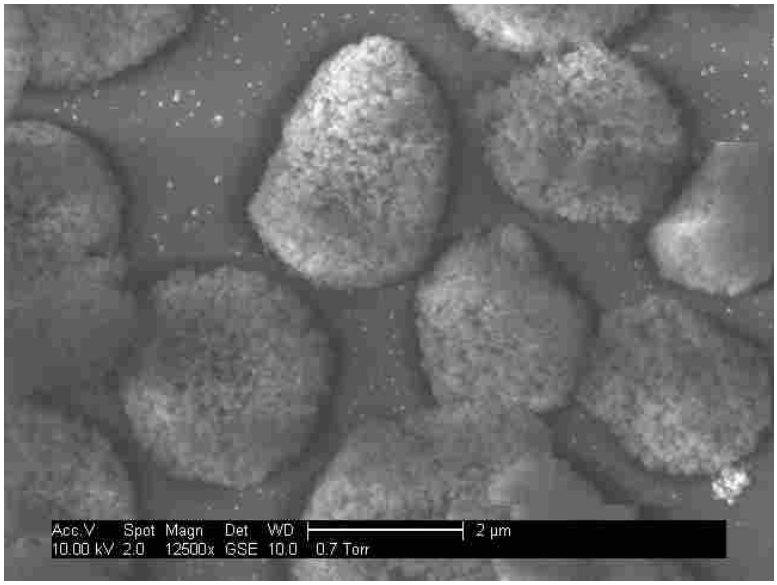

Figure 4.1 Irregular diamond cores coated with nanodiamond/polymer shells.

4.4.2 Zirconia Core Materials

4.4.2.1 Surface Imaging

Zirconium oxide (zirconia) was next considered as a core material because it is known to have high chemical and mechanical stability, which are required under the high pressures and extreme pH conditions of our separations.[20] It could also be purchased as a more spherical core

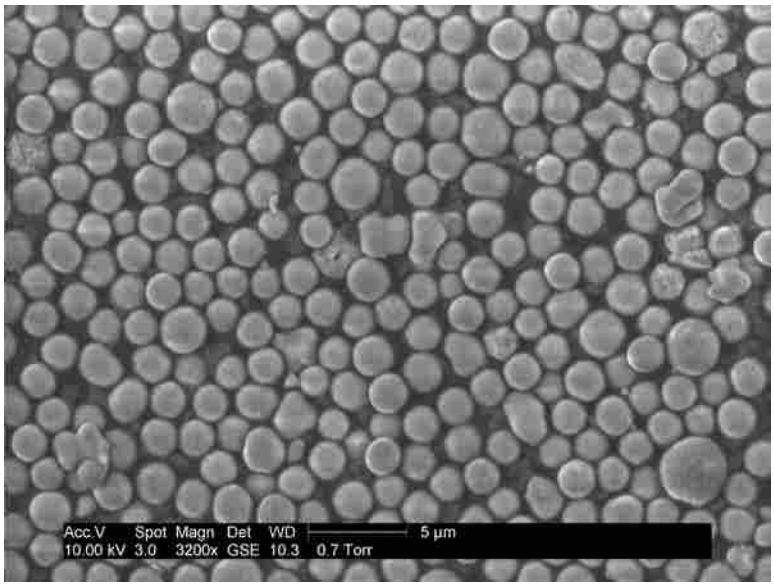

Figure 4.2 Bare zirconia cores.

Figure 4.3 Coated zirconia cores: (top) Imaged using secondary electron mode, (bottom) Imaged using gaseous secondary electron mode.

Figure 4.4 Magnified image of nanodiamond/polymer surface on a zirconia core.

material (see Figure 4.2) in comparison to the diamond core particles (see Figure 4.1). To image the core-shell particles with zirconia cores, we found through trial and error that viewing the particles in secondary electron mode gave more surface detail than images obtained in gaseous secondary electron (GSE) mode (see Figure 4.3). GSE mode is a low pressure analysis technique where ca. 0.1 torr of a polarizable gas (water) is used in the analysis mode. This helps to mitigate charging effects from the surface, but typically lowers or distorts fine feature surface resolution. Under secondary electron mode we saw details of the surface beyond what we had seen with our diamond-based materials (see Figure 4.4). These images confirmed that we had completely covered the core particles with PAAm/nanodiamond shells, that those shells were intact and that our particles were largely spherical. While we had found good conditions to image the surface, we still desired to measure shell and core dimensions simultaneously.

4.4.2.2 Ion Milling

The Helios NanoLab gave us the ability to image both the core and the shell of the particles simultaneously. Our first approach here was ion milling, where after the particles were coated with a protective and conductive layer of platinum, the zirconia-PAAm/nanodiamond particles were milled with a focused beam of Ga^+ ions and cross-sectional images were acquired (see Figure 4.5). This analysis revealed that the particles had 2 μm zirconia cores with 0.5 μm shells and that the shells were fairly uniform. While powerful, this method was time consuming, i.e., if we wanted to examine the shell thickness/uniformity over an entire particle, we would have to ion mill/shave off one portion of the particle at a time.

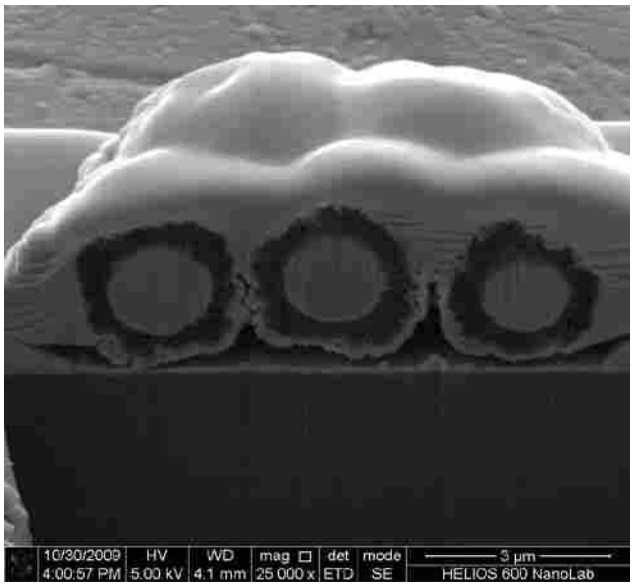

Figure 4.5 Ion milled zirconia core-shell particles with platinum coating.

4.4.2.3 “Halo” Imaging

Serendipitously, we imaged the zirconia core-shell particles with a high accelerating potential and discovered an interesting effect: the zirconia core appeared through the shell and was brighter than its carbon surroundings. To wit, as we increased the accelerating potential from 5 keV (Figure 4.6 top) to 20 keV (Figure 4.6, middle), the core became visible. At 30 keV, the cores were plainly observed (Figure 4.6, bottom). We call these images “Halo” images. We hypothesized that this effect occurred because zirconium is a higher Z material than carbon and it more efficiently backscatters primary electrons or releases more secondary electrons. We further assumed that as we increased the accelerating potential, the mean free path of the electrons would increase, allowing simultaneous imaging of the zirconia core and the polymer/nanodiamond shells.

Various studies have indeed shown that as the accelerating potential increases, electrons penetrate deeper into a sample, and that the secondary electrons are generated from the top of a teardrop profile.[50] Research by Drouin *et al.*[51] and Hovington *et al.*[52,53] demonstrated this effect via a CASINO simulation. They showed that electrons penetrated into a silicon substrate (Z = 14) to varying depths based on the accelerating voltage, i.e., electrons with greater energy have a longer mean free path.[54] When E_0 = 5 keV, penetration of about 200 nm was observed. When E_0 = 30 keV, the penetration depth increased to 4584 nm. Another simulation performed by the same group compared penetration of electrons using the same acceleration potential, but with different Z materials. They compared carbon and gold and showed that electrons penetrate much deeper into a lower Z material. They stated that the range of electrons into carbon was about six times larger than their penetration depth into gold.

Figure 4.6 Core-shell zirconia particles imaged with different accelerating potentials: (top) imaged at 5 keV, (middle) imaged at 20 keV, and (bottom) imaged at 30 keV.

To compare the measurements between halo images and milled cross sections, we used the same sample (see Figures 4.5 and 4.6). Images were analyzed using Image J. The shell thicknesses measured by both techniques corroborated each other. However, as halo imaging was not as time-consuming as ion milling, we were able to analyze many particles simultaneously with this approach (see Figure 4.7). Indeed, this technique allowed us to determine the deposition rate of our PAAm/nanodiamond bilayers through direct measurement rather than by taking the difference in particle diameters before and after layer-by-layer deposition (see Figure 4.8). After 14 bilayers had been applied, the shell thickness was 0.24 μm and after 28 bilayer depositions the shell was 0.48 μm indicating a linear deposition rate of about 17 nm per bilayer.

The discoveries made with the zirconia core particles suggested that we would have an improved *A*-term because of the spherical nature of our particles, which would reduce the flow nonuniformity through a packed bed comprised of these particles. We would also have an improved *C*-term, because of the superficially porous nature of the particles.

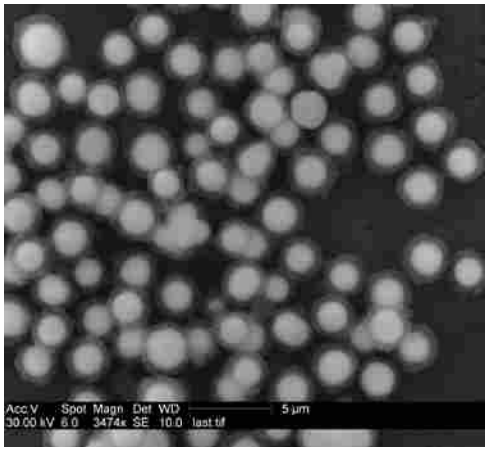

Figure 4.7 Low magnification image of many zirconia core-PAAm/nanodiamond shell particles. Halo image taken at 30 keV.

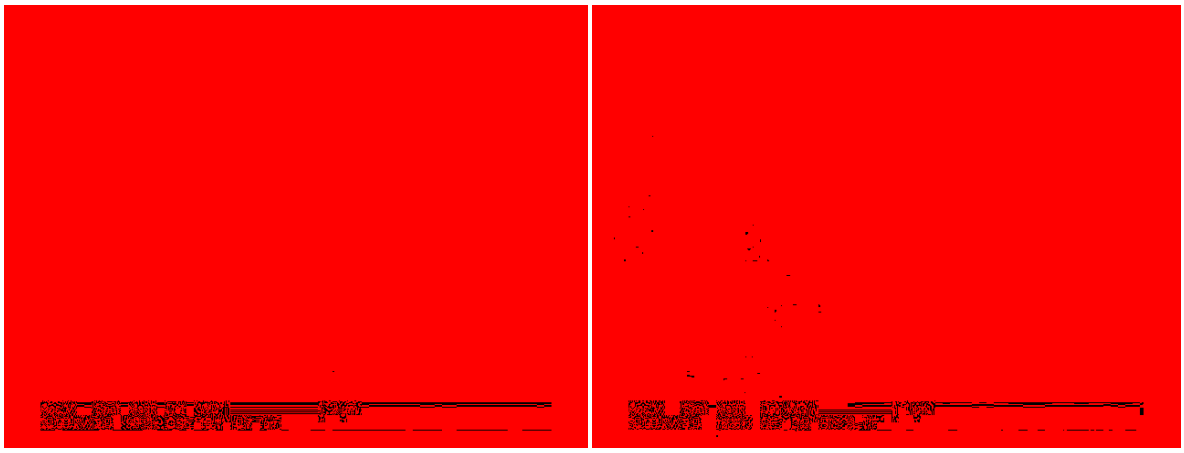

Figure 4.8 Halo images showing different shell thickness after deposition of (left) 14 PAAm/nanodiamond bilayers (0.24 µm shell), and (right) 28 PAAm/nanodiamond bilayers (0.48 µm shell).

4.4.2.4 Energy-Dispersive X-ray Spectroscopy (EDAX)

We used EDAX as a materials characterization technique. A single point measurement of the particles showed carbon, zirconium, oxygen, aluminum, and magnesium (see Figure 4.9). To clarify these results and better determine where these signals were coming from, we obtained an x-ray map of our sample (see Figure 4.10). When compared to the standard SEM image, the emitted carbon and zirconium x-ray images corresponded to the particles, where, as expected, lobes in the carbon images extended out further than those in the zirconia images. Aluminum and magnesium scans showed that those signals came from the stub, suggesting that magnesium was a contaminant in the aluminum. An oxygen map was also obtained, but gave inconclusive results, as oxygen-containing species, aluminum oxide and zirconia (zirconium oxide), were present in both the background and foreground, respectively.

Figure 4.9 EDAX single point measurment showing the presence of carbon, oxygen, zirconium, aluminum and magnesium.

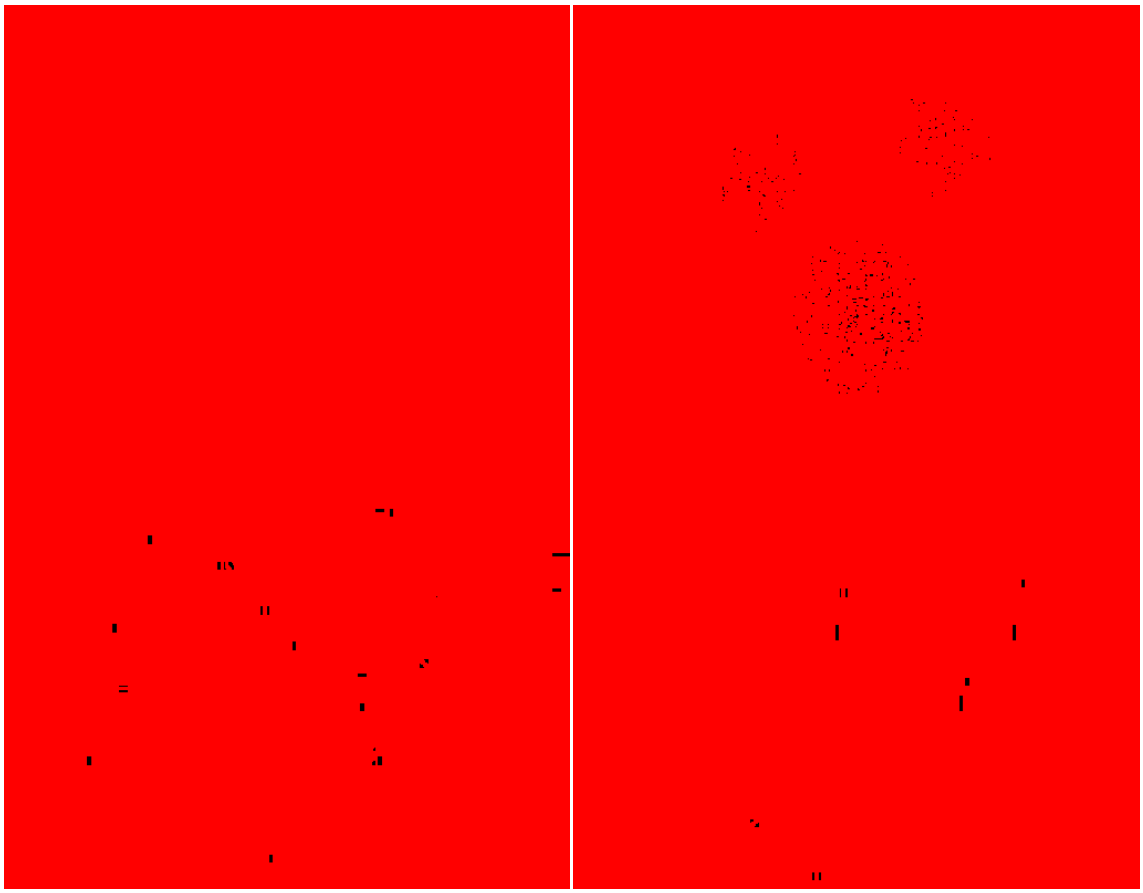

Figure 4.10 Images of core-shell particles with zirconia cores. Standard SEM image (upper left), and 2D x-ray maps of aluminum (upper right), zirconium (lower left), and carbon (lower right).

4.4.2.5 Chromatographic Performance of Zirconia Core-PAAm/Nanodiamond Shell Particles

Zirconia core-PAAm/nanodiamond shell particles were functionalized with a reversed-phase ligand and packed into a liquid chromatography column. We separated a mixture of benzene, toluene, xylenes and mesitylene with this column using a 50:50:0.1 water/acetonitrile/triethylamine (pH 11.3) mobile phase at 0.5 mL/min (see Figure 4.11). The efficiency for mesitylene on this zirconia-based column was 41,700 N/m, which was an improvement over the previous column prepared from irregular diamond cores (36,300 N/m for mesitylene). We also saw a slight separation (not baseline) of the xylene isomers, which was not observed with the diamond core column.

As we continued using the column, we noticed steadily increasing back pressures, which prevented us from obtaining van Deemter curves. The increasing back pressures, likely caused by clogged pores from fractured nanodiamond shells, were indicative of column failure and over a short period of time, the retention time of analytes on this material decreased drastically (see Figure 11). We verified the column degradation by performing a post-mortem on the column via SEM, and saw that the shells on the particles had been damaged (see Figure 4.12). While the particles in this column yielded better efficiencies than the irregular-diamond particles, they too lacked mechanical stability and fell apart too quickly to be commercially viable. Improvements needed to be made to increase the mechanical stability of the shell.

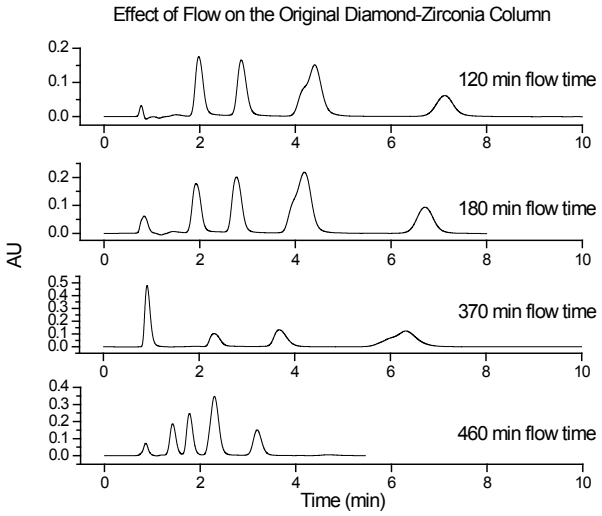

Figure 4.11 Chromatographic performance as a function of time of an alkylbenzene test mixture (from left to right: benzene, toluene, xylenes, and mesitylene) on a 1,2-epoxyoctadecane functionalized ($C_{18)}$ zirconia core column.

Figure 4.12 Post mortem analysis of the zirconia core-PAAm/nanodiamond shell column. Notice the particle irregularity and broken shells on the particles, which was not observed in previous images.

4.4.3 Carbon Core Materials

4.4.3.1 Glassy Carbon Core Materials

As the zirconia cores were prohibitively expensive, we decided to use a different core material. Supelco donated to us some glassy carbon test particles, which were used as the new core material. This glassy carbon material was coated with polymer/nanodiamond bilayers in the same manner as the zirconia core. However, the particles were functionalized with both 1,2,7,8-diepoxyoctane (a crosslinker) and 1,2-epoxyoctadecane in a 1:20 w/w ratio. The added crosslinker gave greater mechanical stability, lowered the column back pressure, and made van Deemter analysis possible. However, the first van Deemter curve obtained with this material had a much higher *C*-term than expected (see Figure 4.13A). To understand these results, SEM and PSD measurements were performed on the particles.[39] The PSD analysis showed that the particles were far from uniform and likely had many agglomerates. SEM confirmed this finding, showing large agglomerates that would likely increase the *A*- and *C*-terms.

To improve these particles, sieving and sonication were employed. SEM analysis and PSD measurements indicated that these changes to the procedure improved the particle size distributions (see Figure 4.13 B and C). The van Deemter curves obtained with these better particles showed improved (flatter) *C*-terms, but the *A*-terms increased with each successive particle improvement. As the effective particle diameter improved, one would reasonably expect the *A*-term to also improve; however, packing efficiency also has an effect on the *A*-term, which suggests that our particle packing procedure became less effective as the particles became more uniform.

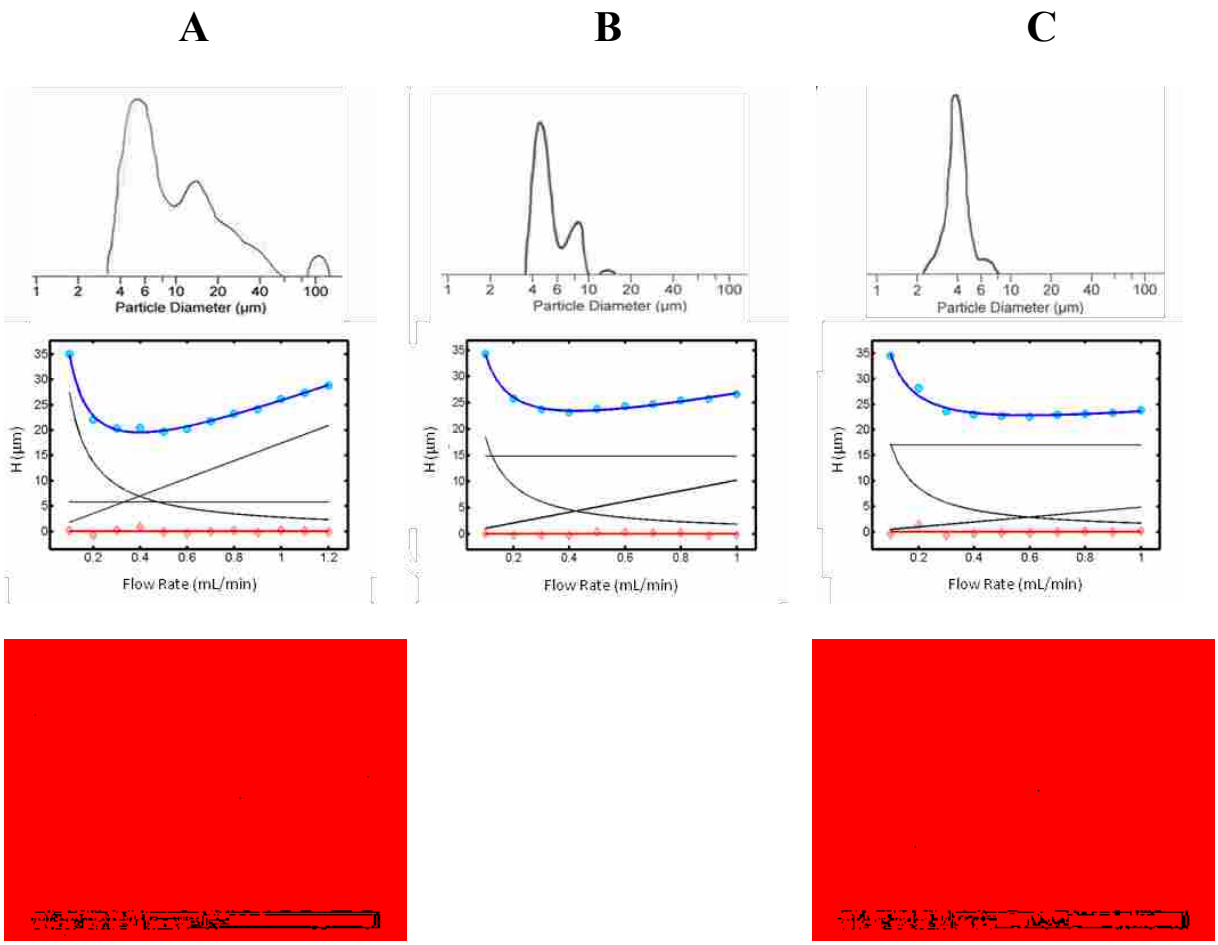

Figure 4.13 PSDs and corresponding SEM images of glassy carbon core-shell particles. (A) 14 µm mean particle diameter, no sieving, no sonication, (B) 5 µm mean particle diameter, sieved, no sonication, (C) 4 µm mean particle diameter, sieved and sonicated.

Despite these improvements, the *C*-terms were still higher than we expected for a core-shell phase. SEM was then used to analyze the glassy carbon cores in greater detail. Imaging of the core material (see Figure 4.14) showed surface roughness that could be indicative of particle porosity. Focused ion beam milling performed on random cores revealed that the particles had varying degrees of porosity, some of which were quite high (see Figure 4.15). We had believed these particles were nonporous. Nevertheless, SEM and FIB had revealed that they often showed a large degree of porosity. These results could help explain the larger than expected *C*-terms.

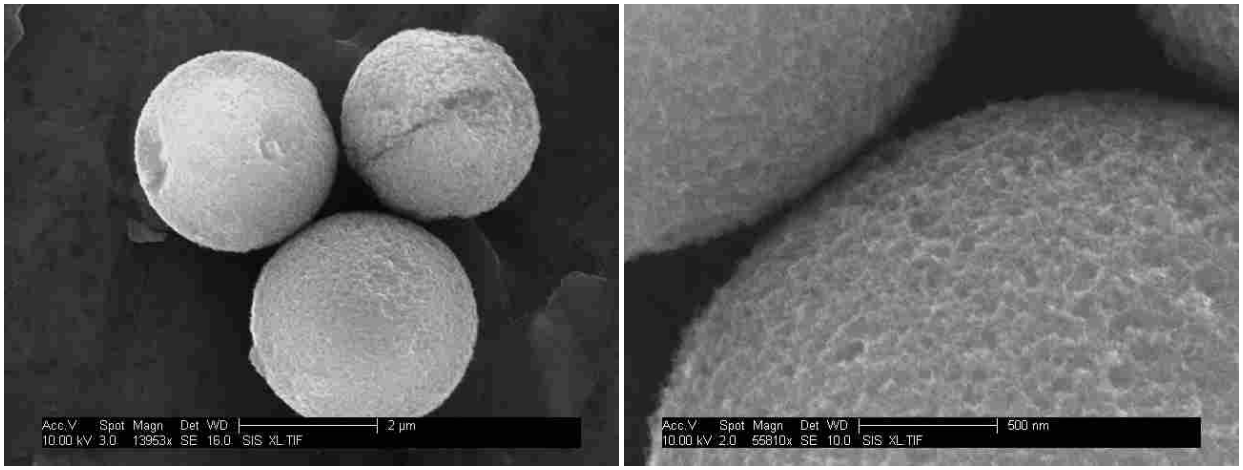

Figure 4.14 Bare glassy carbon cores from Supelco. The surface appears to be rough in the magnified image.

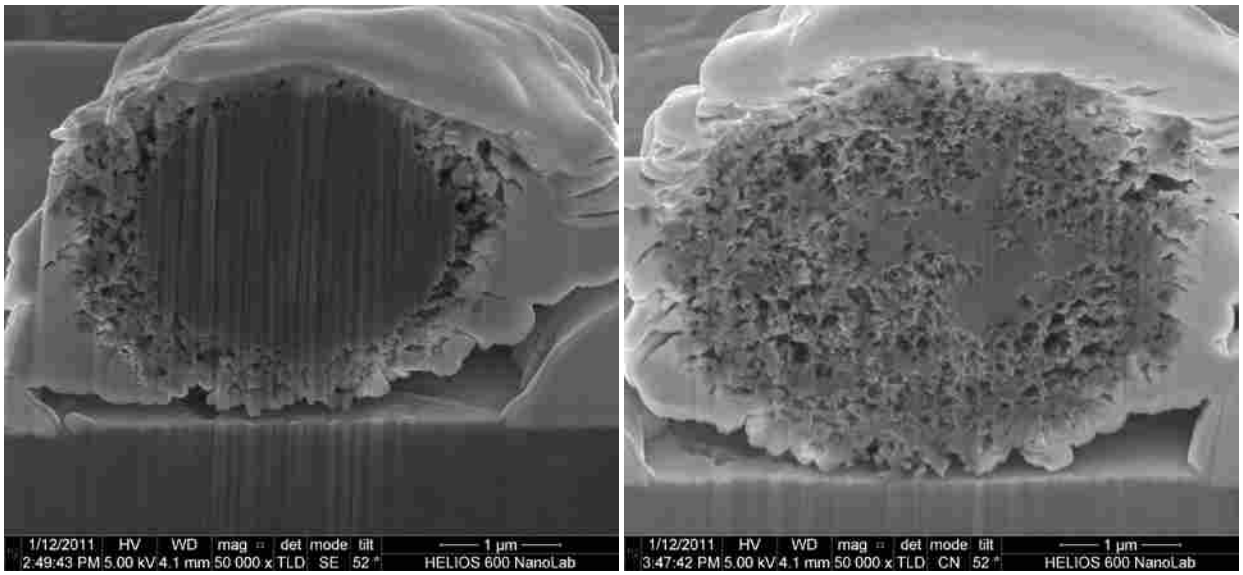

Figure 4.15 Cross sections of glassy carbon core-shell particles obtained by ion milling. Particle on the left shows little porosity. Particle on the right shows significant porosity, i.e., the internal porosity of the particle is indistinguishable from its porous shell.

4.4.3.2 In-House Prepared, Carbonized PolyDVB Cores

Without core porosity, the diffusion pathways for solutes will be decreased, thereby reducing the *C*-term. More uniform and spherical particles are also expected to improve the *A*-term. Accordingly, to obtain a nonporous material with better sphericity and uniformity we created our own carbon cores (see Figure 4.16).[40] These particles had improved sphericity and appeared to be nonporous. They were formed from polydivinylbenzene (PolyDVB) spheres created in our lab via a combination of procedures from various publications.[38-40,55-59] The PolyDVB spheres[60,61] were then oxidized,[58] carbonized[62] and acid treated/oxidized[63,64] to allow improved adhesion of the PAAm layer. Deposition of the polymer/nanodiamond bilayers was performed in the same manner as for the glassy carbon material, except that all of the particles were sonicated. To remove large agglomerates, some of the particles were sieved. FIB was performed on these materials and no core porosity was observed (see Figure 4.17). Columns were then packed and van Deemter curves obtained. These columns showed improved *A*- and *C*-terms (see Table 4.2), but it is difficult to directly compare these results to the previous results because of the different particle sizes and analytes.

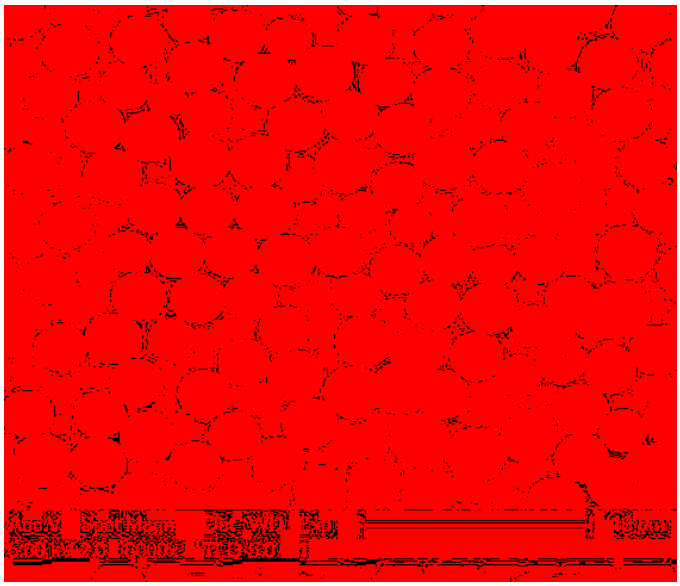

Figure 4.16 In-house synthesized, carbonized PolyDVB particles appear smoother and more spherical than previous materials.

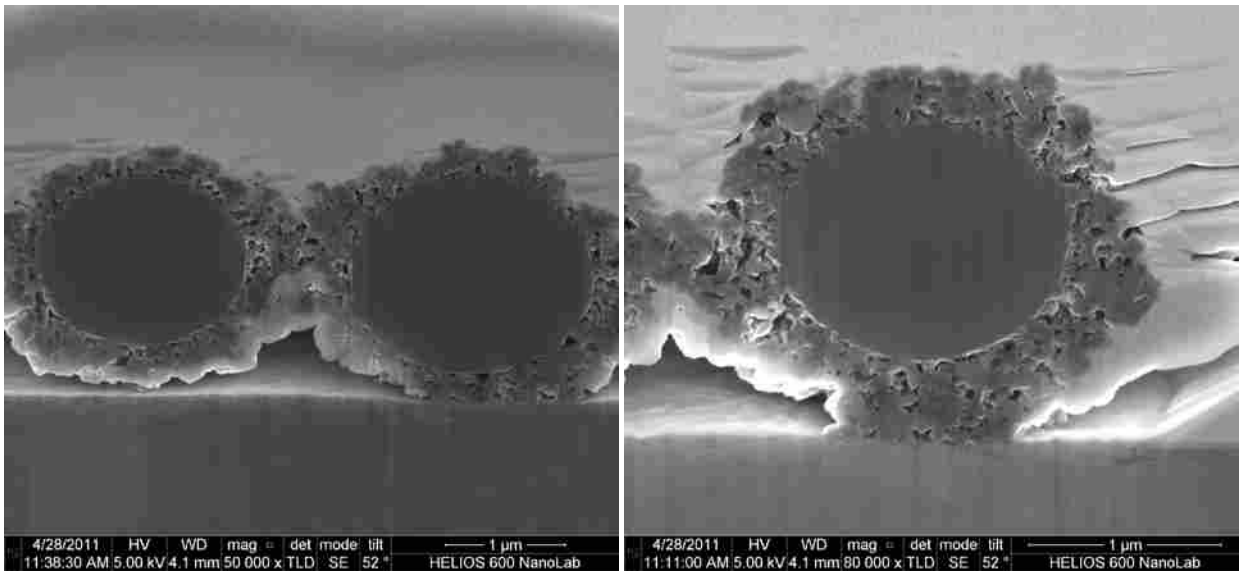

Figure 4.17 Ion milled (cross sectioned) core-shell particles made with in-house synthesized, carbonized polyDVB spheres show no visible porosity.

Table 4.1 Conditions and analytes under which each van Deemter curve was obtained.

	Analyte	k	MP	pH modifier	pH	T (°C)
Glassy carbon cores	Butylbenzene	2.55	40:60	0.1 % Triethylamine	11.3	35
In-house prepared carbonized polyDVB	Decylbenzene	8.75	40:60	0.1 % Triethylamine	11.3	35
Commercially obtained carbonized polyDVB	Hexylbenzene	4.31	50:50	10 mM Phosphate buffer	12	35

Table 4.2 Van Deemter terms for each generation of carbon core-shell particle.

Core Type	Column Name	d_p (μm)	A (μm)	B (μm·cm/s^{-1})	C (μm·s/cm^{-1})
Glassy carbon	From particles shown in Fig. 4.13A[a]	14	3.89	0.33	167.33
	From particles shown in Fig. 4.13B[b]	5	14.80	0.18	101.59
	From particles shown in Fig. 4.13C[b]	4	17.00	0.17	48.21
In-house	In-House Column 1	3.3	6.02	0.18	43.82
	In-House Column 2	3.3	10.86	0.10	41.93
	In-House Column 3	3.3	7.84	0.17	26.66
	In-House Column 4[a]	3.3	6.06	0.18	43.62
	In-House Column 5[b]	3.3	5.58	0.17	27.59
Commercial[b]	Commercial 1 Thicker Shell	4	4.97	0.13	37.65
	Commercial 2 Thicker Shell	4	4.51	0.11	47.11
	Commercial 3 Thicker Shell	4	4.41	0.14	45.52
	Commerical 1 Thinner Shell	4	8.28	0.13	23.34
	Commerical 2 Thinner Shell	4	5.39	0.15	27.65
	Commerical 3 Thinner Shell	4	4.73	0.16	29.83
	Commerical 4 Thinner Shell	4	4.09	0.13	28.05

[a]Particles not sieved. [b]Particles sieved.

4.4.3.3 Carbonized, Commercially Obtained PolyDVB Cores

The previous two types of carbon core materials (the glassy carbon particles from Supelco and the in-house synthesized particles) were improvements over their predecessors. A newer core-shell particle was next created with a more uniform polyDVB core obtained from a commercial vendor. The improvement sought with the commercially obtained polyDVB cores was to increase the uniformity of the core, thereby improving d_{90}/d_{10}. With these particles, we also attempted to optimize the shell thickness. As before, this material was oxidized, carbonized and acid treated. PSD measurements revealed a very uniform core with a tight PSD,[40] and SEM analysis corroborated that finding (see Figure 4.18).

To optimize the shell thickness, SEM micrographs were taken frequently during PAAm/nanodimaond bilayer depositions. The particle diameters were then measured from the micrographs using ImageJ. About 40 – 60 particle diameters were measured from a single SEM image at most stages in the particle growth. The standard deviation approximately doubled after 30 bilayer depositions (see Figure 4.19). This could potentially increase the *A*-term and affect batch to batch reproducibility. Because the standard deviation remained fairly constant for the first 15 bilayer depositions, we decided to decrease the number of bilayer depositions from 30 to 15. While this change should decrease the capacity of the column, it would also be expected to decrease the *C*-term. Images of the core taken after depositions of 3, 7, 11, and 15 bilayers are presented in Figure 4.20.

While these particles did have a larger diameter than the in-house polyDVB material, the *A*-terms were lower than the previous materials, suggesting that we had improved the packing of the column (see Table 4.2). The *C*-terms for these materials were also somewhat smaller,

suggesting that decreasing the shell thickness improved *C*. We also obtained the best batch-to-batch reproducibility we had found in any of our materials.

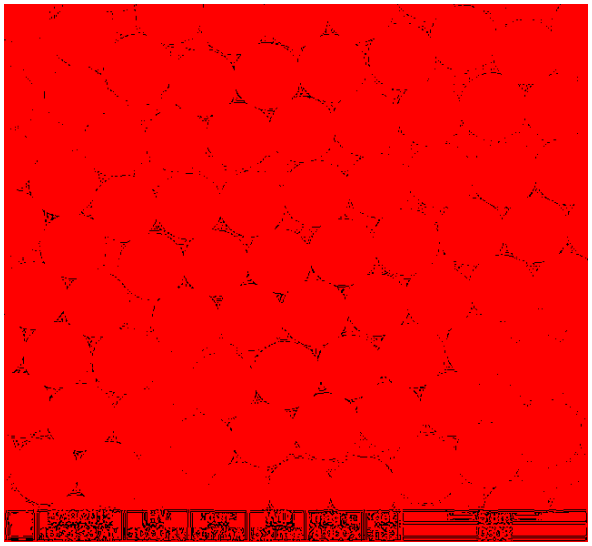

Figure 4.18 Bare, carbonized, commercially obtained polyDVB cores.

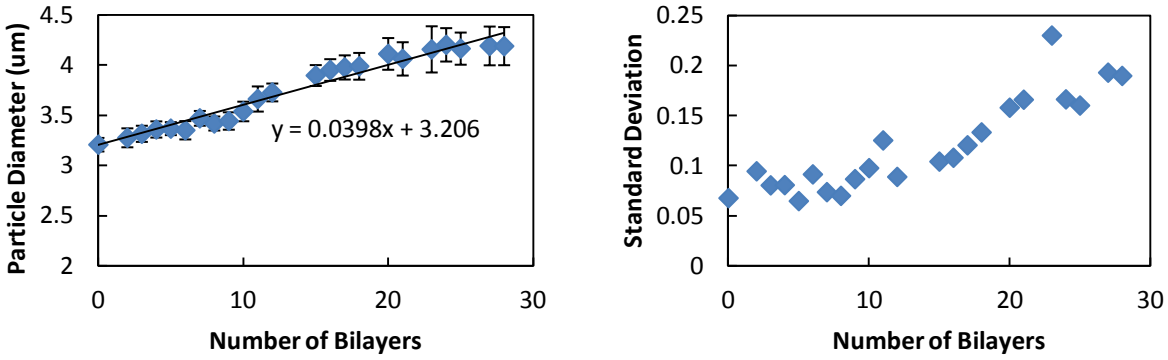

Figure 4.19 Average particle diameter (left), and corresponding standard deviations (right) for layer-by-layer growth on carbonized, commercially obtained polyDVB cores.

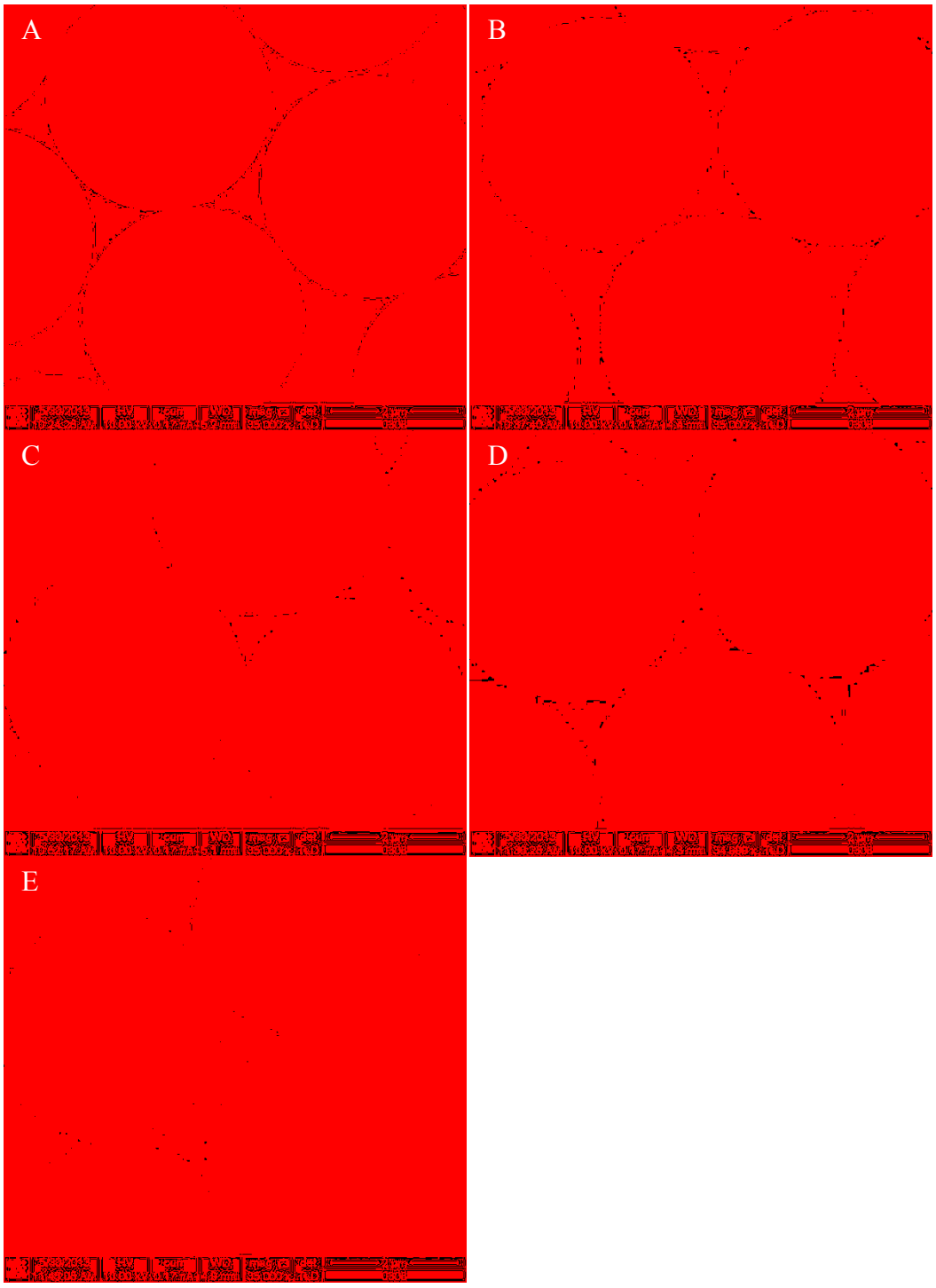

Figure 4.20 Carbonized, commercially obtained polyDVB particles imaged after (A) zero layers, (B) 3 layers, (C) 7 layers, (D) 11 layers, and (E) 15 layers.

4.4.3.4 Van Deemter Analysis of Carbonized, Commercially Obtained PolyDVB Core-Shell Phases

We compared particle diameter and roughness to the *A*-term and shell thickness to the *C*-term, where the particles ranged in size from 3.90 – 3.95 µm with shell thickness of 0.392 – 0.416 µm. That is, because the *A*-term is governed by particle diameter and packing efficiency, we compared the average particle diameter of each batch to the *A*-term. The particle diameter and the *A*-term did not correlate. The particle roughness ratio, calculated by taking the ratio of the experimental circumference to the theoretical circumference, was also compared to the *A*-term (see Figure 4.21 and Table 4.3). While there is scatter in the data, and a an R^2 value of 0.8443, there does appear to be an upward trend that associates particle roughness with an increasing *A*-term even if it is a somewhat rough fit. These data suggest that particle roughness had a greater effect on the *A*-term than the particle diameter. We also compared the shell thickness to the *C*-term (see Figure 4.22 and Table 4.4).Greater scatter existed with this data (R^2 = 0.5466), but the seven different columns (from four particle batches) suggested some correlation between an increasing *C*-term with increasing shell thickness (see Figure 4.22).

Table 4.3 Correlation of *A*-term with surface roughness ratio. Data are averages of multiple columns from the same particle batch.

	Experimental diameter (µm)	Theoretical diameter (µm)	Particle roughness Ratio	*A*
Commerical 1 Thinner shell	13.696	12.075	1.134	8.05
Commerical 2 Thinner shell	13.590	12.192	1.115	5.39
Commerical 3 Thinner shell	13.404	12.186	1.100	4.73
Commerical 4 Thinner shell	13.460	12.110	1.111	5.00

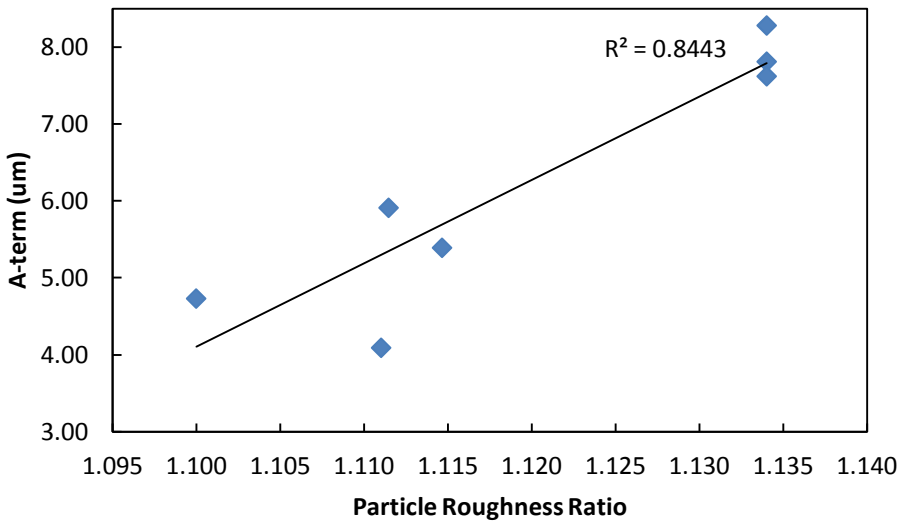

Figure 4.21 *A*-term vs. particle roughness ratio. A general correlation is seen between roughness and the *A*-term. Each individual column is represented in this plot.

Table 4.4 Correlation of the *C*-term with shell thickness. Data are averages of multiple columns from the same particle batch.

	Core diameter (µm)	Particle diameter (µm)	Shell thickness (µm)	C-term
Commerical 1 Thinner shell	3.510	3.902	0.392	23.3
Commerical 2 Thinner shell	3.529	3.936	0.407	27.6
Commerical 3 Thinner shell	3.530	3.946	0.416	29.8
Commerical 4 Thinner shell	3.504	3.907	0.403	28.0

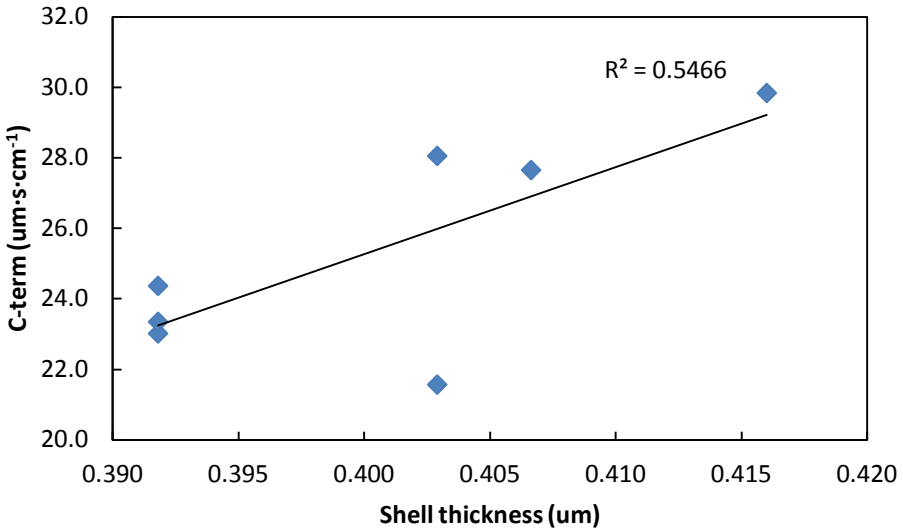

Figure 4.22 Correlation of *C*-term with shell thickness. Each data point represents a different column.

4.4.3.5 Improvement of Carbon Core, Packed Chromatographic Columns as Shown by the *A*- and *C*-Terms

As discussed above, improvents were made with each successive generation of carbon core material. The glassy carbon material gave inconsistent *A* and *C*-terms. The in-house prepared carbon cores showed a large improvement over the glassy carbon cores in both *A* and *C*, where the values of these terms were also more consistent, indicating improved reproducibility in column preparation. As expected, the best performing columns were produced with the carbon cores made from the commercial source. They had both the tightest grouping and lowest values of *A* and *C* overall. The plot of *A* vs. *C* is shown below (see Figure 4.23) where the points closest to the origin represent better columns.

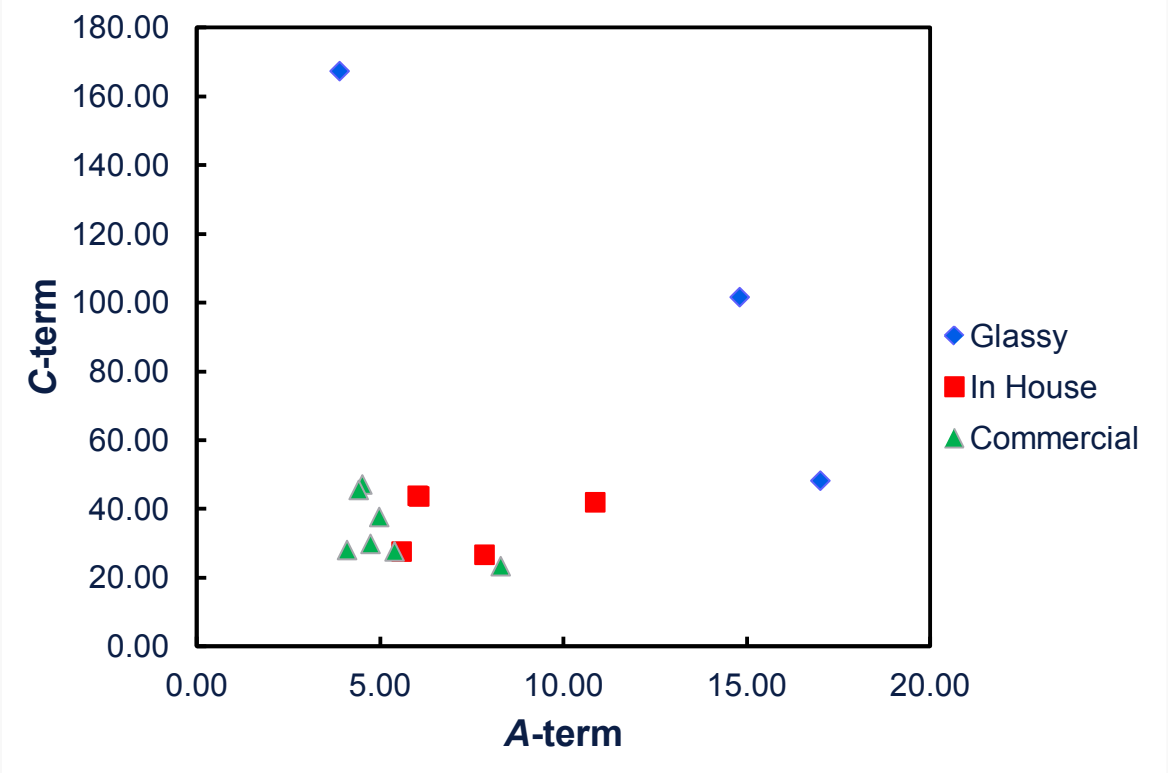

Figure 4.23 Plot of the *A*-term vs. the *C*-term for the best performing analytes from columns in this study.

4.5 Conclusions

SEM, FIB, and EDAX characterized the zirconia core particles with polymer/nanodiamond shells. Our "Halo" imaging and ion milling provided corroborating data on our particle shell thicknesses and gave us methods to characterize our particles more effectively.

As zirconia was prohibitively expensive, we sought a new core material that was both more economical and more spherical. To this end, we used a glassy carbon core donated by Supelco. With this material, we increased the particle stability by crosslinking the PAAm during functionalization.

FIB allowed us to detect the core porosity of the glassy carbon material, which led us to develop a polyDVB-based core that was nonporous. Data obtained from SEM and van Deemter curves helped us identify potential improvements that could be made with subsequent syntheses. Van Deemter curves and SEM validated each other throughout this process and helped identify the effects of agglomeration, poor packing, particle porosity, particle roughness, particle uniformity, and shell thickness on column efficiency, as well as individual van Deemter terms, specifically the *A*- and *C*-terms. We have seen improvements in particle uniformity, particle stability, and column efficiency in this study, and have associated the effects of particle roughness and shell thickness with the *A*- and *C*-terms, respectively. Overall, SEM, FIB, and van Deemter curves have been vital in the development of our core-shell materials during the past six years.

ACKNOWLEDGEMENTS

I thank US Synthetic Corporation for funding this research and Michael Standing for assistance with microscopy.

4.6 References

(1) Miller, J. M. *Chromatography: Concepts and Contrasts*; 2nd ed.; John Wiley & Sons, Inc: Hoboken, NJ, 2005.

(2) Snyder, L. R.; Kirkland, J. J.; Glajch, J. L. *Practical HPLC Method Development*; 2nd ed.; John Wiley: New York, 1997.

(3) Dai, J.; Yang, X. Q.; Carr, P. W. *J. Chromatogr. A* **2003**, *1005*, 63.

(4) Davies, N. H.; Euerby, M. R.; McCalley, D. V. *J. Chromatogr. A* **2008**, *1178*, 71.

(5) Kirkland, J. J.; van Straten, M. A.; Claessens, H. A. *J. Chromatogr. A* **1998**, *797*, 111.

(6) McCalley, D. V. *J. Chromatogr. A* **1997**, *769*, 169.

(7) McCalley, D. V. *J. Chromatogr. A* **1999**, *844*, 23.

(8) McCalley, D. V. *J. Sep. Sci.* **2003**, *26*, 187.

(9) McCalley, D. V. *J. Chromatogr. A* **2005**, *1075*, 57.

(10) McCalley, D. V. In *Advances in Chromatography, Vol 46*; Grushka, E., Grinberg, N., Eds. 2008; Vol. 46, p 305.

(11) Luo, H.; Ma, L. J.; Zhang, Y.; Carr, P. W. *J. Chromatogr. A* **2008**, *1182*, 41.

(12) Ma, L. J.; Luo, H.; Dai, J.; Carr, P. W. *J. Chromatogr. A* **2006**, *1114*, 21.

(13) Trammell, B. C.; Ma, L. J.; Luo, H.; Hillmyer, M. A.; Carr, P. W. *J. Chromatogr. A* **2004**, *1060*, 61.

(14) Zhang, Y.; Carr, P. W. *J. Chromatogr. A* **2011**, *1218*, 763.

(15) Zhang, Y.; Luo, H.; Carr, P. W. *J. Chromatogr. A* **2012**, *1228*, 110.

(16) O'Gara, J. E.; Wyndham, K. D. *J. Liq. Chromatogr. R. T.* **2006**, 29, 1025.

(17) Wyndham, K. D.; O'Gara, J. E.; Walter, T. H.; Glose, K. H.; Lawrence, N. L.; Alden, B. A.; Izzo, G. S.; Hudalla, C. J.; Iraneta, P. C. *Anal. Chem.* **2003**, *75*, 6781.

(18) Dunlap, C. J.; McNeff, C. V.; Stoll, D.; Carr, P. W. *Anal. Chem.* **2001**, *73*, 598A.

(19) Li, J. W.; Carr, P. W. *Anal. Chem.* **1997**, *69*, 2193.

(20) Nawrocki, J.; Rigney, M. P.; McCormick, A.; Carr, P. *J. Chromatogr. A* **1993**, *657*, 229.

(21) Trüdinger, U.; Müller, G.; Unger, K. K. *J. Chromatogr. A* **1990**, *535*, 111.

(22) Xiang, Y. Q.; Yan, B. W.; McNeff, C. V.; Carr, P. W.; Lee, M. L. *J. Chromatogr. A* **2003**, *1002*, 71.

(23) Elfakir, C.; Lafosse, M. *J. Chromatogr. A* **1997**, *782*, 191.

(24) Forgacs, E.; Cserhati, T. *Advances in Chromatography, Vol 40* **2000**, *40*, 359.

(25) Jensen, D. S.; Wiest, L. A.; Vail, M. A.; Dadson, A.; Linford, M. R. *Abstr. Pap. Am. Chem. S.* **2009**, *237*, 338.

(26) Pereira, L. *J. Liq. Chromatogr. R. T.* **2008**, 31, 1687.

(27) Ross, P. *LC GC N. Am.* **2000**, *18*, 14.

(28) West, C.; Elfakir, C.; Lafosse, M. *J. Chromatogr. A* **2010**, *1217*, 3201.

(29) Kobayashi, A.; Takezawa, K.; Takasaki, H.; Kanda, T.; Kutsuna, H. *J. Chromatogr. A* **2005**, *1073*, 163.

(30) Penner, N.; Nesterenko, P.; Ilyin, M.; Tsyurupa, M.; Davankov, V. *Chromatographia* **1999**, *50*, 611.

(31) Martin, A. J.; Synge, R. L. *Biochem. J.* **1941**, *35*, 1358.

(32) van Deemter, J. J.; Zuiderweg, F. J.; Klinkenberg, A. *Chem. Eng. Sci.* **1956**, *5*, 271.

(33) Gritti, F.; Guiochon, G. *Chem. Eng. Sci.* **2010**, *65*, 6310.

(34) Gritti, F.; Cavazzini, A.; Marchetti, N.; Guiochon, G. *J. Chromatogr. A* **2007**, *1157*, 289.

(35) Abrahim, A.; Al-Sayah, M.; Skrdla, P.; Bereznitski, Y.; Chen, Y. D.; Wu, N. J. *J. Pharmaceut. Biomed.* **2010**, *51*, 131.

(36) Cunliffe, J. M.; Maloney, T. D. *J. Sep. Sci.* **2007**, *30*, 3104.

(37) Salisbury, J. J. *J. Chromatogr. Sci.* **2008**, 46, 883.

(38) Saini, G.; Jensen, D. S.; Wiest, L. A.; Vail, M. A.; Dadson, A.; Lee, M. L.; Shutthanandan, V.; Linford, M. R. *Anal. Chem.* **2010**, *82*, 4448.

(39) Wiest, L. A.; Jensen, D. S.; Hung, C.-H.; Olsen, R. E.; Davis, R. C.; Vail, M. A.; Dadson, A. E.; Nesterenko, P. N.; Linford, M. R. *Anal. Chem.* **2011**, *83*, 5488.

(40) Hung, C.-H.; Wiest, L. A.; Singh, B.; Diwan, A.; Valentim, M. J. C.; Christensen, J. M.; Davis, R. C.; Miles, A. J.; Jensen, D. S.; Vail, M. A.; Dadson, A. E.; Linford, M. R. *Submitted to J. Sep. Sci.* **2013**.

(41) Yang, L.; Jensen, D. S.; Vail, M. A.; Dadson, A.; Linford, M. R. *J. Chromatogr. A* **2010**, *1217*, 7621.

(42) Jee, A.-Y.; Lee, M. *Curr. Appl. Phys.* **2009**, *9*, e144.

(43) Telepchak, M. J. *Chromatographia* **1973**, *6*, 234.

(44) Nesterenko, P. N.; Fedyanina, O. N. *J. Chromatogr. A* **2010**, *1217*, 498.

(45) Nesterenko, P.; Haddad, P. *Anal. Bioanal. Chem.* **2010**, *396*, 205.

(46) Fedyanina, O. N.; Nesterenko, P. N. *Russ. J. Phys. Ch. A* **2011**, *85*, 1773.

(47) Saini, G.; Yang, L.; Lee, M. L.; Dadson, A.; Vail, M. A.; Linford, M. R. *Anal. Chem.* **2008**, *80*, 6253.

(48) Saini, G.; Wiest, L. A.; Herbert, D.; Biggs, K. N.; Dadson, A.; Vail, M. A.; Linford, M. R. *J. Chromatogr. A* **2009**, *1216*, 3587.

(49) Ferreira, T.; Rasband, W.; NIH: 2012.

(50) Demers, H.; Ramachandra, R.; Drouin, D.; de Jonge, N. *Microsc. Microanal.* **2012**, *18*, 582.

(51) Drouin, D.; Hovington, P.; Gauvin, R. *Scanning* **1997**, *19*, 20.

(52) Hovington, P.; Drouin, D.; Gauvin, R. *Scanning* **1997**, *19*, 1.

(53) Hovington, P.; Drouin, D.; Gauvin, R.; Joy, D. C.; Evans, N. *Scanning* **1997**, *19*, 29.

(54) Seah, M. P.; Dench, W. A. *Surf. Interface Anal.* **1979**, *1*, 2.

(55) Ramanathan, T.; Fisher, F. T.; Ruoff, R. S.; Brinson, L. C. *Chem. Mater.* **2005**, *17*, 1290.

(56) Li, K.; Stöver, H. D. H. *J. Polym. Sci., Part A: Polym. Chem.* **1993**, *31*, 3257.

(57) Downey, J. S., McMaster University, 2000.

(58) Li, L.; Song, H.; Chen, X. *Mater. Lett.* **2008**, *62*, 179.

(59) Hirano, S.; Ozawa, M.; Naka, S. *J. Mater. Sci.* **1981**, *16*, 1989.

(60) Bai, F.; Yang, X. L.; Huang, W. Q. *Macromolecules* **2004**, *37*, 9746.

(61) Li, W. H.; Stover, H. D. H. *Macromolecules* **2000**, *33*, 4354.

(62) Partouche, E.; Margel, S. *Carbon* **2008**, *46*, 796.

(63) El-Hendawy, A. N. A. *Carbon* **2003**, *41*, 713.

(64) Morenocastilla, C.; Ferrogarcia, M. A.; Joly, J. P.; Bautistatoledo, I.; Carrascomarin, F.; Riverautrilla, J. *Langmuir* **1995**, *11*, 4386.

Chapter 5: Conclusions and Future Work

5.1 Conclusions

My graduate studies focused on the creation of core-shell particles that could be used for liquid chromatography under extreme pH conditions and elevated temperatures. For this to become a successful endeavor, the material needed to be stable at low pH (below 2), high pH (above 11) and elevated temepratures. It also needed to have a useful selectivity for LC and be synthesized reproducibly.

An early prototype of my work used zirconia as the core with layer-by-layer deposited nanodiamond/polymer shells. The development of this material assisted us in learning to characterize our material using SEM. We were able to determine our shell thickness with two techniques: focused ion beam milling and "Halo" imaging. The reversed-phase column made from this material lacked mechanical stability, yet this prototype was a step in the right direction from the irregular diamond cores we had started with.

The next prototype used a glassy carbon shell from Supelco as the core with the same layer-by-layer deposition of nanodiamond and polymer. These particles were simultaneously functionalized and crosslinked with a C_{18} epoxide and a diepoxide resulting in a much more mechanically stable material.

A column packed with these particles was stability tested at pH 11.3 and pH 13 and showed very little degradation over the entire period of the test. Alkylbenzenes, cholesterol, phenols, pesticides, and TCAs were separated on this column. Again, this column was an improvement over previous generations, however further study revealed that this core was in fact porous and the cores were not entirely spherical.

The next columns used carbonized polyDVB as the core. These cores were much more spherical and far less porous than the previous glassy carbon material. Studies at elevated temperature were performed and while catastrophic failure was never observed, repeated heating and cooling of the column appeared to substantially decrease the efficiency of the column over time. TCAs were separated at pH 7 and 12 and a drastic difference in selectivity was observed. At this point, we realized that our amine backbone likely gave a mixed mode character to our ccolumn, resulting in a C_{18}/WAX phase. Depending on pH, the phase would function more as a reversed phase or more as a weak anion exchanger.

Overall this column has proven to be more reproducible than previous prototypes and efficiencies of ca. 100,000 N/m (*k* ca. 4.5) are commonly seen. Many analyte mixtures have been separated such as essential oils, β_2-agonists, amphetamines, TCAs, phenols, alkylbenzenes and triazine herbicides.

5.2 Future Work

While many advances have taken place during my time on this project, some deficiencies still exist with the column that should be addressed in future work. The current particles have a broad pore size distribution and low surface area, which needs to be improved. This might be done by using a smaller nanodiamond, and/or nanodiamond with a narrower particle size distribution. As the core is currently 3.5 μm in diameter, smaller cores should be manufactured so as to give higher efficiencies and make faster and higher resolution separations possible. The shell also needs to be optimized. Currently, the pore size distribution is very broad. Smaller nanodiamond may reduce the pore size and increase surface area.

It may also be possible to improve PAAm adhesion to the nanodiamond by carboxyl terminating the diamond. Hünig's base may improve surface functionalization by setting the protonatation state of the PAAm. Other S_N2 reactive molecules (alkylhalides) could be reacted with the amine surface which would remove polar moieties currently present with the current epoxide chemistry.

The column degradation observed with the repeated heating and cooling during the van't Hoff studies is of concern. It is not known whether the particles were degrading, or the particle bed was becoming increasingly disordered. A test in which a column goes through repeated temperature cycles with regular testing with a hexylbenzene standard and another column is kept at high temperature with continual testing with the same analyte would determine the source of this degradation.

If the column could be made stable to elevated temperatures for extended periods of time, water-only separations and FID detection could be possible, and should be attempted along with thermal gradients. Supercritical fluid chromatography might also be possible, considering the potential stability of the column.

Other functionalities should be attempted as well. Varying the alkyl chain length on the column could give different selectivity to the column. Other ligands, such as biphenyl, perfluoro, phenylhexyl and HILIC-type phases might also be possible, considering the amine coated support on this column.

Finally, other sizes of columns or traps should be packed making applications in UHPLC, proteomics and MudPIT potentially viable.

Appendix 1: Flare Mixed-Mode Column: β_2-Agonists and Amphetamines*

A1.1 Introduction

Amphetamines are a class of chemicals that can act as stimulants, decongestants, and hallucinogens, where some compounds in this category are illicit substances.[1] All are primary or secondary amines giving these compounds higher pK_a values (9.3 – 9.8). At pH < 9.3 – 9.8 the molecules are increasingly protonated, generally reducing retention on C_{18} columns, but at pH > 9.3 – 9.8 they are increasingly deprotonated (neutral), which can facilitate a reversed-phase retention mechanism. Because of the lack of stability of most silica-based columns at elevated pH, there are relatively few reports of the separation of these compounds in their neutral form on silica-based C_{18} columns. Accordingly, it is often necessary to derivatize them.[2] Here we show their direct analysis at elevated pH using the Flare mixed-mode column.

Many β_2-agonists are used to treat asthma and other pulmonary diseases by relaxing smooth muscle tissue via action on the β_2-adrenergic receptor.[3] Some of them are used illegally to increase the muscle to fat ratios in livestock.[4] These chemicals are also amines – they are basic analytes. Similar to the amphetamines, it is advantageous to operate at elevated pH when separating them by a reversed-phase mechanism.

Separations of amphetamines and β_2-agonists were performed at pH 12 using the Flare Mixed-Mode column from Diamond Analytics. This column is the first functionalized, carbon-based phase.[5] As this column is diamond-based, it has stability under extreme pH conditions.[6]

*This chapter has been published as an application note by Diamond Analytics (Landon A. Wiest, David S. Jensen, Andrew Miles, Andrew Dadson, Matthew R. Linford)

A1.2 Experimental

Analytes: Cimaterol, tulobuterol, mabuterol and mapenterol were purchased from Sigma-Aldrich. (St. Louis, MO). Phenylpropanolamine and methamphetamine were obtained from Restek (Bellefonte, PA).

Sample: Analyte mixtures were created in the mobile phase as ca. 1 mg/mL solutions.

Column: Diamond Analytics Flare Mixed-Mode (2.1 mm × 50 mm, 4 μm)

System: Agilent 1290 UHPLC, binary pump, DAD, ChemStation software

Injection volume: 1.0 μL

Temperature: 35 °C

Flow rate: 0.2 mL/min

Detection: UV/Vis Diode Array Detector (254 nm)

Needle wash: 1 min with methanol

Mobile Phase: 70:30 10 mM aqueous phosphate buffer (pH 12)/acetonitrile, isocratic

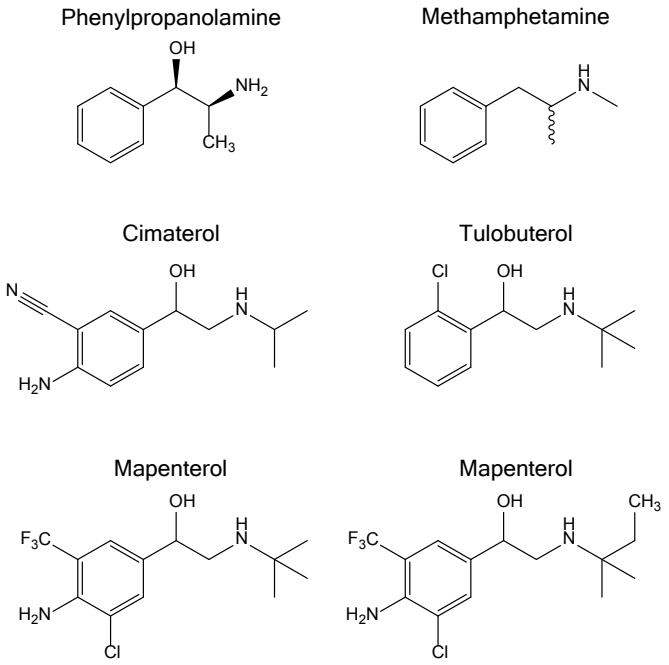

Scheme 1. Structure of the β_2-agonists and amphetamines used in this application note.

A1.3 Results and Discussion

Figure A1.1 shows baseline separation of four β_2-agonists in under three min. For the latter two compounds in the separation, efficiencies exceed 50,000 N/m and tailing factors are close to 1. Figure A1.2 shows the baseline separation of two amphetamines and three β_2-agonists in under three min. Efficiencies of the latter two compounds are again in excess of 50,000 N/m and tailing factors are ca. 1.

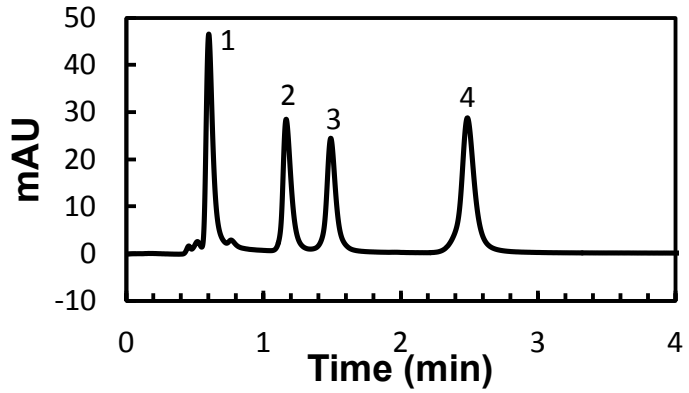

Figure A1.1 Separation of four β_2-agonists: (1) Cimaterol, (2) Tulobuterol, (3) Mabuterol, (4) Mapenterol.

Table A1.1 Retention of Various β_2-Agonists.

	Analyte	t_r	N/m	T_f
1.	Cimaterol	0.601	14960	1.74
2.	Tulobuterol	1.164	38060	1.40
3.	Mabuterol	1.489	52580	1.15
4.	Mapenterol	2.485	73220	1.05

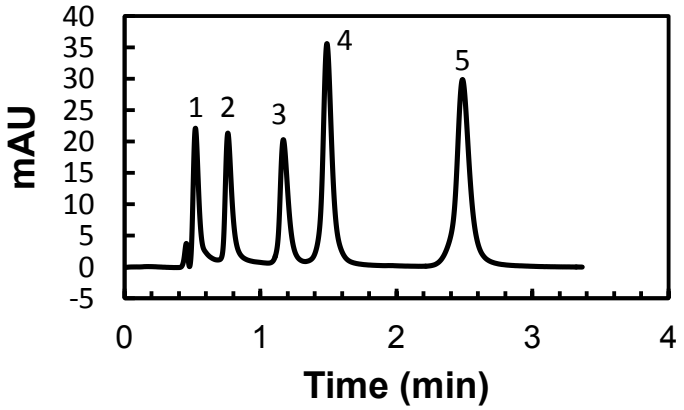

Figure A1.2 Separation of β_2-agonists and amphetamines: (1) Propanolamine, (2) Methamphetamine, (3) tulobuterol, (4) Mabuterol, (5) Mapenterol.

Table A1.2 Retention of Amphetamines and β_2-Agonists.

	Analyte	t_r	N/m	T_f
1.	Phenylpropanolamine	0.521	15520	2.25
2.	Methamphetamine	0.760	25060	
3.	Tulobuterol	1.168	37620	1.36
4.	Mabuterol	1.488	52580	1.15
5.	Mapenterol	2.485	73400	1.06

A1.4 References

(1) Report to accompany H.R. 5246 19 Sep 86.

(2) Herráez-Hernández, R.; Campíns-Falcó, P.; Sevillano-Cabeza, A. *Anal. Chem.* **1996**, *68* (5), 734-739.

(3) Tashkin, D. P.; Fabbri, L. M. *Resp. Res.* **2010**, *11* (149).

(4) Sai, F.; Hong, M.; Yunfeng, Z.; Huijing, C.; Yongning, W. *J. Agr. Food Chem.* **2012**, *60* (8), 1898-1905.

(5) Zhang, Y.; Zhang, Z.; Sun, Y.; Wei, Y. *Journal J. Agr. Food Chem.* **2007**, *55* (13), 4949-4956.

(6) Saini, G.; Jensen, D. S.; Wiest, L. A.; Vail, M. A.; Dadson, A.; Lee, M. L.; Shutthanandan, V.; Linford, M. R. *Anal. Chem.* **2010**, *82* (11), 4448-4456.

(7) Wiest, L. A.; Jensen, D. S.; Hung, C.-H.; Olsen, R. E.; Davis, R. C.; Vail, M. A.; Dadson, A. E.; Nesterenko, P. N.; Linford, M. R. *Anal. Chem.* **2011**, *83* (14), 5488-5501.

Appendix 2: Flare Mixed-Mode Column: Triazine Herbicides*

A2.1 Introduction

Triazine herbicides have been widely used, e.g., by Midwestern corn farmers in the United States for weed control.[1] And while generally effective, there is a major concern of these herbicides entering the water supply. In particular, the more hydrophilic herbicides and their degradation products can be carried by runoff into streams and the more hydrophobic varieties and their degradation products can be absorbed by the soil and ultimately enter the ground water.[1] Triazine herbicides act as photosystem II inhibitors, reducing the electron flow from water to $NADPH_2^+$ at the photochemical step in photosynthesis, which causes intolerable oxidation in plants that eventually results in their death.[2]

Chromatographic methods, such as gas chromatography (GC) with electron capture detection (ECD), have been used to determine the concentrations of triazine herbicides in water. Nevertheless HPLC has some advantages over GC. HPLC allows analysis of polar, non-volatile, and/or thermally labile analytes, where these analytes may be separated together with non-polar analytes in a single run.[3]

The Flare mixed-mode column from Diamond Analytics was used to separate a mixture of five triazine herbicides at pH 12 (see Scheme 1). Elevated pH values activate/accentuate the reversed-phase retention mechanism of this column, which is the first functionalized, carbon/nanodiamond-based phase. These materials give the column extraordinary stability under extreme pH conditions.[4-5]

*This chapter has been published as an application note by Diamond Analytics (Landon A. Wiest, David S. Jensen, Andrew Miles, Andrew Dadson, Matthew R. Linford)

A2.2 Experimental

Analytes: Cyanazine, simazine, atrazine, propazine and prometryn were purchased from Sigma-Aldrich. (St. Louis, MO)

Sample: 2 mg of each analyte was dissolved in 6 mL mobile phase and 4 mL isopropanol

Column: Diamond Analytics Flare Mixed-Mode (4.6 mm × 33 mm, 4 μm)

System: Waters 1525 HPLC binary pump, Waters Column Heater (CH5), Breeze 3.30 SPA software

Injection volume: 5.0 μL

Temperature: 35 °C

Flow rate: 0.7 mL/min

Detection: Waters 2487 Dual λ Absorbance Detector @ 254 nm

Mobile Phase: 70:30 10 mM aqueous phosphate buffer (pH 12)/acetonitrile, isocratic

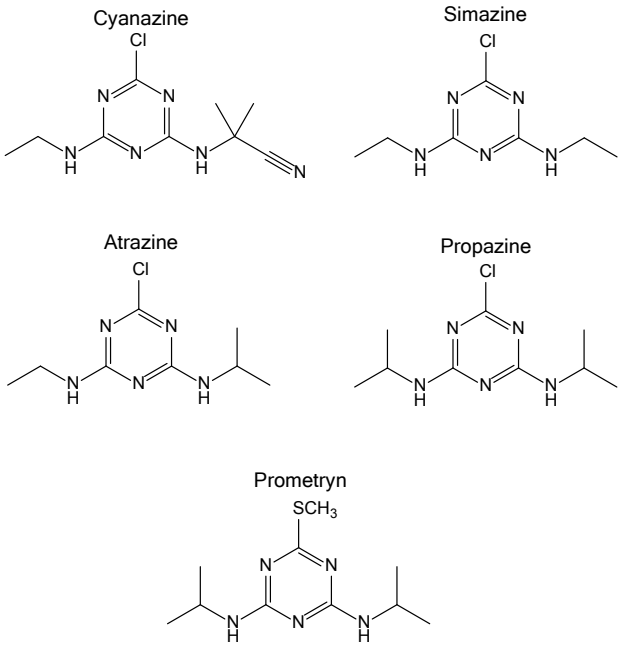

Scheme 1. Structure of separated triazine herbicides

A2.3 Results and Discussion

Figure A2.1 shows separation of five triazine herbicides in less than 2.5 min. For the last compound in the separation, the efficiency exceeded 36,000 N/m and tailing factors were 1.4 – 1.5 for all analytes.

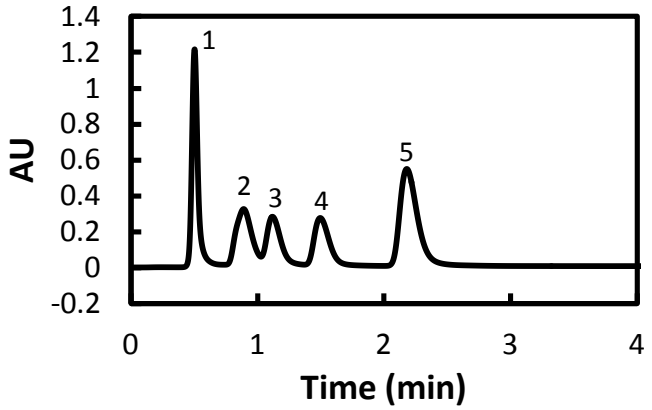

Figure A2.1 Separation of five triazine herbicides: (1) cyanazine, (2) simazine, (3) atrazine, (4) propazine, (5) prometryn.

Table A2.1 Retention of Triazine Herbicides.

	Analyte	t_r	N/m	T_f	R
1.	Cyanazine	0.501	19636	1.42	—
2.	Simazine	0.889	6242	—	2.40
3.	Atrazine	1.117	14152	—	1.01
4.	Propazine	1.495	22273	1.43	1.77
5.	Prometryn	2.179	36394	1.53	2.91

A2.4 References

(1) Scribner, E.A., Thurman, E.M., Goolsby, D.A., Meyer, M.T., Battaglin, W.A., and Kolpin, D.W., 2005, Summary of significant results from studies of triazine herbicides and their degradation products in surface water, ground water, and precipitation in the Midwestern United States during the 1990s: U.S. Geological Survey Scientific Investigations Report 2005–5094, 27 p.

(2) Stryer, L. *Biochemistry*; 4th ed.; W.H. Freeman and Company, 1995.

(3) Lintelmann, J.; Mengel, C.; Kettrup, A. *Fresenius J. Anal. Chem.* **1993**, *346*, 752-756.

(4) Saini, G.; Jensen, D. S.; Wiest, L. A.; Vail, M. A.; Dadson, A.; Lee, M. L.; Shutthanandan, V.; Linford, M. R. *Anal. Chem.* **2010**, *82*, 4448-4456.

(5) Wiest, L. A.; Jensen, D. S.; Hung, C.-H.; Olsen, R. E.; Davis, R. C.; Vail, M. A.; Dadson, A. E.; Nesterenko, P. N.; Linford, M. R. *Anal. Chem.* **2011**, *83*, 5488-5501.

Appendix 3: Separation of Lavender Essential Oil Using Gradient Elution on the Diamond Analytics Flare Mixed-Mode/C_{18} Column*

A3.1 Introduction

The Flare Mixed-Mode/C_{18} column by Diamond Analytics was used to separate the components in lavender essential oil.

Lavender essential oil has been used topically to treat allergies,[1] herpes,[2] and the appearance of stretch marks.[3] Its oral uses have included the treatment of menopausal conditions,[4] insomnia,[5] and premenstrual conditions.[3] Lavender has also been used aromatically as a relaxant, and sleep aid.[5-6]

While these previous uses are perhaps somewhat anecdotal, recent studies suggest that lavender can be used as an analgesic,[7] antifungal,[8] anti-inflammatory,[7] anti-microbial,[8-9] anti-tumor[10] and anti-mutagenic agent.[11] Lavender has also been used as a sedative and to treat anxiety.[12-13]

Lavender is composed of many compounds, including alcohols, esters, monoterpenes, sesquiterpenes, phenols, aldehydes, coumarins, ketones and lactones.[3]

*This chapter has been published as an application note by Diamond Analytics (Landon A. Wiest, David S. Jensen, Andrew Miles, Andrew Dadson, Matthew R. Linford)

A3.2 Experimental

Gradient elution was used to separate the mixture of compounds that comprise the lavender essential oil. Known components of the oil including linalool, linalyl acetate, and β-ocimene were purchased from Sigma-Aldrich (St. Louis, MO).

Sample: 5 μL of lavender essential oil from dōTERRA Intl., Orem, UT, dissolved in 1mL of acetonitrile

Column: Flare Mixed-Mode Column (4.6 mm × 3.3 mm, 4.0 μm)

System: Agilent 1290 UHPLC, binary pump, DAD, ChemStation software

Injection volume: 2 μL

Temperature: 35 °C

Flow rate: 1.0 mL/min

Detection: Multiwavelength UV/Vis Diode Array (214, 230 nm)

Needle wash: 1 min with methanol

Mobile Phase: Gradient

A: 10 mM phosphate buffer, pH 8

B: Acetonitrile

Time	Water	ACN
0	70	30
12	30	70

A3.3 Results and Discussion

The retention times of linalool (A), linalyl acetate (B) and β-ocimene (C) were obtained by individually injecting each compound on the Flare column. These retention times were compared with peaks present in the lavender essential oil. They appeared at the following retention times: 1.03 min (linalool), 2.50 min (linalyl acetate) and 3.92 min (β-ocimene) (see Figure A3.1).

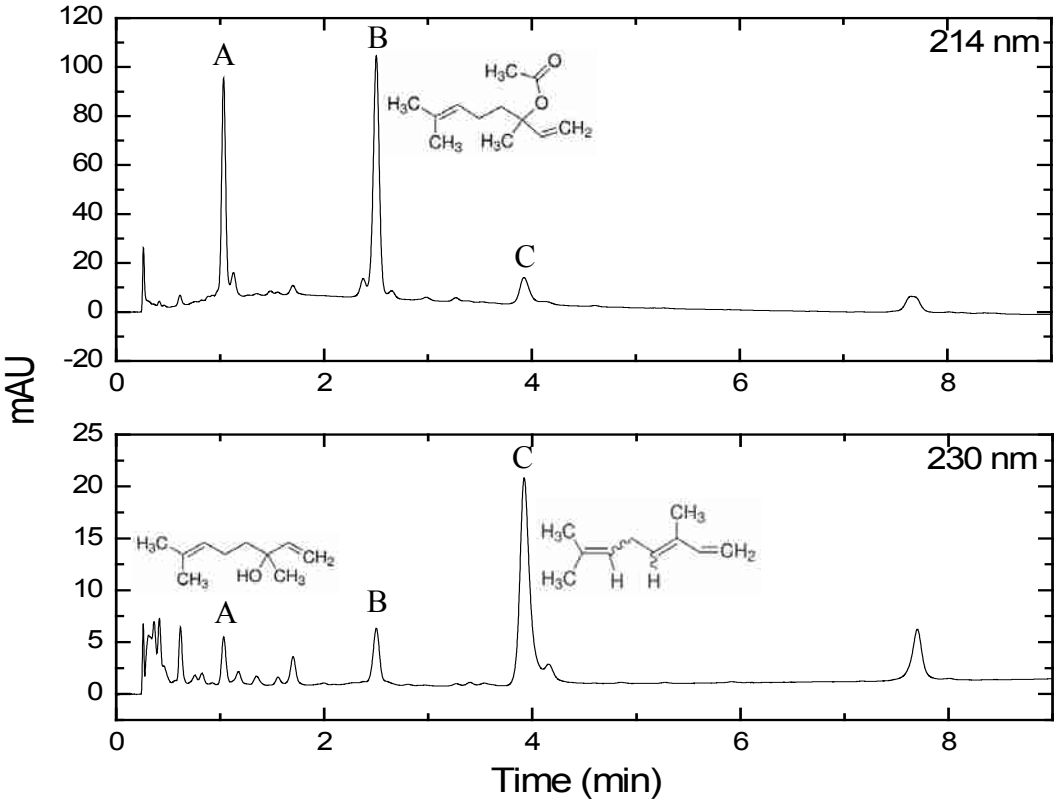

Figure A3.1 Gradient separation of lavender essential oil (214, 230 nm).

A3.4 References

(1) Kim, H. M.; Cho, S. H. *J. Pharm. Pharmacol.* **1999**, *51* (2), 221-226.

(2) Yucharoen, R.; Chansakaow, S.; Tragoolpua, Y. *Afr. J. Biotechnol.* **2011**, *10* (68), 15394-15401.

(3) *Modern Essentials*; 3rd ed.; Abundant Health: Spanish Fork, UT, 2011.

(4) Yamada, K.; Mimaki, Y.; Sashida, Y. *Biol. Pharm. Bull.* **2005**, *28* (2), 378-379.

(5) Lee, I.-S.; Lee, G.-J. *Taehan Kanho Hakhoe chi* **2006**, *36* (1), 136-143.

(6) Dunn, C.; Sleep, J.; Collett, D. *J. Adv. Nurs.* **1995**, *21* (1), 34-40.

(7) Hajhashemi, V.; Ghannadi, A.; Sharif, B. *J. Ethnopharmacol.* **2003**, *89* (1), 67-71.

(8) D'Auria, F. D.; Tecca, M.; Strippoli, V.; Salvatore, G.; Battinelli, L.; Mazzanti, G. *Med. Mycol.* **2005**, *43* (5), 391-396.

(9) Moon, T.; Wilkinson, J. M.; Cavanagh, H. M. A. *Parasitol. Res.* **2006**, *99* (6), 722-728.

(10) Mills, J. J.; Chari, R. S.; Boyer, I. J.; Gould, M. N.; Jirtle, R. L. *Cancer Res.* **1995**, *55* (5), 979-983.

(11) Evandri, M. G.; Battinelli, L.; Daniele, C.; Mastrangelo, S.; Bolle, P.; Mazzanti, G. *Food Chem. Toxicol.* **2005**, *43* (9), 1381-1387.

(12) Buchbauer, G.; Jirovetz, L.; Jager, W.; Dietrich, H.; Plank, C.; Karamat, E. *Zeitschrift Naturforsch. C* **1991**, *46* (11-12), 1067-1072.

(13) Guillemain, J.; Rousseau, A.; Delaveau, P. *Ann. Pharm. Fr.* **1989**, *47* (6), 337-343.

Appendix 4: Separation of Melaleuca Essential Oil Using Gradient Elution on the Diamond Analytics Flare Mixed-Mode/C_{18} Column*

A4.1 Introduction

The Flare Mixed-Mode/C_{18} column by Diamond Analytics was used to separate the components in melaleuca essential oil.

Melaleuca tree, *melaleuca alternifolia*, (tea tree) was used by aboriginal tribes to treat wounds and skin infections.[1] According to an essential oils handbook, melaleuca has twelve times the antiseptic power of phenol and strong immune building properties.[1] Recent studies suggest that melaleuca can be used as an antibacterial,[2-8] antifungal,[9-13] anti-inflammatory,[14-17] and antiviral agent.[18] Melaleuca has also been used to treat boils and acne.[17,19-20]

Melaleuca is composed of many compounds including monoterpenes, phenols, sesquiterpenes, alcohols and sesquiterpene alcohols.[1]

*This chapter has been published as an application note by Diamond Analytics (Landon A. Wiest, David S. Jensen, Andrew Miles, Andrew Dadson, Matthew R. Linford)

A4.2 Experimental

Gradient elution was used to separate the mixture of compounds that comprise the melaleuca essential oil. A known component of the oil was purchased from Sigma-Aldrich (St. Louis, MO).

Sample: 5 μL of Melaleuca essential oil (dōTERRA Intl., Orem, UT) dissolved in 1 mL of acetonitrile

Column: Flare Mixed-Mode Column (4.6 mm × 3.3 mm, 4.0 μm)

System: Agilent 1290 UHPLC, binary pump, DAD, ChemStation software

Injection volume: 2 μL

Temperature: 35 °C

Flow rate: 1.0 mL/min

Detection: Multiwavelength UV/Vis Diode Array (214 nm)

Needle wash: 1 min with methanol

Mobile Phase: Gradient

A: 10 mM phosphate buffer, pH 8

B: Acetonitrile

Time	Water	ACN
0	70	30
12	30	70

A4.3 Results and Discussion

The retention time of terpineol (A) was obtained by injecting it on the Flare column. The retention time was compared with the peak present in the melaleuca essential oil. Its retention time was 0.88 min (see Figure A4.1).

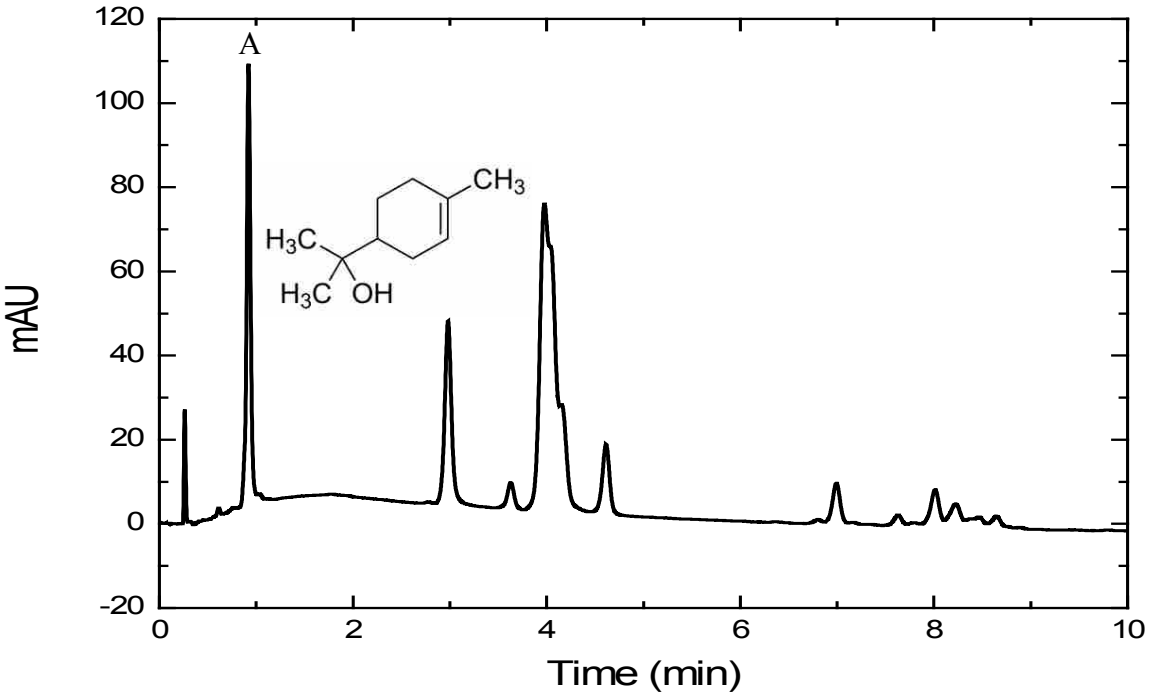

Figure A4.1 Gradient separation of melaleuca essential oil (214 nm).

A4.4 References

(1) *Modern Essentials*; 3 ed.; Abundant Health: Spanish Fork, UT, 2011.

(2) Banes-Marshall, L.; Cawley, P.; Phillips, C. A. *Brit. J. Biomed. Sci.* **2001**, *58* (3), 139-145.

(3) Carson, C. F.; Cookson, B. D.; Farrelly, H. D.; Riley, T. V. *Journal of Antimicrobial Chemotherapy* **1995**, *35* (3), 421-424.

(4) Carson, C. F.; Hammer, K. A.; Riley, T. V. *Microbios* **1995**, *82* (332), 181-185.

(5) Carson, C. F.; Hammer, K. A.; Riley, T. V. *J. Antimicrob. Chemoth.* **1996**, *37* (6), 1177-1178.

(6) Ferrini, A. M.; Mannoni, V.; Aureli, P.; Salvatore, G.; Piccirilli, E.; Ceddia, T.; Pontieri, E.; Sessa, R.; Oliva, B. *Int. J. Immunopath. Ph.* **2006**, *19* (3), 539-544.

(7) Hammer, K. A.; Carson, C. E.; Riley, T. V. *Int. J. Antimicrob. Ag.* **2008**, *32* (2), 170-173.

(8) Longbottom, C. J.; Carson, C. F.; Hammer, K. A.; Mee, B. J.; Riley, T. V. *J. Antimicrob. Chemoth.* **2004**, *54* (2), 386-392.

(9) Buck, D. S.; Nidorf, D. M.; Addino, J. G. *J. Fam. Practice* **1994**, *38* (6), 601-605.

(10) Hammer, K. A.; Carson, C. F.; Riley, T. V. *Am. J. Infect. Control* **1996**, *24* (3), 186-189.

(11) Hammer, K. A.; Carson, C. F.; Riley, T. V. *J. Antimicrob. Chemoth.* **2004**, *53* (6), 1081-1085.

(12) Mondello, F.; De Bernardis, F.; Girolamo, A.; Cassone, A.; Salvatore, G. *Bmc Infectious Diseases* **2006**, *6*.

(13) Satchell, A. C.; Saurajen, A.; Bell, C.; Barnetson, R. S. C. *The Australasian Journal of Dermatology* **2002**, *43* (3), 175-178.

(14) Caldefie-Chezet, F.; Fusillier, C.; Jarde, T.; Laroye, H.; Damezi, M.; Vasson, M. P.; Guillot, J. *Phytother. Res.* **2006**, *20* (5), 364-370.

(15) Caldefie-Chezet, F.; Guerry, M.; Chalchat, J. C.; Fusillier, C.; Vasson, M. P.; Guillot, J. *Free Radical Res.* **2004**, *38* (8), 805-811.

(16) Hart, P. H.; Brand, C.; Carson, C. F.; Riley, T. V.; Prager, R. H.; Finlay-Jones, J. J. *Inflamm. Res.* **2000**, *49* (11), 619-626.

(17) Koh, K. J.; Pearce, A. L.; Marshman, G.; Finlay-Jones, J. J.; Hart, P. H. *Brit. J. Dermatol.* **2002**, *147* (6), 1212-1217.

(18) Farag, R. S.; Shalaby, A. S.; El-Baroty, G. A.; Ibrahim, N. A.; Ali, M. A.; Hassan, E. M. *Phytother. Res.* **2004**, *18* (1), 30-35.

(19) Bassett, I. B.; Pannowitz, D. L.; Barnetson, R. S. *Med. J. Australia* **1990**, *153* (8), 455-&.

(20) Enshaieh, S.; Jooya, A.; Siadat, A. H.; Iraji, F. *Indian J. Dermatol. Venereol. Leprology* **2007**, *73* (1), 22-25

Appendix 5: Separation of Eucalyptus Essential Oil Using Gradient Elution on the Diamond Analytics Flare Mixed-Mode/C_{18} Column*

A5.1 Introduction

The Flare Mixed-Mode/C_{18} column by Diamond Analytics was used to separate the components in eucalyptus essential oil.

Eucalyptus essential oil vapor is used for asthma,[1] bronchitis,[2] flu,[3] respiratory viruses,[4] and for sanitizing.[5-6] Topical uses include help with bronchitis,[7] congestion,[8] ear inflammation,[9] inflammation,[10-11] lice,[12] and overextended muscles and pain.[13]

Recent studies suggest that eucalyptus can also be used as an analgesic,[14] antibacterial,[15-16] anti-inflammatory,[10] antiviral,[17] and insecticidal agent,[18-19] and can also reduce blood pressure.[20]

Eucalyptus is composed of many compounds, including monoterpenes, alcohols and aldehydes.[13]

*This chapter has been published as an application note by Diamond Analytics (Landon A. Wiest, David S. Jensen, Andrew Miles, Andrew Dadson, Matthew R. Linford)

A5.2 Experimental

Gradient elution was used to separate the mixture of compounds that comprise the eucalyptus essential oils. Know components of the oil, including pinene and terpineol, were purchased from Sigma-Aldrich (St. Louis, MO).

Sample: 5 μL of Eucalyptus essential oil (dōTERRA Intl., Orem, UT) dissolved in 1 mL of acetonitrile

Column: Flare Mixed-Mode Column (4.6 mm × 3.3 mm, 4.0 μm)

System: Agilent 1290 UHPLC, binary pump, DAD, ChemStation software

Injection volume: 2 μL

Temperature: 35 °C

Flow rate: 1.0 mL/min

Detection: Multiwavelength UV/Vis Diode Array (214 nm)

Needle wash: 1 min with methanol

Mobile Phase: Gradient

A: 10 mM phosphate buffer, pH 8

B: Acetonitrile

Time	Water	ACN
0	70	30
12	30	70

A5.3 Results and Discussion

The retention times of terpineol (A) and pinene (B) were obtained by individually injecting each compound on the Flare column. These retention times were compared with peaks present in the eucalyptus essential oil. They appeared at the following retention times: 0.88 min (terpineol) and 4.63 min (pinene) (see Figure A5.1).

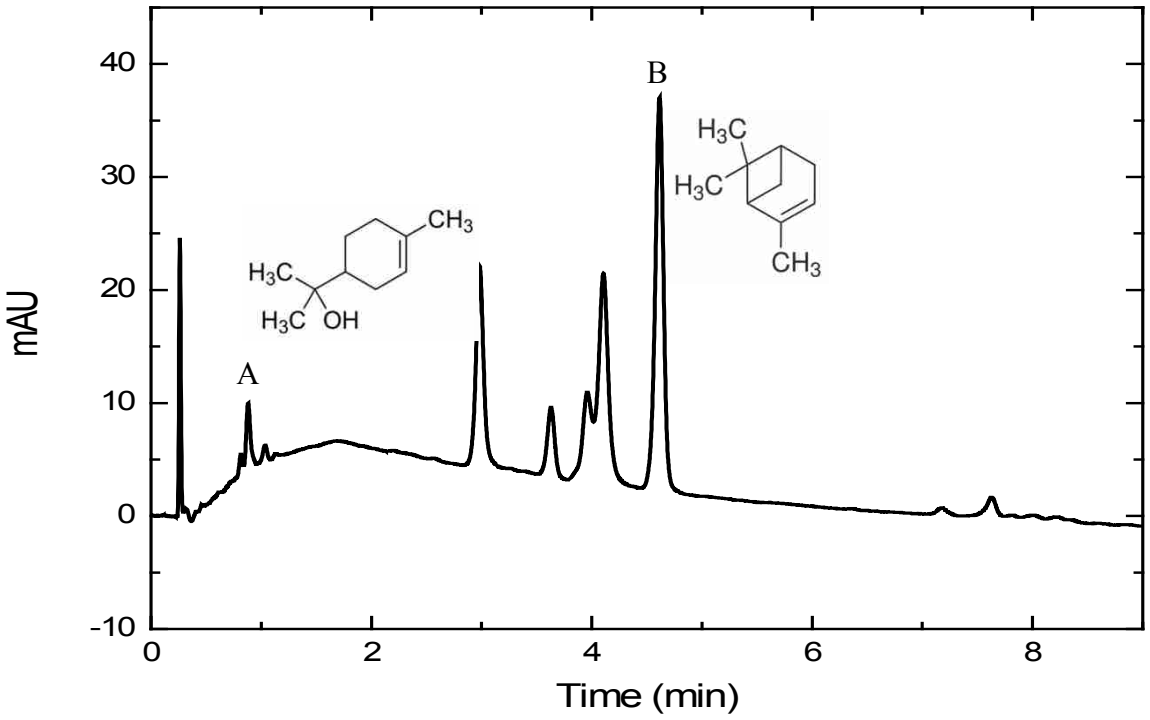

Figure A5.1 Gradient separation of eucalyptus essential oil (214 nm).

A5.4 References

(1) Juergens, U. R.; Dethlefsen, U.; Steinkamp, G.; Gillissen, A.; Repges, R.; Vetter, H. *Resp. Med.* **2003**, *97* (3), 250-256.

(2) Lu, X.-q.; Tang, F.-d.; Wang, Y.; Zhao, T.; Bian, R.-l. *China journal of Chinese materia medica* **2004**, 29 (2), 168-171.

(3) Pyankov, O. V.; Usachev, E. V.; Pyankova, O.; Agranovski, I. E. *Aerosol Sci. Tech.* **2012**, *46* (12), 1295-1302.

(4) Cermelli, C.; Fabio, A.; Fabio, G.; Quaglio, P. *Curr. Microbiol.* **2008**, *56* (1), 89-92.

(5) Sartorelli, P.; Marquioreto, A. D.; Amaral-Baroli, A.; Lima, M. E. L.; Moreno, P. R. H. *Phytother. Res.* **2007**, *21* (3), 231-233.

(6) Delaquis, P. J.; Stanich, K.; Girard, B.; Mazza, G. *Int. J. Food Microbiol.* **2002**, *74* (1-2), 101-109.

(7) Siurin, S. A. *Klin. Med. Moscow* **1997**, *75* (10), 43-45.

(8) Paul, I. M.; Beiler, J. S.; King, T. S.; Clapp, E. R.; Vallati, J.; Berlin, C. M. *Pediatrics* **2010**, *126* (6), 1092-1099.

(9) Atta, A. H.; Alkofahi, A. *J. Ethnopharmacol.* **1998**, *60* (2), 117-124.

(10) Grassmann, J.; Hippeli, S.; Dornisch, K.; Rohnert, U.; Beuscher, N.; Elstner, E. F. *Arzneimittel-Forsch.* **2000**, *50* (2), 135-139.

(11) Silva, J.; Abebe, W.; Sousa, S. M.; Duarte, V. G.; Machado, M. I. L.; Matos, E. T. A. *J. Ethnopharmacol.* **2003**, *89* (2-3), 277-283.

(12) Williamson, E. M.; Priestley, C. M.; Burgess, I. F. *Fitoterapia* **2007**, *78* (7-8), 521-525.

(13) *Modern Essentials*; 3 ed.; Abundant Health: Spanish Fork, UT, 2011.

(14) Gobel, H.; Schmidt, G.; Soyka, D. *Cephalalgia* **1994**, *14* (3), 224-234.

(15) Charles, C. A.; Amini, P.; Gallob, J.; Shang, H. Y.; McGuire, J. A.; Costa, R. *Am. J. Dent.* **2012**, *25* (4), 195-198.

(16) Rasooli, I. International Journal of Infectious Diseases **2008**, 12 E167-E167.

(17) Schnitzler, P.; Schon, K.; Reichling, J. *Pharmazie* **2001**, *56* (4), 343-347.

(18) Ootani, M. A.; Aguiar, R. W. D.; de Mello, A. V.; Didonet, J.; Portella, A. C. F.; do Nascimento, I. R. *Bioscience Journal* **2011**, *27* (4), 609-618.

(19) Singh, G.; Upadhyay, R. K. *J. Sci. Ind. Res. India* **1993**, *52* (10), 676-683.

(20) Lahlou, S.; Figueiredo, A. F.; Magalhaes, P. J. C.; Leal-Cardoso, J. H. *Can. J. Physiol. Pharm.* **2002**, *80* (12), 1125-1131.

Appendix 6: Separation of Peppermint Essential Oil Using Gradient Elution on the Diamond Analytics Flare Mixed-Mode/C_{18} Column*

A6.1 Introduction

The Flare Mixed-Mode/C18 column by Diamond Analytics was used to separate the components in peppermint essential oil.

Peppermint essential oil has been used medicinally to treat asthma,[1-2] bronchitis, candida,[3-5] diarrhea,[6] flu,[7] halitosis,[8] hot flashes,[9] indigestion,[10] migraines,[11] nausea,[12] and vomiting.[13] Peppermint oil is also documented to have antibacterial,[14-16] anti-inflammatory,[17-18] antispasmodic,[2] and antiviral properties,[19-22] and is an aid for digestion and indigestion.[6,23]

Peppermint is composed of many compounds, including phenolic alcohols, ketones, monoterpenes, esters, furanoids, phenols, alcohols, furanocoumarins and sulphides.[13]

*This chapter has been published as an application note by Diamond Analytics (Landon A. Wiest, David S. Jensen, Andrew Miles, Andrew Dadson, Matthew R. Linford)

A6.2 Experimental

Gradient elution was used to separate the mixture of compounds that comprise the peppermint essential oil. Known components of the oil including menthone and pinene were purchased from Sigma-Aldrich (St. Louis, MO).

Sample: 5 μL of peppermint essential oil from dōTERRA Intl., Orem, UT, dissolved in 1mL of acetonitrile

Column: Flare Mixed-Mode Column (4.6 mm × 3.3 mm, 4.0 μm)

System: Agilent 1290 UHPLC, binary pump, DAD, ChemStation software

Injection volume: 2 μL

Temperature: 35 °C

Flow rate: 1.0 mL/min

Detection: Multiwavelength UV/Vis Diode Array (230 nm)

Needle wash: 1 min with methanol

Mobile Phase: Gradient

A: 10 mM phosphate buffer, pH 8

B: Acetonitrile

Time	Water	ACN
0	70	30
12	30	70

A6.3 Results and Discussion

The retention times of menthone (A) and pinene (B) were obtained by individually injecting each compound onto the Flare column. These retention times were compared with peaks present in the peppermint essential oil. They appeared at the following retention times: 1.40 min (menthone) and 4.64 min (pinene) (see Figure A6.1).

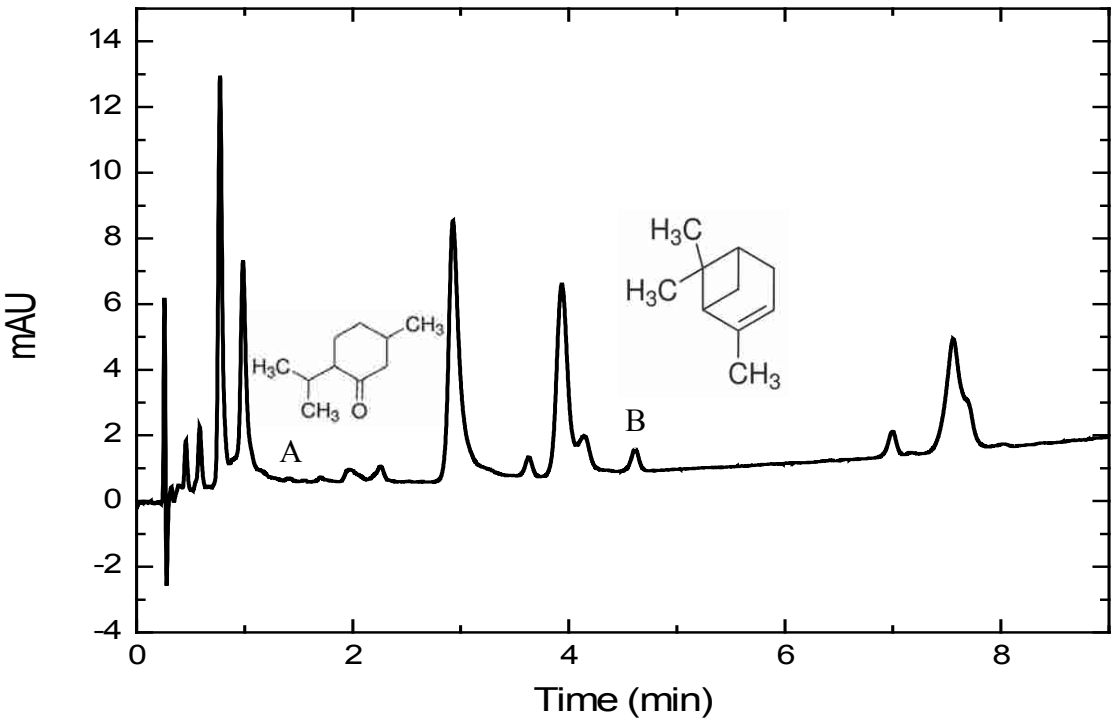

Figure A6.1 Gradient separation of peppermint essential oil (230 nm).

A6.4 References

(1) Bielory, L. *Ann. Allerg. Asthma Im.* **2004**, 93 (2), S45-S54.

(2) de Sousa, A. A. S.; Soares, P. M. G.; de Almeida, A. N. S.; Maia, A. R.; de Souza, E. P.; Assreuy, A. M. S. *J. Ethnopharmacol.* **2010**, *130* (2), 433-436.

(3) Agarwal, V.; Lal, P.; Pruthi, V. *Mycopathologia* **2008**, *165* (1), 13-19.

(4) Agarwal, V.; Lal, P.; Pruthi, V. *J. Microbiol. Immunol. Infection* **2010**, *43* (5), 447-451.

(5) Ezzat, S. M. *World J. Microb. Biot.* **2001**, 17 (7), 757-759.

(6) Grigoleit, H. G.; Grigoleit, P. *Phytomedicine* **2005**, *12* (8), 601-606.

(7) Barbour, E. K.; Yaghi, R. H.; Jaber, L. S.; Shaib, H. A.; Harakeh, S. *Int. J. Appl. Res. Vet. Med.* **2010**, *8* (1), 60-64.

(8) Hur, M. H.; Park, J.; Maddock-Jennings, W.; Kim, D. O.; Lee, M. S. *Phytotherapy Research* **2007**, *21* (7), 641-643.

(9) Williams, A.; Connell, J.; Starmaker Products LLC: 2011.

(10) Spirling, L. I.; Daniels, I. R. *J. R. Soc. Promot. Health* **2001**, *121* (1), 62-63.

(11) Borhani-Haghighi, A.; Motazedian, S.; Rezaii, R. *Med. Hypotheses* **2007**, *69* (2), 455-455.

(12) Tate, S. *J. Adv. Nurs.* **1997**, *26* (3), 543-549.

(13) *Modern Essentials*; 3 ed.; Abundant Health: Spanish Fork, UT, 2011.

(14) Jirovetz, L.; Buchbauer, G.; Bail, S.; Denkova, Z.; Slavchev, A.; Stoyanova, A.; Schmidt, E.; Geissler, M. *J. Essential Oil Res.* **2009**, *21* (4), 363-366.

(15) Sandasi, M.; Leonard, C. M.; Van Vuuren, S. F.; Viljoen, A. M. *S. Afr. J. Bot.* **2011**, *77* (1), 80-85.

(16) Imai, H.; Osawa, K.; Yasuda, H.; Hamashima, H.; Arai, T.; Sasatsu, M. *Microbios.* **2001**, *106* 31-39.

(17) Adam, B.; Liebregts, T.; Best, J.; Bechmann, L.; Lackner, C.; Neumann, J.; Koehler, S.; Holtmann, G. *Scand. J. Gastroentero.* **2006**, *41* (2), 155-160.

(18) Juergens, U. R.; Stober, M.; Vetter, H. *Eur. J. Med. Res.* **1998**, *3* (12), 539-545.

(19) Geuenich, S.; Goffinet, C.; Venzke, S.; Nolkemper, S.; Baumann, I.; Plinkert, P.; Reichling, J.; Keppler, O. T. *Retrovirology* **2008**, *5*.

(20) Koch, C.; Reichling, J.; Schneele, J.; Schnitzler, P. *Phytomedicine* **2008**, *15* (1-2), 71-78.

(21) Schuhmacher, A.; Reichling, J.; Schnitzler, P. *Phytomedicine* **2003**, *10* (6-7), 504-510.

(22) Yucharoen, R.; Meepowpan, P.; Tragoolpua, Y. *Chiang Mai Journal of Science* **2012**, *39* (1), 97-110.

(23) Cappello, G.; Spezzaferro, M.; Grossi, L.; Manzoli, L.; Marzio, L. *Digest. Liver Dis.* **2007**, *39* (6), 530-536.

Appendix 7: Diamond Coating by Living Polymerization*

A7.1 Overview

A7.1.1 Abstract

A method for coating a diamond where an initiation site is provided on the diamond surface or initiation of a living polymerization on the site and the initiation site is reacted with a monomer having a site the reacts with and bonds to the initiation site to form an chemically attached chain with a new initiation site on the chain for further reaction with a monomer. An article with a coating upon a diamond surface, the coating the reaction product of a living polymerization reaction with initiation site on the diamond surface.

A7.1.2 Statement of Attribution

My major contribution to this work is section A7.3.13. In it I reduced/hydroxylated an oxidized diamond surface using $LiAlH_4$. I then verified the surface functionalization using ToF-SIMS and DRIFTS. The work in sections A7.3.14 – A7.3.14.2.2 is from a paper by Dr. Li Yang who is primarily responsible for this content. Dr. Yang is also an inventor on the patent.

*This appendix has been publsihed as a United States Patent, US 8,147,985 B2. Issued April 3, 2012.

A7.2 Summary of Invention

An aspect is a method for coating a diamond where an initiation site is provided on the diamond surface for initiation of a living polymerization on the site. The initiation site is reacted with a monomer having a site that reacts with and bonds to the initiation site to form a chemically attached chain with a new initiation site on the chain for further reaction with a monomer. An article with a coating upon a diamond surface can be made where the coating is the reaction product of a living polymerization reaction with initiation site on the diamond surface.

A7.3 Detailed Description

Living polymerization involves first providing an initiator, or an initial reactive site, which then reacts with a monomer. The monomer extends as a chain from the reactive site, and a new reactive site forms on the end of the chain and the reaction is repeated with new monomer molecule. In the process of the present invention, the initiator/reactive site is provided on the diamond surface. Accordingly, as the chain forms, it extends from the diamond surface.

As is further described below, the initiating reactive sites on the diamond surface may include, but are not limited to, –H, –OH, halogen (e.g. Cl or Br), and carbon-carbon double bond for ring opening metathesis polymerization (ROMP)

The reactive site may be bonded directly to the diamond surface. For example, diamond usually has –OH radicals attached to the surface, and can be used as is. Alternately, –H sites can be applied by reaction of the surface with hydrogen. Halogens can be applied by reaction of –H sites with halogen under suitable conditions. A surface with halogen sites can be treated with a strong base to convert same to hydroxyl –OH sites. Hydroxyl sites can be treated with a strong base such as NaH, $NaNH_2$ or NaC≡CH, sodium methoxide, alkyl lithium or Grignard reagent to provide an –O–, which can used to as in initiator in a ring-opening reaction to attach epoxide, and the like. The surface of diamond can be treated so that it will contain carbon-carbon double bonds.

The reaction sites may also be indirectly bonded. For example, a molecule with an initiating active group can be bonded directly to the bonded surface, such surface with hydroxyl groups (–OH) can be treated with a compound like 2-bromoisobutyryl bromide to provide a reactive bromine for initiating ATRP.

Living polymerization systems are characterized by a rate of chain initiation that is fast compared with the rate of chain propagation, so that the number of kinetic-chain carriers is essentially constant throughout the polymerization. Living polymerization can also be described as a chain growth process without irreversible chain breaking reactions (transfer and termination). Such a polymerization provides endgroup control. Side reactions can occur but only to an extent which does not considerably disturb the control of the molecular structure of the polymer chain. Examples of living polymerization include cationic, ring-opening metathesis, group transfer, and radical polymerizations.

Characteristics of living polymerization may include, slow initiation, reversible formation of species with various activities and lifetimes, reversible formation of inactive (dormant) species (reversible deactivation), and reversible transfer (in some cases). Living polymerization does not involve irreversible deactivation (i.e., termination), or irreversible transfer.

Reversible termination or reversible deactivation is a process where active species are in a dynamic equilibrium with inactive (dormant) species. Examples include cationic, group transfer, and radical polymerizations where the dormant species (P) are covalent and the active ones (P*) can be ions, ion pairs, or radicals. A catalyst, co-initiator, or/activator may by used in reaction of the active species, which becomes a deactivator or product of the activation process. Reversible transfer can be a bimolecular reaction between a dormant and an active polymer chain which only differ in their degree of polymerization or a reaction with a low molecular compound with a structure similar to the chain end, e.g., addition of alcohols in the anionic ring-opening polymerization of epoxides.

Since in living polymerization the ability of a growing polymer chain to terminate has essentially been removed, chain transfer reactions are absent or insignificant. The rate of chain

initiation is also much larger than the rate of chain propagation. The result is that the polymer chains grow at a more constant rate than seen in traditional chain polymerization and their lengths remain very similar.

Living polymerization for production of polymers is described in Macromolecular Nomenclature Note No. 12, NAMING OF CONTROLLED, LIVING AND "LIVING" POLYMERIZATIONS, Krzysztof Matyjaszewski and Axel H. E. Müller, at http://www.polyacs.org/nomcl/mnn12.html; Living Ziegler-Natta Polymerization, Richard J. Keaton, Department of Chemistry and Biochemistry, University of Maryland, at http://organicdivision.org/essays 2002/keaton.pdf, and "Living Polymers"—50 years of evolution, Moshe Levy, Department of Materials and Interfaces, Weizmann Institute of Science, Rehovot at http://www.weizmann.ac.il/ICS/booklet/18/pdf/levy.pdf.

Living polymerization as applied to the present process involves creating a living polymerization initiating or active site on a diamond surface, and reacting this site with an appropriate monomer. Thus, a polymer chain is grown on the surface from the original reactive site on the surface. The monomer is chosen to impart to the diamond surface a selected property. For example, a monomer with aromatic groups, primary, secondary, tertiary, or quaternary amine groups, carboxyl groups, hydroxyl groups, sulfonic acid groups, cyano groups, alkyl chains, or any other suitable chemistry.

The initiator/reactive site can be attached to the diamond surface by conventional chemical bonding techniques. The choice of initiator/reactive site and monomer or monomers depends on the living polymer system that is being used. The monomer also depends on the surface properties that are to be imparted to the diamond by the coating. For example, the monomer may have chemistry or reactive sites that impart a desired property, or sites that can be

further reacted to impart the property, for example, aromatic groups, hydroxyl, carboxyl, amine, aromatic groups, primary, secondary, tertiary, or quaternary amine groups, carboxyl groups, hydroxyl groups, sulfonic acid groups, cyano groups, alkyl chains, or any other suitable chemistry. For example, a monomer with an aromatic group will provide a surface with sites for conversion to an anionic surface (e.g., by sulfonation) for separations. Such aromatic groups could also undergo alkylation or acylation. The monomer should not be reactive in a way that would materially interfere with the living polymerization.

Living polymerization techniques that may be used in the present process include free radical living polymerization, living cationic polymerization, ring opening metathesis polymerization, group transfer polymerization, anionic living polymerization, living Ziegler-Natta polymerization, and free radical living polymerization.

A7.3.1 Free Radical Living Polymerization

Free radical living polymerization involve catalytic chain transfer polymerization, iniferter mediated polymerization, stable free radical mediated polymerization (SFRP), atom transfer radical polymerization (ATRP), reversible addition-fragmentation chain transfer (RAFT) polymerization, and iodine-transfer polymerization. Other examples include Stable free radical mediated polymerization (SFRP) (also called nitroxide mediated polymerization (NMP)).

A7.3.2 Free Radical—Atom Transfer Radical Polymerization (ATRP)

Atom transfer radical polymerization (ATRP) involves the chain initiation of free radical polymerization by a halogenated organic species in the presence of a metal halide species. The metal has a number of different oxidation states that allows it to abstract a halide from the

organohalide, creating a radical that then starts free radical polymerization. After initiation and propagation, the radical on the chain active chain terminus is reversibly terminated (with the halide) by reacting with the catalyst in its higher oxidation state. Thus, the redox process gives rise to an equilibrium between dormant (Polymer-Halide) and active (Polymer-radical) chains. The equilibrium is designed to heavily favor the dormant state, which effectively reduces the radical concentration to sufficiently low levels to limit bimolecular coupling. ATRP is disclosed in U.S. Pat. No. 5,763,548, issued to Matyjaszewski, et al on Jun. 9, 1998, which is hereby incorporated by reference.

ATRP and other free radical methods are used to provide the diamond coating by first creating a free radical active site on the diamond surface. For ATRP this is accomplished by applying a halogen to the surface of the diamond. The metal abstracts the halide from the diamond surface, creating a free radical reactive site that starts free radical polymerization with a monomer.

A7.3.3 Free Radical—Reversible Addition Fragmentation Chain Transfer (RAFT)

Reversible Addition Fragmentation chain Transfer (RAFT) polymerization is a degenerative chain transfer process and is free radical in nature. Most RAFT agents contain thiocarbonyl-thio groups, and it is the reaction of polymeric and other radicals with the C═S that leads to the formation of stabilized radical intermediates. In an ideal system, these stabilized radical intermediates do not undergo termination reactions, but instead reintroduce a radical capable of reinitiation or propagation with monomer, while they themselves reform their C═S bond. The cycle of addition to the C═S bond, followed by fragmentation of a radical, continues

until all monomer is consumed. Termination is limited in this system by the low concentration of active radicals.

A7.3.4 Free Radical—Iodine-Transfer Polymerization

Iodine-transfer polymerization, typically uses a mono- or diiodo-perfluoroalkane as the initial chain transfer agent. This fluoroalkane may be partially substituted with hydrogen or chlorine. The energy of the iodine-perfluoroalkane bond is low and, in contrast to iodo-hydrocarbon bonds, its polarization small. Therefore, the iodine is easily abstracted in the presence of free radicals. Upon encountering an iodoperfluoroalkane, a growing poly(fluoroolefin) chain will abstract the iodine and terminate, leaving the now-created perfluoroalkyl radical to add further monomer. But the iodine-terminated poly(fluoroolefin) itself acts as a chain transfer agent. As in RAFT processes, as long as the rate of initiation is kept low, the net result is the formation of a monodisperse molecular weight distribution. (see "Living Polymers by the use of Trithiocarbonates as Reversible Addition—Fragmentation Chain Transfer (RAFT) Agents: ABA Triblock Copolymers by Radical Polymerization in Two Step" by Roshan T. A. Mayadunne, et al., CSIRO Molecular Science, Bag 10, Clayton South, Victoria 3169 Australia. Macromolecules 2000, 33, 243-245.)

A7.3.5 Free Radical—Selenium-Centered Radical-Mediated Polymerization

Diphenyl diselenide and several benzylic selenides have been explored as photoiniferters in polymerization of styrene and methyl methacrylate. Their mechanism of control over polymerization is proposed to be similar to the dithiuram disulfide iniferters. However, their low

transfer constants allow them to be used for block copolymer synthesis but give limited control over the molecular weight distribution.

A7.3.6 Free Radical—Telluride-Mediated Polymerization (TERP)

Telluride-Mediated Polymerization or TERP appears to mainly operate under a reversible chain transfer mechanism by homolytic substitution under thermal initiation. Alkyl tellurides of the structure Z—X—R, were Z=methyl and R=a good free radical leaving group, give the better control for a wide range of monomers, phenyl tellurides (Z=phenyl) giving poor control. Polymerization of methyl methacrylates are only controlled by ditellurides. The importance of X to chain transfer increases in the series O<S<Se<Te, makes alkyl tellurides effective in mediating control under thermally initiated conditions and the alkyl selenides and sulfides effective only under photoinitiated polymerization.

A7.3.7 Free Radical—Stibine-Mediated Polymerization

Stibine-mediated polymerization uses an organostibine transfer agent with the general structure Z(Z′)—Sb—R (where Z=activating group and R=free radical leaving group). A wide range of monomers (styrenics, (meth)acrylics and vinylics) can be controlled, giving narrow molecular weight distributions and predictable molecular weights under thermally initiated conditions. Bismuth alkyls can also control radical polymerizations via a similar mechanism.

A7.3.8 Ring Opening Metathesis Polymerization

Ring opening metathesis polymerization (ROMP) is a polymerization method in which (generally strained) cyclic olefins (e.g. norbornene or cyclopentene) are polymerised with a

metathesis catalyst. As used in the present system, a diamond surface is first provided with olefin, cyclic olefin, or –C≡C sites, that by means of a metatheses catalyst can be opened and attached to a cyclic olefin monomer.

A7.3.9 Group Transfer Polymerization (GTP)

Group transfer polymerization is disclosed in U.S. Pat. No. 4,940,760, which is hereby incorporated by reference. Group Transfer Polymerization (GTP) is a process for preparing a "living" polymer. The process involves contacting under polymerizing conditions in a polymerization medium at least one acrylic or maleimide monomer with an initiator, which is a tetracoordinate organosilicon, organotin or organogermanium compound having at least one GTP initiating site, and a catalyst which is an anion or is a source of an anion, which is selected from the group consisting of bifluoride, fluoride, cyanide, azide or a selected oxyanion, or a selected Lewis acid or Lewis base. The initiator or the anion or Lewis acid catalyst is chemically attached (grafted) to a solid support that is insoluble in the polymerization medium. GTP is applied in the present process for coating diamonds by bonding on the surface of the diamond the initiator or the anion or Lewis acid catalyst, which provides the initiating site, and treating with acrylic or maleimide monomer.

A7.3.10 Anionic Living Polymerization

Anionic living polymerization is a vinyl polymerization and involves polymerization of monomers containing double bonds. Anionic living polymerization begins with an initiator which forms an ion. In the present process, the initiator can be attached to the diamond surface, which can be an alkyl chain with a pendant lithium. The initiator is involved in an equilibrium

where lithium ions and carbanions are formed. The carbanion pendant end then reacts with a double bond in a monomer, which lengthens the chain and forms a new carbanion at the end of the chain.

A7.3.11 Living Ziegler-Natta Polymerization

Ziegler-Natta polymerizations are described in "Living Ziegler-Natta Polymerization" by Richard J. Keaton, cited above. Ziegler-Natta polymerization is a type of coordination polymerization in which the catalytically active species in solution are believed to be metal alkyl cations. Generation of these active centers stems from the reaction of a metal dialkyl with a borane ($B(C_6F_5)_3$), a borate ($[Ph_3C][B(C_6F_5)_4]$), or an alkyl aluminum, the most common of which is methylaluminoxane. After partial or complete abstraction of one alkyl group, a cationic metal center is formed with a coordinative site of unsaturation. The mechanism by which chain growth occurs for Ziegler-Natta polymerizations is called the Cossee-Arlman mechanism. Monomer coordination to the cationic metal causes insertion of the polymer chain to the π-coordinated olefin. This chain elongation goes through a metallocyclobutane transition state with the olefin insertion occurring with cis addition across the double bond. The migratory insertion step provides a new vacant site for a new molecule of monomer to bind, and this subsequently inserts providing the original vacant site.

A7.3.12 Epoxide Ring Opening Reactions

Living anionic polymerizations or copolymerizations of various monomers, including epoxide and cyclic ester monomers, can be accomplished by creating –O– sites on the diamond surface. These sites can be introduced in different ways. The first is to take advantage of the

–OH groups that are often formed at the surfaces of diamond materials when they are created, removing the hydrogen ions from these hydroxyl moieties. The second is to introduce –OH groups at the diamond surface, or on a group that has been grafted into the diamond surface. This could be done by hydrogen (or deuterium) terminating a diamond surface, halogenating it, and then allowing this surface to react with hydroxide ions (–OH). The hydrogen ions can be removed from –OH groups at or near the diamond surface by reaction with a strong base such as an alkyl lithium reagent, an alkyl Grignard reagent, sodium amide ($NaNH_2$), sodium hydride, potassium hydride, or sodium acetylide. The resulting deprotonated diamond surfaces could then be rinsed with a dry solvent to remove unreacted base. A cyclic monomer could then be introduced, which would react with the surface sites, see below:

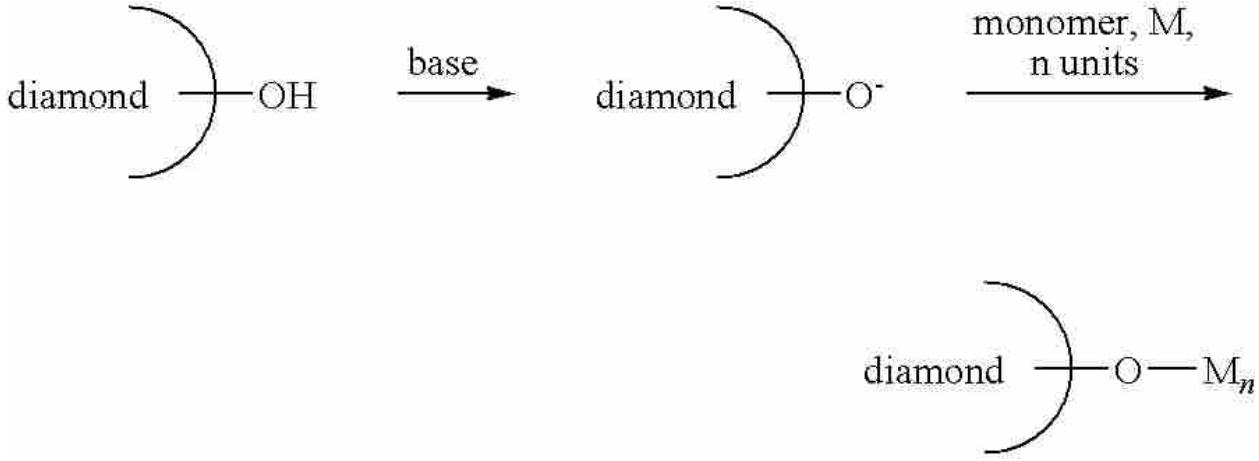

In the case of an epoxide, the chemistry would be as follows:

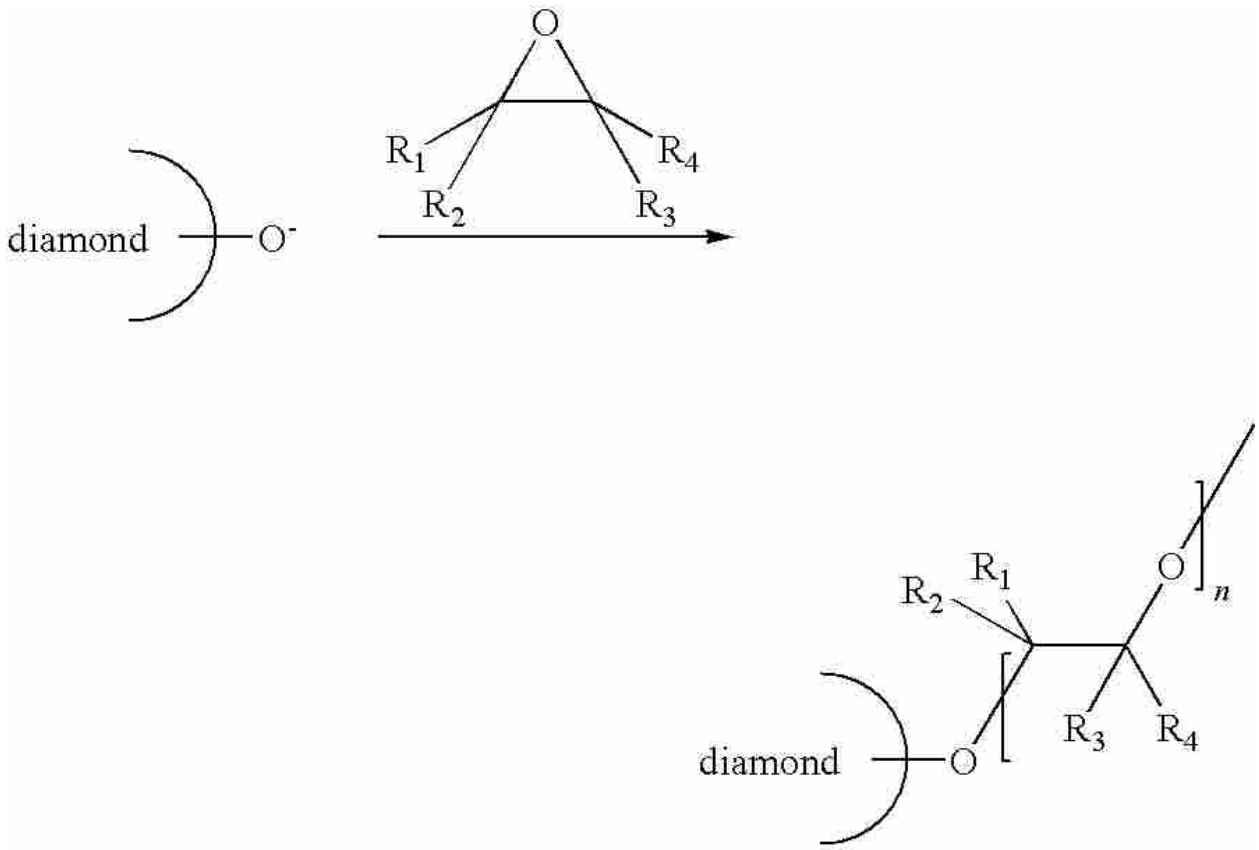

In the above reaction schemes, R1, R2, R3, and R4 could be different radicals, including hydrogen. Of course, there will be a cation paired with the O− at the diamond surface. This cation itself could be ligated to one or more ligands.

Note that the epoxide could be chiral, and give chirality to the coating it forms.

Below is an example of ring opening polymerization from an –O– group at a diamond surface using a cyclic ester.

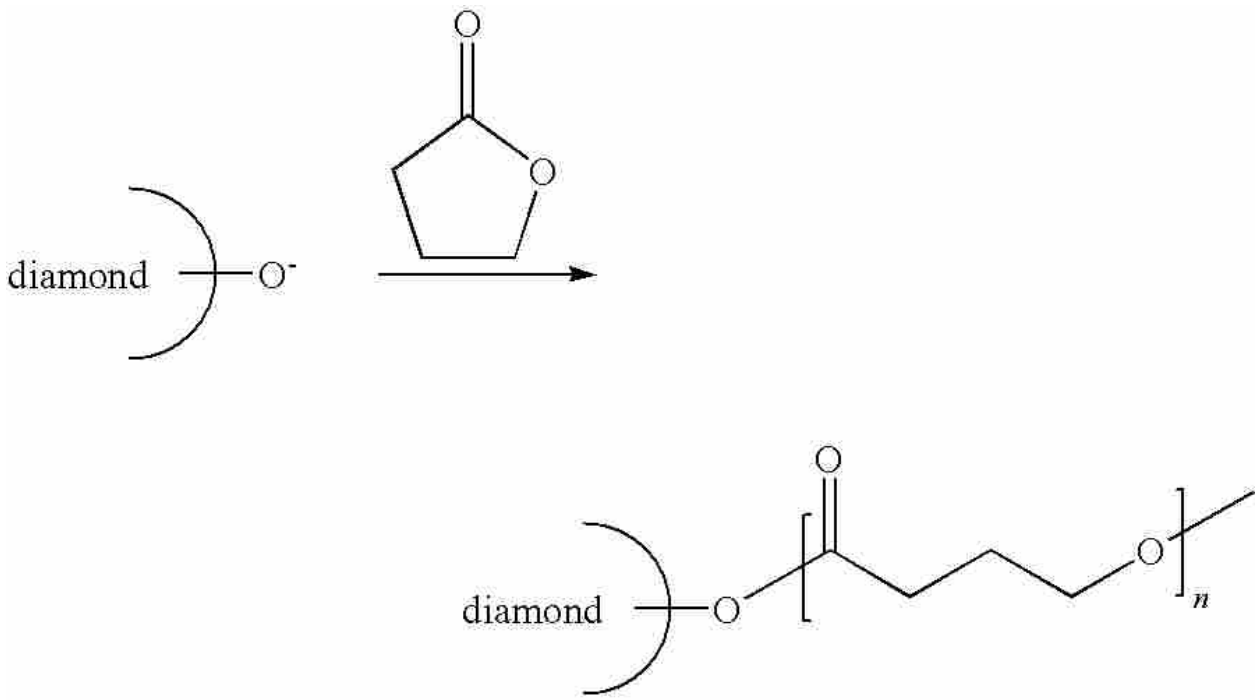

Many heterocyclic compounds can be polymerized by ring opening under certain conditions with ionic initiators, to produce linear macromolecules. Amongst these are cyclic ethers, cyclic sulfides, cyclic acetals, cyclic esters (lactones), cyclic amides (lactams), and cyclic amines. Ring opening polymerizations are carried out under similar conditions, and frequently with similar initiators to those used for ionic polymerizations of unsaturated monomers.

The ring-opening polymerization of cyclic ethers having 3-, 4-, and 5-membered rings (e.g., epoxides, oxetanes, THF) yields polymeric ethers.

Epoxides such as epoxyethane (ethylene oxide) can be polymerized cationically (e.g., with Lewis acids) and anionically (e.g., with alcoholates or organometallic compounds). Polymers of propylene oxide and generally substituted ethylene oxides can be produced in both atactic amorphous and isotactic crystalline forms. Optically active poly(propylene oxide)s can be obtained from chiral propylene oxide.

Polymerization of four-membered cyclic ethers (oxetanes) is also brought about by cationic initiators (e.g., Lewis acids) and by anionic initiators (e.g., organometallic compounds). Like THF, cyclic acetals (e.g., 1,3-dioxolane and 1,3,5-trioxane) are polymerizable only with cationic initiators.

Cyclic esters of omega-hydroxycarboxylic acids can be polymerized by ring-opening to give linear aliphatic polyesters.

Some specific monomers that could be polymerized by ring opening methods from either an anionic or a cationic initiator on diamond are L-lactide, D-lactide, meso-lactide, glycolide, methylglycolide, epsilon-caprolactone, delta-valerolactone, gamma-butyrolactone, epichlorohydrin, 2-pyrrolidinone, 2-azetidinone, delta-valerolactam (2-piperidinone), cyclohexene oxide, exo-2,3-epoxynorbornane, 7-oxabicyclo[4.1.0]heptan-2-one, 4-vinyl-1-cyclohexene 1,2-epoxide, 6-acetoxy-3-oxatriclyclo-(3,2,1,0 2,4)-octane, trimethoxy[2-(7-oxabicyclo[4.1.0]hept-3-yl)ethyl]silane, (R)-(+)-1,2-epoxybutane, (S)-(−)-1,2-epoxybutane, cyclopentene oxide, 1,2-epoxypentane, 1,2-epoxy-5-hexene, (R)-(+)-1,2-epoxyhexane, (S)-4-chloro-1,2-epoxybutane, 1,2-epoxyoctane, 1,2-epoxydodecane, 1,2-epoxyoctadecane, 1,2-epoxyeicosane, (S)-(−)-1,2-epoxyoctane.

Note that carbon dioxide can be incorporated into some of these living polymers.

Note that a diepoxide or a triepoxide could be used as a crosslinking agent, e.g., vinylcyclohexene dioxide, dicyclopentadiene dioxide (mixture of endo and exo isomers), 1,3-butadiene diepoxide.

A7.3.13 Introducing –OH Groups onto the Diamond Surface

A method for introducing –OH groups to a diamond surface is by treatment with $LiAlH_4$. Diamond treated with $LiAlH_4$ has an increased density of hydroxyl groups. These hydroxyl groups can then be reacted with monomer to form living polymers on the diamond surface. Due to the higher density of hydroxyl groups, the polymer growth will also be denser. The evidence of this actually working is seen by reference to Figures A7.1 – A7.3.

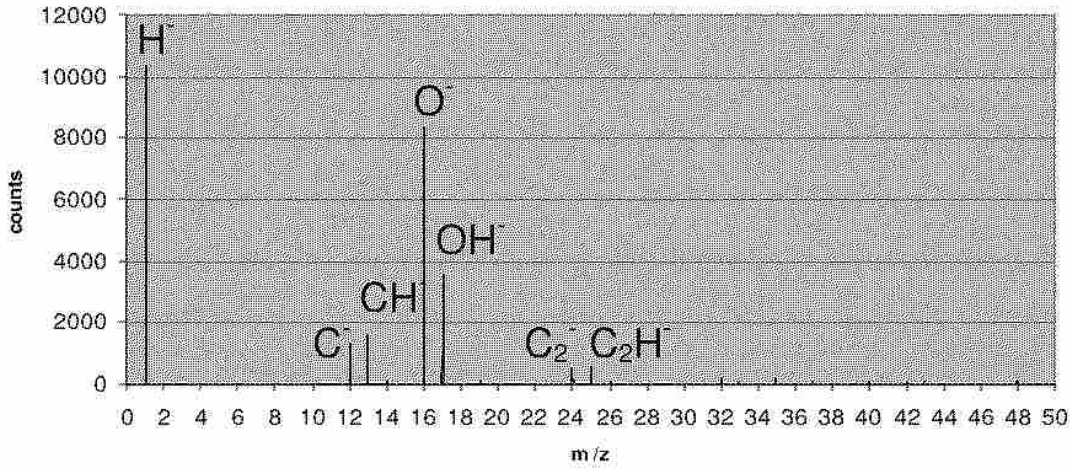

Figure A7.1. SIMS spectrum of Piranha cleaned diamond in negative ion mode.

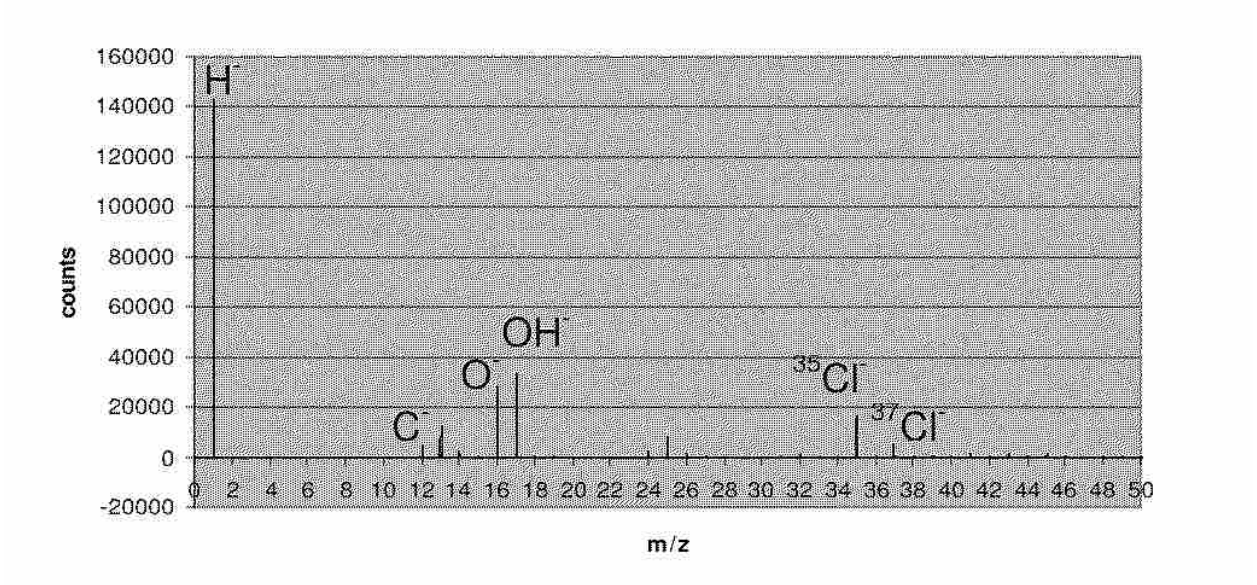

Figure A7.2 SIMS spectrum of LAH treated diamond in negative ion mode.

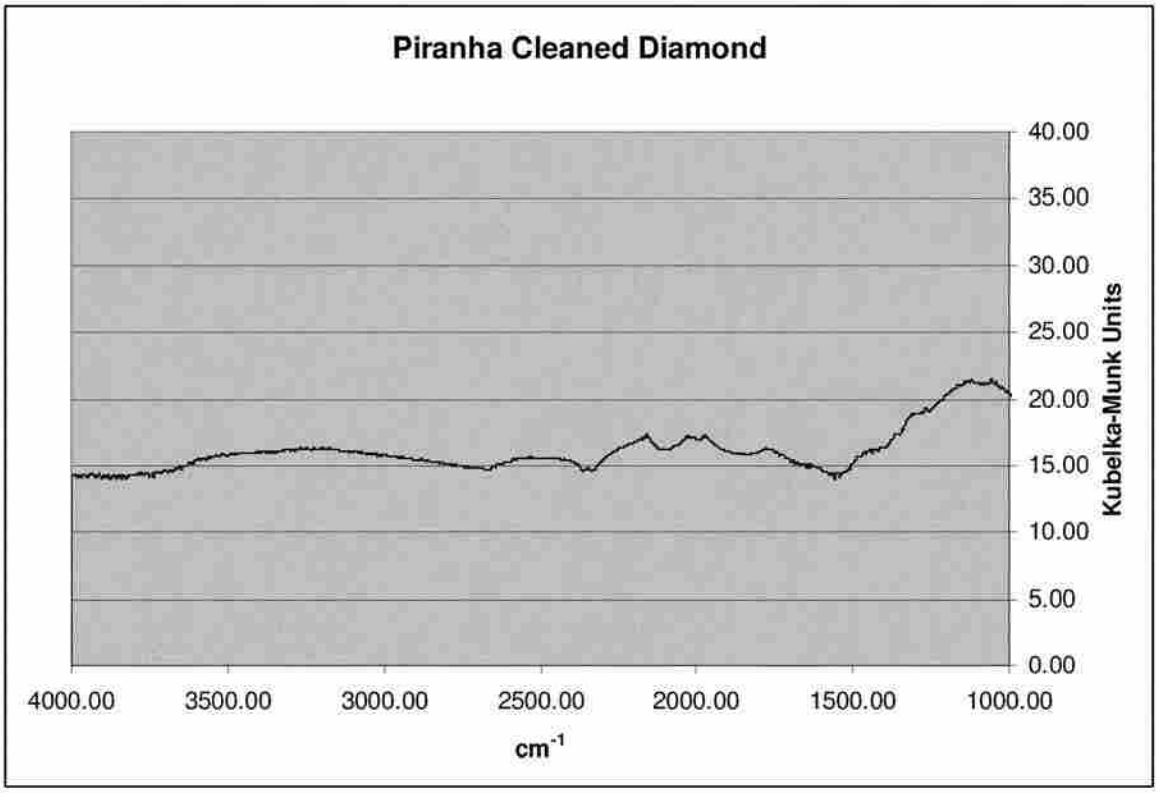

Figure A7.3 DRIFT spectrum of Piranha cleaned diamond.

With reference to Figure A7.4, the reaction is as follows. The piranha solution (H_2SO_4 and H_2O_2) treated diamond is placed in a vessel, which is subsequently flushed with an inert atmosphere. $LiAlH_4$ (1M $LiAlH_4$ in tetrahydrofuran (THF)) is then added to the diamond through a septum via syringe. The reaction is then allowed to occur for 24 – 68 h, with occasional swirling. The result is a increased number of hydroxyl groups on the surface.

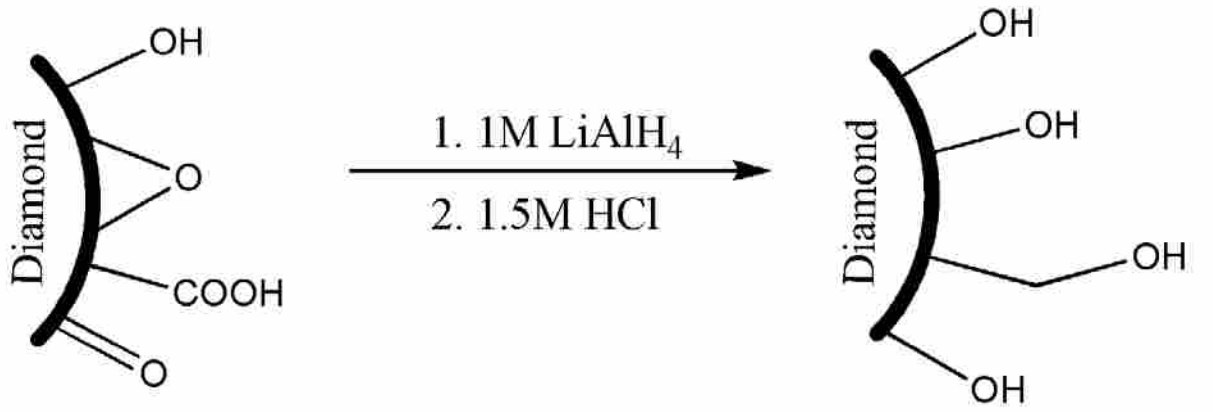

Figure A7.4 Shows scheme for $LiAlH_4$ treatment of diamond to increase number of hydroxyl groups on the surface of the diamond. Piranha cleaned diamond is allowed to react with 1M $LiAlH_4$ in THF for 24 – 68 h. at room temperature.

The peaks seen at 3500 cm^{-1} in the DRIFT spectra in Figures A7.5 – A7.7 are indicative of an increased amount of –OH groups on the surface. The SIMS spectra in Figure A7.2 also shows an increased amount of hydrogen on the surface, which would be consistent with more –OH groups on the diamond surface.

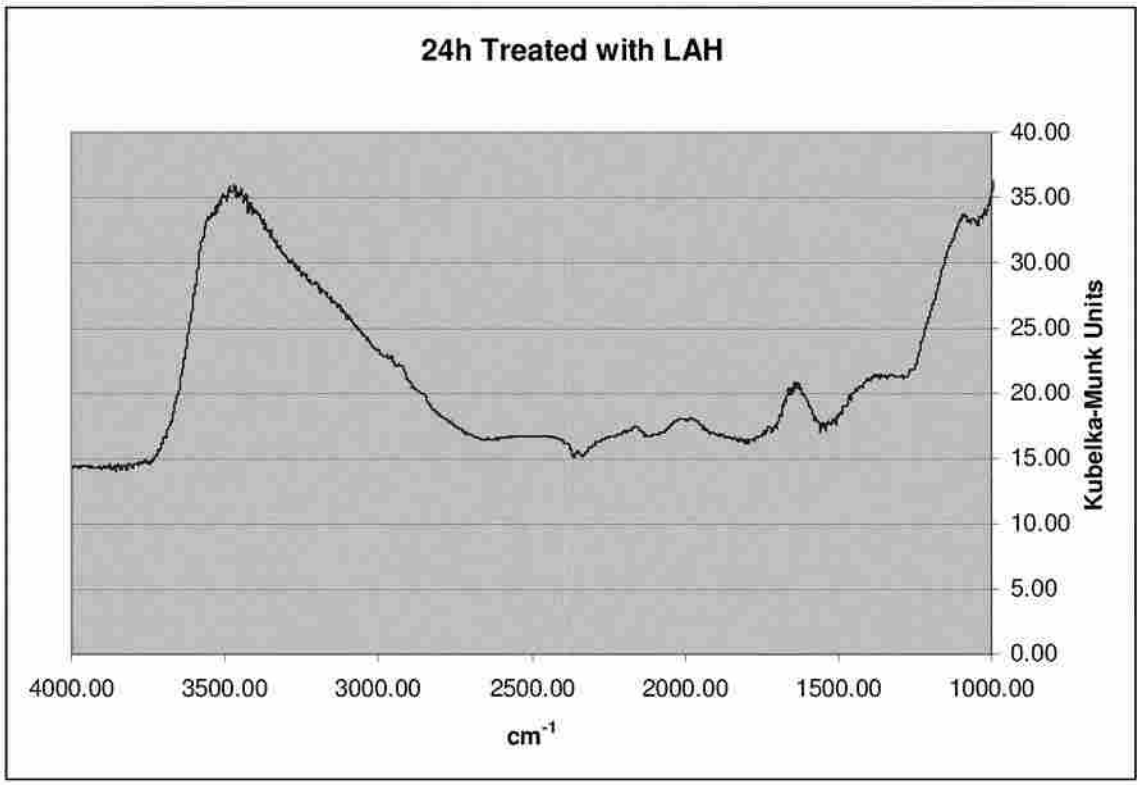

Figure A7.5 DRIFT spectrum of diamond reacted with LAH for 24 h. Diamond size 1.7 μm.

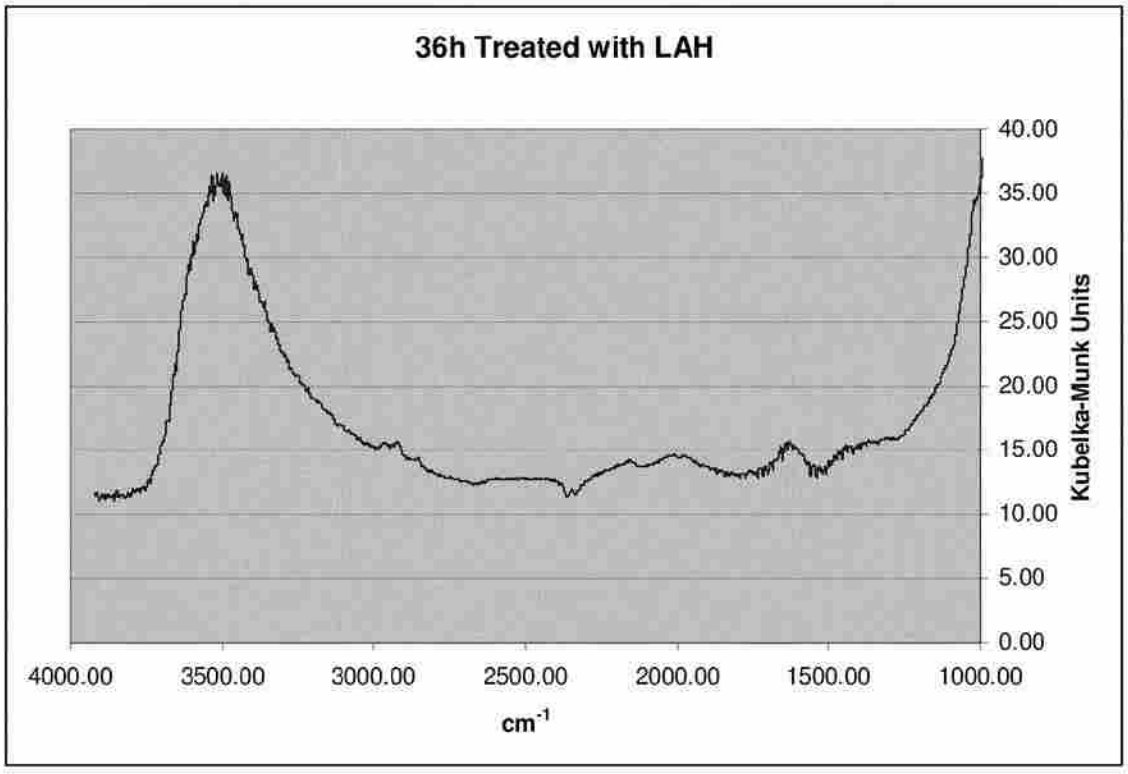

Figure A7.6 DRIFT spectrum of diamond reacted with LAH for 36 h. Diamond size 1.7 μm.

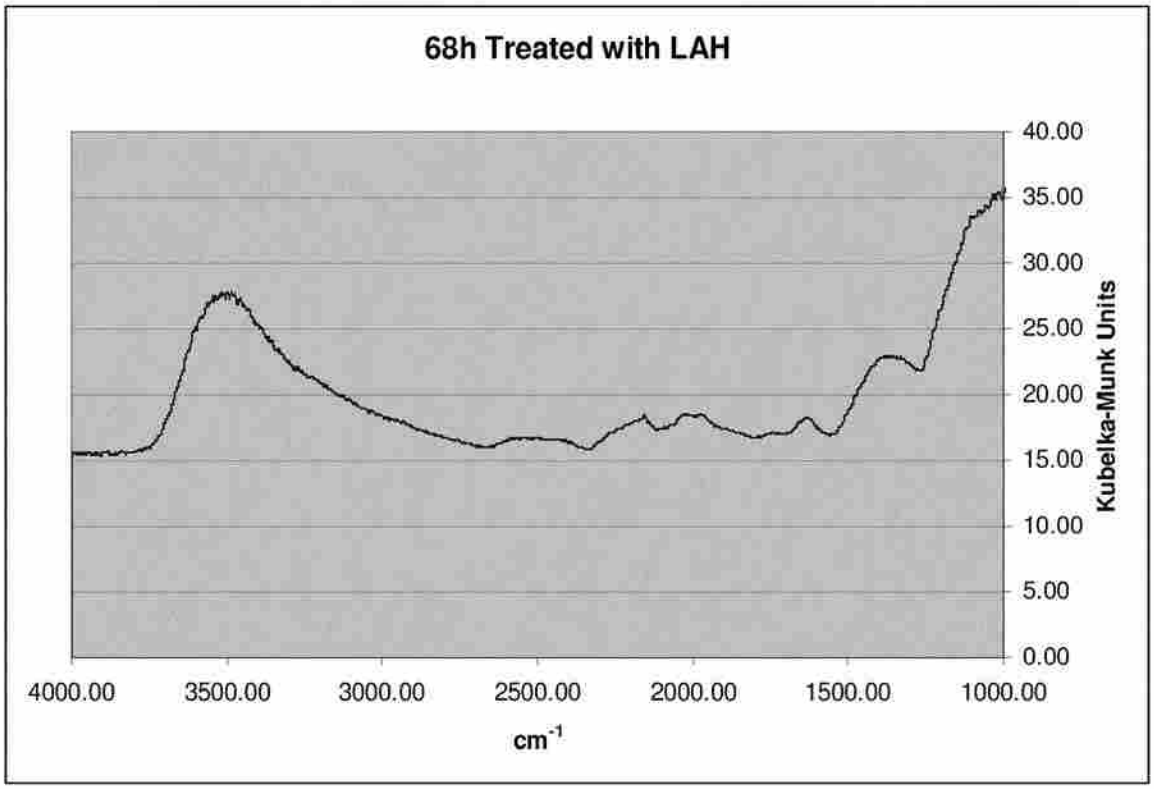

Figure A7.7 DRIFT spectrum of diamond reacted with LAH for 68 h. Diamond size 5 μm.

A7.3.14 Example I - Direct Polymer Attachment and Growth on Deuterium/Hydrogen-Terminated Diamond Substrates with Atom Transfer Radical Polymerization and Solid Phase Extraction on the Resulting Sorbents

Atom transfer radical polymerization (ATRP) is applied to grow polymers on diamond surfaces. Before ATRP, the ATRP initiator should be introduced. There are two ways to immobilize the ATRP initiators. One method is putting the hydrogen- or deuterium-terminated diamond in bromine under light. The other method is reacting piranha cleaned diamond with 2-bromoisobutyryl bromide. Polystyrene (PS) or crosslinked polystyrene can be grown on the diamond powders by ATRP. These phases have excellent stability in both highly acidic and highly basic media. Thicker polymer layers are obtained when a crosslinking agent, such as divinylbenzene is employed as part of the monomer mixture. Sulfonation of these phenyl phases is demonstrated with a H_2SO_4/CH_3COOH mixture. Solid phase extraction is performed on the resulting strong cation exchange material using 1-aminonaphthalene.

A7.3.14.1 Experimental Section

A7.3.14.1.1 Reagents

All chemicals were used as received, except that all monomers were passed through an inhibitor removing column prior to use, as follows: tetrahydrofuran (Aldrich, spectra grade); styrene (Spectrum, 99%, inhibited with 50 ppm p-tert-butylcatechol); divinylbenzene (DVB) (Aldrich, 80%, remainder mostly 3- and 4-ethyl vinyl benzene, inhibited with 1000 ppm p-tert-butylcatechol).

All monomers were passed through an inhibitor-removing column to remove polymerization inhibitors prior to use. The adsorbants for removing MEHQ and tert-butylcatechol were obtained from Aldrich.

The mixture gases including 5% deuterium/hydrogen in argon (99.999% pure) were purchased from Airgas Inc. Commercial diamond powder was provided by US Synthetic. The average diameter is 70 μm.

A7.3.14.1.2 Preparation of Deuterium/Hydrogen-Terminated Diamond Powder.

Diamond powder was used as substrate. The diamond powder was treated in flowing 5% D_2 or H_2 (in Ar) gas at 900 °C. for 28 hours. 5% deuterium or hydrogen (in Ar) is not a flammable mixture, and therefore much safer to work with than pure D_2 or H_2 gas. The Mini-Mite Tube Furnace of Lindberg/Blue M (model number is TF55030A-1) was purchased from the Thermo Electron Corporation. During the reaction, the diamond powder was shaken twice to evenly deuterate the surface and it was then cooled in flowing 5% D_2 or H_2 (in Ar). After this treatment, the diamond powder was terminated with deuterium or hydrogen. The resulting deuterium/hydrogen-terminated diamond powder was used as a starting material.

A7.3.14.1.3 Introduction Initiators by Two Methods

There are two ways to immobilize the ATRP initiators. One method is putting the hydrogen- or deuterium-terminated diamond in bromine under light to introduce the initiator. The light wavelength range could be 250-600 nm.

The other way, the diamond powder was cleaned in piranha solution (70% H_2SO_4:30 % conc. H_2O_2) at 100 °C. for 1 h, and then thoroughly washed with deionized water. Clean, untreated diamond powder was slurried in a dry THF solution containing 0.5 M 2-bromoisobutyryl bromide and 0.55 M pyridine. After 24 h, diamond powder was washed thoroughly with methanol and deionized water.

A7.3.14.1.4 Polymerization on the Diamond Powder

Diamond particles containing initiator (3 g) and CuBr (0.26 g) were placed in a flask and degassed with nitrogen. Subsequently, degassed 2,2′-bipyridine (bipy) (0.58 g) in 10.0 g styrene (or 4 g styrene and 6 g divinylbenzene) and 10 mL 1,4-dioxane was mixed with it. The mixture was stirred with a magnetic stir bar, heated to 110 °C. under nitrogen, and the reaction continued for 19 h. The particles were washed and sonicated with THF and methanol/glacial acetic acid (95/5) until the solvent was colorless.

A7.3.14.1.5 Sulfonation of Polystyrene Functionalized Diamond Powder

The method of PS-DVB resin sulfonation described by Dumont and Fritz was followed. 2 g polystyrene or polystyrene-divinylbenzene (PS-DVB) functionalized diamond powder was slurried in 5 mL acetic acid followed by 50 mL concentrated sulfuric acid in an ice bath. Then the reaction was set at 90° C. for 5 hours and finally poured over ice to quench the reaction. The diamond powder was filtered and washed with water until the pH of water was neutral.

A7.3.14.1.6 Stability Studies

Approximately 1.0 M NaOH and 1.0 M HCl solutions were prepared for pH stability studies. 0.2 g of each adsorbent was immersed separately in either the NaOH or HCl solution for 72 h. Finally, the particles were captured on a filter funnel as before (vide supra) and rinsed with copious quantities of Millipore water.

A7.3.14.1.7 Characterization of the Diamond Surfaces

Time-of-flight secondary ion mass spectrometry (ToF-SIMS) was performed with an ION-TOF ToF-SIMS IV instrument using monoisotopic 25 keV 69^{+} ions. X-ray photoelectron spectroscopy was performed with an SSX-100 x-ray photoelectron spectrometer with a monochromatic Al Kα source and a hemispherical analyzer. An electron flood gun was employed for charge compensation. Survey scans as well as narrow scans were recorded with an 800 × 800 μm spot. The diamond surface was characterized by a Magna-IR 560 spectrometer from Nicolet (Madison, Wis.). The DRIFT spectra were obtained over the range of 4000-400

cm^{-1}. For each spectrum, 64 scans were collected at a resolution of 4 cm^{-1}. The diffuse reflectance was converted into Kubelka-Munk function units.

A7.3.14.1.8 Solid Phase Extraction (SPE)

SPE of 1-naphthylamine was performed with packings prepared in our laboratory. For our experiments, the material in a commercially available cartridge was replaced by our sulfonated stationary phase. A control experiment was performed that showed that neither the plastic cartridge nor the frits retained analytes. The same volume of packing material was used in all of our experiments. To improve packing, the cartridges were washed with water and pumped on with the house vacuum during loading. Finally, the columns were dried using the house vacuum.

Prior to SPE, cartridges containing our sulfonated polystyrene diamond phase were first conditioned with 6 column volumes of methanol, and then with six column volumes of phosphate buffer (10 mM, pH=1.9). 50 μL of 1-naphthylamine (1 mg/mL) in phosphate buffer (10 mM, pH=1.9) was loaded into the column. This analyte was used to test sulfonation of polystyrene coated diamond. In this procedure, the analyte is not eluted with phosphate buffer (10 mM, pH=1.9), but eluted with phosphate buffer (10 mM, pH=1.9, NaCl, ionic strength 0.2 M) and methanol (The ratio is 1:1).

In practice, sulfonated polystyrene modified diamond SPE adsorbents could be repeatedly used without noticeable degradation. After each reuse, the column was washed with phosphate buffer (10 mM, pH=1.9, NaCl, ionic strength 0.2 M) several times to regenerate the cation exchange column.

A7.3.14.1.9 Breakthrough Curves

The analyte used for determination of breakthrough volumes was 1-naphthylamine. The column was first conditioned using the procedures mentioned above. After conditioning, the analyte solution (0.02 mg/mL) was loaded onto the cartridge. The column was kept wet, and the flow rate was kept constant during the process. Equal volumes of the fractions eluting from the column were collected in separate vials. Finally, ESI-MS was done to analyze these fractions.

Breakthrough curves had sigmoidal shapes. The breakthrough volume was calculated from the point on the curve corresponding to 5% of the average value at the maximum (plateau region).

A7.3.14.1.10 Electrospray MS (ESI-MS)

Electrospray MS (ESI-MS) was performed on an Agilent Technologies LC/MSD TOF system by direct infusion of several μLs of sample along with the mobile phase: 75 % MeOH and 25 % water with 5 mM ammonium formate. In positive ion mode, the charging voltage and the capillary voltage were set at 900 V and 3500 V, respectively, and the skimmer was operated at 60 V. The nebulizer was at 35 psi and the gas temperature was 350° C. The flow rate of the nitrogen drying gas was set at 12 L/min. All of the instrument parameters in negative ion mode were identical to those in positive ion mode, except the capillary voltage and drying gas flow rate, which were set at 4000 V and 8 L/min, respectively.

A7.3.14.1.11 Stability Test

Sulfonated polystyrene coated diamond was immersed in 1M NaOH and 1M HCl solution for 72 hours respectively to test the stability in strong base or strong acid. XPS, TOF-SIMS and IR were used to characterize these diamond powders.

A7.3.14.2 Results and Discussion

A7.3.14.2.1 Polymerization and Sulfonation on the Diamond Powder by ATRP

Before atom transfer radical polymerization, an ATRP initiator should be introduced. Two methods can be used. One is by photoreaction, the other one is addition of 2-bromoisobutyryl bromide, performed according to the procedure of Carl mark and Malmstrom. Then these brominated diamond powder react with styrene or styrene/DVB, Cu(I) Br and bipyridine at 110 °C. Finally polystyrene or polystyrene-divinylbenzene functionalized diamond powders are sulfonated. The whole procedure (Scheme 1) is shown below.

Scheme 1: ATRP from surface of particle initiators.

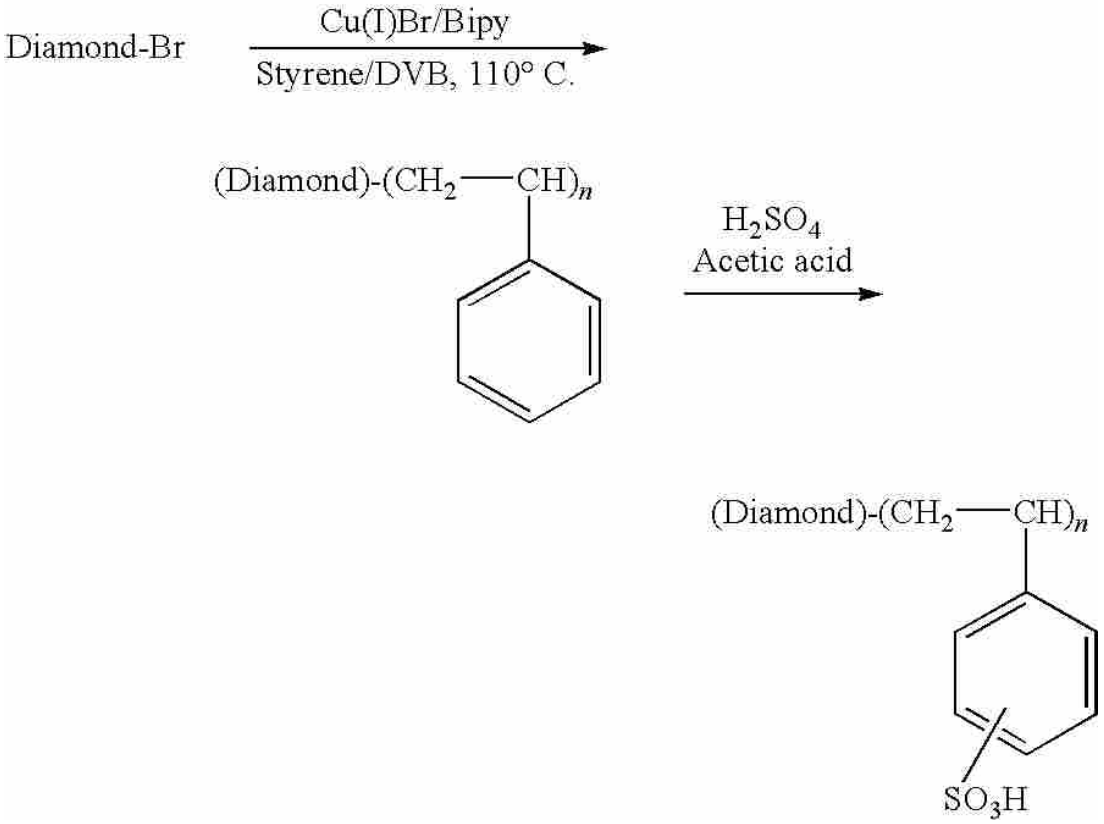

An obvious bromine signal is present in the x-ray photoelectron spectroscopy (XPS) survey spectrum of brominated diamond powder from deuterium-terminated diamond powder (see Figure A7.8a) and brominated diamond powder from piranha cleaned diamond powder (see Figure A7.8b). The diamond powder brominated with 2-bromoisobutyryl bromide showed a significant oxygen peak, compared with the diamond powder with photoreaction. The increased oxygen signal is consistent with the carbonyl group of 2-bromoisobutyryl bromide. The brominated diamond powder is then treated with styrene or styrene/DVB, Cu(I) Br and bipyridine at 110 °C. XPS shows a significant reduction in the oxygen signal (see Figure A7.8c) and the C/O ratio is increased. These results show that polystyrene has grown on the diamond surface since more carbon signal is introduced. Table A7.1 shows the compositions of all diamond surfaces.

Table A7.1 Compositions of the surfaces of diamond powders.

	C	O	Br	S
D-Br	90.2	8.8	1.0	
Isobromide	77.1	22.5	0.4	
PS	88.0	12.0		
PS-sulfonation	82.5	15.7		1.8

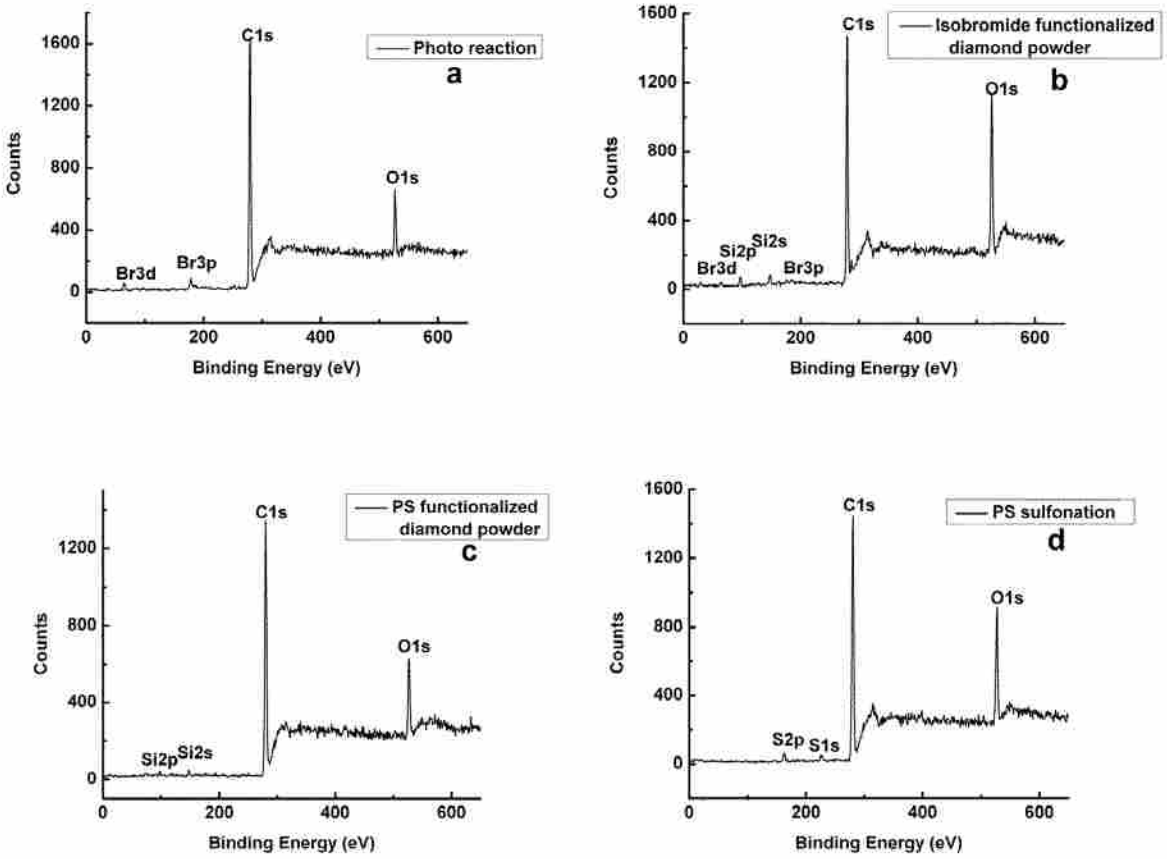

Figure A7.8 x-ray photoelectron spectroscopy (XPS) for diamond powders: a) hydrogen-terminated diamond reacted with bromine under light, b) piranha treated diamond reacted with isobromide, c) brominated diamond functionalized with polystyrene by ATRP and d) sulfonated polystyrene diamond powder.

In time of flight-secondary ion mass spectrometry (ToF-SIMS), after polymerization, there are numerous hydrocarbon peaks and the characteristic peaks are mostly the same as those peaks of standard polystyrene. The relative intensities of characteristic peaks matched the standard well. This is especially, true for the higher masses region for the main characteristic peaks such as 103, 105, 115, 117 and 128. This result shows that the brominated diamond is functionalized by polystyrene. In contrast, before polymerization, characteristic peaks such as 103, 105, 115, 117 and 128 do not match with standard polystyrene positive ToF-SIMS spectra.

Regardless of how the surface was brominated, the infrared spectrum of the diamond after ATRP showed the C—H stretching peaks of aromatic rings (3000 – 3200 cm^{-1}) and alkyl chains (2800 – 3000 cm^{-1}) (see Figures A7.9 d, e and f). In addition, the standard IR spectrum of polystyrene (see Figure A7.2 a) is compared with the spectrum of the diamond powder functionalized by polystyrene.

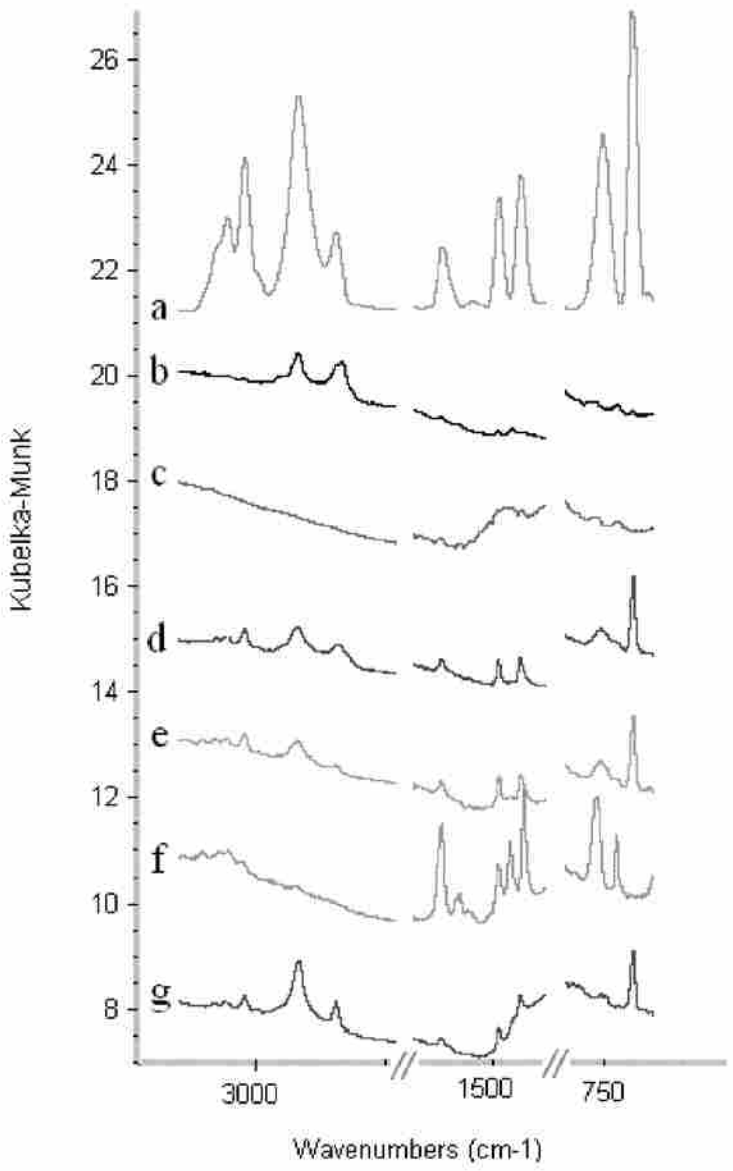

Figure A7.9 DRIFT-IR for diamond powders: a) infrared spectrum of neat polystyrene, b) hydrogen-terminated diamond, c) piranha-treated diamond, d) polystyrene functionalized diamond obtained by photoreaction and ATRP, e) polystyrene functionalized diamond obtained by reaction with 2-bromoisobutyryl bromide and ATRP, f) polystyrene-DVB functionalized diamond obtained by 2-bromoisobutyryl bromide and ATRP and g) polystyrene functionalized diamond obtained by di-tert-amyl peroxide and styrene.

Most of the other peaks matched very well, such as the monobenzene peak at 700 cm^{-1} and the other characteristic peaks at 1450 cm^{-1}, 1500 cm^{-1} and 1600 cm^{-1} (see Figures A7.11 a, d, e and f), which are assigned as combined ring vibrations. Two controls were also performed. They are deuterium-terminated diamond powder and piranha solution cleaned diamond powder which did not have not the ATRP initiators. There were allowed to react with styrene, Cu(I) Br and bipyridine at 110 °C. Figure A7.9 b and c showed no C–H stretching peaks of aromatic rings (3000 – 3200 cm^{-1}). In addition, the other characteristic peaks of polystyrene at 1450 cm^{-1}, 1500 cm^{-1} and 1600 cm^{-1} were not present.

This evidence suggests that our functionalization is successful. During this reaction, styrene (or adding crosslinker DVB) can be polymerized on the diamond surfaces.

Polystyrene (PS) or polystyrene-divinylbenzene (PS-DVB) functionalized diamond powder was slurried in 5 mL acetic acid followed by 50 mL concentrated sulfuric acid in an ice bath. Then the reaction temperature was raised to 90 °C. for 5 hours and finally the PS or PS-DVB was sulfonated. XPS shows an obvious sulfur signal (see Figure A7.8 d), which was not present before the sulfonation. The composition of this diamond surface is shown in Table A7.1.

Chemical stability tests were performed by immersing sulfonated polystyrene coated diamond particles into 1.0 M HCl or 1.0 M NaOH for 70 h. Following this treatment, approximately one-tenth and one-third of the sulfur was removed from the surface; after exposures to acid and base, respectively. These results were compared to the stability of a commercially available SPE stationary phase (Phenomenex Strata SCX, 55 μM, 70 Å). Prior to stability tests, the S2p-to-C1s ratio by XPS was 0.16 ± 0.03. After immersion of these particles in 1.0 M NaOH for 8 h, the particles completely dissolved. To further verify the dissolution of these particles, the resulting clear solution was filtered. It easily passed through the filter, leaving no material behind. The Phenomenex particles were also immersed in 1 M HCl for 70 h. A small decrease in the S2p/C1s ratio was observed (down to 0.15 ± 0.02), which suggests that 6% of the sulfur-containing coating on the particles had been lost. Thus, the deposited PS-sulfonated coatings on diamond have almost the same stability in acid as a commercially available SCX SPE packing material, while being much more stable to base.

A7.3.14.2.2 Strong Cation Exchange SPE Procedure and Breakthrough Curve

These sulfonated PS diamond powders were packed into a strong cation exchange SPE column. The column was conditioned with 6 column volumes of methanol followed by 6 column volumes phosphate buffer (H_3PO_4 and NaH_2PO_4, pH=1.9). The analyte used to test the SPE columns was 1-naphthylamine. 1-naphthylamine (molecular weight: 143.1) was loaded into the column by depositing a 50 μL sample of 1-naphthylamine dissolved in buffer (pH=1.9) (1 mg/mL). Then 3 column volumes of the same buffer were used for washing the column and the analyte did not elute (see Figure A7.10) because it was retained by the column. Finally, the

analyte was eluted by the same buffer but mixed with sodium chloride (pH=1.9, ionic strength is 0.2 M) and methanol (The ratio is 1:1) (see Figure A7.11). All the fractions from the SPE column were analyzed by electrospray ionization mass spectroscopy. (Note: Peak 121.0 is a reference peak. Peak 164.1 might be from the matrix. Peak 144.1 is the $[M+H]^+$ of the analyte.)

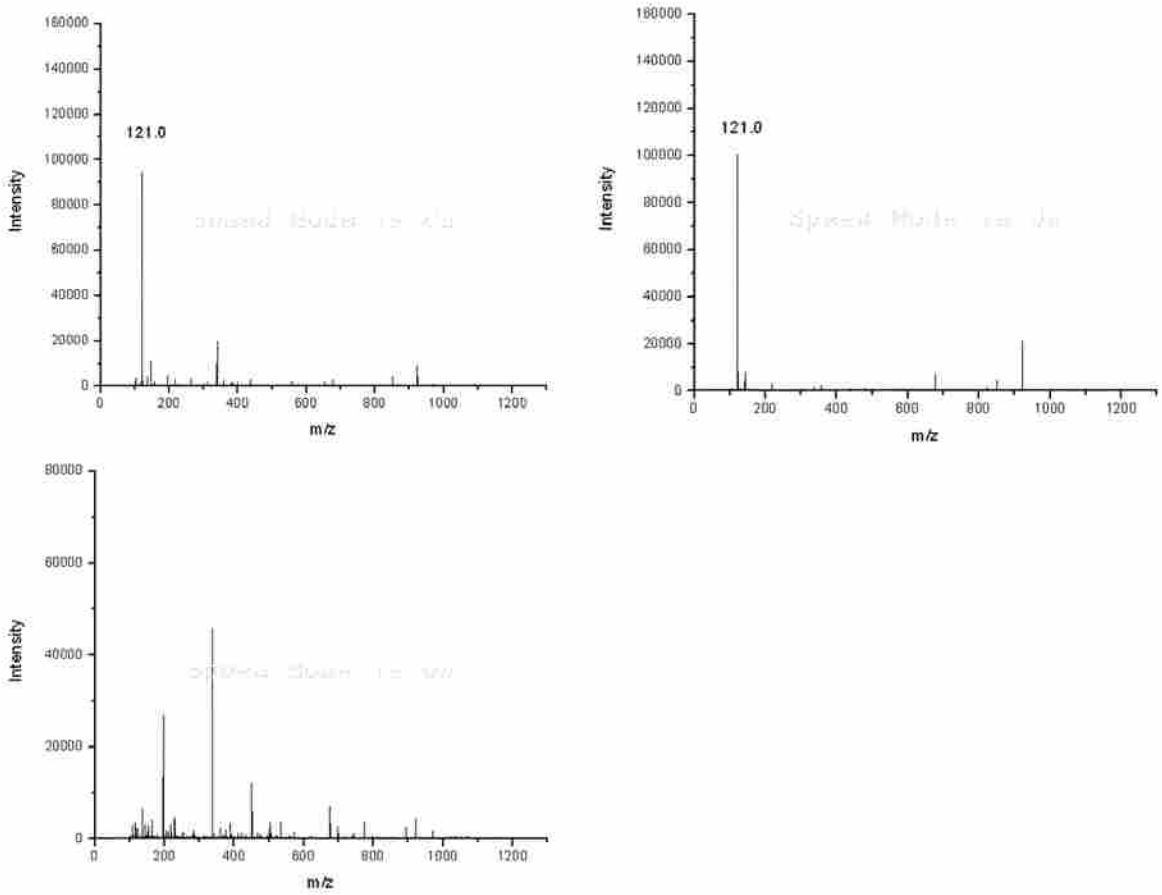

Figure A7.10 shows electrospray ionization mass spectra of three fractions by washing the column with buffer (pH=1.9).

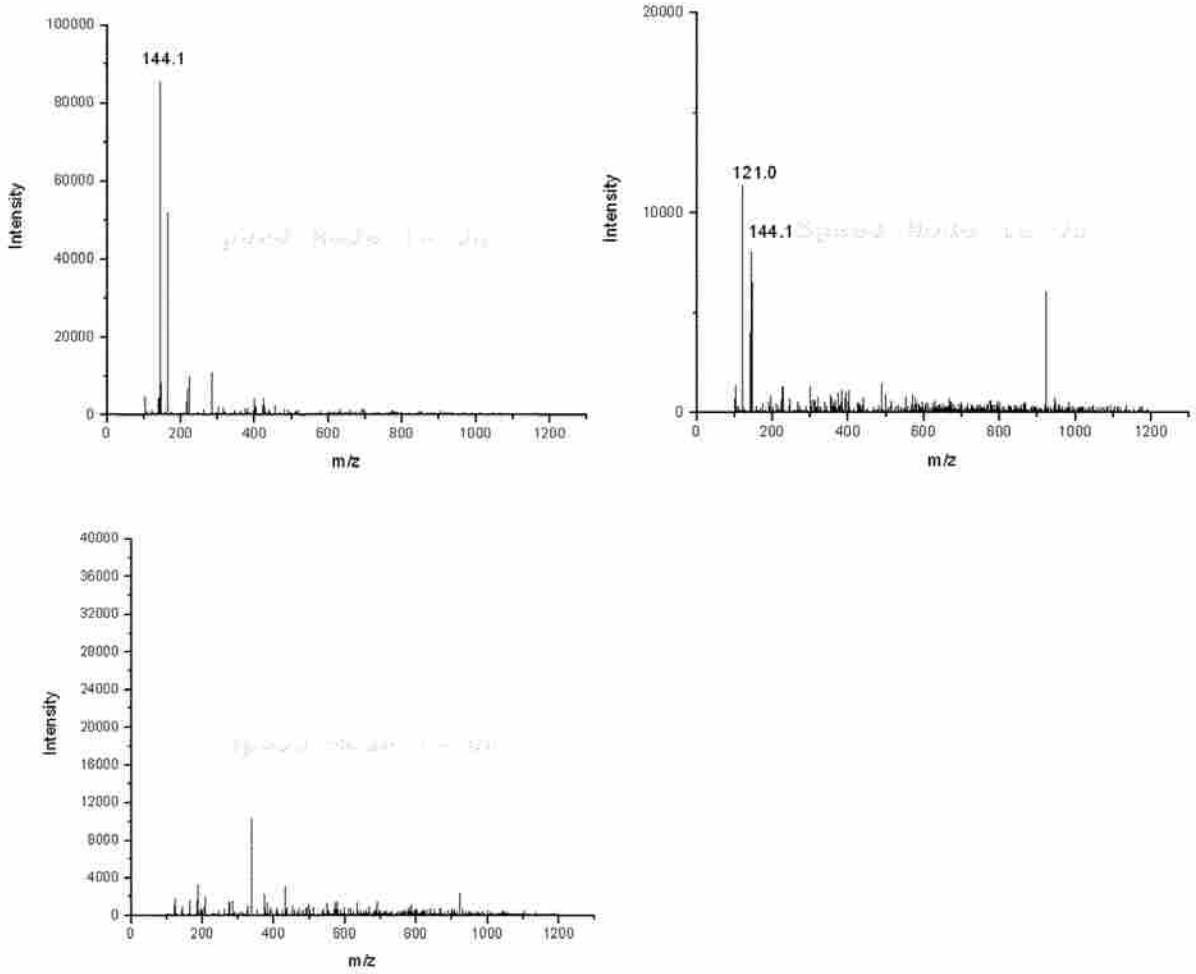

Figure A7.11. Electrospray ionization mass spectra of three fractions by eluting the column with buffer (pH=1.9, NaCl, ionic strength 0.2M) and methanol (The ratio is 1:1).

Breakthrough curves were obtained for the SPE column using 1-naphthylamine as an analyte for determination of breakthrough volumes of the cation exchange SPE column. The columns were conditioned with 6 column volumes of methanol followed by 6 column volumes phosphate buffer (H_3PO_4 and NaH_2PO_4, pH=1.9). The solution of 1-naphthylamine dissolved in buffer (pH=1.9) (0.02 mg/mL) was allowed to flow through the column at a constant flow rate while the breakthrough curves were being obtained. Equal volumes of the fractions eluting from the column were collected in separate vials. The samples were then analyzed using electrospray ionization mass spectrometry to obtain the breakthrough curves based on the presence of 1-naphthylamine in the collected fractions. The breakthrough curve is shown in Figure A7.12. The breakthrough volume was taken from the point on the breakthrough curve corresponding to 5% of the average value at the maximum (i.e., the breakthrough curve plateau region). From these breakthrough curves, a column capacity for cation exchange SPE column was found to be 0.087 mg. Figure A7.13 is the dynamic range of the solution of 1-naphythamine in ESI-MS. This linear relationship demonstrates the breakthrough curve is under this range and the plateau region of the breakthrough curve is the saturation of the SCX SPE column, not the saturation of the ESI-MS detector.

References to other publications and patents have been made in this disclosure, all of which are incorporated herein by reference.

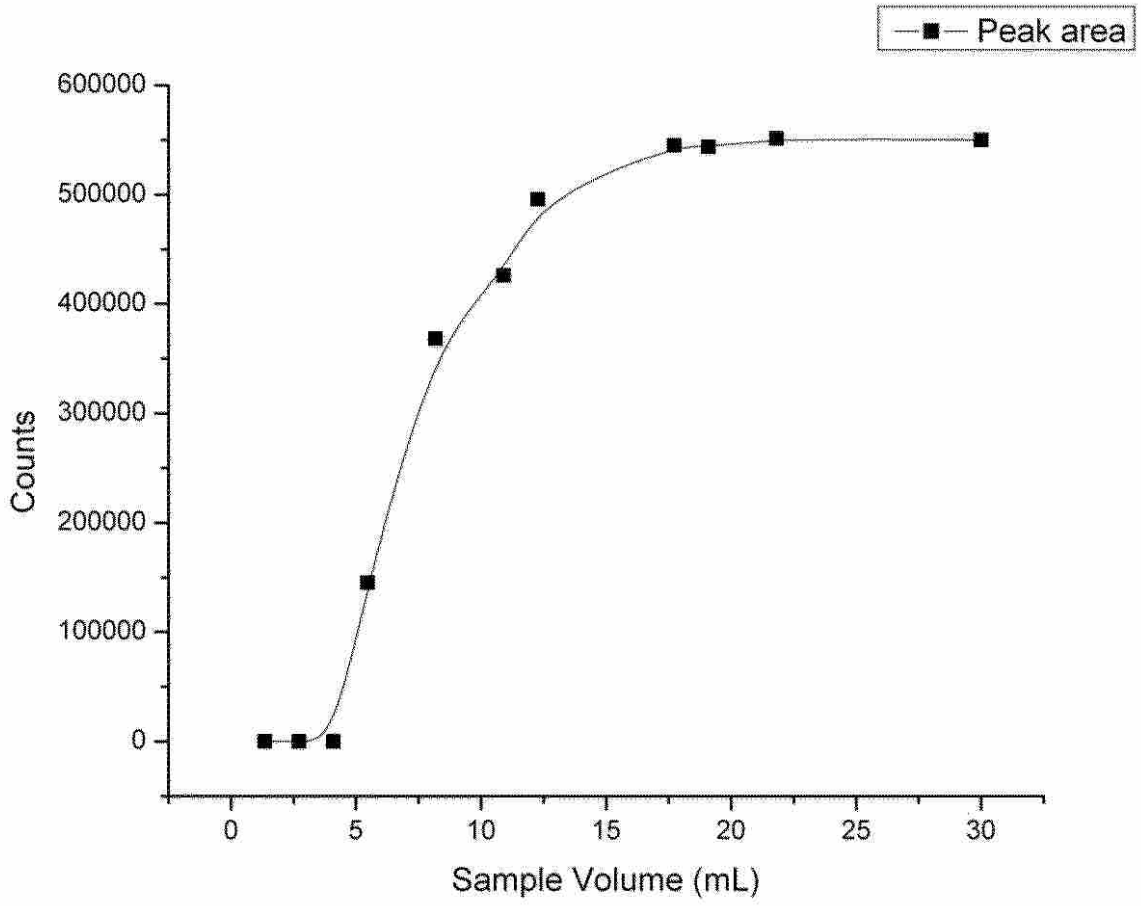

Figure A7.12 Breakthrough curve of SCX SPE column. Each point represents the peak area of the analyte from the positive ESI-MS spectra.

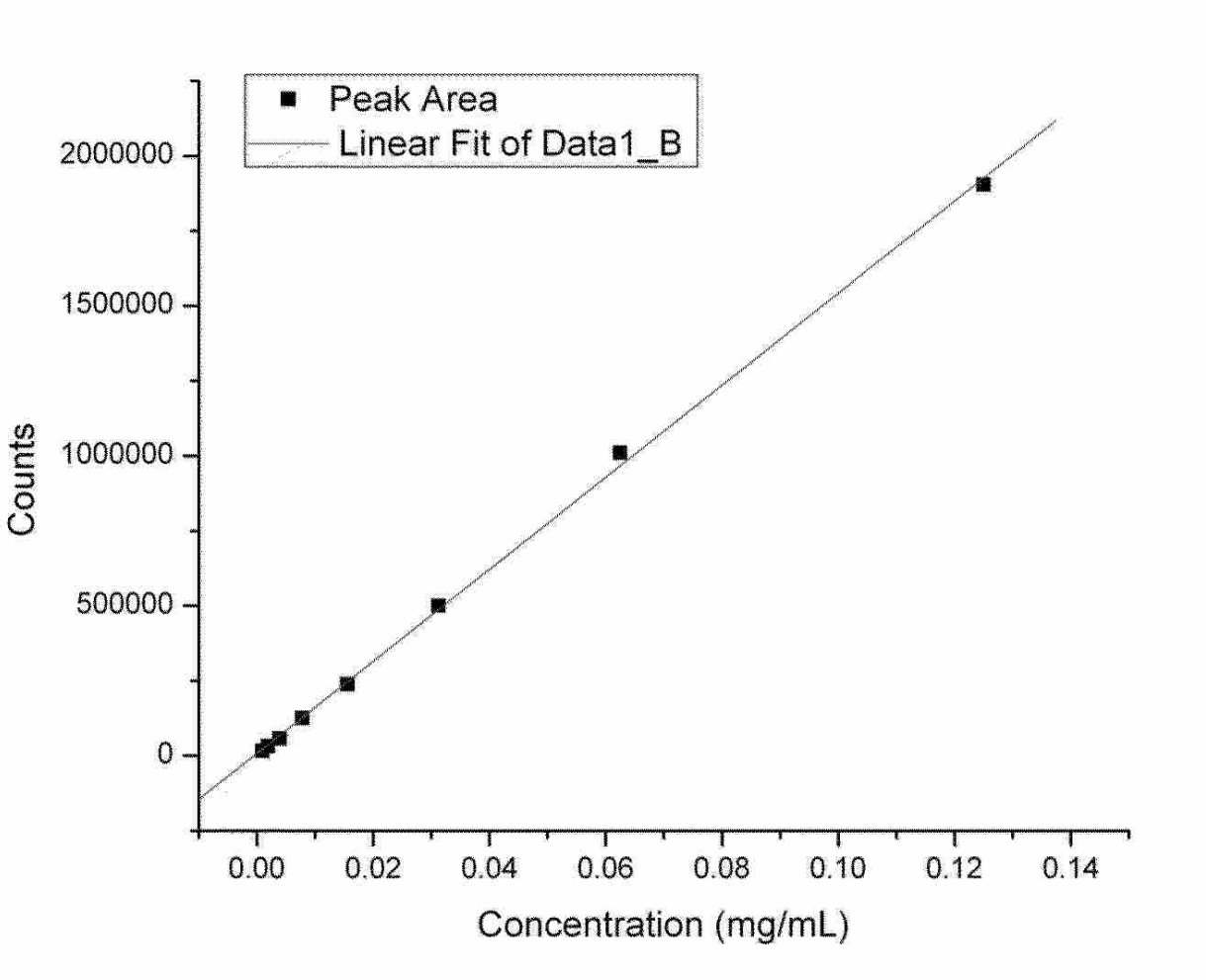

Figure A7.13. Dynamic range of the phosphate buffer (pH=1.9) solution of 1-naphythamine in ESI-MS.

A7.4 Claims

1. A method for coating a diamond surface comprising: providing surface initiation sites on the diamond surface for initiation of a living polymerization on the site; reacting the surface initiation sites with a monomer having a site that reacts with and bonds to an initiation site to form an chemically attached chain with a new initiation site on the chain for further reaction with a monomer, the surface initiation site being carbon-carbon double bond, and the reacting the surface initiation site comprising ring opening metathesis polymerization.

2. A method for coating a diamond surface comprising: providing surface initiation sites on the diamond surface for initiation of a living polymerization on the site; reacting the surface initiation sites with a monomer having a site that reacts with and bonds to an initiation site to form an chemically attached chain with a new initiation site on the chain for further reaction with a monomer, the surface initiation site being –O– and the reacting the surface initiation site comprising epoxide ring opening reactions.

3. A method for coating a diamond surface comprising: providing surface initiation sites on the diamond surface for initiation of a living polymerization on the site; reacting the surface initiation sites with a monomer having a site that reacts with and bonds to an initiation site to form an chemically attached chain with a new initiation site on the chain for further reaction with a monomer, the diamond surface first treated with $LiAlH_4$ to increase the number of –OH sites and the surface initiation sites include the added –OH sites, where H is hydrogen or deuterium.

4. A method for producing a diamond with a coated surface comprising; reacting –OH groups in the surface with 2-bromoisobutyryl bromide to produce bromide surface initiation sites on the surface; reacting the surface initiation sites with a monomer reactive with the surface initiation sites under an atom transfer radical polymerization reaction system.

5. A method as in claim 4 wherein the coated surface comprises polystyrene.

6. A method for producing a diamond with a coated surface comprising; reacting the diamond surface to form –H groups on the surface, where H is hydrogen or deuterium, reacting the –H groups with Br_2 to produce bromide surface initiation sites on the surface, reacting the surface initiation sites with a monomer reactive with the surface initiation sites under an atom transfer radical polymerization reaction system.

7. A method for producing a diamond with a coated surface comprising; deprotonating –OH groups on the diamond surface to form –O– initiation sites on the surface, reacting the surface initiation sites with a monomer having a site that reacts with and bonds to the initiation site to form an chemically attached chain with a new initiation site on the chain for further reaction with a monomer.

8. The method of claim 7 wherein the monomer is an epoxide.

9. A method as in claim 6 wherein the monomer contains a group or groups that impart activity to the coating.

10. A method as in claim 9 wherein the monomer contains one or more of aromatic groups, hydroxyl, carboxyl, amine, primary, secondary, tertiary, or quaternary amine groups, carboxyl groups, hydroxyl groups, sulfonic acid groups, cyano groups, alkyl chains.

11. An article comprising a coating upon a diamond surface, the coating the reaction product of a living polymerization reaction with surface initiation sites on the diamond surface where the living polymerization reaction comprises reacting the surface initiation sites with a monomer having a site the reacts with and bonds to an initiation site to form an chemically attached chain with a new initiation site on the chain for further reaction with a monomer, the surface initiation site being carbon-carbon double bond, and the reacting the surface initiation sites comprising ring opening metathesis polymerization.

12. An article as in claim 11 wherein the coating imparts to the diamond surface an activity derived from group or groups contained in the monomer.

13. An article as in claim 12 the monomer contains one or more of aromatic groups, hydroxyl, carboxyl, amine, primary, secondary, tertiary, or quaternary amine groups, carboxyl groups, hydroxyl groups, sulfonic acid groups, cyano groups, alkyl chains.

14. An article comprising a coating upon a diamond surface, the coating the reaction product of a living polymerization reaction with surface initiation sites on the diamond surface where the living polymerization reaction comprises; reacting the surface initiation sites with a monomer having a site the reacts with and bonds to an initiation site to form an chemically

attached chain with a new initiation site on the chain for further reaction with a monomer, the surface initiation site being –O– and the reacting the surface initiation site comprising epoxide ring opening reactions.

15. An article comprising a coating upon a diamond surface, the coating the reaction product of a living polymerization reaction with surface initiation sites on the diamond surface where the living polymerization reaction comprises; reacting the surface initiation sites with a monomer having a site the reacts with and bonds to an initiation site to form an chemically attached chain with a new initiation site on the chain for further reaction with a monomer, the diamond surface first treated with $LiAlH_4$ to increase the number of –OH sites and the surface initiation sites include the added –OH sites, where H is hydrogen or deuterium.

16. An article comprising a coating upon a diamond surface, the coating the reaction product of deprotonating –OH groups on the diamond surface to form –O– initiation sites on the surface, and reacting the surface initiation sites with a monomer having a site that reacts with and bonds to the initiation site to form a chemically attached chain with a new initiation site on the chain for further reaction with a monomer.

17. An article as in claim 16 wherein the monomer is an epoxide.

18. An article as in claim 16 wherein the reacting the surface initiation sites includes epoxide ring opening reactions.

19. An article as in claim 16 wherein the coating imparts to the diamond surface an activity derived from group or groups contained in the monomer.

20. An article as in claim 16 the monomer contains one or more of aromatic groups, hydroxyl, carboxyl, amine, primary, secondary, tertiary, or quaternary amine groups, carboxyl groups, hydroxyl groups, sulfonic acid groups, cyano groups, alkyl chains.

A7.5 References

Patent Citations

(1) US7276283 B2, Denes, F.S.; Manolache, S.O.; Cruz-Barba, L.E.; Lagally, M.G.; Larson, B.J., 10/2007, Wisconsin Alumni Research Foundation, Plasma-enhanced functionalization of carbon-containing substrates

(2) US2008/0249229 A1, Lukehart, C.M.; Davidson, J.L.; Strauss, A.M.; Li L.; Branson, B.T., 10/2008, Vanderbilt University, Diamond polymer brushes

Non Patent Citations

(1) Li et al. *Carbon*, 44, **2006**, 2308-2315.

(2) Qin et al, *Macromolecules*, **2004**, 37, 752-757.

(3) Qin et al, *J. Am. Chem. Soc.*, **2004**, 126, 170-176.

Appendix 8: Modified Diamond Particle Surfaces and Method*

A8.1 Overview

A8.1.1 Abstract

A method for preparing modified diamond particles for use in chromatography where hydroxyl groups at the diamond surfaces are reacted with a reactive molecule to introduce a desired functional group at the diamond surface.

A8.1.2 Statement of Attribution

My major contributions to this work are in sections A8.2 – A8.4. These sections contain a study performed on microdiamond where the oxidized surface was reduced using $LiAlH_4$. Octadecylisocyanate was then reacted with the reduced/hydroxylated surface to form a hydrophobic surface. Each step of surface functionalization is verified using DRIFTS, ToF-SIMS and XPS.

*This appendix has been published as a United States Patent, US 8,202,430 B2. Issued June 19, 2012.

A8.2 Background

Since the inception of modern chromatography, silica based stationary phases have dominated the world of chemical separations. Unfortunately, silica has certain limitations. Under acidic conditions, silica tends to lose its functionality and under basic conditions it dissolves entirely after a matter of hours. Not until recently have alternatives to silica been available such as polymer based stationary phases. These tend to swell when exposed to organic solvents and are therefore not ideal for reversed-phase separations.

Chemists have worked around the limitations of available stationary phases, but these workarounds often result in less than ideal outcomes. For instance, certain separations may need to occur under basic or acidic conditions because the analyte of interest may only be stable under a certain pH range. It is would therefore be ideal to find a phase that could perform a separation under extreme pHs that current phases cannot successfully do separations at.

Diamond has usually been assumed to be inert and relatively little has been done to investigate the possibility of diamond as the basis for a stationary phase. Nosterenko et al. has performed separations of proteins using oxidized/cleaned diamond and Saini et al. has been successful in coating the diamond surface with poly(allylamine). This coated diamond was then used as a normal phase in Solid-phase Extraction (SPE). Saini's study also showed that his phase was extremely stable under extreme pH conditions (from pH 0-pH 14) for 24 h. The SPE column was able to be reused many times and showed no signs of degradation. It also performed in the same manner experiment after experiment and only required a flush with ethyl acetate in between uses.

These two groups have shown that separations can indeed be performed with diamond as the basis for a stationary phase. Nesterenko's study lacked good resolution in it HPLC spectra and Saini's capacity was quite low, but efforts are being made to remedy the capacity issue.

A8.3 Summary

A new phase is directly bonded to the diamond surface which has been largely hydroxyl terminated. In a specific example, diamond cleaned with piranha solution is treated with lithium aluminum hydride (LAH). This reaction greatly increases the amount of hydroxyl groups on the diamond surface. Since hydroxyl groups are reactive to various functional groups, this chemistry is exploited to attach ligands directly to the diamond surface. For example, isocyanates and acyl halides (primarily Br and Cl) are reactive to the hydroxyl functional group and form urethane and ester linkages respectively, that are directly bonded to the diamond surface. (see Figure A8.1)

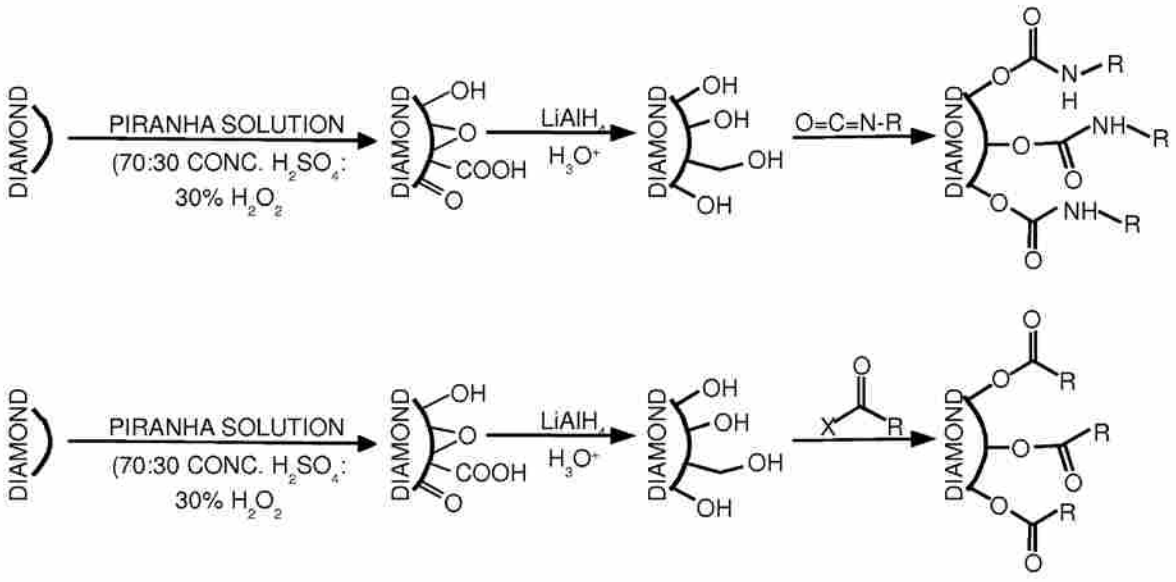

Figure A8.1 Scheme outlining basic chemistry for the formation of the isocyanate and acyl halide reacted diamond particles.

Bases do have the ability to hydrolyze this linkage at the carbonyl site, so bulky groups (methyl, isopropyl, tert-butyl, phenyl etc.) can be attached to the α-carbon of the ligand to sterically hinder the binding site and prevent bases from accessing the partially negative carbon. This should give this type of linkage greater stability in the presence of acids and bases. The reusability and consistency of the column is also expected to be similar to that of Saini's column and this chemistry can be applied to HPLC and SPE stationary phases.

An aspect is a method for preparing modified diamond particles for use in chromatography where hydroxyl groups at the diamond surfaces are reacted with a reactive molecule to introduce a desired functional group at the diamond surface. An example is the reaction of isocyanates and acyl halides with hydroxyl-terminated diamond to form HPLC/SPE stationary phases.

Another aspect is a method for preparing modified diamond particles for use in chromatography where i) diamond particles are reacted with an oxidizing agent that introduces carboxyl groups at the surface of the diamond, ii) the carboxyl groups are reduced to primary alcohols, and iii) the primary alcohols are reacted with a reactive molecule to introduce a desired functional group at the diamond surface.

The diamond particles of the present method can be used in any suitable type of chromatography type. These include, for example, high performance liquid chromatography (HPLC), ultra performance liquid chromatography (HPLC), solid phase extraction, electrochromatography, size-exclusion chromatography, ion chromatography, affinity chromatography.

The chromatography may be practiced at any suitable pressure, such as for example, between 1000 psi and 15000 psi.

The diamond surface may be prepared by reducing the surface with a suitable reducing agent prior to reaction with the reactive molecule. Any suitable reducing agent is contemplated, such as, for example, lithium aluminum hydride.

The reactive function group may be any suitable functional group with the desired reactivity, and may have attached to the reactive group an alkyl group or aryl group. The alkyl group may have the form $–(CH_2)_nCH_3$, where n = 0 – 25. The alkyl group may be branched or unbranched. The alkyl group may be partially or fully fluorinated, the aryl group may have the form $–C_6H_6$. The aryl group may be partially or fully fluorinated.

Examples of the reactive functional groups include, one of or a mixture of an alkyl isocyanate, an aryl isocyanate, an acid chloride with an aromatic group, an acid chloride with an alkyl group, an acid bromide, an alkyl halide, an aryl halide, a benzyl halide, a benzyl triflate, a benzyl mesylate, an alkyl mesylate, an alkyl tosylate, and an alkyl triflate.

The reactive functional group may contain more than one other group near the reactive site of the molecule, which provides steric hindrance for the adsorbed species.

The reactive molecule may contain C–H bonds. The reactive molecule may contain an electrophilic site and a leaving group.

Another aspect is a diamond particle for use in chromatography containing groups tethered to the diamond surface through ether, ester, or urethane linkages.

A8.4 Detailed Description

A8.4.1 Example Experimental

Micro-diamond or diamond powder is treated with piranha solution (3:7 30% H_2O_2:conc. H_2O_2:conc. H_2SO_4) or any other suitable cleaning/etching solution. This cleans/etches

the diamond surface and exposes the various functional groups that naturally occur on the diamond surface. The diamond must be dried thoroughly before the next step. This can be performed by pulling argon through the powder or placing the powder in a vacuum for many hours. The dryness can be verified by diffuse reflectance infrared Fourier transform (DRIFT).

The cleaned dry diamond is then treated with 1M $LiAlH_4$ (LAH) suspended in THF (or any other strongly reducing base)[1] for 24 – 68 h at room temperature (about 1 g diamond:5 mL LAH solution). Warning: LAH is extremely reactive to water. Use proper PPE. The reaction must be performed under inert atmosphere (argon) and all glassware must be dry. The reaction is quenched by 1M HCl. This should be added very slowly due to the reactivity of LAH with water and HCl. Once the reaction is quenched, the diamond is filtered over a fine fritted Buchner funnel and washed with copious amounts of water. If white particles are present, rinse with more 1 M HCl to dissolved the reacted LAH. Once thoroughly rinsed, the powder is dried completely. This gives hydroxyl terminated diamond.

The reduced surface has been disclosed US patent,[2] the reaction of the hydroxylated surface with various functional groups is not disclosed. The present method is an improvement over the disclosed diamond-based chromatographic processes.

Another US patent[2] discloses powders "attached with hydrocarbon, amino, carboxylic acid, or sulfonic acid groups." The present method is specifically targeting the reaction of the hydroxylated surface with a reactive molecule to introduce a desired functional group at the diamond surface, such as, for example, reactive isocyanates and acyl halides, and this chemistry and these functional groups are not disclosed.

In a specific example, for this final step the hydroxyl terminated diamond is then placed in a reaction vessel which is subsequently flushed with inert atmosphere. Then a reactive

molecule is added to the powder. For example, a desired isocyanate or acyl halide is added to the powder (about 0.5 mL:1 g hydroxyl terminated diamond) then add enough dry tetrahydrofuran (THF) or ether to completely dissolve the isocyanate or acyl halide. The reaction should then react for at least 18 h at room temperature. Filter the diamond over a fine fritted Buchner funnel and wash with a large amount of THF or ether to rinse away the unreacted isocyanate or acyl halide. Dry the powder completely. The powder is then suspended in a solvent and pressed into an HPLC column.

A8.4.2 Results and Discussion

Thus far, only octadecyl isocyanate has been reacted with the hydroxyl terminated diamond. The evidence of the successive reactions can be seen in Figure A8.2 by the DRIFT, ToF-SIMS and XPS spectra. There is a decrease in the height of the alcohol peak (~3500 cm^{-1}) seen in the octadecyl isocyanate DRIFT spectrum as compared to the LAH spectrum. It is clear that not all of the alcohol functional groups are reacted and this is attributed to the steric hindrance of the diamond surface. The 2° amine peak at 3342.43 cm^{-1}, asymmetric and symmetric C–H stretches at 2920.95 cm^{-1} and 2848.21 cm^{-1} and the carbonyl stretches at 1612.33 cm^{-1} and 1572.64 cm^{-1} are indicative of successful bonding of octadecyl isocyanate to the hydroxyl terminated surface as evidenced by the urethane (carbamate) linkage.

The ToF-SIMS data shows an increase of hydrocarbon fragments in the positive ion spectra and a decrease of O (16 m/z) and OH (17 m/z) fragments in the negative ion spectra. This result is predicted because fewer O and OH groups would be exposed on the diamond surface once the isocyanate group has reacted with the OH functional group. The XPS spectrum shows the presence of nitrogen which is absent from the piranha and LAH treated diamond powders.

The only source of nitrogen in this experiment is from the isocyanate group. This therefore further confirms the formation of the carbamate linkage on the diamond surface.

In another embodiment, an HPLC column is packed with 5 μm octadecyl isocyanate reacted diamond powder. If non-porousdiamond is used, few plates are expected to be present on the column. This should be remedied by using porous diamondpowder.

The chemistry of the present method is expected to work with various isocyanates and acyl halides, including compounds with the disubstituted α-carbons (see Figure A8.3 for some examples). The acyl halide derivatives of these compounds would also be used including the tert-butyl group not shown in the figure. Other functional groups past the functionalized α-carbon could include but are not limited to phenyl, naphthyl, chiral, perfluorinated, C_8, and C_{10}.

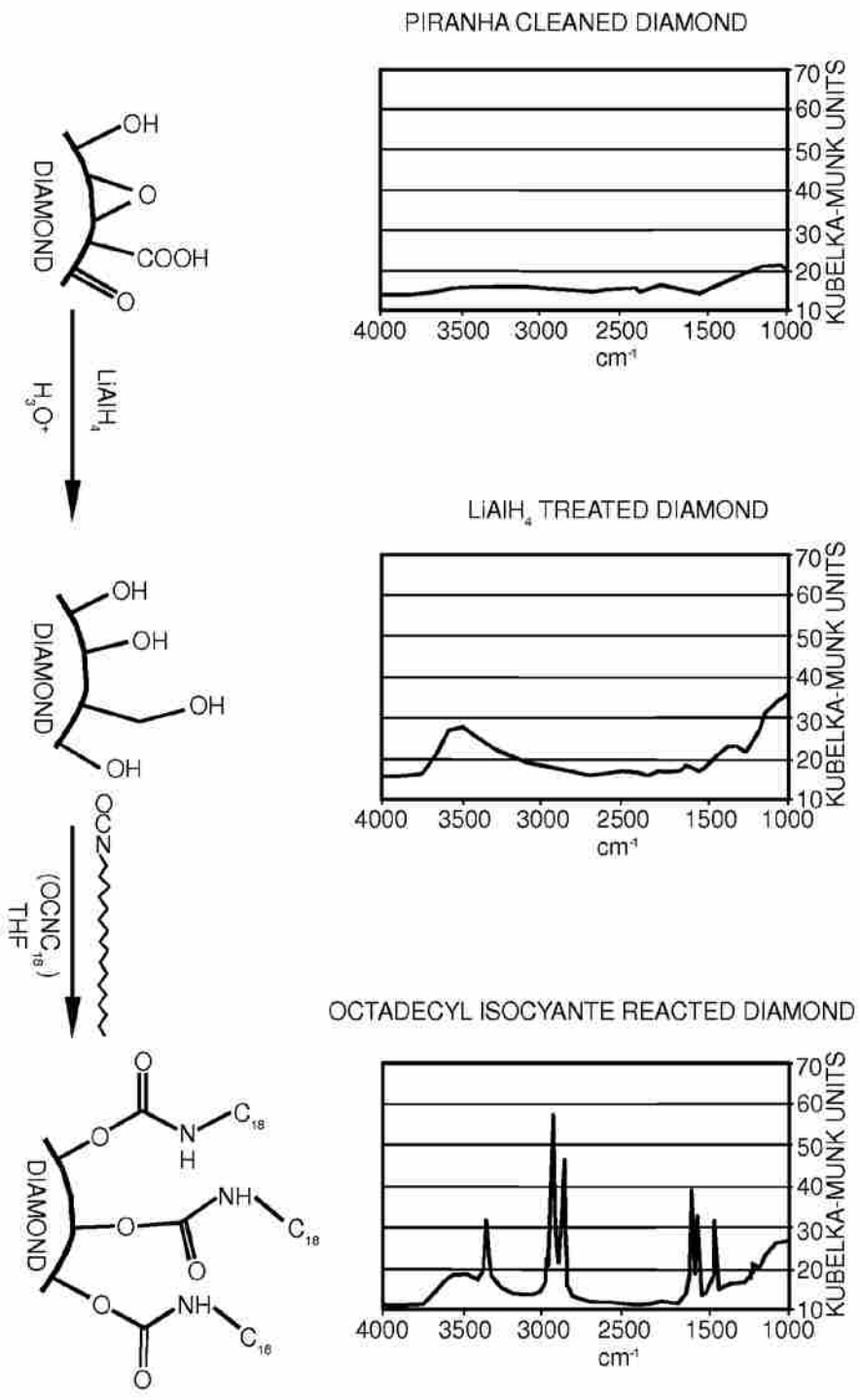
PIRANHA CLEANED DIAMOND
DIAMOND
OH
O
COOH
O
H_3O^+
$LiAlH_4$
4000 3500 3000 2500 1500 1000
cm-1
KUBELKA-MUNK UNITS
10 20 30 40 50 60 70
$LiAlH_4$ TREATED DIAMOND
DIAMOND
OH
OH
OH
OH
(OCNC18)
THF
OCN
4000 3500 3000 2500 1500 1000
cm-1
KUBELKA-MUNK UNITS
10 20 30 40 50 60 70
OCTADECYL ISOCYANTE REACTED DIAMOND
DIAMOND
O
N
H
C18
NH
C18
O
NH
C16
4000 3500 3000 2500 1500 1000
cm-1
KUBELKA-MUNK UNITS
10 20 30 40 50 60 70

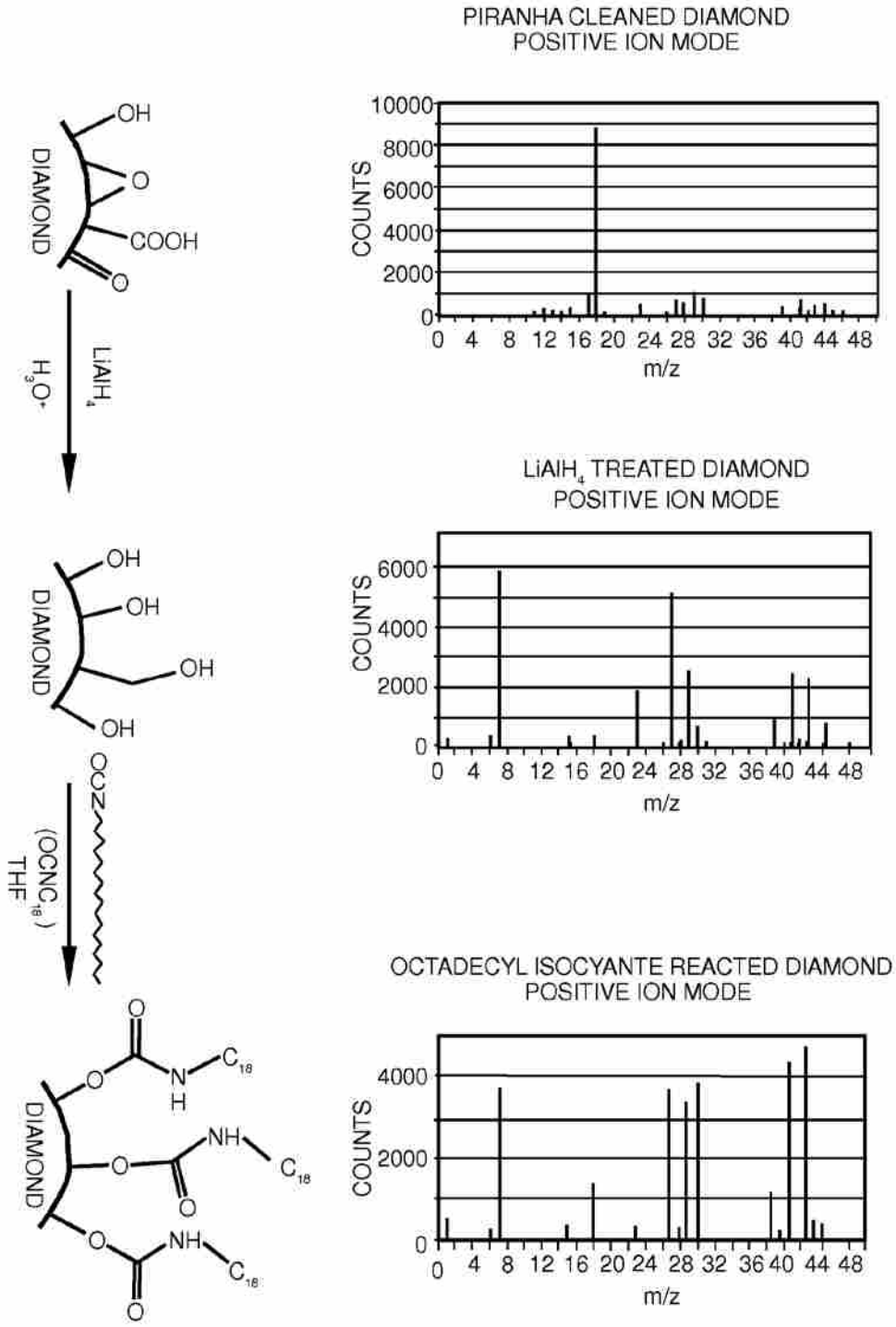
PIRANHA CLEANED DIAMOND
POSITIVE ION MODE
COUNTS
m/z
LiAlH4 TREATED DIAMOND
POSITIVE ION MODE
COUNTS
m/z
OCTADECYL ISOCYANTE REACTED DIAMOND
POSITIVE ION MODE
COUNTS
m/z
DIAMOND
OH
O
COOH
H3O+
LiAlH4
(OCNC18)
THF
C18
NH

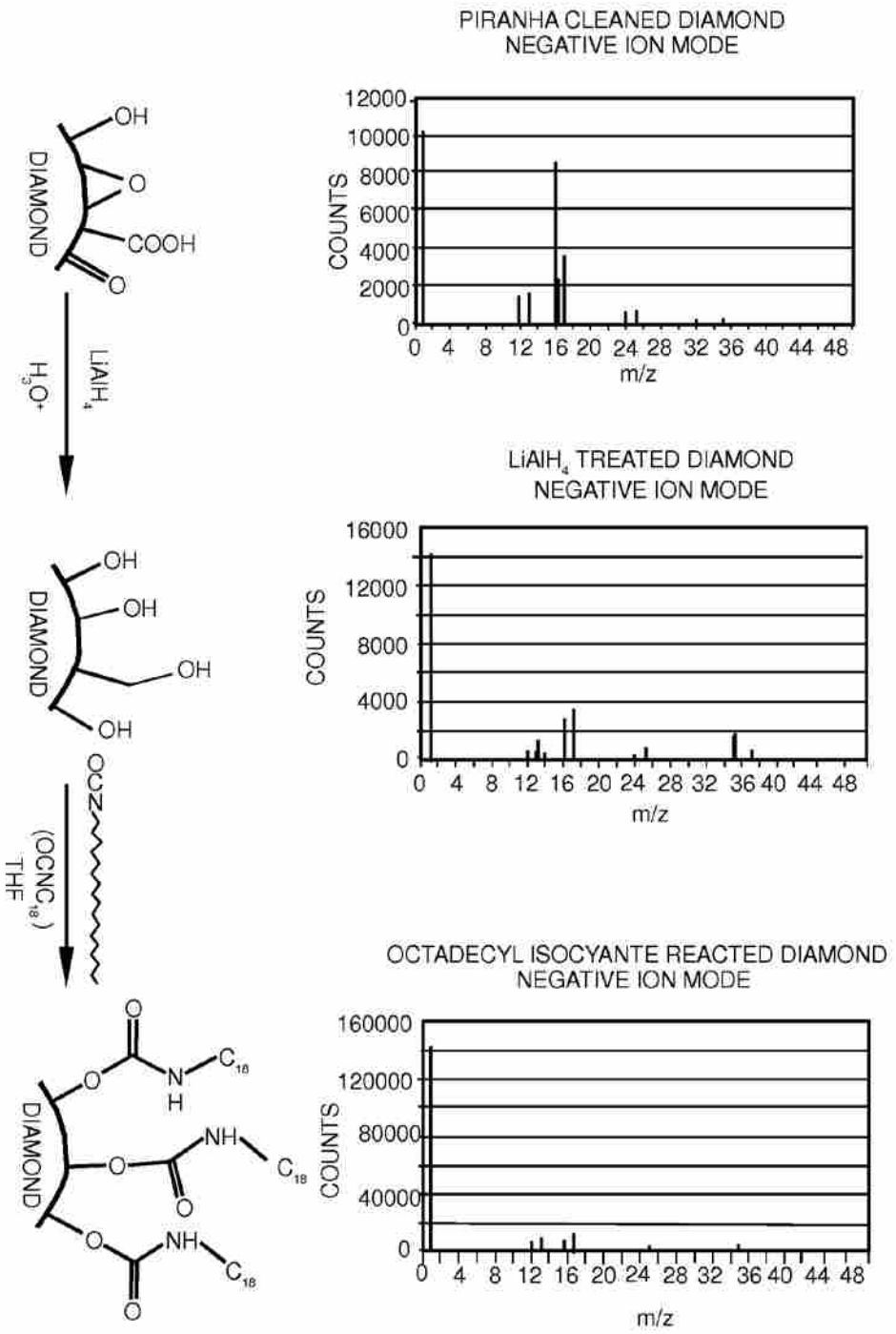
PIRANHA CLEANED DIAMOND
NEGATIVE ION MODE
COUNTS
m/z
DIAMOND
OH
O
COOH
O
H_3O^+
$LiAlH_4$
$LiAlH_4$ TREATED DIAMOND
NEGATIVE ION MODE
COUNTS
m/z
DIAMOND
OH
OH
OH
OH
(OCNC$_{18}$)
THF
OCN
OCTADECYL ISOCYANTE REACTED DIAMOND
NEGATIVE ION MODE
COUNTS
m/z
DIAMOND
O
N
H
C_{18}
NH
C_{18}
NH
C_{18}

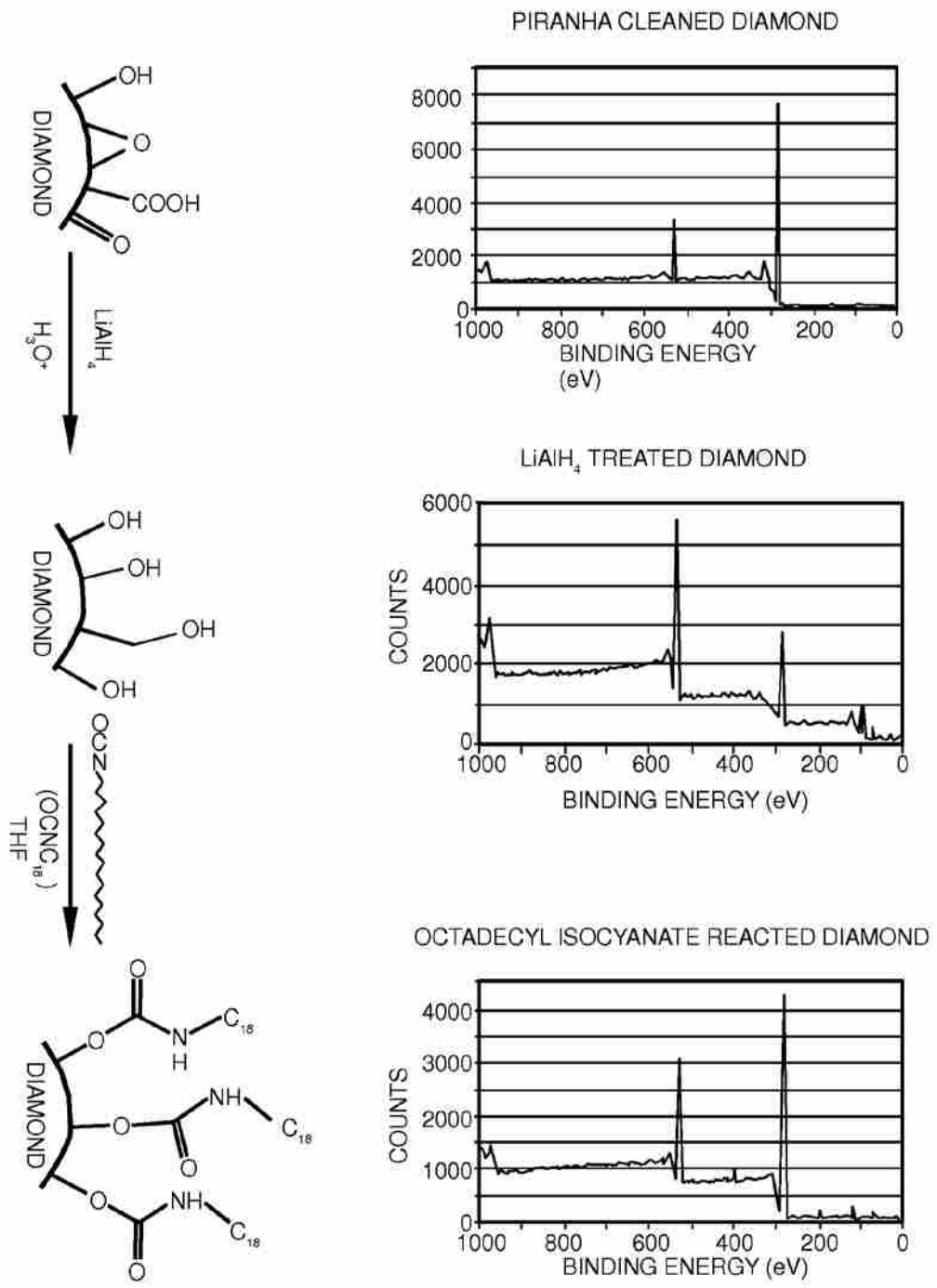

Figure A8.2 Spectra confirming the step by step synthesis of a carbamate linked C_{18} chain to the diamond surface.

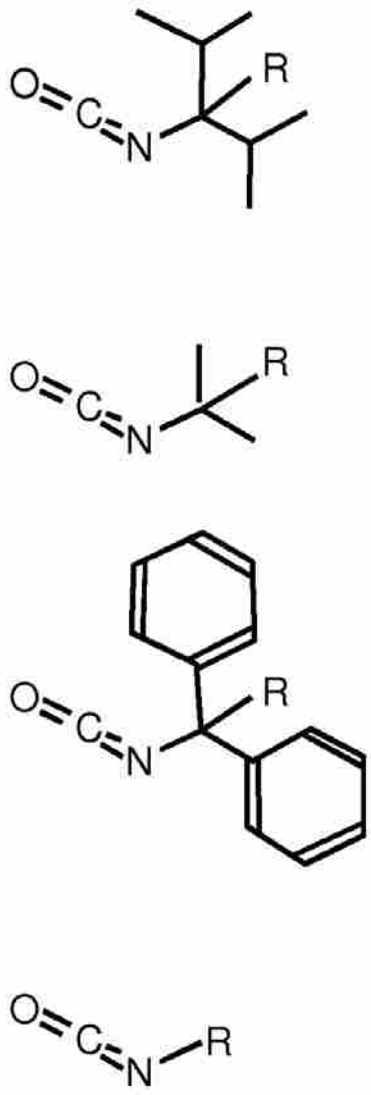

Figure A8.3 Possible examples of the types of groups attached at the α-carbon site to increase sterics of the area in order to prevent nucleophilic attack of a base at the carbonyl resulting in hydrolysis of the ether or urethane linkage.

A8.4.3 Conclusion

The chemistry for creating urethane (carbamide) linkages to the diamond surface is straight forward and should prove useful in the creation of diamond-based HPLC and SPE stationary phases. The attachment of octadecyl isocyanate to the diamondsurface has been verified and other isocyanates/acyl halides should also react in a similar manner to the hydroxyl terminateddiamond surface.

Once a diamond-based HPLC column is successfully created and used, the added stability, reusability and consistency of these diamond columns will exceed that of its similarly functionalize silica-based counterparts. This strength comes from the urethane and/or ester linkages which bind the diamond and the functional group together. This will result in greater stability at more extreme pHs and the disubstituted α-carbon should help increase the stability further in basic conditions.

While invention has been described with reference to certain specific embodiments and examples, it will be recognized by those skilled in the art that many variations are possible without departing from its scope and spirit, and that any invention, as described by the claims, is intended to cover all changes and modifications that do not depart from the spirit of the invention.

A8.5 Claims

1. A method for preparing modified diamond particles for use in chromatography comprising reacting hydroxyl groups at the diamond surfaces with a reactive molecule to introduce a desired functional group at the diamond surface.

2. A method for preparing modified diamond particles for use in chromatography comprising reacting hydroxyl groups at the diamond surfaces with a reactive molecule to introduce a desired functional group at the diamond surface, the reactive functional group being one or more of an alkyl isocyanate, aryl isocyanate, an acid chloride with an aromatic group, an acid chloride with an alkyl group, acid bromide, alkyl halide, aryl halide, benzyl halide, benzyl triflate, benzyl mesylate, alkyl mesylate, alkyl tosylate, and alkyl triflate.

3. A method for preparing modified diamond particles for use in chromatography comprising reacting hydroxyl groups at the diamond surfaces with a reactive molecule to introduce a desired reactive functional group at the diamond surface, the reactive functional group, in addition to a reactive site, having one of or more from alkyl groups, and aryl groups.

4. The method of claim 3 wherein the alkyl group is $-(CH_2)_nCH_3$, where n = 0 – 25.

5. The method of claim 3 wherein the alkyl group is branched.

6. The method of claim 3 wherein the alkyl group is partially or fully fluorinated.

7. The method of claim 3 wherein the aryl group is $-C_6H_5$.

8. The method of claim 3 wherein the aryl group is partially or fully fluorinated.

9. The method of claim 3 in which the reactive functional group comprises one or more of alkyl isocyanate, aryl isocyanate, acid chloride with an aromatic group, acid chloride with an alkyl group, acid bromide, alkyl halide, aryl halide, benzyl halide, benzyl triflate, benzyl mesylate, alkyl mesylate, alkyl tosylate, and alkyl triflate.

10. A method for preparing modified diamond particles for use in chromatography comprising reacting hydroxyl groups at the diamond surfaces with a reactive molecule to introduce a desired reactive functional group at the diamond surface, the reactive functional group, in addition to a reactive site, having one or both of an alkyl group, and an aryl group,
wherein the reactive functional group has more than one other group near the reactive site of the molecule, which provides steric hindrance for adsorbed species.

11. A method for preparing modified diamond particles for use in chromatography comprising reacting hydroxyl groups at the diamond surfaces with a reactive molecule to introduce a desired functional group at the diamond surface, the reactive functional group being one or more of alkyl isocyanate, aryl isocyanate, acid chloride with an aromatic group, acid chloride with an alkyl group, acid bromide, alkyl halide, aryl halide, benzyl halide, benzyl triflate, benzyl mesylate, alkyl mesylate, alkyl tosylate, and alkyl triflate.

12. A method for preparing modified diamond particles for use in chromatography comprising i) reacting diamond particles with an oxidizing agent that introduces carboxyl groups at the surface of the diamond, ii) reducing said carboxyl groups to primary alcohols, and iii) reacting the primary alcohols with a reactive molecule to introduce a desired functional group at the diamond surface.

13. The method of claim 12 additionally comprising conducting a chromatography process with the diamond particles, where the chromatography process is high performance liquid chromatography (HPLC), ultra performance liquid chromatography (HPLC), solid phase extraction chromatography, electrochromatography, size-exclusion chromatography, ion chromatography, or affinity chromatography.

14. The method of claim 13 in which the chromatography process is practiced at a pressure of between 1000 psi and 15,000 psi.

15. The method of claim 12 in which the diamond surface is reduced with a reducing agent prior to reacting with the reactive molecule.

16. The method of claim 15 in which the reducing agent is lithium aluminum hydride.

17. The method of claim 12 in which the reactive molecule contains C–H bonds.

18. The method of claim 12 in which the reactive molecule contains an electrophilic site and a leaving group.

19. A method for preparing modified diamond particles for use in chromatography comprising i) reacting diamond particles with an oxidizing agent that introduces carboxyl groups at the surface of the diamond, ii) reducing said carboxyl groups to primary alcohols, and iii) reacting the primary alcohols with a reactive molecule to introduce a desired reactive functional group at the diamond surface; the reactive functional group, in addition to a reactive site, having one or both of an alkyl group, and an aryl group.

20. The method of claim 19 wherein the alkyl group is $-(CH_2)_nCH_3$, where n = 0 – 25.

21. The method of claim 19 wherein the alkyl group is branched.

22. The method of claim 19 wherein the alkyl group is partially or fully fluorinated.

23. The method of claim 19 wherein the aryl group is $-C_6H_5$.

24. The method of claim 19 wherein the aryl group is partially or fully fluorinated.

25. The method of claim 19 wherein the reactive functional group has more than one other group near the reactive site of the molecule, which provides steric hindrance for adsorbed species.

26. The method of claim 19 in which the reactive functional group comprises one or more of alkyl isocyanate, aryl isocyanate, acid chloride with aromatic group, acid chloride with an alkyl group, acid bromide, alkyl halide, aryl halide, benzyl halide, benzyl triflate, benzyl mesylate, alkyl mesylate, alkyl tosylate, and alkyl triflate.

27. A method for preparing modified diamond particles for use in chromatography comprising;

i) reacting diamond particles with an oxidizing agent that introduces carboxyl groups at the surface of the diamond,

ii) reducing said carboxyl groups to primary alcohols, and

iii) reacting the primary alcohols with a reactive molecule to introduce a desired reactive functional group at the diamond surface; the reactive functional group one or more of an alkyl isocyanate, aryl isocyanate, an acid chloride with an aromatic group, an acid chloride with an alkyl group, acid bromide, alkyl halide, aryl halide, benzyl halide, benzyl triflate, benzyl mesylate, alkyl mesylate, alkyl tosylate, and alkyl triflate.

28. A method for preparing modified diamond particles for use in chromatography comprising; treating diamond particle surfaces to produce hydroxyl groups on the surface, treating the surfaces having hydroxyl groups with isocyanate or acyl halide to produce reactive functional groups on the surfaces.

29. A method for preparing modified diamond particles for use in chromatography comprising; treating diamond particle surfaces to produce hydroxyl groups on the surface,

treating the surfaces having hydroxyl groups with isocyanate or acyl halide to produce reactive functional groups on the surfaces; reactive functional groups having more than one other group near the reactive site of the molecule, which provides steric hindrance for adsorbed species.

A8.6 References

Patent Citations

(1) US4298500, Abbott, S.R., Nov 3, 1981, Varian Associates, Inc., Mixed phase chromatographic compositions

(2) US7326837, Han, C.C.; Chang, H-.,C.; Lee, S-.,C.; Chen, W-.,H., Feb 5, 2008, Academia Sinica, Clinical applications of crystalline diamond particles

(3) US7427361, Frey, D.W.; Hayden, C.G.; Small, R.J.; Tredinnick, B., Sep 23, 2008, Dupont Air Products Nanomaterials Llc, Particulate or particle-bound chelating agents

(4) US20020158022, Huang, J., Chou, H-.,P.; Unger, M.A., Oct 31, 2002, Fluidigm Corporation, Microfluidic chromatography

(5) US20040118762, Bowden, E.; Xu, J, Jun 24, 2004, Bowden Edmond Packing materials for liquid chromatography using chemically modified diamond powders

(6) US20040121070, Bowden, E.; Xu, J, Jun 24, 2004, Bowden Edmond, Connect diamond powders by cycloaddition reactions

(7) US20050158549, Yao, A., Jul 21, 2005, William Marsh Rice University Functionalization of nanodiamond powder through fluorination and subsequent derivatization reactions

(8) US20050189279, Bowden, E.; Xu, J, Sep 1, 2005, Bowden Edmond, Stationary phase for liquid chromatography using chemically modified diamond surfaces

(9) US20060024434, Wang, H.; Quanci, J.; Partch, R.; Barney, N., Feb 2, 2006, Barney Nathaniel A Manufacturing of polymer-coated particles for chemical mechanical polishing

(10) US20060154304, Han, C.C.; Chang, H-.,C.; Chen, W-.,H.,; Lee, S-.,C., Jul 13, 2006, Academia Sinica, Clinical applications of crystalline diamond particles

(11) US20060234269, Asplund, M.; Linford, M.; Jiang, G., Oct 19, 2006, Asplund Matthew Laser Modification and Functionalization of Substrates

(12) US20060269467, Khabashesku, V.; Liu, Y.; Halas, N., Nov 30, 2006, William Marsh Rice University Fluorinated nanodiamond as a precursor for solid substrate surface coating using wet chemistry

(13) US20090218276, Linford, M.R.; Saini, G., Sep 3, 2009, Brigham Young University Functionalized diamond particles and methods for preparing the same

(14) US20100089832, Linford, M.R.; Jensen, D.S.; Wiest, L.A., Apr 15, 2010, Brigham Young University, Modified diamond particle surfaces and method

Foreign Patent Documents

(1) JP2004051937A Takashi, S.; Shoichiro, Y.; Akiyoshi, I.; Kazuki, R., Feb 19, 2004 University Nihon, Polymer composite material and method for producing the same

Non-Patent Citations

(1) Akesson-Nilsson, G. *J. Chromatogr. A* **2003**, 996, 173-180.

(2) Ando, T., et al. *Diam. Relat. Mater.* **1996**, 5, (10), 1136-1142.

(3) Ando. T., et al*., J. Chem. Soc. Faraday T.* **1993**, 89 (11), 1783-1789.

(4) Bateman, H. G., *Food Chem.* **1997**, 45, 132-134.

(5) Bodennec, J. et al., *J. Lipid Res.* **2000**, 41, 1524-1531.

(6) Bodennec, J., et al., *J. Lipid Res.* **2000**, 41, 1524-1531.

(7) Chen, W. H., et al., *Anal. Chem.* **2006**, 78, 4228-4234.

(8) Cicero, R.L., *Langmuir* **2000**, 16, 5688-5695.

(9) Cicero, R.L., *Langmuir* **2002**, 18, 305.

(10) Clare, T. L. et al., *Langmiur* **2005**, 21, 6344-6355.

(11) Dyer, M. A., et al., *Langmuir* **2007**, 23, 7018-7023.

(12) Fabre, B., et al., *Chem. Commun.* **2002**, 2904-2905.

(13) Fabre, B., et al., *J. Phys. Chem. B* **2003**, 107, 14326-14335.

(14) Fu, G.D., et al., *J. Phys. Chem. B* **2003**, 107, 13902-13910.

(15) Hahn, M.,et al., *J. Adhes. Sci. Technol.* **2005**, 19, 1039-1052.

(16) Hamers, R. J. et al., *Diam. and Relat. Mater.* **2005**, 14, 661-668.

(17) Harris, J. J., et al., *J. Am. Chem. Soc.* **1999**, 121, 1978-1979.

(18) Ida, S, *Langmuir* **2003**, 19, 9693-9698.

(19) Ida, S., *Diam. Relat. Mater.* **2003**, 12, 601-605.

(20) Ida, S., et al., *Phys. Chem. Chem. Phys.* **2002**, 4, 3881-3886.

(21) Jiang, T, et al., *J. Chem. Soc. Faraday T.* **1996**, 92, 3401-3406.

(22) Kaluzny, M. A., et al., *J. Lipid* **1985**, 26, 135-140.

(23) Kendall, R. A., *Computer Phys. Comm.* **2000**, 128, 260-283.

(24) Kim, N. Y., et al. *J. Am. Chem. Soc.* **1999**, 121, 7162.

(25) Knickerbocker, T. et al., *Langmiur* **2003**, 19, 1938-1942.

(26) Kondo, T. et al., J. *Phys. Chem. C.* **2007**, 111, 12650-12657.

(27) Kong, X. L., et al. *Anal. Chem.* **2005**, 77, 4273-4277.

(28) Krysinski. P., et al., *J. Am. Chem. Soc.* **2003**, 125, 12726-12728.

(29) Lasseter, T., et al., *J. Am. Chem. Soc.* **2004**, 126, 10220-10221.

(30) Lee, M V., et al., *Chem. Vap. Deposition* **2005**, 11, 437-443.

(31) Lee, M. V., et al., *Chem. Mater.* **2007**, 19(21), 5052-5054.

(32) Linford, M. R., et al., *J. Am. Chem. Soc.***1993**, 115, 12631-12632.

(33) Linford, M. R., et al., *J. Am. Chem. Soc.***1995**, 117, 3145-3155.

(34) Liu, Y. et al., *Chem. Mater.* **2004**, 16, 3924-3940, 3924.

(35) Miller, J.B. et al., *Langmiur* **1996**, 12, 5809-5817.

(36) Nakamura, T. et al., *Langmuir* **2004**, 20, 5846-5849.

(37) Nakamura, T., et al., *Chem. Commun.* **2003**, 7, 900-901.

(38) Nesterenko, P. N. et al., *Analyst* **2007**, 132, 403-405.

(39) Nesterenko, P. N. et al., *J. Chromatogr. A* **2007**, 1155, 2-7.

(40) Nichols, B.M., et al., *J. Phys. Chem. B* **2005**, 109, 20938-20947.

(41) Notsu, H. et al., *Electrochem. Solid-State Lett.* **1999**, 2 (10) 522-524.

(42) Ohta, R. et al., *J. Vac. Sci. Technol. A* **2004**, 22, 2005-2009.

(43) Ouyang, T., *J. Phys. Chem. B* **2006**, 110, 5611-5620.

(44) Sabu, S. et al., *Anal. Biochem.* **2007**, 367, 190-200.

(45) Scruggs, B. et al., *J. Phys. Chem.* **1993**, 97, 9187-9195.

(46) Strother, T. et al., *Langmuir* **2002**, 18, 968-971.

(47) Tillman, N., et al., *J. Am. Chem. Soc.* **1988**, 110, 6136-6144.

(48) Tse, K.-Y., et al., *J. Phys. Chem. B* **2005**, 109, 8523-8532.

(49) Tsubota T., et al., *Phys. Chem. Chem. Phys.* **2002**, 4, 806-811.

(50) Tsubota T., et al., *Diam. Relat. Mater.* **2002**, 11, 1374-1378.

(51) Tsubota, T. et al., *Phys. Chem. Chem. Phys.* **2002**, 4, 3881-3886.

(52) Tsubota, T., et al., *Diam. Relat. Mater.***2004**, 13, 1093-1097.

(53) Tsubota, T., et al., *Hyomen Gijutsu* **2003**, 54, 758.

(54) Tsubota, T., et al., *Phys. Chem. Chem. Phys.* **2003**, 5, 1474-1480.

(55) Ushizawa, K., et al., *Chem. Phys. Lett,* **2002**, 351, 105-108.

(56) Vereir, I.E., et al., *Appl. Phys. Lett.* **1999**, 74, 3860.

(57) Visbal, H. et al., *J. Ceram. Soc. Jpn* **2004**, 112, 95-98.

(58) Wang, G.T., et al., *J. Am. Chem. Soc.***2000**, 122, 744-745.

(59) Wang, S, et al., *J. Phys, Chem. C.* **2007**, 111, 3986-3995.

(60) Yang, W, et al., *Langmuir* **2004**, 20, 6778-6787.

(61) Yeap, W. S., *Langmuir* **2009**, 25, 185-191.

(62) Yushin, G.N, et al., Effect of Sintering on Structure of Nanodiamond, Science Direct, 2005, 14 pp. 1721-1729 (9 pages).

(63) Zhang, J. P., *Biochemistry-US* **2002**, 41, 4612-4617.

(64) Zhong, Y. L., *Chem. Mater.* **2008**, 20, 3137-3144